Estudio de las alteraciones en el patrón de metilación del DNA del huésped inducidas por un viroide nuclear

Memoria presentada por: Mayte Castellano Pérez

Para optar al título de Doctor por la Universidad Politécnica de Valencia

Directores:

Profesor Vicente Pallás Benet

Doctor Gustavo Germán Gómez

Noviembre 2016

CSIC
Consejo Superior de Investigaciones Científicas

ibmcp
Instituto de Biología Molecular y Celular de Plantas

Universitat Politècnica de València

A Tere y Diego

UNIVERSITAT POLITÈCNICA DE VALÈNCIA

Don Vicente Pallás Benet, Doctor en Ciencias Biológicas, Profesor de Investigación del Consejo Superior de Investigaciones Científicas del Instituto de Biología Molecular y Celular de Plantas (Universidad Politécnica de Valencia-Consejo Superior de Investigaciones Científicas) de Valencia.

Don Gustavo Germán Gómez, Doctor en Biología, Científico Titular del Consejo Superior de Investigaciones Científicas del Instituto de Biología Molecular y Celular de Plantas (Universidad Politécnica de Valencia-Consejo Superior de Investigaciones Científicas) de Valencia.

CERTIFICAN:

Que Doña Mayte Castellano Pérez, Ingeniera Agrónoma por la Universidad Politécnica de Valencia, ha realizado bajo su dirección el trabajo que con título "Estudio de las alteraciones en el patrón de metilación del DNA del huésped inducidas por un viroide nuclear" presenta para optar al grado de Doctor en Biotecnología por la Universidad Politécnica de Valencia.

Y para que así conste a los efectos oportunos, firman el presente certificado en Valencia a 13 de enero de 2017.

Vicente Pallás Benet **Gustavo Germán Gómez**

ÍNDICE DE CONTENIDOS

ÍNDICE

ABREVIATURAS.

AGO: Argonaute protein. Proteina Argonauta.

ASBVd : Avocado sunblotch viroid. Viroide del manchado solar del aguacate.

ATP: Adenosine triphosphate. Trifosfato de adenosina.

C: Central domain. Dominio central.

CAP (extremo): Cap. Caperuza o casquete del RNA mensajero.

CChMVd: Chrysanthemun chlorotic mottle viroid. Viroide del moteado clorótico del crisantemo.

CCR: Central conserved region. Región central conservada.

cDNA: Complementary DNA. DNA complementario.

CEVd: Citrus exocortis viroid. Viroide de la exocortis de los cítricos.

Cis-Nats: Cis-natural antisense transcripts. Transcritos naturales antisentido.

CLSY: Chromatin remodeling. Remodelador de la cromatina.

CTM2: Cromomethylase 2. Cromometilasa 2.

CMT3: DNA Cromomethylase 3. Cromometilasa 3.

cRNA: Copy RNA. RNA copia.

DCL: Dicer-like RNase III. RNasa III de tipo dicer-like.

DDM1: Nucleosome remodeler. Remodelador de la cromatina.

DNA: Deoxyribonucleic acid. Ácido desoxiribonucleico.

dsRNA: Double stranded RNA. RNA bicatenario.

ELVd: Eggplant latent viroid. Viroide latente de la berenjena.

GFP: Green fluorescence protein. Proteina verde fluorescente.

GYSVd1: Grapevine yellow speckle viroid 1. Viroide 1 del moteado amarillo de la vid.

HC-pro: Viral helper component-protease. Proteasa del componente ayudante viral.

hc-siRNAs: Heterochromatic small interfering RNAs. Pequeños RNAs interferentes heterocromáticos.

HDA6: Histone deacetylase 6. Histona deacetilasa 6.

HDACs: Histone deacetylase. Deacetilasasde histonas.

HEN1: miRNA methyltransferase. Pequeño RNA Metiltransferasa

His: Histidine. Histidina.

HST: HASTY.

HSVd : Hop stunt viroid. Viroide del enanismo del lúpulo.

MET1: DNA methyltrasferase 1. DNA metiltransferasa 1.

MIR : Primary micro RNA coding gene. Gen que codifica para un miRNA primario.

miRNA: Micro RNA. micro RNA

mRNA: Messenger RNA. RNA mensajero.

NAT: Natural antisense transcripts. Transcritos naturales antisentido.

nat-siRNAs: Natural antisense small interfering RNAs. Pequeños RNAs interferentes naturales antisentido.

Nb: *Nicothiana benthamiana*.

ncRNA: Non-coding RNA. RNA no codificante.

NRPD1b: Nuclear DNA-dependent RNA polymerase IV b subunit. Subunidad b de la RNA polimerasa nuclear dependiente de DNA IV.

nts: Nucleotides. Nucleótidos.

P: Pathogenic domain. Dominio patogénico.

PAMP: Pathogen-associated molecular patterns. Patrones moleculares asociados a patógenos.

PLMVd: Peach latent mosaic viroid. Viroide del mosaico latente del melocotonero.

pre-miRNA: Pre-micro RNA.

Pre-rRNAs: Preribosomal RNA. Formas precursoras del RNA ribosomal.

pri-miRNA: Primary micro RNA. micro RNA primario

PSTVd: Potato spindle tuber viroid. Viroide del tubérculo fusiforme de la patata.

PTGS: Post-transcriptional gene silencing. Silenciamiento génico postranscripcional.

ra-siRNAs: Repeat associated small interfering RNAs. Pequeños RNAs de interferencia asociados a repeticiones.

rb-sRNAs: ribosomal-dervided sRNAs. Pequeños RNAs ribosomales.

rDNA: Ribosomal DNA. DNA ribosomal.

RdDM: RNA-directed DNA methylation. Metilación del DNA mediada por RNA.

RDR: RNA dependent RNA polymerase. Polimerasa de RNA dependiente de RNA.

RISC: RNA-induced silencing complex. Complejo inductor del silenciamiento de RNA.

RNA : Ribonucleic acid. Ácido ribonucleico.

RNA pol I: RNA polymerase I. RNA polimerasa I.

RNA-pol II: RNA polymerase II. Polimerasa de RNA II.

RNA pol IV: RNA polymerase IV. RNA polimerasa IV.

RNA pol V: RNA polymerase V. RNA polimerasa V.

RNasa: Ribonuclease. Ribonucleasa.

rRNA: Ribosomal RNA. RNA ribosomal.

SGS: Supressor of gene silencing. Supresor del silenciamiento génico.

siRNA: Small interfering RNA. Pequeño RNA interferente

sRNA: Small RNA. Pequeño RNA

ssRNA: Single stranded RNA. RNA monocatenario.

TAS (loci): Trans-acting small interfering RNA gene loci. Loci de un gen que produce pequeños RNAs interferentes con actividad en trans.

ta-siRNA o tasiRNA: Trans acting small interfering RNA. Pequeño RNA interferente con actividad en trans.

TCR: Terminal conserved region. Región terminal conservada.

TE: Transposable element. Transposón.

te-sRNAs: Transposable element sRNAs. Pequeño RNA derivado de un transposón.

TGS: Transcriptional gene silencing. Silenciamiento génico transcripcional.

TL: Left terminal domain. Dominio terminal izquierdo.

TMV. Tobacco mosaic virus. Virus del mosaico del Tabaco.

TR: Right terminal domain. Dominio terminal derecho.

Trans-Nats: Trans-antisense transcripts. Transcritos antisentido Trans.TRSV: Tobacco ringspot virus. Virus de la mancha anular del tabaco.

UV: Ultraviolet. Radiación ultravioleta

V: Variable domain. Dominio variable.

VdIRS: Viroid-induced RNA silencing. Silenciamiento de RNA inducido por un RNA viroidal.

vdRNAs: Viriod small RNAs. Pequeños RNAs viroidales.

RESUMEN

Los viroides son los patógenos de plantas con menor complejidad biológica descritos hasta el momento. Sin embargo y a pesar de estar compuestos por una cadena de RNA no codificante poseen la capacidad de infectar plantas y en algunos casos interferir en su metabolismo, provocando alteraciones en la homeostasis del huésped. Los mecanismos por los que estos RNAs no codificantes (ncRNAs) interfieren en las rutas metabólicas no están aun del todo descifrados. En los últimos años, se ha propuesto la existencia de una estrecha relación entre la patogénesis viroidal y el mecanismo del silenciamiento de RNA. Según esta hipótesis los pequeños RNAs derivados del viroide (vd-sRNAs) mediarían el silenciamiento post-transcripcional de RNAs endógenos del huésped y provocarían, de esta forma, la expresión de los síntomas. A pesar de que las evidencias que soportan la relación entre patogénesis y silenciamiento son robustas en algunas interacciones planta-viroide, existen indicios que sugieren que las alteraciones inducidas por el viroide en el huésped podrían ser producto de procesos más complejos que involucren por ejemplo, la alteración transcripcional de determinados genes de la planta. Para tratar de comprender, al menos en parte, esta compleja red de interacciones patógeno-planta se estableció como objetivo principal de este trabajo tratar de dilucidar las alteraciones que, a nivel transcripcional, se producían en la planta tras una infección viroidal.

En el primer capítulo determinamos que plantas de pepino infectadas con el viroide del enanismo del lúpulo (*HSVd*) acumulaban altos niveles de sRNAs derivados del RNA ribosomal (rb-sRNAs). Además, este efecto se correlacionó con un aumento de la transcripción de los precursores de los RNAs ribosomales (rRNAs) debido a una disminución de la metilación del DNA en su región promotora poniendo de manifiesto que ciertos genes ribosomales (normalmente silenciados) reactivaban su actividad transcripcional durante la infección. Estos resultados indicaban que, al menos en la interacción *HSVd*-pepino, el viroide inducía la desregulación de mecanismos de transcripción que estaban modulados por modificaciones epigenéticas (metilación de citosinas).

En el siguiente capitulo y con el objetivo de determinar si este proceso podía ser un fenómeno común a otros sistemas planta-patógeno, analizamos plantas de *N.benthamiana* transgénicas que expresaban de forma constitutiva la secuencia dimérica del viroide. Se observó cómo la acumulación de los sRNAs en plantas transgénicas era similar a la observada en los pepinos infectados, promoviendo el desequilibrio de la acumulación de rb-sRNAs. Mediante secuenciación de DNA bisulfitado demostramos que este fenómeno volvía a estar ligado con la pérdida de metilación de citosinas en un contexto simétrico. Al igual que en pepino este fenómeno correlacionaba con un aumento de la transcripción de estas zonas de DNA hipometiladas. Estos datos apoyaban la idea de que el HSVd era capaz de interferir en los mecanismos de

regulación a nivel epigenético del huésped (metilación), lo que sugería que este fenómeno podía ocurrir de forma general en otros sistemas viroide-huésped.

En el tercer capítulo y mediante ensayos de immuno-precipitación, fue posible determinar que tanto en pepino como en *N. benthaminana* el HSVd formaba complejos estables *in vivo* con la proteína HISTONA DEACETILASA 6 (HDA6), un componente clave del proceso de metilación de diversos DNAs repetitivos, entre los que se encuentra el DNA ribosomal. Estos resultados sugerían que esta interacción HSVd-HDA6 generaría un déficit funcional de HDA6 que podría ser responsable de las alteraciones epigenéticas observadas en el huésped durante la infección. Esta hipótesis fue consistente con la observación de que la sobreexpresión transitoria de HDA6 en plantas infectadas revirtió el estado de hipometilación del rDNA inducido por el viroide. Inesperadamente, observamos que la sobreexpresión de HDA6 inducía una significativa reducción en los niveles de acumulación del viroide en la planta infectada. Además, la acumulación del viroide en las células infectadas aumentó al silenciar de forma transitoria la expresión de HDA6 evidenciando la existencia de una relación antagónica entre la concentración de HDA6 y la del viroide. Una hipótesis que permite explicar los datos obtenidos y correlacionarlos con un incremento de eficacia biológica del viroide en el huésped se describe de manera detallada en la discusión de este capitulo.

Una vez demostrado que, en tejidos vegetativos del huésped, el HSVd induce alteraciones en el mapa epigenético de las zonas promotoras del rDNA, en el último capítulo de esta tesis analizamos si tejidos reproductivos del huésped mostraban alteraciones similares durante la infección. Para ello se analizaron granos de polen de flores provenientes de plantas de pepino infectadas por el HSVd. El análisis estructural de estas células reproductivas indico que la acumulación de *HSVd* inducía la descondensación de la cromatina nucleolar responsable de la transcripción de los rRNAs en el núcleo generativo. Esta alteración correlacionó con una significativa desmetilación de DNAs ribosomales y los asociados a Elementos Transponibles (TEs). Mediante análisis de qRT-PCR fue posible determinar que esta alteración en los patrones de metilación se correspondía con un significativo aumento de su actividad transcripcional lo que permite afirmar que al igual que lo observado en hoja, la infección por HSVd induce alteraciones a nivel de los mecanismos de regulación transcripcional también en tejidos reproductivos del huésped. Esta observación permite especular con la posibilidad de que estas modificaciones epigenéticas podrían pasar a la siguiente generación de plantas, confiriendo de esta manera al viroide una ventaja en la adaptación al huésped.

En resumen, los resultados presentados en esta tesis doctoral constituyen la primera descripción de una interacción física y funcional entre un patógeno de RNA y un componente del mecanismo de

silenciamiento de RNA del huésped, proporcionando nuevos datos que evidencian el potencial de los viroides para rediseñar el entorno celular del huésped y reprogramar sus mecanismos reguladores.

RESUM

Els viroides són els patògens vegetals amb menor complexitat biològica descrits fins al moment. Tanmateix i malgrat estar compostos per una cadena d'RNA no codificant, tenen la capacitat d'infectar plantes i en alguns casos interferir en el seu metabolisme, provocant alteracions en l'homeòstasi de l'hoste. Els mecanismes pels quals aquests RNA no codificants (ncRNA) interfereixen en les rutes metabòliques no estan del tot desxifrats. En els últims anys, s'ha proposat l'existència d'una estreta relació entre la patogènesi viroidal i el mecanisme del silenciament d'RNA. Segons aquesta hipòtesi, els petits RNA derivats del viroide (vd-sRNA) intervindrien en el silenciament posttranscripcional d'RNA endògens de l'hoste i provocarien, d'aquesta forma, l'expressió dels símptomes. A pesar que les evidències que admeten la relació entre patogènesi i silenciament són robustes en algunes interaccions planta-viroide, hi ha indicis que suggereixen que les alteracions induïdes pel viroide en l'hoste podrien ser producte de processos més complexos que involucren, per exemple, l'alteració transcripcional de determinats gens de la planta. Per a tractar de comprendre, almenys en part, aquesta complexa xarxa d'interaccions patogen-planta, es va establir com a objectiu principal d'aquest treball tractar de dilucidar les alteracions que, a nivell transcripcional, es produïen en la planta després d'una infecció viroidal.

En el primer capítol determinem que plantes de cogombre infectades amb el viroide del nanisme del llúpol (HSVd) acumulaven alts nivells d'sRNA derivats de l'RNA ribosòmic (rb-sRNA). A més, aquest efecte es va correlacionar amb un augment de la transcripció dels precursors dels RNA ribosòmics (rRNA) a causa d'una disminució de la metilació del DNA en la seua regió promotora, i va posar de manifest que certs gens ribosòmics (normalment silenciats) reactivaven la seua activitat transcripcional durant la infecció. Aquests resultats indicaven que, almenys en la interacció HSVd-cogombre, el viroide induïa la desregulació de mecanismes de transcripció que estaven modulats per modificacions epigenètiques (metilació de citosines).

En el següent capítol i amb l'objectiu de determinar si aquest procés podia ser un fenomen comú a altres sistemes planta-patogen, analitzem plantes de *N. benthamiana* transgèniques que expressaven de forma constitutiva la seqüència dimèrica del viroide. Es va observar como l'acumulació dels sRNA en plantes transgèniques era similar a l'observada en els cogombres infectats, promovent el desequilibri de l'acumulació d'rb-sRNA. Mitjançant la seqüenciació del DNA bisulfitat vam demostrar que aquest fenomen tornava a estar lligat a la pèrdua de metilació de citosines en un context simètric. De la mateixa forma que en el cogombre, aquest fenomen es correlacionava amb un augment de la transcripció d'aquestes zones

de DNA hipometilades. Aquestes dades donaven la idea que l'HSVd era capaç d'interferir en los mecanismes de regulació a nivell epigenètic de l'hoste (metilació), la qual cosa suggeria que aquest fenomen podia ocórrer de forma general en altres sistemes viroide-hoste.

En el tercer capítol, mitjançant assajos d'immunoprecipitació, va ser possible determinar que tant en cogombre com en *N. benthaminana*, l'HSVd formava complexos estables *in vivo* amb la proteïna HISTONA DEACETILASA 6 (HDA6), un component clau del procés de metilació de diversos DNA repetitius, entre els quals es troba el DNA ribosòmic. Aquests resultats suggerien que aquesta interacció HSVd-HDA6 generaria un dèficit funcional d'HDA6 que podria ser responsable de les alteracions epigenètiques observades en l'hoste durant la infecció. Aquesta hipòtesi va ser consistent amb l'observació que la sobreexpressió transitòria d'HDA6 en plantes infectades revertia l'estat d'hipometilació de l'rDNA induït pel viroide. Inesperadament, observem que la sobreexpressió d'HDA6 induïa una significativa reducció en els nivells d'acumulació del viroide en la planta infectada. A més, l'acumulació del viroide en les cèl·lules infectades va augmentar en silenciar de forma transitòria l'expressió d'HDA6, evidenciant l'existència d'una relació antagònica entre la concentració d'HDA6 i la del viroide. Una hipòtesi que permet explicar les dades obtingudes i correlacionar-les amb un increment d'eficàcia biològica del viroide en l'hoste, que es descriu de manera detallada en la discussió d'aquest capítol.

Una vegada determinat que, en teixits vegetatius de l'hoste, l'HSVd indueix alteracions en el mapa epigenètic de les zones promotores de l'rDNA, en l'últim capítol d'aquesta tesi analitzem si teixits reproductius de l'hoste mostraven alteracions similars durant la infecció. Amb aquesta finalitat, es van analitzar grans de pol·len de flors provinents de plantes de cogombre infectades per l'HSVd . L'anàlisi estructural d'aquestes cèl·lules reproductives va indicar que l'acumulació d'HSVd induïa la descondensació de la cromatina nucleolar responsable de la transcripció dels rRNA en el nucli generatiu. Aquesta alteració es va correlacionar amb una significativa desmetilació de DNA ribosòmics i els associats a elements *transposables* (TE). Mitjançant anàlisi de qRT-PCR va ser possible determinar que aquesta alteració en els patrons de metilació es corresponia amb un significatiu augment de la seua activitat transcripcional, la qual cosa va permetre afirmar que, igual que l'observat en la fulla, la infecció per HSVd induïa, també en els teixits reproductius de l'hoste, alteracions dels mecanismes de regulació transcripcional. Aquesta observació va permetre especular amb la possibilitat que aquestes modificacions epigenètiques pogueren passar a la següent generació de plantes, conferint d'aquesta manera al viroide un avantatge d'adaptació a l'hoste.

En resum, els resultats presentats en aquesta tesi doctoral constitueixen la primera descripció d'una interacció física i funcional entre un patogen d'RNA i un component del mecanisme de silenciament d'RNA

de l'hoste, que proporcionen noves dades que evidencien el potencial dels viroides per a redissenyar l'entorn cel·lular de l'hoste i reprogramar els seus mecanismes reguladors.

SUMMARY

Viroids are plant pathogens with the less biological complexity described until now. However, and despite being composed of a non-coding RNA, they have the ability to infect plants and in some cases to interfere in their metabolism, causing alterations in the host homeostasis.

The mechanisms by which these non-coding RNAs (ncRNAs) interfere in the metabolic routes are not yet totally deciphered. In recent years, it has been proposed the existence of a close relationship between viroid pathogenesis and the RNA silencing mechanism. According to this hypothesis, the small RNAs derived of the viroid (vd-sRNAs) would mediate the post-transcriptional silencing of endogenous RNAs of the host resulting in the expression of symptoms. Despite evidences supporting the relationship between pathogenesis and silencing are strong in some plant-viroid interactions, there are signs to suggest that alterations induced by the viroid in the host could be the result of more complex processes involving for example, the transcriptional alteration of certain genes in the plant. In order to try to understand, at least in part, this complex network of pathogen-plant interactions, it was established as the main objective of this work to try to elucidate alterations that, at the transcriptional level, were produced in the plant after a viroid infection.

In the first chapter, we determined that cucumber plants infected with hop stunt viroid (HSVd) accumulated high levels of sRNAs derived of ribosomal RNA (rb-sRNAs).Moreover, this effect was correlated with an increase of the transcription of the ribosomal RNAs precursors (rRNAs) due to a decrease in DNA methylation in its promoter region, revealing that certain ribosomal genes (usually silenced) reactivated its transcriptional activity during the infection. These results indicated that, at least in the HSVd-cucumber interaction, the viroid induced the deregulation of transcriptional mechanisms that were modulated by epigenetic modifications (cytosine methylation).

In the following chapter and in order to determine whether this process could be a common phenomenon to other plant-pathogen systems, we analyzed *N.benthamiana* transgenic plants that expressed, in a constitutive way, the viroid dimeric sequence. It was observed that the accumulation of the sRNAs in transgenic plants was similar to the one seen in infected cucumbers, promoting the imbalance of the rb-sRNAs accumulation. By bysulfited DNA sequencing we proved that this phenomenon turned to be linked with the loss of cytosine methylation in a symmetrical context. As with that observed in cucumber, this phenomenon was correlated with an increase of the transcription of these hypomethylated DNA

regions. These data supported the idea that the HSVd was able to interfere with the regulation mechanisms in the host epigenetic level (methylation), suggesting that this phenomenon could happen generally in other viroid-host systems.

In the third chapter, by immunoprecipitation essays, it was possible to determine that both in cucumbers in N. benthamiana plants, the HSVd formed an in vivo stable complex with the HISTONE DEACETYLASE 6 (HDA6), a key component in the process of methylation of diverse repetitive DNAs. These results suggested that the interaction HSVd-HDA6 would generate a functional deficit of HDA6 that might be responsible of the epigenetic alterations observed in the host during the infection. This hypothesis was consistent with the observation that the transient overexpression of HDA6 in infected plants reverted to the hypomethylation status of the rDNA. Unexpectedly, we observed that the HDA6 overexpression induced a significant reduction in the accumulation levels of the viroid in the infected plants. Also, the viroid accumulation in the infected cells increased when we transiently silenced the HDA6 expression, demonstrating the existence of an antagonistic relationship between the HDA6 concentration and the viroid. A hypothesis that allows explaining the information obtained and correlating them with an increase of biological viroid efficacy in the host is described in detail in the discussion of this chapter.

Once determined that, in vegetative host tissue, the HSVd induces alterations in the epigenetic map of the promotor areas of rDNA, in the last chapter of this thesis we analyzed whether or not reproductive host tissue showed similar alterations during the infection. We analyzed pollen grains of infected cucumber plants. The structural analysis of these reproductive cells indicated that the HSVd accumulation induced a nuclear chromatin decodensation, responsible of the rRNAs transcription in the nucleus of the generative cell. This alteration was correlated with a significant demethylation of the ribosomal DNAs and transposable elements. By RT-PCR analysis it was possible to determine that this methylation pattern alteration correlated with a significant increase of transcriptional activity. This observation revealed that the HSVd infection also induced alterations in the transcriptional regulation mechanisms in the host reproductive tissue. This result allowed speculating with the possibility that these epigenetic modifications could happen in the next generation plants, awarding to the viroid an advantage for host adaptation.

In short, the results presented in this thesis constitute the first description of a physical and functional interaction between a RNA pathogen and a host component of the silencing machinery, providing new information that demonstrates the potential of the viroids to redesign the host cellular environment and reschedule its regulative mechanisms.

INTRODUCCIÓN GENERAL

INTRODUCCIÓN.

1. Características generales de los viroides

Los viroides son patógenos que se caracterizan por poseer un genoma de RNA de cadena simple, circular y de tamaño pequeño (de 246 a 401nt). Son exclusivos de plantas, incluyendo monocotiledóneas y dicotiledóneas, herbáceas y leñosas, agronómicas y plantas ornamentales. Se replican autónomamente parasitando la maquinaria transcripcional de sus huéspedes, y por tanto necesitan interaccionar con los componentes de las vías metabólicas de la planta para poder infectarla (Diener, 2001; Flores *et al.*, 2005; Ding, 2009; Gómez *et al*., 2009; Gómez y Pallás, 2013).

La estructura primaria de los viroides presenta una alta auto-complementariedad de bases, generalmente con una gran proporción en citosina y guanina, lo que genera una robusta estructura secundaria (Flores *et al*., 2005). A pesar de no codificar proteínas, tienen la capacidad de infectar plantas y causar enfermedades (Diener, 2003; Tabler y Tsagris, 2000; Daròs *et al*., 2006; Ding y Itaya, 2007; Gómez y Pallás, 2013). Inicialmente se especuló con la idea de que los viroides fueran los precursores primitivos de los virus, pero sus características moleculares y biológicas hacían poco probable esta hipótesis. También se propuso un posible origen a partir de intrones, elementos transponibles o plásmidos (Diener, 1981; 1989). Sin embargo, el descubrimiento posterior de la presencia de ribozimas en algunos de ellos ha llevado a considerarlos como potenciales fósiles moleculares que tuvieron su origen en el mundo del RNA, que se cree, antecedió a la aparición de la vida celular basada en el DNA y las proteínas (Diener, 1989; Flores *et al*., 2014; Diener, 2016).

Al ser RNAs patogénicos que no poseen capacidad codificante, su ciclo de vida es estrictamente dependiente de los factores del huésped. Esta característica ha hecho de los viroides un atractivo sistema modelo para analizar diferentes aspectos de la biología del RNA, tales como el conocimiento de la relación entre la estructura y la función del RNA, su procesamiento o su transporte entre otros (Flores *et al.,* 2005; Flores *et al.* 2004; Daròs *et al.,* 2006; Ding y Itaya 2007; Tsagris *et al.,* 2008).

Los viroides se descubrieron y caracterizaron en la primera mitad de la década de los 70 tratando de dilucidar los agentes causales de la enfermedad del tubérculo fusiforme de la patata (PSTVd) (Diener 1971) y de la enfermedad de la exocortis de los cítricos (CEVd) (Semancik y Weathers, 1972). En ambos casos, tras múltiples experimentos, fue posible determinar que presentaban propiedades de un RNA de bajo peso molecular, circular y de características muy distintas a los virus de RNA.

Desde el punto de vista funcional, su simplicidad molecular se contrarresta con su capacidad para interactuar con la maquinaria celular del huésped y así llevar a cabo todas las funciones necesarias de su ciclo infectivo. Los viroides interaccionan con factores del huésped y, debido a ello, pueden (en algunas interacciones patógeno-huésped) inducir síntomas. Diversos estudios demostraron que moléculas circulares o lineales del viroide PSTVd interactuaban con histonas, proteínas nucleares desconocidas y la RNA polimerasa II de germen de trigo (Goodman *et al*., 1984; Wolff *et al*., 1985). Otra aproximación experimental, empleando la combinación de la unión mediante UV seguida de una digestión con RNasa, permitió identificar diversos complejos viroide-proteína aislados del núcleo (Goodman *et al*., 1984). Más recientemente se ha descrito otra proteína que interaccionaba con PSTVd en tomate (VirP1), un miembro de la familia de los reguladores transcripcionales asociados con la remodelación de la cromatina (Martinez de Alba *et al*., 2003).

A día de hoy se han caracterizado molecular y biológicamente 30 especies de viroides y numerosas variantes de secuencia de las mismas (Di Serio *et al*., 2014 Tabla 1 clasificándolas en dos familias; la familia *Pospiviroidae*, cuya especie tipo es el viroide fusiforme de la patata (PSTVd) (Gross *et al*., 1978), y la *Avsunviroidae*, cuya especie tipo es el viroide del manchado solar del aguacate (*Avocado sunblotch viroid*, ASBVd) (Symons, 1981).

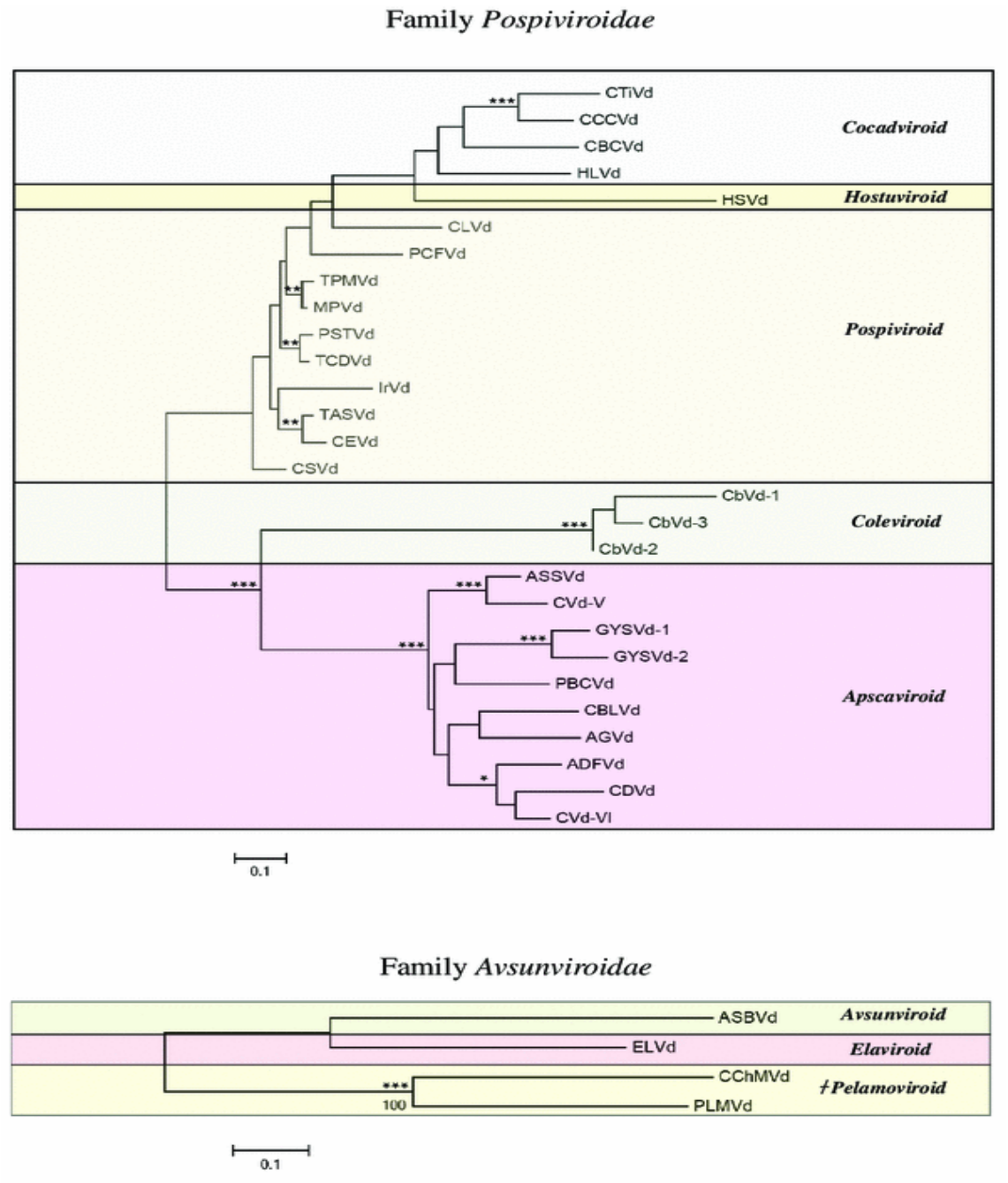

En la **Tabla1.** (Di Serio *et al*., 2014) se muestran los árboles filogenéticos de las familias Pospiviroidae y Avsunviroidae, que contienen 5 y 3 géneros respectivamente. Los viroides se agrupan en función de su respectiva posición taxonómica dentro de los géneros reconocidos (indicado a la derecha de cada cuadro de color). Se representan las siglas del nombre completo del viroide.

Los viroides de la familia *Pospiviroidae* se replican y acumulan en el núcleo (para consultar detalles sobre el proceso de replicación de los viroides nucleares ver Gas *et al*., 2007). Un análisis mutacional de la estructura secundaria puso de manifiesto que los miembros de la familia *Pospiviroidae* adoptan una estructura en varilla con cinco dominios conservados (Keese y Symons, 1985): uno central, el cual integra una región central conservada (CCR), flanqueada por los dominios patogénico (P) y variable (V), y los dos dominios terminales derecho (TR) e izquierdo (TL), éste último conteniendo una región terminal conservada (TCR) o una horquilla terminal conservada (TCH), tal y como se muestra en la Figura 1. En función de la secuencia de la CCR y la presencia o ausencia de la región terminal conservada y la horquilla, los miembros de esta familia se clasifican en cinco géneros (Tabla 1) (Flores *et al.*, 2005).

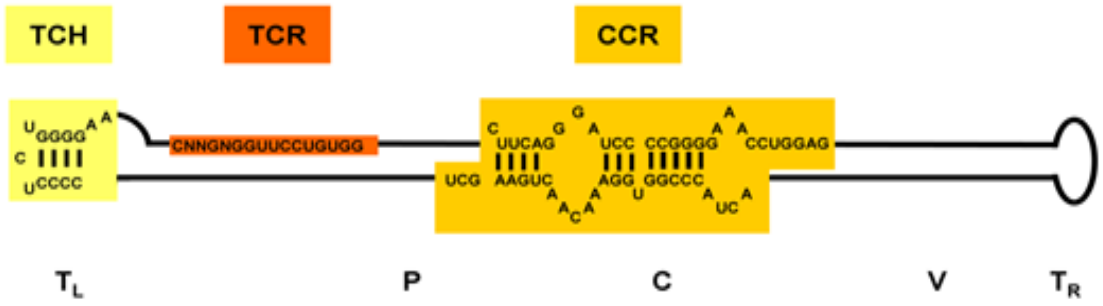

Figura 1. Representación esquemática de la estructura secundaria de tipo varilla propuesta para los viroides del género Pospiviroid de la familia *Pospiviroidae*. En la parte inferior se indica la localización de los diferentes dominios. A color se representan los nucleótidos conservados de cada una de las regiones.

Respecto a los viroides de la familia *Avsunviroidae*, hay que destacar que carecen de los motivos conservados típicos de los *Pospiviroidae* y que a diferencia de éstos pueden formar estructuras de cabeza de martillo con actividad ribozimática. Estos dominios no aceptan ningún cambio nucleotídico en el centro catalítico del ribozima. Sólo se han detectado mutaciones en las zonas adyacentes que forman los bucles y siempre están asociados a mutaciones compensatorias para no afectar a la estabilidad de las hélices. A diferencia de los *Pospiviroidae* los viroides de esta familia se replican y acumulan en el cloroplasto (Navarro y Flores, 1997; Ambrós *et al*., 1998; Navarro *et al*., 2000; Nohales *et al.,* 2012 a y b).

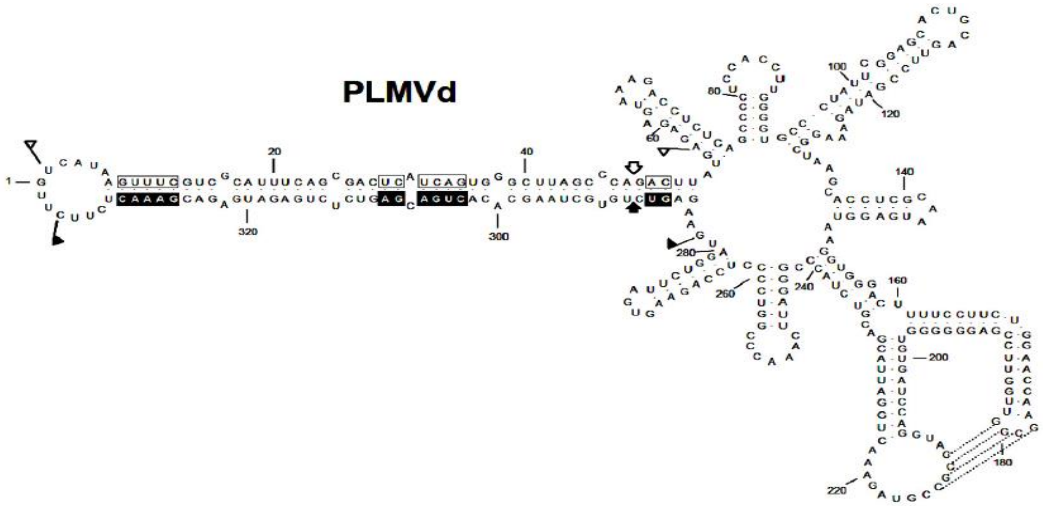

Figura 2. Representación de la estructura secundaria de tipo cuasi-varilla y ramificada del PLMVd de la familia *Avsunviroidae*.

Como ya se ha comentado anteriormente, los viroides presentan un elevado grado de estructura secundaria debido a la alta autocomplementariedad de sus secuencias. Los modelos estructurales predichos, por lo general, presentan tramos apareados alternados con pequeños bucles desapareados, lo que les confiere una estructura de tipo cuasi-varilla o ramificada en el caso exclusivo de algunos miembros de la familia *Avsunviroidae* (Figura 2).

1.1 Replicación de los viroides.

Mediante estudios de centrifugación diferencial y más tarde por experimentos de hibridación *in-situ* y microscopía electrónica, se confirmó la localización subcelular de los viroides de la familia *Pospiviroidae*, observándose su acumulación fundamentalmente en el núcleo y el nucléolo (Diener 1971; Bonfiglioli *et al*., 1996; Harders *et al*., 1989). Estos viroides se encuentran en diferentes formas dentro del núcleo, siendo la más abundante el monómero viroidal con una determinada polaridad a la que se le atribuye arbitrariamente la polaridad positiva (Branch y Robertson, 1984). Por su parte, los miembros de la familia *Avsunviroidae* se replican y acumulan preferentemente en el cloroplasto y es en este orgánulo dónde se localizan mayoritariamente los monómeros circulares de ambas polaridades (Mohamed y Thomas 1980; Bonfiglioli *et al*., 1994; Lima *et al*., 1994; Bussière *et al*., 2000). Se asume que, esta diferencia de localización subcelular entre las dos familias de viroides podría implicar diferencias en la interacción con los componentes del huésped.

La replicación y propagación de los viroides depende de los factores de la planta; se ha demostrado que la RNA polimerasa DNA dependiente II interviene en la replicación de los viroides localizados en el núcleo (Tabler y Tsagris, 2004), mientras que los viroides cloroplásticos se replican a través de una RNA polimerasa cloroplástica codificada en el núcleo o una RNA polimerasa codificada en los plastidios (Flores

et al., 2004). La naturaleza circular de los viroides y la falta de intermediarios de DNA homólogos o complementarios a su secuencia (Zaitlin *et al*., 1980; Branch y Dickson, 1980) determinan que la replicación de los viroides siga el modelo de círculo rodante. En este mecanismo de replicación intervienen solamente intermediarios de RNA y se basa en la presencia de moléculas de ambas polaridades que se acumulan a distintas concentraciones.

En función de la familia del viroide, el mecanismo de replicación tiene diversas variantes (Figura 3). Los viroides de la familia *Pospiviroidae* siguen la vía asimétrica, cuya molécula circular de polaridad positiva sirve de molde para la síntesis de oligómeros lineales de polaridad negativa que a su vez sirven de molde para la síntesis de oligómeros de polaridad positiva. Los miembros de la familia *Avsunviroidae* sigue la vía simétrica (Branch y Robertson, 1984; Darós *et al*, 1994; Navarro *et al*, 1999). La molécula circular de polaridad positiva sirve de síntesis de los oligómeros lineales de polaridad negativa que se autocortan y circularizan, obteniendo moléculas viroidales de polaridad negativa que servirán a su vez como molde para generar monómeros de polaridad positiva que serán recircularizados, encontrándose de nuevo en el punto de partida (Figura 3).

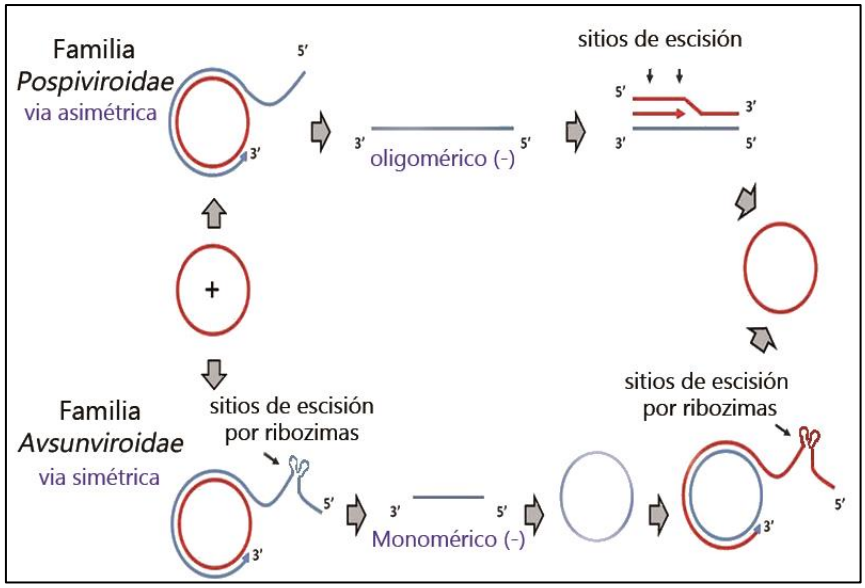

Figura 3. Replicación de los viroides mediante el modelo de círculo rodante. Vías simétrica y asimétrica de los viriodes pertenecientes a las familias *Pospiviroidae* y *Avsunviroidae,* respectivamente (adaptado de Flores *et al*., 2005).

1.1.1 RNA polimerasas DNA dependientes implicadas en la síntesis de los RNAs viroidales nucleares.

Para investigar qué RNA polimerasa nuclear se encuentra implicada en la replicación de los miembros de la familia *Pospiviroidae* se realizaron estudios *in vivo* e *in vitro* con α-amanitina, un octapéptido fúngico capaz de inhibir a las RNA polimerasas II y III a bajas y altas concentraciones respectivamente, pero no

así a la RNA polimerasa I (Roeder, 1976; Marzluff y Huang, 1984; Cox y Golberg, 1988). Siguiendo esta metodología se demostró que la enzima implicada en la transcripción del PSTVd (Schindler y Mülbach, 1992), CEVd (Flores y Semancik, 1982; Flores, 1989; Rivera-Bustamante y Semancik, 1989) y HSVd (Mühlbach y Sänger, 1979; Yoshikawa y Takahashi, 1986), era la RNA polimerasa II. Esta hipótesis quedó sustentada por los resultados de un trabajo dónde la RNA polimerasa II purificada de plantas de tomate sanas era capaz de transcribir *in vitro* un RNA de polaridad positiva del PSTVd (Rackwitz *et al*., 1981).
Años más tarde se demostró la interacción *in vivo* de la RNA polimerasa II y el CEVd. Se realizó un ensayo de inmunoprecipitación partiendo de una fracción enriquecida en cromatina purificada de plantas de tomate infectadas por este viroide, donde se pudo inmunoprecipitar la RNA polimerasa II asociada a RNAs viroidales de ambas polaridades con un anticuerpo monoclonal específico del dominio carboxiterminal de la subunidad mayor de dicha polimerasa (Warrilow y Symons, 1999).

1.2 Movimiento viroidal.

Dada la naturaleza no codificante del RNA viroidal y su pequeño tamaño, junto con el renovado interés en los estudios de la translocación de los RNAs endógenos, los viroides se han convertido recientemente en sistemas modelo idóneos para estudiar el transporte de RNA intra e intercelular (Wang y Ding, 2010). Una infección convencional de una planta huésped comprende una serie de pasos coordinados. Los viroides inician su proceso de infección generalmente a través de heridas provocadas por instrumentos de poda aunque lo pueden hacer también en algunos casos a través de vectores biológicos o a través del polen y/o semillas. Una vez en el interior de la célula vegetal y para poder invadir sistémicamente al huésped los viroides deben acometer al menos tres tipos diferentes de movimiento que normalmente están coordinados: i) intracelular, en el interior de la célula; ii) intercelular; a través de los plasmodesmos y iii) vascular, a través del floema para alcanzar las partes distales de la planta (Ding y Itaya, 2007; Flores *et al*., 2005; Gora-Sochacka, 2004; Tabler *et al*., 2004; Wang *et al*., 2010) (Figura 4).

1.2.1 Movimiento intracelular.

Los viroides poseen dos sitios de replicación bien determinados en la célula infectada en función de la familia a la que pertenezcan, bien el núcleo, para los miembros de la familia *Pospiviroidae*, o el cloroplasto, para los de la familia *Avsunviroidae*. Al no poseer capacidad codificante, se ven obligados a interactuar directamente con los factores de la célula huésped para lograr la compartimentalización subcelular adecuada y que su replicación sea eficiente. Los estudios con viroides nucleares, esencialmente con el PSTVd, han puesto de manifiesto que el transporte al núcleo se produce a través de un receptor no

saturable e independiente de la ruta del citoesqueleto (Woo *et al*., 1999). En el transporte al núcleo de este viroide es crítica la participación de la hebra superior de la CCR (Abraitiene *et al*., 2008). Una proteína del huésped con un bromodominio (VirP1) parece ser esencial en la compartimentalización nuclear de este viroide (Martínez de Alba *et al*., 2003).

Los pocos estudios acerca del movimiento intracelular de viroides cloroplásticos han revelado la posible existencia de un paso intermedio nuclear para llegar al cloroplasto mediado por un dominio de RNA localizado en la región terminal izquierda del viroide (Gómez y Pallás, 2012).

1.2.2 Movimiento intercelular y vascular.

Ding y Wang (2009) demostraron de manera inequívoca que los viroides, de la misma forma que los virus, se mueven de una célula a otra a través de los plasmodesmos. Es de destacar que para el movimiento entre las células del parénquima en empalizada y las del mesófilo espongiforme se requiere el concurso de un motivo del RNA viroidal, denominado 'loop 6', que podría ser reconocido por distintos factores celulares (Takeda *et al*., 2011). Una vez en el floema los viroides son transportados como complejos ribonucleoproteicos formados entre el RNA viroidal y la proteína floemática 2 (PP2) (Owens *et al*., 2001; Gómez y Pallás, 2001) que presenta un dominio de unión a RNA de doble cadena y es capaz de facilitar la translocación del RNA viroidal a través de injertos intergenéricos (Pallás y Gómez, 2013). Es importante destacar que la invasión del tejido vascular está mediada por un dominio del RNA virodal que forma un pequeño lazo y que otro dominio es necesario para la descarga floemática (Ding y Wang, 2009) lo que pone de manifiesto la complejidad en los requerimientos estructurales del RNA viroidal en los distintos tipos de movimiento.

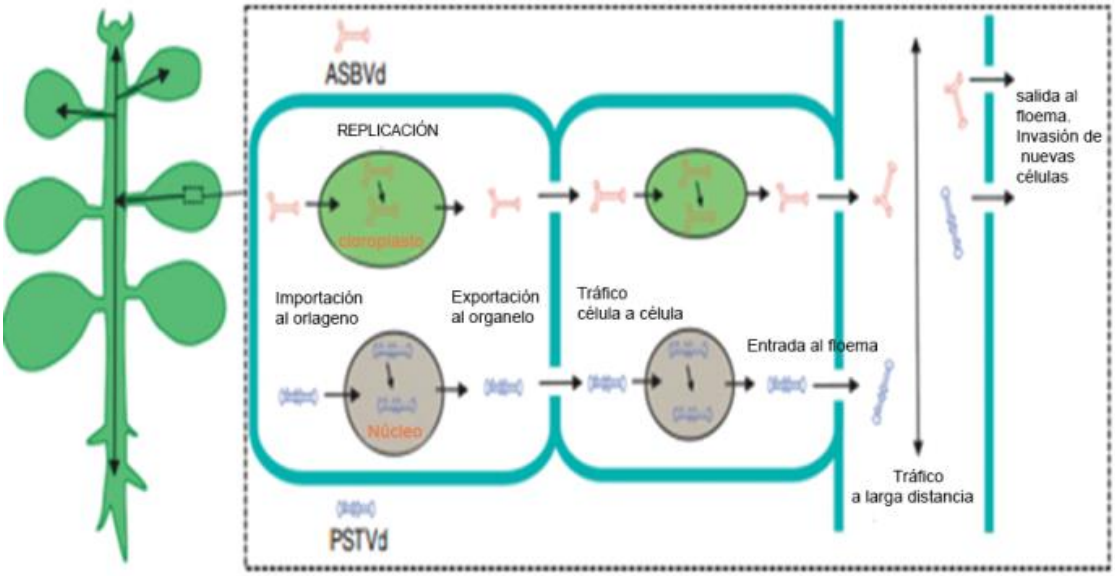

Figura 4. Esquema del movimiento viroidal de ambas familias intra e intercelular (adaptado de Ding *et al,* 2005).

1.3 Patogénesis viroidal y su relación con el silenciamiento.

Como consecuencia de la infección, en algunas interacciones viroide-huésped, la planta puede desarrollar alteraciones morfológicas reconocidas como síntomas. Si bien la naturaleza y gravedad de estas alteraciones son en general específicas de cada interacción, los síntomas más comunes incluyen retraso en el crecimiento, enanismo, epinastia, manchas cloróticas y necróticas, chancros, malformaciones de flores, frutos y tubérculos. Cabe mencionar que en algunas interacciones, ciertos viroides (como por ejemplo el ELVd) desarrollan una infección latente caracterizada por la ausencia de síntomas externos evidentes (Fadda *et al*., 2003). En el caso de aislados extremadamente virulentos, este proceso puede ocasionar la muerte de la planta infectada (Kovalskaya y Hammond, 2014) (Figura 5).

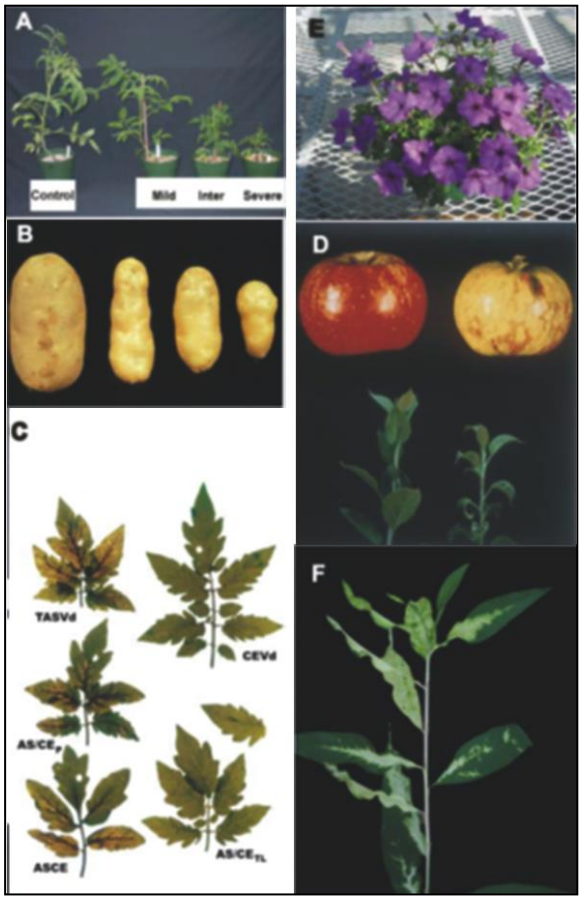

Figura 5. Síntomas asociados a la infección por viroide. (A) Infección de diferentes aislados de PSTVd ocasionan diferente sintomatología en tomate. (B). Diferentes viroides de la misma familia inducen síntomas diferentes como retraso en el crecimiento, epinastia y necrosis venal. (C) Síntomas de PSTVd en su huésped natural (patata); el tubérculo control de la izquierda es de planta sana. (D) A la izquierda se muestra una manzana sana y a la derecha una infectada con ASSVd. (F) Infección de melocotonero producida por PLMVd. (E) Petunia asintomática infectada por TCDVd. (Adaptado de Robert A. Owens y Rosemarie W. Hammond, 2009)

Teniendo en cuenta que los viroides son RNAs no codificantes, se asume que las alteraciones fisiológicas asociadas a la aparición de síntomas deben ser consecuencia de la interacción directa entre el RNA viroidal y los factores del huésped. Esta idea se sustenta en trabajos que demuestran que existen variaciones nucleotídicas en la secuencia del viroide asociadas a alteraciones en la intensidad de la repuesta patogénica. Por ejemplo, la alteración de un sólo nucleótido del viroide del enanismo del lúpulo (HSVd) es suficiente para ocasionar la cachexia de los cítricos (Serra *et al*., 2008); las alteraciones de dos nucleótidos adyacentes en CEVd resultaron ser importantes en la patogenicidad de determinados huéspedes (Murcia *et al*., 2011), además, se identificaron secuencias responsables de producir albinismo (Navarro *et al*., 2012) y clorosis en el melocotonero (Wang *et al*., 2013) de diferentes aislados del PLMVd.

El descubrimiento de la presencia de siRNAs derivados del viroide en plantas infectadas resultó ser un indicio indirecto de que estos patógenos inducían silenciamiento post-trascripcional (PTGS) en su huésped (Itaya *et al.*, 2001; Markarian *et al.*, 2004; Martínez de Alba *et al.*, 2002; Papaefthimiou *et al.*, 2001). La detección de la acumulación de pequeños RNAs derivados del viroide en tomate infectado con PSTVd (Papaefthimiou *et al*., 2001) sugirió la posible relación entre el proceso de infección viroidal y el silenciamiento de RNA. Una evidencia aún mayor de este fenómeno se obtuvo al conseguir modelos transgénicos demostraron que los viroides y/o sus intermediarios de replicación inducían este fenómeno, denominado silenciamiento de RNA inducido por un RNA viroidal (VdIRS) (Vogt *et al*., 2004).

Durante la infección, las células de la planta están expuestas a estructuras de RNA de doble cadena (dsRNA), formadas a partir de regiones del genoma del patógeno altamente autocomplementarias (Molnar *et al*., 2005) o bien generadas como consecuencia de su replicación (Mlotshwa *et al*., 2008).
Estos dsRNAs actúan como un patrón molecular asociado a patógenos (PAMP), el cual es detectado por la maquinaria de silenciamiento de RNA del huésped, induciendo un mecanismo de defensa que se activa como respuesta a la presencia de ácidos nucleicos externos. Las enzimas Dicer-like (DCLs) procesan estos dsRNAs en pequeños dúplex de 21, 22 o 24 pares de bases, presentando dos nucleótidos protuberantes en su extremo 3' (siRNAs) (Axtell, 2013), que se acumulan en tejido infectado y son incorporados al complejo AGO-RISC, dirigiendo el corte específico hacia su hebra complementaria (Mlotshwa *et al*., 2008).
Se ha propuesto que los viroides son capaces de escapar de la actividad del complejo RISC debido a la estructura compacta de su genoma (Gómez y Pallás, 2007; Itaya *et al*., 2007; Wang *et al*., 2004). Así, Itaya *et al*. (2007) demostraron que el RNA del PSTVd expresado transitoriamente en protoplastos de *Nicotiana benthamiana*, resultó ser resistente a la degradación mediada por RISC debido a su estructura compacta. Simultáneamente y en un estudio independiente, se demostró que formas circulares del HSVd resistían la

degradación mediada por el silenciamiento de RNA y eran capaces de translocarse sistémicamente a través de injertos (Gómez y Pallás, 2007). Estas evidencias sustentan la idea de que evolutivamente los viroides habrían estado condicionados a mantener su estructura secundaria compacta para escapar de esta vía de defensa de las plantas (Wang *et al*. 2004; Elena *et al*., 2009).

Por tanto, estos resultados proporcionan una visión unificada en la que el RNA viroidal es al mismo tiempo inductor, diana y evasor del fenómeno del silenciamiento (Flores *et al*, 2005; Gómez *et al*., 2009; Itaya *et al*, 2007; Vogt *et al*, 2004; Wang *et al*, 2004), ya que son patógenos que están obligados a utilizar las vías regulatorias de los RNAs no codificantes (ncRNAs) de las plantas.
Debido a que este tema ha sido uno de los puntos principales para el desarrollo de la presente tesis, se abordará de forma más extensa en el apartado de la interrelación entre patogénesis asociada a la infección con HSVd y silenciamiento de RNA.

1.4 El viroide del enanismo del lúpulo (HSVd)

El viroide del enanismo del lúpulo (HSVd) pertenece al género *Hostuviroid* de la familia *Pospiviroidae*, y presenta un tamaño entre 294-303 nucleótidos. Fue identificado por primera vez en Japón en los años 70 como agente causal de un severo enanismo en plantas de lúpulo (Sasaki y Shikata, 1977). Es un patógeno generalista que está extendido en un gran número de países (Pallás *et al*., 2003). Ha sido descrito en pepino, lúpulo, vid, cítricos, ciruela, melocotón y pera (Shikata, 1990), así como en albaricoquero y almendro (Astruct *et al*., 1996, Cañizares *et al*, 1999).

En algunas especies, como la vid, la infección suele ser latente (Shikata, 1990; Polivka *et al*., 1996); en cambio, en otras como el lúpulo, los cítricos, el ciruelo y el albaricoquero, ciertas variantes de secuencia pueden producir síntomas como retraso en el crecimiento, rugosidad y moteado del fruto y caquexia (Diener *et al*., 1988; Sano *et al*., 1989, Shikata, 1990, Ragozzino *et al*., 2002, Amari *et al*., 2007; Serra *et al*.,2008).

Históricamente, los primeros análisis filogenéticos y de homología de secuencia dividieron los aislados de HSVd en tres grupos: tipo ciruelo (plum-type), tipo lúpulo (hop-type) y tipo cítrico (citrus-type) (Hsu *et al*., 1995; Shikata, 1990). Pero la caracterización y el análisis filogenético de nuevas variantes de secuencia de tres especies de prunus revelaron la aparición de dos nuevos grupos, que, muy probablemente, deriven de eventos de recombinación (Kofalvi *et al*., 1997). Además, este análisis reveló que posiblemente un cierto número de aislados podrían haber derivado de eventos de recombinación y

que de hecho, el grupo tipo lúpulo podría ser el resultado de recombinaciones entre los grupos tipo ciruelo y cítrico (grupo P-C) (Kofalvi *et al*., 1997; Amari *et al*., 2001). Un nuevo grupo filogenético ha sido descrito recientemente para aislados de vid procedentes de un banco de germoplasma de la Comunidad Valenciana (España) (Fiore *et al*., 2016).

2. Silenciamiento génico de RNA.

El silenciamiento génico es un mecanismo de regulación dependiente de secuencia y mediado por RNA, presente en la mayoría de los organismos eucariotas (excepto en la levadura *Saccharomyces cerevisiae*). En plantas, además de regular la expresión génica endógena, participa en la defensa contra RNAs patogénicos (virus y viroides) y protege la estabilidad del genoma frente a transposones y transgenes (Baulcombe, 2004). El descubrimiento del silenciamiento mediado por RNA ha estado estrechamente ligado al mundo vegetal y muy particularmente a la Virología de plantas (Pallás, 2013). Sin embargo, fueron los experimentos realizados por Fire *et al*. (1998) en *C. elegans* los que demostraron de manera definitiva que la molécula inductora de dicho proceso de silenciamiento era el RNA de doble hebra (dsRNA).

2.1 Características generales.

En plantas, el silenciamiento de RNA abarca una serie de procesos que actúan a nivel transcripcional (transcripcional gene silencing, TGS) o postranscripcional (posttranscriptional gene silencing, PTGS). Ambos reconocen específicamente secuencias de DNA o RNA respectivamente, e intervienen en varias funciones como el mantenimiento de la estabilidad del genoma (Vaucheret, 2006; Liu *et al*., 2010), la regulación de procesos del desarrollo (Chen, 2009) y la defensa frente a ácidos nucleicos invasores (Ruiz-Ferrer y Voinnet, 2009).

El término silenciamiento de RNA comprende un conjunto de procesos que, gracias a experimentos en genética y bioquímica, han podido ser organizados en un modelo general (Figura 6) además de identificar sus factores necesarios.

Como norma general, el proceso se inicia a partir de un transcrito bicatenario (dsRNA) cuyo origen puede ser endógeno (transcriptos estructurados tipo "*hairpin*" transposones, transgenes, transcritos antisentido, etc.) o exógeno (RNAs patogénicos virales o sub-virales) (Vance y Vaucheret, 2001; Voinnet, 2001; Waterhouse *et al*., 2001; Baulcombe, 2002). La doble hebra de RNA (dsRNA) es cortada por una familia de ribonucleasas tipo III (RNasa III), denominadas en plantas proteínas Dicer-Like (DCLs), en moléculas bicatenarias de 21-24 nucleótidos (pequeños RNAs (sRNAs)) (Bernstein *et al*., 2001; Hamilton and Baulcombe, 1999; Zamore *et al*., 2000) que presentan dos nucleótidos protuberantes en el extremo 3'

en ambas cadenas (Elbashir *et al*., 2001a, b). La producción de sRNAs mediante la actividad DCL es un proceso ATP dependiente (Bernstein *et al*., 2001; Zamore *et al*., 2000) en el que están involucradas interacciones con otras proteínas (Tabara *et al*., 2002). A continuación, una RNA helicasa separa ambas cadenas y una de ellas es reclutada a un complejo proteico denominado RNA Induced Silencing Complex (RISC) (Hammond *et al*., 2000), que, como componente funcional principal, contiene una proteína Argonauta (AGO) que posee actividad RNasa H.

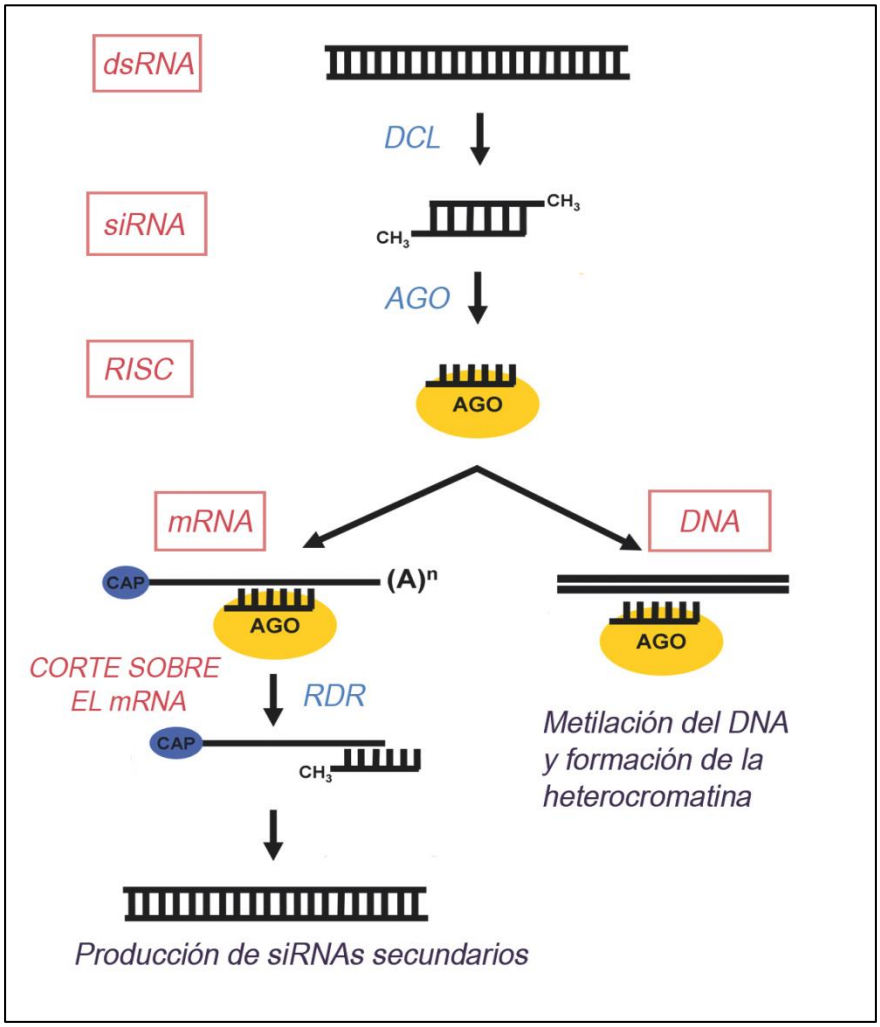

Figura 6. Esquema del proceso de silenciamiento de RNA. Se inicia con un dsRNA, el cual es digerido por DCL en moléculas de siRNA, éstos son cargados en complejos RISC, cuyo componente principal es una proteína AGO, teniendo dos posibles destinos, cortar un mRNA de secuencia homóloga al siRNA (inhibiendo su traducción), o actuar sobre el DNA metilando la citosina o las histonas, formando la heterocromatina.

En el caso del silenciamiento post-transcripcional este complejo proteína-RNA es guiado por el sRNA a un RNA mensajero de secuencia complementaria, provocando su degradación o la inhibición de su traducción (Bernstein *et al*., 2001; Elbashir *et al*., 2001a; Hammond *et al*., 2000, 2001; Zamore *et al*., 2000). En el silenciamiento transcripcional (TGS), el complejo es guiado hasta un DNA diana de secuencia

complementaria a la que se une e induce su metilación, bloqueando así su transcripción mediante la modulación estructural de la heterocromatina (Voinnet, 2008).

Esta respuesta es amplificada mediante la síntesis de nuevos RNAs bicatenarios gracias a la acción de una RNA polimerasa dependiente de RNA (RDR), la cual utiliza como molde los ssRNAs que se generan tras el corte por el complejo RISC. Estos dsRNAs vuelven a entrar en la ruta de silenciamiento siendo cortados, de nuevo, por las DCL para generar los sRNAs secundarios. En general, estas polimerasas actúan sobre RNAs derivados de virus, transposones, y otros RNAs percibidos por la célula como aberrantes o extraños (Voinnet, 2008)

2. 2 Las rutas del silenciamiento de RNA en plantas

Hay diferentes rutas de silenciamiento de RNA en plantas, pero todas presentan los cuatro pasos característicos de este proceso; 1) inicio del silenciamiento provocado por la formación de un dsRNA, 2) corte de dicho dsRNA en sRNAs de 20 a 24 nucleótidos, 3) metilación en 2'-O del sRNA y, por último, 4) incorporación al complejo RISC que se asociará con un RNA o DNA con una homología total o parcial al sRNA (Ruiz-Ferrer y Voinnet, 2009) (Figura 7).

El origen de los dsRNAs puede ser diverso, los mecanismos más comunes suelen ser la expresión de genes antisentido, de RNAs aberrantes, de transgenes (cuya expresión exceda un valor umbral) o de loci endógenos con una alta estructura secundaria (Matzque y col, 2002). De forma alternativa, el dsRNA puede sintetizarse por la acción de alguna de las RNA polimerasas (RDR1-6) a partir de mRNAs aberrantes (o procedentes del corte por miRNAs) o de transcritos producidos por la RNA Pol IV (Brodersen y Voinnet, 2006; Chapman y Carrington, 2007; Ruiz-Ferrer y Voinnet, 2009). En *Arabidopsis*, el dsRNA se procesa en duplos de sRNAs de un tamaño determinado dependiendo de cuál de las 4 DCLs actúe sobre ellos. DCL1 genera sRNAs de entre 18 y 21 nts, DCL2 de 22 nts, DCL3 de 24 nts y DCL4 de 21. Este corte es facilitado por 1 de las 5 proteínas de unión a dsRNA (HYL1, DRB2-5) que interaccionan directamente con la DCL. Tras este corte los extremos 3' de los sRNAs (extremos con dos nucleótidos no apareados) son O-metilados en 2' por la metiltransferasa HEN1, lo que les protege de la degradación o de la oligo-uridilación. Estos duplos de sRNAs estabilizados pueden tener dos destinos: 1) ser retenidos en el núcleo para actuar sobre la cromatina o 2) ser exportados al citoplasma por un homólogo de la exportina-5, HASTY (HST) para iniciar el PTGS. Una de las dos hebras se incorpora a RISC que escaneará la célula buscando ácidos nucleicos de secuencia complementaria sobre los que ejecutará su función que podría ser: 1) corte endonucleolítico en el centro del híbrido sRNA-diana, 2) represión de la traducción mediante mecanismos todavía desconocidos y 3) metilación del residuo citosina del DNA o de las histonas con la

ayuda de la subunidad b de la Pol IV (NRPD1b) (Baulcombe, 2004; Herr y Baulcombe, 2004; Chapman y Carrington, 2007; Brodersen *et al*., 2008; Xie y Qi, 2008; Jamalkandi y Masoudi-Nejad, 2009; Ruiz-Ferrer y Voinnet, 2009).

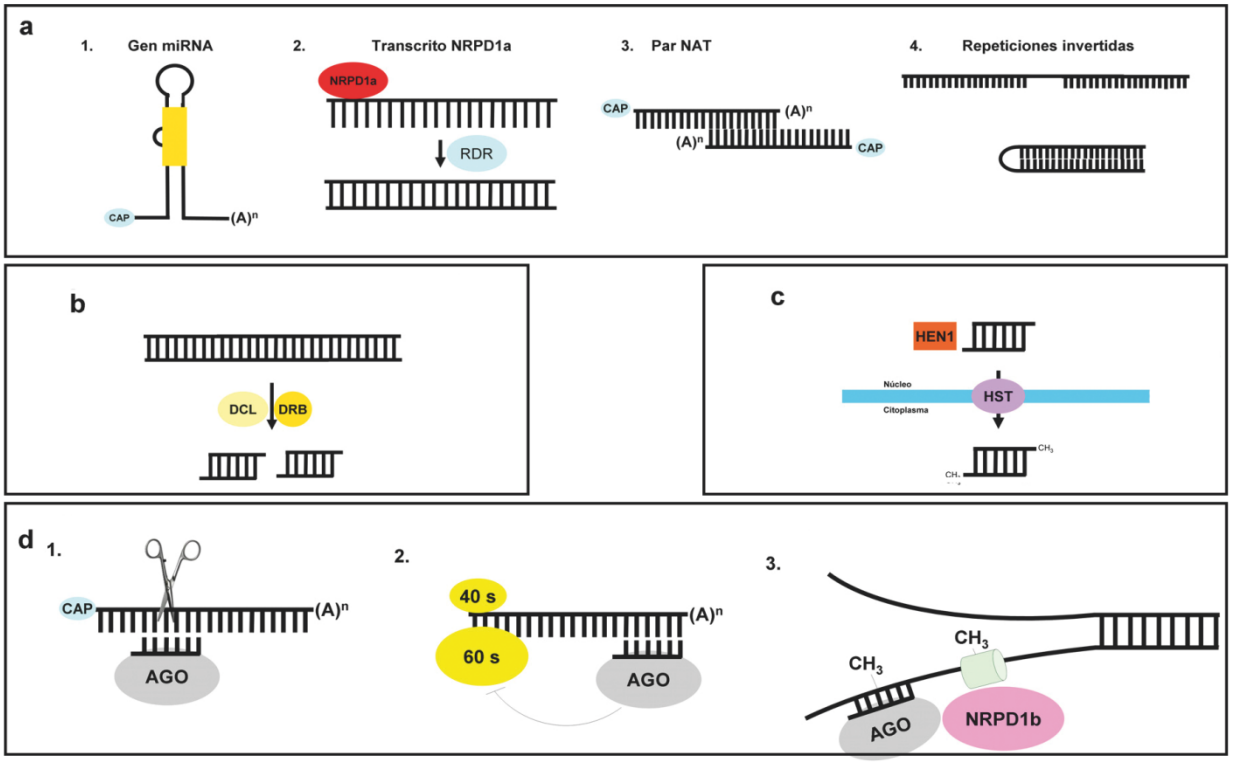

Figura 7. Esquema de los cuatro pasos conservados en la producción de pequeños RNAs. En el apartado a) se representa los distintos orígenes de un RNA de doble cadena: 1) gen de micro RNA, 2) transcrito de la NRPD1a o la RNA polimerasa II amplificado por alguna de las 6 RNA polimerasas RNA dependientes,3) par de genes NAT que tienen una región de homología entre las que forman un RNA de doble cadena y 4) transcritos con repeticiones invertidas que forman un hairpin. En al apartado b) se representa la producción de sRNAs por el procesamiento de dicho dsRNA mediante la enzima Dicer-Like junto a una proteína de unión a RNA de doble cadena (DRB). El apartado c) representa la metilación de dichos sRNAs producidos en el paso anterior por HEN1 y su exportación al citoplasma desde el núcleo por HST. En el último bloque d) se representa los distintos destinos de los sRNAs una vez cargados en el complejo efector del silenciamiento (RISC) cuya proteína principal es Argonauta (AGO). Estos destinos pueden ser: 1) corte de mensajeros homólogos en secuencia al sRNA, 2) inhibición de la traducción por mecanismos aún desconocidos y 3) metilación del residuo citosina o de las histonas del DNA (adaptado de Ruiz-Ferrer y Voinnet, 2009).

2.2.1. Silenciamiento génico post-transcripcional (PTGS)

Los pequeños RNAs han sido identificados como los factores claves de la regulación post-transcripcional en plantas.

Avances en las técnicas de secuenciación masiva y clonado de estos pequeños riboreguladores han revelado que la población de sRNAs en la planta modelo *Arabidopsis thaliana* se encuentra ampliamente dominado por microRNAs (miRNAs) y por pequeños RNAs interferentes (siRNAs) identificados como ta-

siRNAs y nat-siRNA entre otros (Rajagopalan *et al*., 2006; Fahlgren *et al*., 2007; Parent *et al*., 2012). Ambos tipos de sRNAs se forman a partir de una región de RNA con una alta estructura secundaria o a partir de una doble hebra de RNA (dsRNA), respectivamente.

Los miRNAs son los sRNAs más estudiados y desempeñan papeles esenciales en muchos aspectos de la planta, como por ejemplo, el control de la formación de la hoja y la flor (Aukerman y Sakai, 2003; Baker *et al*., 2005; Guo *et al*., 2005), o el desarrollo de raíces laterales (Rhoades *et al*., 2002; Chen, 2005; Zhang *et al*., 2006). Durante los últimos años se han realizado estudios sobre los sRNAs en plantas, especialmente en *Arabidopsis*. Estos estudios identificaron algunos genes relacionados con la biogénesis y las funciones de los pequeños RNAs (Voinnet *et al*., 2009; Castel *et al*., 2013; Liu *et al*., 2011). Gracias a ellos, además de detectar los miRNAs ya conocidos por su alta expresión, también se encontraron miRNAs producidos a partir del mismo loci genómico pero con longitudes variables (isomiRNAs) (Luo *et al*., 2014; Meyers *et al*., 2008; Lelandais-Brière *et al*., 2009; Guo *et al*., 2010).

Las clases funcionales de siRNAs incluyen, entre otras, los ra-siRNAs, generados a partir de transposones, regiones genónimcas heterocromáticas y repetitivas (Vazquez *et al*., 2006); los trans-acting siRNAs (ta-siRNAs) (producidos a partir de genes TAS) que se transcriben en largos RNAs primarios, no codifican proteínas y cuya única función es ser los precursores de la producción de ta-siRNAs (Peragine *et al*., 2004; Vazquez *et al*., 2004; Allen *et al*., 2005); o los transcritos naturales antisentido (nat-siRNAs) que se producen gracias a la proximidad de genes endógenos de la planta, codificantes o no, que comparten una complementariedad de secuencias con otros RNAs (Borsani *et al*., 2005). Dependiendo de si la hebra complementaria se encuentra en el mismo locus (cis) o en otro locus del genoma (trans) se les denomina cis-NAts y trans-NAts respectivamente. Los cis-NATs suelen tener una gran complementariedad entre las hebras sentido y antisentido, mientras que los trans-NATs suelen tener una complementariedad no perfecta (Jin *et al*., 2008).

Además de los grupos mencionados, existen un gran número de sRNAs no clasificados con funciones desconocidas, sin embargo, con la aplicación de las nuevas tecnologías de secuenciación masiva se han podido identificar poblaciones y expresión de sRNAs en diferentes especies de plantas, revelando algunas regiones genómicas enriquecidas en sRNAs (Yong-xing *et al*., 2014).

2.2.1.1. Biogénesis de los miRNAs y siRNAs.

Tanto los miRNAs como los siRNAs provienen de cadenas de RNAs de doble hebra. La diferencia entre ambos sRNAs reside en que los miRNAs se forman a partir de una sola molécula de RNA en forma de horquilla, mientras que los siRNAs generan el dúplex de RNA a partir de dos moléculas de RNA (Voinnet *et al*., 2009).

Hay varios procesos generales comunes que ocurren en la biogénesis de miRNAs. Inicialmente los miRNAs primarios son transcritos por la RNA polimerasa II (Lee *et al*., 2004; Li *et al*., 2013). En plantas los miRNAs primarios se forman a partir de regiones intergénicas, mientras que los miRNAs animales lo hacen a partir de intrones o regiones codificantes de genes (Ruby *et al*., 2007). Estos precursores son procesados por la acción de DL1 en sRNAs de 21 nucleótidos (Kurihara *et al*., 2004), además de otras proteínas tales como DDL (Yu *et al*., 2008), SE (Lobbes *et al*., 2007) y HYL1 (Kurihara *et al*., 2006).
La doble hebra resultante es exportada al citoplasma por la proteína HASTY (Bollman *et al*., 2003) y metilada por HEN1 (Yu *et al*., 2010). Finalmente el miRNA es incorporado al complejo AGO-RISC (Jones-Rhoades *et al*., 2006) donde realiza su función de silenciamiento génico post-transcripcional (Brodersen *et al*., 2008; Li *et al*., 2013).

Por otro lado, los siRNAs se generan a partir de una doble hebra de RNA formada por dos moléculas de RNA de secuencia complementaria (Brosani*et al*., 2005) o por la acción de las RdRPs (Tabach *et al*., 2013). Las moléculas de doble hebra son procesadas por las DCLs en siRNAs y cargadas en el complejo AGO-RISC (Chen *et al*., 2009). La mayoría de ellos presentan una longitud de 24nt, indicando que han sido procesados por la DCL3 y cargados en AGO4 (Catel *et al*., 2013).

2.2.2. Silenciamiento génico transcripcional (TGS)

En el TGS se llevan a cabo las modificaciones covalentes del DNA y las histonas asociadas. Como regla general, el Silenciamiento Génico Transcripcional (TGS) engloba los mecanismos epigenéticos fundamentales que regulan la expresión de los genomas eucariotas. Desempeña un papel importante en la prevención de la reorganización de secuencias repetidas tales como transposones, retroelementos, rDNA, repeticiones centroméricas o regiones metiladas del DNA (Hamilton *et al.*, 2002; Lippman y Martienssen, 2004; Kasschau *et al.*, 2007).

Este proceso está regulado por los siRNAs heterocromáticos (hc-siRNAs), moléculas de 23-25 nts relacionadas con secuencias genómicas repetitivas (Hamilton *et al*., 2002; Lippman y Martienssen, 2004; Kasschau *et al*., 2007). Su biosíntesis se inicia con la transcripción del RNA a partir de loci no metilados mediante la RNA polimerasa IV (POL IV). Estos transcritos no codificantes son reclutados y convertidos en dsRNA por la RDR2. El dsRNA es procesado por DCL3 e incorporado al complejo AGO 4 o AGO 6, para actuar metilando el residuo citosina del DNA o las histonas, uniéndose a transcritos nacientes no codificantes sintetizados por la Pol V y reclutando a diversos factores como DRM2 (una metiltransferasa *de novo*), DRD1 (un miembro de la SWI2-SNF2 familia de proteínas remodeladora de la cromatina) y DMS3 (una proteína de función desconocida involucrada en el mantenimiento estructural de los cromosomas) (Hamilton *et al.*, 2002; Xie *et al.*, 2004; Herr *et al.*, 2005; Lu *et al.*, 2005; Onodera *et al.*, 2005; Xie y Qi, 2008).

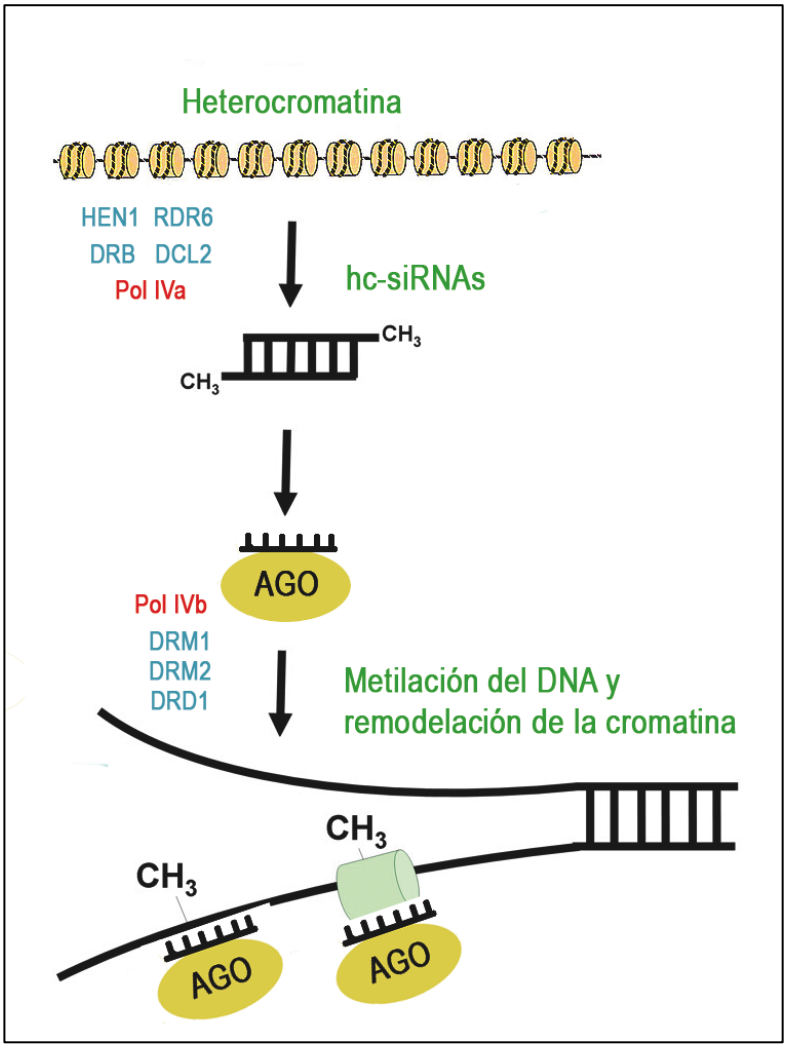

Figura 8. Representación de la ruta de hc-siRNAs. Son producidos a partir de secuencias genómicas repetidas. Se producen por la acción conjunta de Pol IV a, RDR6, DCL2, DRB y HEN1.Estos siRNAs formados son cargados en AGO 4 o 6y actúan metilando la citosina o las histonas , uniéndose a transcritos nacientes no codificantes sintetizados por la Pol IV y reclutando diversos miembros como DRM2, DRD1 y DMS3.

Los aspectos generales de este mecanismo de regulación se desarrollarán de manera más extensa en el apartado 4.

3. Relación entre silenciamiento de RNA y patogénesis

Como ya se ha comentado, el silenciamiento de RNA interviene tanto en funciones de defensa frente a ácidos nucleicos externos como en la regulación del desarrollo de la planta. La interacción planta-patógeno puede activar este mecanismo a dos niveles diferentes. Uno relacionado con la producción de sRNAs derivados del patógeno (controlando su tasa de replicación); y un segundo nivel que interfiere en la población de sRNAs endógenos de la planta que puede modificar la expresión de genes del huésped relacionados con mecanismos de defensa (Ruiz-Ferrer y Voinnet, 2009). Por tanto, cabe esperar un vínculo estrecho entre el silenciamiento de RNA y el proceso de patogénesis (Llave, 2010; Gómez *et al* 2009).

3.1 Relación entre patogénesis inducida por viroides y el silenciamiento de RNA

En un principio se asumió que los síntomas inducidos en la planta durante una infección viroidal podrían ser consecuencia de la competencia huésped-patógeno por los factores celulares necesarios para la transcripción, movimiento célula a célula y movimiento sistémico del patógeno (Tabler y Tsagris, 2004; Flores *et al*., 2005; Owens y Hammond, 2009). Sin embargo, la falta de evidencias experimentales que apoyaran esta idea dio lugar a que comenzara a considerarse la posibilidad de que durante la infección, los viroides alterasen la expresión de genes endógenos de la planta. Se propuso que cambios a nivel transcripcional o post-transcripcional (sin descartar posibles modificaciones traduccionales de los productos génicos), podían ser eventos asociados a la infección por viroides y responsables de la expresión de síntomas (Conejero, 2003; Ding, 2009; Owens y Hammond, 2009). En este escenario, la posible interferencia de RNAs viroidales (tanto genómicos como derivados con homología parcial) en los procesos de regulación de la transcripción mediados por silenciamiento de RNA, emergía como una de las posibilidades más viables para explicar, al menos en parte, las alteraciones inducidas por los viroides en el huésped (Ding, 2009).

En este sentido diversos estudios de hibridación mostraron las primeras evidencias que sugerían que los viroides inducían en la planta una respuesta relacionada con el silenciamiento de RNA. Estos trabajos demostraron que las infecciones producidas por los viroides de ambas familias (*Pospiviroidae* y *Avsunviroidae*) estaban asociadas a la presencia de sRNAs de origen viroidal (vdsRNAs). Los pequeños RNAs comprendían un tamaño entre 20 y 25 nucleótidos y derivaban del genoma del patógeno; estas moléculas fueron detectadas en distintas especies vegetales infectadas por PSTVd (Itaya *et al.*, 2001;

Papaefthimiou *et al.*, 2001), PLMVd (Martinez de Alba *et al.*, 2002), CChMVd (Martinez de Alba *et al.*, 2002), ASBVd (Markarian *et al.*, 2004), CEVd (Markarian *et al.*, 2004) y HSVd (Gómez and Pallás, 2007).

También se vio que en la interacción HSVd-*Nicotiana benthamiana*, la expresión de síntomas fue un proceso estrictamente ligado a la actividad de RDR6 (un componente clave de la maquinaria del silenciamiento) y totalmente independiente a los niveles de acumulación del patógeno en la planta (Gómez *et al*., 2008), aportando la primera evidencia experimental directa sobre la existencia de una estrecha relación entre este aspecto de la patogénesis viroidal y el silenciamiento de RNA específico de viroides, que había sido previamente postulada por diversos autores (Papaefthimiou *et al*., 2001; Markarian *et al*., 2004; Wang *et al*., 2004).

Mediante técnicas convencionales de secuenciación a baja escala se llevaron a cabo las primeras aproximaciones que permitieron comenzar a definir el mapa poblacional de los vdsRNAs. La caracterización de los sRNAs derivados de PSTVd confirmaron que los vd-sRNAs tenían un tamaño comprendido entre 20 y 24 nts, indicando que todas las DCLs estarían implicadas en su producción (Itaya *et al*., 2007; Machida *et al*., 2007). Un rango de tamaño similar (20–24 nts) se describió para los sRNAs derivados del CEVd, con una acumulación mayoritaria de vd-sRNAs de 21 y 22 nts, lo que sugería una acción preponderante de DCL1/DCL4 y de DCL2 (Martin *et al*., 2007). Además (al menos en el caso de los sRNAs derivados del CEVd), tenían un grupo fosfato en su extremo 5' y presentaban un grupo metilo en su extremo 3' (Martin *et al*., 2007). En el caso de infecciones con PLMVd la mayoría de vd-sRNAs recuperados fueron de 21 nts, lo que podía interpretarse como que habían sido producidos principalmente por DCL1 o DCL4 (St-Pierre *et al*., 2009).

La obtención de datos por secuenciación masiva de sRNAs derivados, tanto de viroides nucleares como cloroplásticos, permitió generar un retrato más exacto acerca de los componentes de la maquinaria de silenciamiento y formas precursoras del viroide que podrían estar implicadas en la producción de vd-sRNAs. La observación de que los vd-sRNAs de polaridad positiva y negativa se originaban de manera comparable a lo largo del genoma de HSVd, permitió postular que estos vd-sRNAs estaban originados por la acción de la DCL sobre un RNA viroidal de doble cadena generado a partir de un precursor lineal (Martínez *et al*, 2010). Esta observación se repitió con otros viroides tales como PLMVd (Di Serio *et al*., 2009; Bolduc *et al*., 2010), GYSVd1 (Navarro *et al*., 2009) y PSTVd (Di Serio *et al*., 2010). Estos estudios coincidieron en determinar que los vd-sRNAs estaban distribuidos a lo largo del RNA genómico y que presentaban una acumulación similar de secuencias positivas y negativas.

La distribución de tamaños de los vd-sRNAs en todas las secuenciaciones parecía mostrar una preferencia de acumulación de los vd-sRNAs de 21-22 nts, seguidos de los de 24 (HSVd, GYSVd y PSTVd) o 20 nts (PLMVd), siendo los menos acumulados 23 y 24 nts (PLMVd) o 23 y 20 nts (HSVd, GYSVd y PSTVd). Lo que sugería que varias DCLs podrían estar implicadas en la síntesis de los sRNAs viroidales.

Una vez demostrado que durante la infección el RNA del viroide interactuaba con el mecanismo de silenciamiento de RNA, se propuso que los vd-sRNAs podrían actuar como miRNAs o algún otro tipo de sRNA endógeno y dirigir la degradación o inhibir la traducción de mRNAs del huésped, causando la aparición de síntomas (Papaefthimiou *et al*., 2001; Conejero, 2003; Markarian *et al*., 2004; Wang *et al*., 2004).

La observación de plantas de tomate que expresaban constitutivamente repeticiones invertidas incompletas de PSTVd y reproducían los síntomas asociados a la infección por este viroide, constituyó la primera evidencia experimental que apoyaba este modelo de patogénesis (Wang *et al.*, 2004). Posteriormente se demostró que plantas de *Nicotiana benthamiana* con actividad RDR6 disminuida, no eran capaces de desarrollar síntomas de infección viroidal a pesar de acumular formas maduras de HSVd (Gómez *et al.*, 2008). Además, la demostración de que sRNAs derivados del viroide mediaban la degradación de mRNAs endógenos y promovían el desarrollo de síntomas en la planta infectada, tanto en viroides nucleares como cloroplásticos, constituyó la demostración definitiva de que los vd-sRNAs podían actuar como moduladores de la patogénesis durante el proceso de infección (Papaefthimiou *et al*., 2001; Conejero, 2003; Markarian *et al*., 2004; Wang *et al*., 2004).

Sin embargo, aunque las evidencias que sostienen la relación entre el silenciamiento post-transcripcional y la patogénesis son robustas, no se puede descartar que otras alteraciones en los procesos de regulación transcripcional del huésped (también mediados por RNAs no codificantes) puedan verse también afectadas durante las infecciones con viroides (Flores *et al*., 2015; Gómez y Pallás 2013).

4. Epigenética y metilación

El término epigenética fue acuñado en 1942 por el embriólogo, paleontólogo y genetista escocés Conrad Waddington para designar el estudio de las interacciones entre el genotipo y el fenotipo, es decir, entre la información codificada en los genes y aquella que efectivamente se expresa. La epigenética abarca los cambios heredables en la estructura y organización del DNA que no impliquen cambios en su secuencia y que modulen la expresión génica (Morgan *et al*., 2008; Wang *et al*., 2008; Bártová *et al*.,

2008). Inicialmente se sugirió que la metilación del DNA en plantas era un proceso mediado por DNA. Sin embargo, la demostración de que la replicación del PSTVd (que se realiza sin intermediarios de DNA) inducía la metilación específica de secuencias de PSTVd en plantas de tabaco transgénicas (Wassengger *et al*., 1994), puso de manifiesto que este era un proceso susceptible de ser regulado por RNAs no codificantes (nc-RNAs).

Con el tiempo se ha demostrado que el control epigenético de la expresión génica está mediado por cambios específicos en la estructura de la cromatina. La unión a proteínas específicas cromosómicas, modificaciones post-traduccionales de las histonas, la regulación mediada por RNA y la metilación del DNA son algunos de los mecanismos implicados en el control de los estados de la cromatina (estructura y actividad génica). Por ello, la cromatina es entendida hoy en día como una estructura dinámica e interactiva, que sufre continuos procesos de modificación y remodelación como respuesta a procesos de señalización celular (Huan *et al*., 2012).

El DNA contiene la información genética que necesita ser transcrita de forma selectiva durante las distintas etapas de desarrollo y en respuesta a los estímulos bióticos y abióticos. El silenciamiento epigenético, mediante metilación del DNA y modificación de histonas, ejerce un papel fundamental en la supresión de la transcripción de algunos genes desfavorables y la prevención de la activación de los transposones, manteniendo la integridad del genoma (Chodavarapu *et al*., 2010; Bernatavichute *et al*., 2008).

En las plantas, las modificaciones epigenéticas son de suma importancia, ya que al ser organismos sésiles, están incapacitados para moverse en busca de nutrientes o mejores condiciones ambientales. Además, pueden ser transmisibles a la línea germinal y ser heredadas transgeneracionalmente (Takeda y Paszkowski, 2006). Aunque aún no se ha logrado descifrar completamente cómo opera este lenguaje, sí se conoce que a diferencia de los procesos genéticos, los epigenéticos pueden ser inducidos por el ambiente (Richards, 2006; Jirtle y Skinner, 2007; Feil y Fraga, 2012; Grativol *et al*., 2012; Baulcombe y Dean, 2016).

En la última década, se ha empezado a comprender el mecanismo que regula la metilación del DNA en plantas. Muchos de los avances en este campo han surgido gracias al estudio con mutantes de *Arabidopsis*, con los que se han podido identificar muchos de los factores implicados en este proceso, demostrando que algunos mecanismos están conservados y son compartidos con los de los mamíferos (Hidetoshi *et al*., 2012).

4.1 Metilación del DNA mediada por RNA

La metilación del DNA mediada por RNA (RdDM) constituye la mayor ruta de metilación de DNA. Se define como una modificación a escala genómica basada en la metilación del DNA en contextos de secuencia CG y CHG (metilación simétrica) o CHH (metilación asimétrica), en ambos casos H se define como cualquier nucleótido excepto G. Este proceso está mediado por pequeños RNAs de interferencia (siRNAs) de 24 nucleótidos capaces de reconocer regiones de secuencia complementaria al propio siRNA (Law y Jacobsen 2010; Haag y Pikaard 2011; He *et al*., 2011; Kanno y Habu 2011). En *Arabidopsis*, la RdDM está involucrada en varios procesos biológicos, como repuesta a estreses bióticos y abióticos, desarrollo, floración, etc. (Law y Jacobsen 2010; Haag y Pikaard 2011; He *et al*., 2011; Kanno y Habu 2011). Además, se encarga de mantener silenciados los transposones y las secuencias repetitivas (Law y Jacobsen 2010; Haang y Pikaard 2011; He *et al*., 2011; Kanno y Habu 2011).

El mecanismo molecular de la RdDM presenta dos etapas: en primer lugar la biogénesis de los siRNAs de 24 nucleótidos y, en segundo lugar, la metilación *de novo* en los sitios complementarios a estos siRNAs. Cada etapa requiere una RNA polimerasa DNA dependiente (Pol) diferente (Herr *et al*., 2005; Kanno *et al*., 2005; Onodera *et al*., 2005; Pontier *et al*., 2005). Inicialmente los transcritos son copiados por la Pol IV que luego son copiados a dsRNAs por RDR2 y procesados por la Dicer-like 3 (DCL3) dando lugar a siRNAs que, posteriormente, serán exportados al citoplasma (Wierzbicki *et al*., 2008). Una de las hebras del siRNA es cargada en el complejo AGO4 que es importado al núcleo, dónde los siRNAs lo guían, por complementariedad de secuencia, hacia zonas del DNA que están siendo transcritas por Pol V, principalmente transposones y DNA repetitivo (Wierzbicki *et al*., 2009). Por último, la DNA metiltransferasa es reclutada al complejo para mediar la metilación *de novo* de citosinas (Atzke *et al*., 2009; Wierzbicki *et al*., 2009). Aunque se ha avanzado considerablemente en este campo, estamos lejos de comprender en su totalidad esta ruta de metilación del DNA. Aún falta por descubrir, por qué en plantas se requieren dos RNA polimerasas y otros factores transcripcionales para llevar a cabo la RdDM y cómo éstos encajarían en esta ruta. (He *et al*., 2009; Kanno *et al*., 2010; Wierzbicki *et al*., 2012; Pikaard *et al*., 2012).

4.1.1 Mecanismos de la ruta RdDM

Como ya se ha mencionado esta ruta de metilación requiere una serie de componentes para llevar a cabo la biogénesis de los siRNAs y la metilación del DNA. A continuación se detallan los factores necesarios de este mecanismo de metilación.

DNA metiltransferasas.

En *Arabidopsis*, se han identificado diferentes DNA metiltransfesasas, dos de ellas implicadas en el mantenimiento de la metilación y una en la metilación *de novo*. La DNA metiltransferasa 1 (MET1) cataliza la metilación en los sitios CG, mientras que la cromometilasa 3 (CMT3), una DNA metiltransferasa específica de plantas, lo hace en los sitios CHG. Tanto la secuencia CG como la CHG son simétricas, por tanto, estos patrones de metilación pueden ser transmitidos y conservados en la hebra hermana durante la replicación del DNA mediante la acción de MET1 y CMT3, respectivamente. La metilación asimétrica CHH es catalizada por CMT3 y por metiltransferasa 2 de dominios reorganizados (DRM2), (Cao *et al*., 2003; Chan *et al*., 2005).

Pol IV, biogénesis de los siRNAs.

Gracias al análisis de mutantes defectivos, se ha visto que Pol IV es la responsable de producir más del 90% de los precursores siRNA de 24 nucleótidos (hc-siRNAs), los cuales guían la metilación en la ruta RdDM (Mosher *et al*., 2008; Zhang *et al*., 2007).Aunque sus transcritos no se hayan observado aún *in vivo*, se asume que la Pol IV transcribe los loci diana en cadenas simples de RNA (ssRNAs) y son copiadas por la RDR2 (como consecuencia de su interacción física) (Haag *et al*., 2012; Law *et al*., 2011) para producir dsRNAs.

El remodelador de la cromatina CLASSY 1 (CLSY1) (Law*et al*., 2001; Smith *et al*., 2007) participa en algunos pasos de esta etapa, probablemente para facilitar el paso de la Pol IV a lo largo del locus. La DCL 3 procesa los dsRNAs en siRNAs de 24 nucleótidos (hc-siRNAs), que se estabilizarán por metilación de su extremo 3'-OH por la acción de HEN 1 (Ji *et al*., 2012) y se cargará en AGO4 para formar el complejo efector del silenciamiento (Figura 9A).

Pol V, metilación *de novo.*

Se han detectado *in vivo* transcritos de Pol V y se cree que son trifosforilados o carentes de cola poli A (Wierzbicki *et al*., 2008). Se propuso que la Pol V ayudaba a los siRNAs a reconocer sus loci dianas y mediar así las modificaciones de la cromatina (Wierzbicki *et al*., 2008). Esta idea se basaba en las observaciones dónde la transcripción de Pol V era necesaria para el establecimiento o la modificación del silenciamiento de la cromatina (Wierzbicki *et al*., 2008; Pontier y col, 2005; Kanno *et al*., 2005; Mosher *et al*., 2008). Los transcritos de Pol V interactúan físicamente con AGO4, por lo que se supone que actúa como base para guiar a los complejos siRNAs-AGO4 hacia sus blancos dentro de la cromatina, además de reclutar otros factores del silenciamiento (Wierzbicki *et al*., 2009). Además se ha demostrado que la Pol V se requiere también para la biogénesis de un subconjunto de siRNAs (Lee *et al*., 2012).

Utilizando técnicas de inmunoprecipitación de cromatina seguida de secuenciación (ChIP-seq), se ha podido identificar la asociación de la Pol V con transposones y zonas repetitivas del DNA, relacionadas con siRNAs de 24 nucleótidos; indicando su implicación en la ruta RdDM de esas zonas (Zhong *et al*., 2012; Wierzbicki *et al*., 2012). Sin embargo, alrededor del 25% del DNA donde se encontraba presente Pol V, no presentaban estas características, lo que pone de manifiesto que se requieren otros factores, además de la Pol V, para poner en marcha los mecanismos de RdDM (Wierzbicki *et al*., 2012).

En general, Pol V actúa en un amplio rango de zonas a lo largo del genoma, aunque se ha demostrado que une preferentemente a regiones de eucromatina ricas en pequeños transposones intergénicos, genes que contienen transposones u otras repeticiones en sus promotores e intrones de regiones codificantes (Zhong *et al*., 2012; Zheng *et al*., 2009).

La RdDM parece estar excluida de alguna forma de la heterocromatina pericentromérica (Zemach *et al*., 2013; Schoft *et al*., 2009). Pues, en lugar de sufrir las modificaciones que ocurren en ella (H3K9 y metilación del DNA), principalmente ocurre de forma independiente de los siRNAs y depende del remodelador de cromatina DDM1, de MET1 (metiltransferasa 1), y de la metiltransferasa específica de plantas cromometilasa 2 (CMT2) y 3 (CMT3) (Zemach *et al*., 2013; Stroud *et al*., 2014).

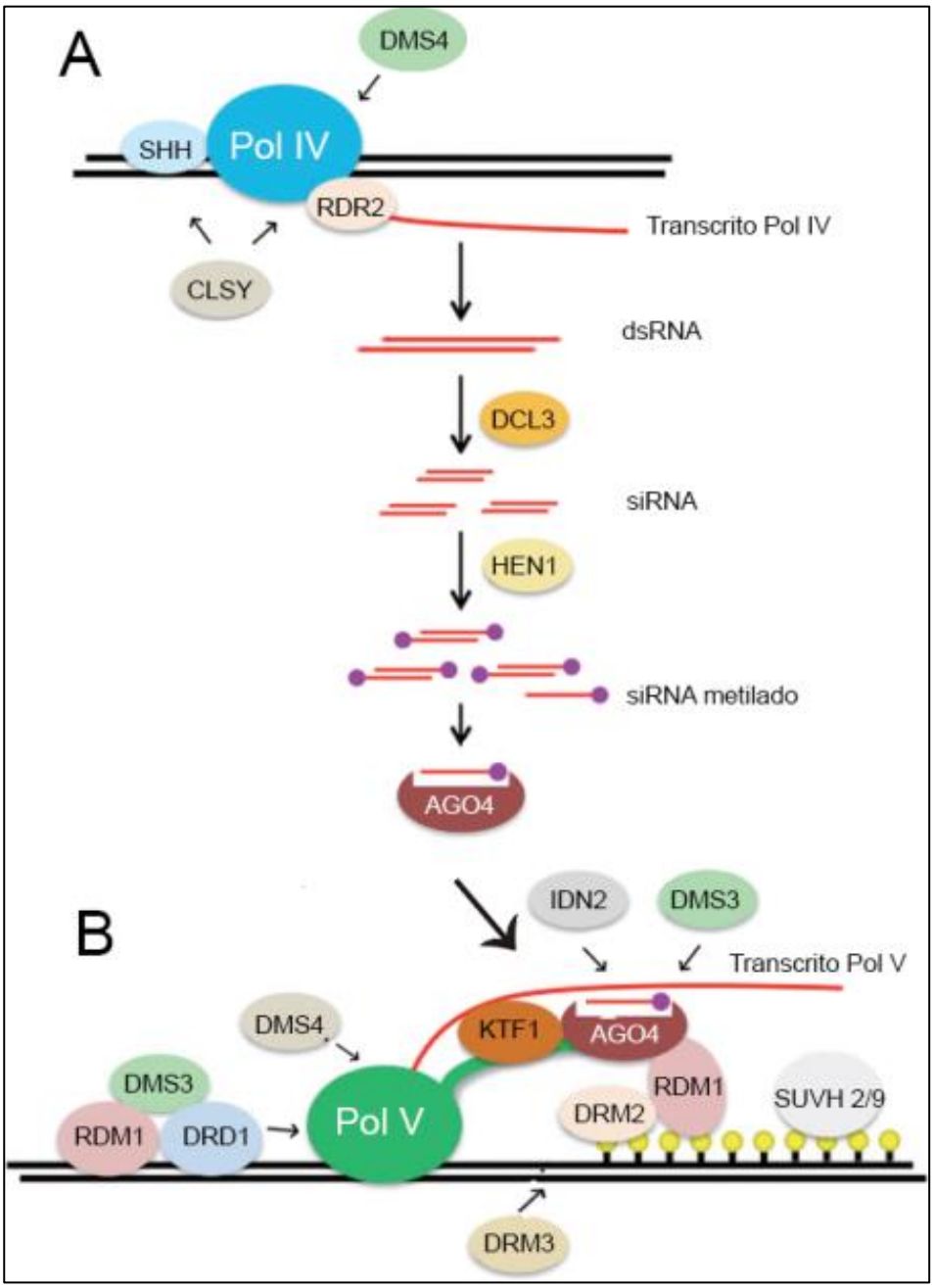

Figura 9. Modelo hipotético de la metilación de DNA mediada por RNA (RdDM). A) Síntesis de siRNAS. La interacción física entre Pol IV y RDR2 provoca la formación de dsRNAs. SHH puede interactuar directamente con la región de DNA diana para facilitar la transcripción de Pol IV. DMS4 puede ser necesario para dirigir el complejo formado a la región destino. CLSY, un remodelador de la cromatina, probablemente participa en las primeras etapas de RdDM. El dsRNA se corta en fragmentos de 24 nt por DCL3, HEN1 añadirá los grupos metilo en los extremos 3' del siRNA, cargándose una de las hebras al complejo AGO4-RISC para formar el complejo de silenciamiento efector.
B). Metilación *de novo* del DNA. Pol V puede transcribir RNA no codificante de la región diana de RdDM, y se cree que este RNA actúa como base para reclutar el complejo de silenciamiento efector a través de la complementariedad de las secuencias de los siRNAs. IDN2, RDM1 y DMS3 podrían ser necesarias para estabilizar el emparejamiento de las bases del siRNA. Además, la posible interacción entre PolV, AGO4 y KTF1 podría contribuir para reclutar a DRM2 en los locus diana. Dado que RDM1 puede interactuar tanto con AGO4 como con DRM2, además de tener capacidad para unirse al DNA metilado, esta proteína puede anclar a DRM2 en la región de DNA que va a ser metilado. DRM3 y SUVH2/SUVH9 pueden ser requeridos para facilitar la metilación *de novo*. DMS3 y RDM1, junto con DRD1facilitan la transcripción de PolV. DMS4 podría ayudar en el reclutamiento de PolV en la zona de DNA que se vaya a metilar. Las citosinas metiladas se indican en amarillo. (Adaptación de Saze *et al., 2012).*

La unión de Pol V a algunas secuencias diana es asistida por SUVH2, SUVH9 y SUVR2, miembros de la familia metiltransferasa SU (var) 3-9 histona (Johnson *et al*., 2012; Liu *et al*., 2014). La transcripción y la asociación de Pol V con la cromatina está facilitada por el complejo DDR (Zhong *et al*., 2012; Law *et al*., 2010). Este complejo está formado por DRD1 (Eun *et al*., 2012; Wierzbicki *et al*., 2008), un remodelador de la cromatina, DMS3, implicado en el mantenimiento de la estructura de los cromosomas (Eun *et al*., 2012; Wierzbicki *et al*., 2010) y RDM1 (Gao *et al*., 2009), una pequeña proteína específica de plantas que puede tener múltiples funciones en el la metilación del DNA mediado por RNA (RdDM).

Pol V recluta AGO4 por el dominio carboxil terminal NRPE1, el cual a su vez, se une a KTF1, un factor de transcripción de elongación (Bies-Etheve *et al*., 2009; He *et al*., 2012). Durante la transcripción mediada por Pol V, el complejo formado por AGO4, siRNA y DMR2, catalizan la metilación *de novo* de los sitios genéticamente homólogos. RDM1 es la responsable de una parte clave del reclutamiento de DMR2, además ha sido la única proteína identificada que interactúa tanto con AGO4 como con DRM2 (Gao *et al*., 2009). IDN2, una proteína relacionada con la unión del dsRNA y el silenciamiento post-transcripcional (Ausin *et al*., 2012; Zhang *et al*., 2012), forma un complejo con IDP1 y IDP2 (Ausin *et al*., 2012; Zhang *et al*., 2012; Xie *et al*., 2012). Este complejo estabiliza la unión entre los siRNAs y Pol V (Ausin *et al*., 2012; Xie *et al*., 2012; Finke *et al*., 2012), facilitando la RdDM mediante la alteración de la posición del nucleosoma a través de las interacciones entre la cromatina y SWI/SNF (Zhu *et al*., 2013) (Figura 9B).

4.1.1.1 Deacetilasas de histonas

Debido a la importancia que tiene dentro de este trabajo de tesis una de las deacetilasas de histonas (HDA6) que intervienen en los procesos de metilación, se va a desarrollar este apartado para clarificar el papel que desempeña. La función deacetilasas de histonas (HDACs) está relacionada con la represión de los genes y la metilación de las histonas, tales como H3K27m3 y la metilación del DNA (Zhou, 2009; Xujun *et al*., 2013; Xuncheng *et al*., 2014).

En *Arabidopsis*, hay 16 genes que codifican HDACs (Pandey *et al*., 2002). Entre todas ellas, hay cuatro HDACs (HDA6, HDA7, HDA9 y HDA19) del tipo RPD3, que actúan como reguladoras de la cromatina, manteniendo la expresión de los genes en levadura, nematodos y metazoos (Pandey *et al*., 2002; Yang y Seto, 2008). HDA19 actúa a nivel del desarrollo, embriogénesis y respuesta a la luz en plantas (Long *et al*., 2006; Tanaka *et al*., 200; Jang *et al*., 2011).

La HISTONA DEACETILASA 6 (HDA6) ha sido extensamente estudiada en la regulación de la actividad genética y el mantenimiento del genoma en plantas (May *et al*., 2005; Earley *et al*., 2006; Aufsatz

et al., 2007; Pontes *et al*., 2007; Tessadori *et al*., 2009; To *et al*., 2011a; To *et al*., 2011b; Zhu *et al*., 2011). Gracias al análisis de mutantes de aumento de expresión se pudo demostrar que la HDA6 está implicada en el mantenimiento de la memoria epigenética (Furner *et al*., 1998; Murfett *et al*., 200; Aufsatz *et al*., 2002), sugiriendo que podría intervenir en la ruta de metilación del DNA mediada por RNA (RdDM) (Aufsatz *et al*., 2002; Aufsatz *et al*., 2007). La HDA6 tiene una fuerte preferencia por silenciar secuencias repetitivas y genes multicopia. En mutantes hda6, la cromatina del RNA ribosómico (rRNA) cambia a un estado activo, observándose un enriquecimiento en la acetilación de las histonas H3K4m3 y la hipometilación del DNA, hechos que indican que la HDA6 está relacionada con el silenciamiento genético, con la deacetiación de las histonas y la metilación del DNA. Gracias a los análisis de transcriptómica e inmunoprecipitación, utilizando un anticuerpo específico del extremo C-terminal de la HDA6, han sido identificadas sus dianas y se ha podido proponer un modelo de acción (To *et al*., 2011a). La HDA6 se encontró asociada a diversas zonas del DNA, entre ellas transposones y varios genes de función desconocida.

Estudios recientes han revelado que la metilación en los contextos CHG y CHH disminuía en las plantas mutantes hda6 en todos los loci estudiados (To *et al*., 2011a). La metilación CG se mantuvo en algunos loci diana que estaban rodeados por regiones de DNA metilado, mientras que la metilación CG disminuyó completamente en los mutantes hda6 que tenían sus dianas en zonas aisladas de DNA metilado (To *et al*., 2011a). Este análisis sugirió que los efectos de la metilación del DNA en el contexto CG de las regiones donde actúa la HDA6, podría estar relacionada con la existencia de otras regiones metiladas alrededor de estas zonas diana.

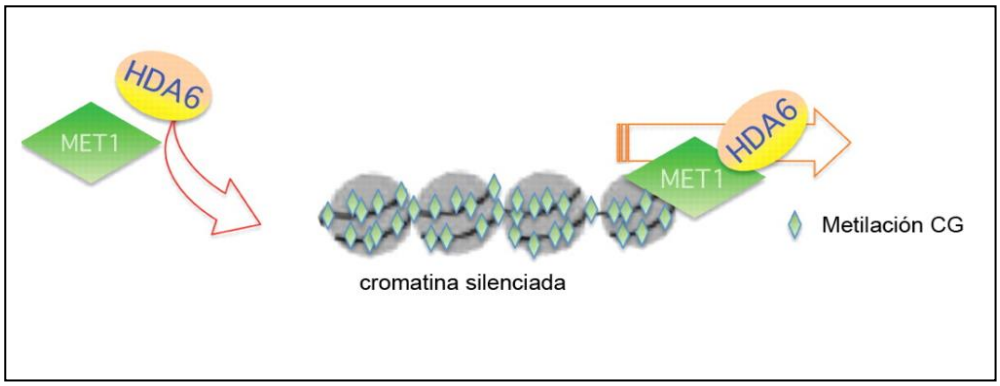

Figura 10. Mecanismo de silenciamiento mediado por HDA6. Para establecer el silenciamiento génico de los sitios CG, MET1 y HDA6 actúan conjuntamente. (Adaptado de Jong-Myong *et al*., 2012).

Además, se ha demostrado que la HDA6 es esencial para la metilación simétrica del DNA (en contexto CG) en la que interviene MET1 en las regiones no flanqueadas por DNA metilado (Figura 10). Gracias a los resultados obtenidos mediante análisis trancriptómicos, se identificó la superposición de forma

significativa entre los mutantes de hda6 y met1 (To *et al*., 2011a). Recientemente se ha descubierto que HDA6 interactúa físicamente con MET1 (Liu *et al*. 2012), sugiriendo que actúan como un complejo en el silenciamiento genético heterocromático para las dianas de HDA6. Recientes evidencias, además, han revelado que la HDA6 actúa específicamente como regulador del mantenimiento de metilación del DNA (debido a la interacción con MET1) de Elementos Transponibles (TEs), DNA ribosomal (rDNA) y transgenes (Aufsatz *et al*., 2002; Probst, *et al*., 2004; May *et al*., 2005; To *et al*., 2011; Liu *et al*., 2012, Hristova 2015).

4.2 Modificaciones de las histonas

Aproximadamente el 70% de las dianas de RdDM tienen como objetivo la modificación del residuo de la lisina 9 de la histona 3 (H3K9), una marca de represión de la cromatina (Bernatavichute *et al*., 2008) que actúa retroalimentándose, reforzando el TGS. Para mantener la metilación del DNA y promover la metilación de H3K9 se requieren enzimas modificadoras de histonas que eliminen marcas activas, tales como la acetilación, H3K4me, y la ubiquitilación H2B (Johnson *et al*., 2012; Enke *et al*., 2011). Como ya se ha comentado en el punto anterior, la HISTONA DEACETILASA 6 (HDA6) actúa junto a MET1 para mantener la metilación CG y promover la metilación de H3K9 mediante la deacetilación de las histonas. Por tanto la HDA6 desempeñaría dos funciones, por un lado la deacetilación de las histonas y por otro el mantenimiento de la metilación CG actuando junto a MET1 (Liu *et al*., 2012; To *et al*., 2011). La metilación H3K9 está mediada por un conjunto de proteínas esenciales para el silenciamiento de los transposones y el propio desarrollo de la planta (Jackson *et al*., 2002; Malagnac *et al*., 2002; Ding *et al*., 2007).

En los genomas vegetales, la metilación H3K9 está enriquecida en secuencias repetitivas y está asociada tanto con la metilación del DNA como con la de los pequeños RNAs (Bernatavichute *et al*., 2008; Lister *et al*., 2008; Zhou *et al*., 2010). En *Arabidopsis* se han identificado 15 proteínas homólogas de la H3K9 metiltransferasa SU (VAR) 39 (Baumbush *et al*., 2001). De entre todas estas, se vio que KYP/SUVH4 metilaba junto con los homólogos SUVH5 y SUVH6 el residuo 9 de lisina de la histona 3 (H3K9) de secuencias repetitivas de una forma redundante (Jackson *et al*., 2002; Malagnac *et al*., 2002; Ebbs and Bender ,2006; Bernatavichute *et al*., 2008). Por otro lado, un estudio reciente mostró que un conjunto de proteínas con dominio SUVH4 trimetilaban, sobre todo en presencia de ubiquitina, el residuo de lisina 9 de la histona 3 que estuviera monometilada, y, esta actividad afectaba al silenciamiento transcripcional de los transposones (Veiseth *et al*., 2011).

En plantas, la metilación H3K9 es reconocida por CTM3, una DNA metiltrasnferasa específica (Lindroth *et al*., 2004). CTM3 media la metilación del DNA CHG (Bartee *et al*., 2001; Lindroth *et al*., 2001). En *Arabidopsis*, la familia SUVH contiene un dominio SRA en el extremo N terminal, que preferentemente enlaza con la citosina metilada (Arita *et al*., 2008; Rajakumara *et al*., 2011). Así, la histona H3K9 es reclutada por el dominio SRA que, probablemente, añadirá la marca de metilación a ese loci. Los sitios de metilación H3K9 se pueden unir a la cromatina codificada por CMT3, formando un bucle de auto-refuerzo de las marcas epigenéticas represivas de los loci heterocromáticos (Johnson *et al*., 2007).

Como se ha comentado anteriormente, aún no están totalmente descifrados los mecanismos que regulan el proceso general de metilación. Sin embargo se ha propuesto que la RdDM y la metilación de las histonas podrían estar interconectadas en plantas, ya que, por ejemplo, con la inactivación de ambas vías de metilación en *Arabidopsis*, se observaron defectos pleiotrópicos en el desarrollo que no se observaron en los mutantes individuales de cualquiera de las dos rutas (Chan *et al*. 2006).

Además de la metilación H3K9 y las histonas metiltransferasas, otras modificaciones de histonas y cromatina pueden influir en el mantenimiento de la metilación del DNA. En particular, las rutas implicadas en la eliminación de marcas epigenéticas activas en la heterocromatina tales como la monoubiquitinación de la histona H2B asociada con la activación transcripcional (Schmitz*et al*. 2009). Por tanto, las modificaciones de las histonas están equilibradas y coordinadas por reguladores tanto positivos como negativos, pudiendo definir los dominios funcionales de la cromatina a lo largo del cromosoma (Roudier *et al*. 2011).

4.3 Modificaciones de la cromatina

El genoma de los organismos eucarióticos está muy compactado debido a la cromatina. Su estructura regula la actividad y accesibilidad de los factores y cofactores de todos los procesos de transcripción del DNA. La estructura fundamental de la cromatina es el nucleosoma, el cual está formado por 146 pb y un octámero de histonas (contienen dos copias de cada una de las cuatro histonas H2A, H2B, H3 Y H4). Y es considerado como una barrera de aproximación al DNA para los factores de regulación (Berger 2007). La estructura y función de la cromatina está regulada por múltiples mecanismos epigenéticos, incluidas las modificaciones de las histonas, la metilación del DNA, su remodelación , la posición de las histonas y la regulación por RNA no codificante (Lister *et al*., 2008; Zilberman *et al*., 2007).

Además de la metilación del DNA, las modificaciones en el extremo N-terminal de las histonas, tales como la acetilación, metilación, fosforilación o ubiquitinación constituyen parte de un complejo escenario de las modificaciones epigenéticas. Los aminoácidos protuberantes de los extremos N-terminal de las histonas H3 y H4 son más fáciles de modificar (Figura 11).

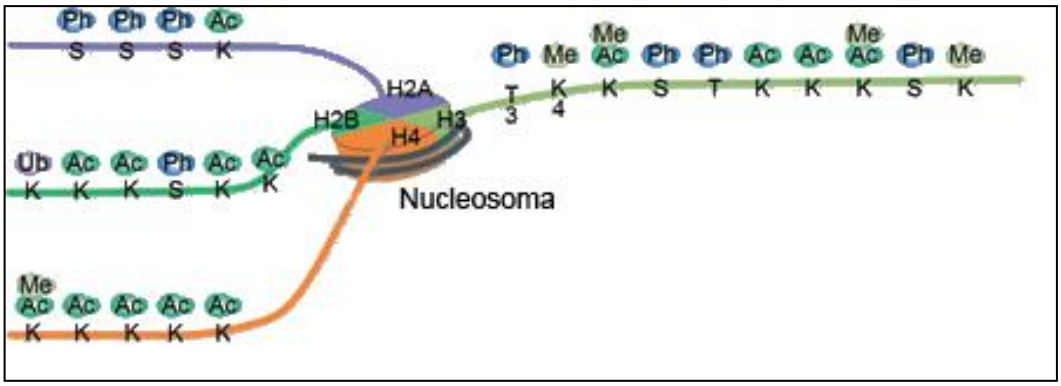

Figura 11. Breve ilustración de las modificaciones de las histonas en el genoma de la planta. El nucleosoma está compuesto por dos copias de cada H2A, H2B, H3 y H4 (cada par se muestra en un color diferente). Los aminoácidos protuberantes de las colas de las histonas pueden ser modificados por diversas marcas, acetilación, fosforilación, ubiquitinación y metilación. (Adaptado de Chen *et al*., 2010).

La expresión genética se activa mediante la acetilación, la fosforilación y la ubiquitinación, mientras que la metilación H3K9 (residuo de lisina 9 de la histona 3) y la H3K27 la reprimen. La mayoría de modificaciones covalentes en las histonas se dan en la lisina de la histona H3. Estos residuos de lisina pueden estar mono, di o trimetilados, confiriendo cada una un significado distinto desde el punto de vista biológico (Cloos *et al*. 2008).

A diferencia del tejido vegetativo, el patrón de metilación de DNA del tejido reproductivo, parece mantenerse constante generación tras generación. Sin embargo, se ha demostrado que la reactivación de transposones y la pérdida de metilación a lo largo de todo el genoma ocurre durante la gametogénesis masculina y femenina respectivamente, indicando que los patrones de metilación en plantas son dinámicos durante el desarrollo (Reik *et al*., 2007; Sasaki *et al*., 2008). Estos estudios sugieren que estos cambios podrían reforzar el silenciamiento de los transposones de las células espermáticas en *Arabidopsis thaliana* (Slotkin *et al*., 2009; Hsieh *et al*., 2009; Gehring *et al*., 2009).

Durante la gametogénesis masculina, el grano de polen tricelular contiene el núcleo vegetativo y son producidas dos células espermáticas (Huh *et al*., 2008). Varios análisis de expresión de transposones en diferentes tejidos de la planta revelaron que los transposones que estaban metilados y silenciados en la

mayoría de los tejidos, eran expresados y móviles en el grano de polen (Slotkin *et al*., 2009). Además, la reactivación de los transposones parece estar restringida al núcleo vegetativo, proporcionando la información genética a las siguientes generaciones (Huh *et al*., 2008). Sin embargo y a diferencia de lo observado en tejidos vegetativos, a día de hoy no se ha descrito ninguna relación entre patogénesis y alteración de los patrones de metilación en células germinativas.

5. Metilación y patogénesis

Como ya se ha indicado, los patrones de metilación del DNA son susceptibles a situaciones de estrés del organismo, pudiendo contribuir en las adaptaciones heredables relacionadas con los cambios de metilación de su genoma. Esos efectos transgeneracionales no necesariamente persisten durante generaciones sucesivas (Boyko *et al*., 2010). Las plantas han encontrado un equilibrio en el mantenimiento estable de los patrones epigenéticos, evitando efectos negativos en la expresión de sus genes, conservando la estructura de su genoma pero manteniéndolo flexible para inducir variación epigenética rápida ante nuevas condiciones ambientales. Aunque aún no está suficientemente claro si parte de las modificaciones generadas en el DNA (metilación) están directamente relacionadas con la repuesta a estrés, se ha observado que, plantas sometidas a elevadas temperaturas mostraban cambios transitorios en la densidad del nucleosoma, así como la activación de algunos elementos repetitivos (Ito *et al*., 2011; Pecinka *et al*., 2010).

También se realizó un estudio en plantas de tabaco donde se silenció la DNA metiltransferasa I (MET1), observándose una desregulación de la expresión de aproximadamente 30 genes, de los cuales, el 62.5% estaban relacionados con estreses tanto abióticos como bióticos (Wada *et al*., 2004), lo que sugirió que un elevado número de genes modificados por medio de la metilación tenían una relación cercana con la respuesta a estreses.

Resultados similares se observaron en plantas de tabaco infectadas con el virus del mosaico del tabaco (TMV). En estos trabajos se observó que algunos genes de sensibilidad al patógeno, NtAlix1 (Wada *et al*., 2004) y NTGPDL (Choi *et al*., 2007), sufrieron una rápida y dinámica alteración de los niveles de expresión debido a los cambios de su patrón de metilación (Choi *et al*., 2007). Por otra parte en un estudio realizado en plantas de *N. benthamiana* transgénicas para la proteína asociada a la replicación (Rep) de un *Geminivirus*, se determinó que la expresión de esta proteína induce una significativa reducción en los niveles de metilación del DNA (en contexto CG) del huésped (Rodriguez-Negrete, *et al.,*2013). Finalmente alteraciones en los niveles de metilación del huésped también se han asociado a la repuesta a

infección bacteriana en arroz, tabaco y *Arabidopsis* (Yu, *et al*., 2013; Sha *et al*., 2005; Boyko *et al*., 2007). En general estas evidencias son consistentes con la hipótesis de que los procesos de patogénesis (tanto viral como bacteriana) pueden estar estrechamente asociados con la alteración de los patrones de metilación del DNA genómico del huésped.

JUSTIFICACIÓN Y OBJETIVOS

JUSTIFICACIÓN Y OBJETIVOS

Los viroides son los patógenos de plantas conocidos con menor complejidad biológica. Su genoma está formado por una molécula circular de RNA de 230 a 400 pb y no presenta capacidad codificante. A pesar de esta evidente simplicidad estructural son capaces de provocar, en sus huéspedes respectivos, síntomas similares a los causados por otros patógenos de mayor complejidad. Estos agentes patogénicos se clasifican en dos familias: *Pospiviroidae* (con replicación en el núcleo) y Avsunviroidae (con replicación en cloroplastos) (Flores *et al*., 2005; Ding, 2009). El viroide del enanismo del lúpulo (HSVd) es un miembro característico de los viroides con replicación nuclear. El tamaño de su RNA varía entre los 297 a los 303 nts y debido a su amplio número de variantes es el viroide con mayor número de huéspedes naturales, tales como el pepino, la vid, los cítricos, el melocotonero, el peral, el ciruelo (Shikata, 1990), el albaricoquero (Astruc *et al*., 1996) y el almendro (Cañizares *et al*., 1999).

Sin embargo, el mecanismo por el que estos RNAs patogénicos son capaces de interferir en las diferentes rutas de la maquinaria de la célula vegetal permanecen aún sin descifrar completamente. En el momento de iniciar la presente tesis existía un creciente número de evidencias que sustentaban la hipótesis propuesta por Wang *et al*. (2004) que proponía que el silenciamiento de RNA debería desempeñar un papel crítico en el proceso de patogénesis inducido por los viroides (revisiones de Gómez *et al*., 2008 y 2009; Navarro *et al*., 2012a). El término silenciamiento de RNA engloba una serie de eventos reguladores por los que la expresión de uno o más genes se inhibe o estimula por el efecto de una molécula de RNA antisentido. Este mecanismo regulador está conservado en los cuatro reinos eucariotas y sus funciones son diversas: mantenimiento de la estabilidad del genoma (Vaucheret, 2006; Liu *et al*., 2010), regulación de procesos del desarrollo (Chen *et al*., 2010) y defensa frente a ácidos nucleicos invasores (Ruiz-Ferrer y Voinnet, 2009). En plantas, el silenciamiento de RNA actúa a nivel post-transcripcional (Posttranscriptional Gene Silencing, PTGS) o transcripcional (Transcriptional Gene Silencing, TGS). Diversos trabajos realizados en el grupo donde se ha realizado esta tesis han contribuido en los últimos años a esclarecer las relaciones entre el silenciamiento post-transcripcional inducido por los viroides y la expresión de síntomas en el huésped (Gómez y Pallás, 2007; Gómez *et al*., 2008 y 2009). Sin embargo, en el momento de iniciar el presente trabajo, el conocimiento sobre las relaciones que pudieran existir entre la regulación transcripcional mediada por silenciamiento de RNA y la infección viroidal era escaso.

La actividad del genoma a nivel transcripcional está regulada por las modificaciones epigenéticas del DNA y las Histonas (Matzke *et al*., 2009). La metilación de citosinas es un proceso epigenético básico para el mantenimiento de la actividad del genoma que permite la regulación transcripcional de regiones de DNA

con y sin capacidad codificante (Dowen *et al*., 2012). En plantas, la modulación de la metilación de DNA frente a factores ambientales constituye un mecanismo de control que podría estar implicado en la respuesta a estrés y a procesos de desarrollo. En relación a su papel en procesos de patogénesis, en los últimos años se han descrito cambios en la metilación del DNA genómico en repuesta a infecciones bacterianas (Yu *et al*., 2012; Dowen *et al*., 2012) y virales (Rodriguez-Negrete *et al*., 2013). Sin embargo, se desconocía si la infección por viroides inducía en el huésped algún tipo de alteración en este mecanismo de regulación transcripcional mediado por la metilación (Navarro *et al*., 2012b).

Ante una situación de estrés, en la planta se desencadena una cascada de respuestas que se traducen en una adaptación a la condición adversa. Como consecuencia de este retorno a un estado de homeostasis, la planta suele comprometer su desarrollo, lo que en las especies agrícolas se traduce en un significativo descenso en la producción. Por esta razón, ha surgido la necesidad de implementar estrategias innovadoras que combinan transcriptómica, proteómica y metabolómica en un intento de comprender los mecanismos que se desencadenan en la planta en respuesta a estreses tanto abióticos como bióticos. Sin embargo, por regla general, estas aproximaciones excluyen las alteraciones producidas a nivel de los RNAs no codificantes (ncRNAs). Se ha propuesto que en plantas los ncRNAs estarían implicados en funciones tales como regulación del desarrollo y en procesos de respuesta al estrés. No obstante, se desconoce la gran mayoría de los mecanismos funcionales de estos ncRNAs o las potenciales dianas de su actividad. Dado que los viroides son RNAs no codificantes capaces de infectar plantas, pueden utilizarse como sondas moleculares que ayuden a comprender la naturaleza de estos mecanismos de regulación en plantas (Gómez y Pallás, 2013).

Como objetivo general del presente trabajo nos propusimos profundizar en el conocimiento de este proceso de patogénesis en las plantas infectadas. Por otro lado, gracias a las características moleculares de estos patógenos, pretendimos ahondar en el conocimiento general de los procesos de respuesta a estrés mediados por ncRNAs en plantas de interés agronómico. Por otra parte, este trabajo trata de determinar si existen alteraciones en los mecanismos de regulación transcripcional (variaciones de metilación) en el huésped, inducidas como consecuencia de la infección por viroides nucleares, tanto en tejido vegetativo como reproductivo, así como identificar aquellos factores celulares implicados en este proceso.

Este proyecto asume como hipótesis de trabajo la premisa de que el silenciamiento a nivel transcripcional de RNAs es un mecanismo regulador de la expresión génica mediado por RNAs no codificantes, y, por tanto, altamente susceptible de verse afectado en el huésped durante una infección viroidal.

En la presente tesis se ha trabajado con dos sistemas planta-patógeno. Por un lado, hemos estudiado la interacción HSVd-pepino, y por otro lado hemos utilizado plantas transgénicas de *Nicotiana benthamiana* que sobreacumulan la secuencia dimérica del viroide (Gómez y Pallás, 2006).

Para abordar el objetivo global del proyecto arriba enunciado hemos definido 4 objetivos específicos, que se detallan a continuación.

1- Identificar en plantas de pepino infectadas con el viroide del enanismo del lúpulo (Hop stunt viroid, HSVd) y en plantas transgénicas de *Nicotiana benthamiana* que lo sobreacumulan, RNAs endógenos de los huéspedes cuya actividad transcripcional se encuentre alterada durante el proceso de infección.

2- Determinar si dicha alteración en el perfil transcripcional de estos RNAs endógenos es dependiente de modificaciones en los patrones de metilación en sus regiones reguladoras.

3- Identificar vías regulatorias mediadas por ncRNAs (especialmente aquellas relacionadas con el proceso de metilación) que pudieran presentar alguna disfunción como consecuencia de la infección, y componentes celulares propios de las mismas que pudiesen estar interaccionando directa o indirectamente con el viroide.

4- Una vez analizados los cambios transcripcionales en tejido vegetativo, determinar si el mapa epigenético de tejidos reproductivos del huésped se ve alterado como consecuencia de la infección del viroide.

CAPÍTULO PRIMERO

Este capítulo ha dado lugar a la siguiente publicación:

Martínez, G., Castellano, M., Tortosa, M., Pallas, V. and Gómez, G. (2014).

A non-coding RNA induces changes in dynamic DNA methylation of ribosomal RNA genes in host plants. *Nucleic Acids Research*. 42: 1553-1562. Doi: 10.1093/nar/gkt968

Title:

A pathogenic noncoding RNA induces changes in dynamic DNA methylation of ribosomal RNA genes in host plants.

Authors:

German Martinez[1,2], Mayte Castellano[1], Maria Tortosa[1], Vicente Pallas[1] and Gustavo Gomez[1]*

Authors Address:

[1] Instituto de Biología Molecular y Celular de Plantas (IBMCP), Consejo Superior de Investigaciones Científicas (CSIC)-UPV, CPI, Edificio 8 E, Av. de los Naranjos s/n, 46022 Valencia, Spain.

[2] Present addresses: Center for RNA Biology. The Ohio State University, Columbus, OH 43210, USA.

ABSTRACT

Viroids are plant-pathogenic ncRNAs able to interfere with yet poorly known host-regulatory pathways and cause alterations recognized as diseases. The way by which these RNAs coerce the host to express symptoms remains to be totally deciphered. In recent years, diverse studies have proposed a close interplay between viroid-induced pathogenesis and RNA silencing, supporting that viroid-derived sRNAs (vd-sRNAs) mediate the post-transcriptional cleavage of endogenous-mRNAs by acting as elicitors of symptoms expression. Although the evidence supporting the role of vd-sRNAs in pathogenesis is robust, the possibility that this phenomenon can be a more complex process, also involving viroid-induced alterations in plant gene-expression at transcriptional levels, has been considered. Here we show that plants infected with the Hop stunt viroid accumulate high levels of sRNAs derived from ribosomal transcripts. This effect was correlated with an increase in the transcription of rRNAs precursors during infection. We observed that the transcriptional reactivation of rRNA-genes correlates with a modification of DNA methylation in their promoter region and revealed that some rRNA-genes are demethylated and transcriptionally reactivated during infection. This study reports a previously unknown mechanism associated with viroid (or any other pathogenic-RNA) infection in plants providing new insights into aspects of host-alterations induced by viroid infectious-cycle.

INTRODUCTION

Impelled by their need to optimize a humble (250-400 nts) non protein coding genome to guarantee their infectious cycle, viroids have evolved into versatile molecular entities capable of interacting with the host-cell machinery at diverse functional levels (1). In some cases, this crosstalk can affect key host-regulatory pathways and cause phenotypic alterations recognized as plant diseases (2-3). Host factors and/or mechanisms associated with basic aspects of the life cycle of viroids, such as sub-cellular compartmentalization (4-5), replication (6-8) and movement (9-12), have been thoroughly studied in the last years to generate a relatively clear picture of the plant-viroid interaction (13). However, the way by which these tiny non coding RNAs (nc-RNAs) subvert the plant cell machinery by coercing the host to express symptoms remains a conundrum (3).

As viroids lack mRNA activity, it was initially assumed that viroid-induced pathogenesis must result from a direct interaction between their genome and host factors (proteins or nucleic acids). Based on this notion, early pathogenesis models envisioned the plant-symptom expression as a consequence of alterations in the endogenous RNA metabolism induced by base-pair interactions between viroid and host nc-RNAs, like U1 (14) or 7S (15). The identification of sequence/structural elements in the viroid genome (pathogenicity determinants) (16-17) supports the notion that these specific viroid domains may interact with yet-to-be-identified host factors interfering in their physiological role and consequently incite disease (1,3). In recent years, and enhanced by the advent of RNA silencing, diverse studies have provided evidence for the existence of close interplay between viroid-induced pathogenesis and this small RNA-dependent regulatory mechanism. The idea that viroid-derived small RNAs (vd-sRNAs) can mediate the post-transcriptional cleavage of endogenous mRNAs, acting as elicitors of symptoms expression (18-20), was reinforced by the observation that the expression of host symptoms is associated with post-transcriptional RNA silencing in representative members of both *Pospiviroidae* (21) and *Avsunviroidae* (22) families. Despite strong evidence supporting the role of vd-sRNAs as inductors of host-symptoms, the possibility that this phenomenon can be a more complex process, also involving viroid-induced alterations in plant gene-expression at transcriptional levels, cannot be ruled out (3,13).

Genome activity at the transcriptional level in plants is regulated by epigenetic modifications of DNA and histones. Cytosine DNA methylation in plants is a stable epigenetic mark, basic for the maintenance of genome stability, including regulation of coding and non-coding regions (23). Methylation takes place in three different sequence contexts, CG and CHG (symmetric) and CHH (asymmetric, where H refers to A, T or C) (24). *De novo* DNA methylation is regulated by DOMAINS REARRANGED METHYLTRANSFERASE 2 (DRM2), with three different pathways being involved in its maintenance. DNA METHYLTRANSFERASE

1 (MET1) and DNA CHROMOMETHYLASE3 (CMT3) respectively maintain CG and CHG methylation through DNA replication, while CHH methylation requires *de novo* continuous maintenance by DRM2 (24-25). Small RNAs (sRNAs) are important in *de novo* establishment and reinforcement of stable DNA methylation as they can target homologous DNA sequences and induce cytosine DNA methylation in all three contexts. A specific RNA silencing pathway, termed RNA-directed DNA methylation (RdDM), mediates the biosynthesis of these epigenetically active sRNAs (26). In the *Arabidopsis*-RdDM pathway, single-strand transcripts originated by RNA Polymerase IV (PolIV) are used by RNA-dependent RNA polymerase 2 (RDR2) as substrates to generate dsRNAs, which are subsequently processed by Dicer-like 3 (DCL3) into 23-24 nt siRNAs (25). These siRNAs guide *Argonaute* (AGO4/AGO6) proteins (likely through a siRNA-nascent PolV transcripts base-pairing mechanism) to target genomic regions (27). Next DRM2 is recruited to direct both symmetric and asymmetric *de novo* methylation. Conversely, *Arabidopsis* encodes a family of DNA glycosylases/lyases that mediate the active demethylation of methylcytosines (28). Recently, an alternative RDR6 21/22 nt siRNAs-dependent pathway has been described to mediate the initiation of *de novo* DNA methylation of transposable elements (29).

The first evidence linking viroid infection and transcriptional regulation in plants was provided by the demonstration that *Potato spindle viroid* (PSTVd) replication directs *de novo* methylation of cognate DNA sequences in viroid-expressing transgenic tobacco plants (30). Furthermore, other studies have shown that diverse host genes exhibit a transcriptional alteration during PSTVd (31-32), *Citrus viroid* III (CVdIII) (33), *Peach latent viroid* (PLMVd) (34) and *Citrus exocortis viroid* (CEVd) (35) infections. Although all this experimental evidence may support the idea that viroid infection incites alterations in plant gene expression at transcriptional levels (13), viroid-induced methylation of the host gene(s) or disruption of methylation pathways (which may eventually result in symptom expression) have not yet been reported in natural infections (3).

To address this issue, we first analyzed the alteration in the levels of endogenous sRNAs, associated with *Hop stunt viroid* (HSVd) infection in cucumber (*Cucumis sativus*) plants. Our results indicate that HSVd-infected plants differentially accumulate high levels of the sRNAs derived from ribosomal transcripts (rb-sRNAs) associated with an increasing accumulation of 27S-rRNAs precursors during infection. Finally, we observed that deregulation in rRNA transcriptional activity correlates with a dynamic modification of the DNA methylation level during the infection process to provide unprecedented insight into the potential endogenous-regulatory pathways affected during the viroid life cycle in infected plants.

RESULTS

rRNA-derived sRNAs are highly recovered from *HSVd*-infected plants

To evaluate if viroid infection induces alterations in the general profiles of host-endogenous sRNAs, we compared the size distribution of the total reads recovered from HSVd-infected plants with the standard sRNA levels previously described for cucumber (41). As observed in Fig. 1*A* (left panel), 21 nt sRNAs was the dominant size class in infected plants, while 22 and 24 nt in length were the most abundant in non inoculated plants. The 23 and 25 nt sized classes showed similar accumulation levels in both the control and HSVd-infected sRNAs populations. This scenario was in general reproduced (except for the 22 nts reads) when the unique sequences recovered from both datasets were analyzed (Fig. 1*A*, right panel), indicating that HSVd infection is associated with changes in the endogenous sRNA population levels, being the 21 nt and 24 nt species up- and down-regulated in infected plants, respectively.

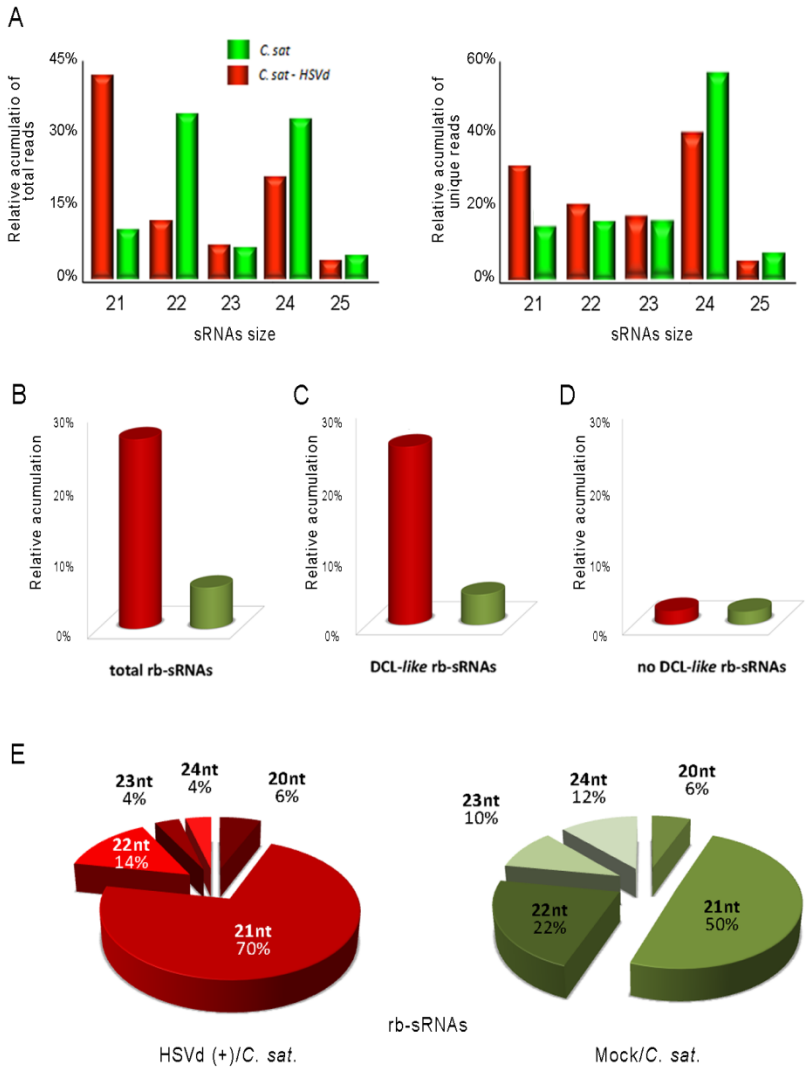

Figure 1. Characterization of the small RNAs recovered from cucumber leaves by deep sequencing. (*A*) Graphic representation of the differential accumulation and distribution of the total (left panel) and unique (right panel) reads of endogenous cucumber sRNAs ranging between 21 and 25 nt recovered from both the control and HSVd-infected samples analyzed at 30 days post-inoculation. (*B*) Differential recovering of ribosomal-derived sRNAs (rb-sRNAs) from infected and healthy tissues. The accumulation of rb-sRNAs is expressed as the percentage of total rb-sRNAs from the overall sRNAs in the library. (*C*) and (*D*) respectively show the relative accumulation of recovered rb-sRNAs with canonical (21-24 nt) and non canonical (<21 and >24 nt) predicted sizes. (*E*) Graphic representation of the distribution of the total reads of rb-sRNAs (ranging between 21 and 25 nt) recovered from both the HSVd-infected (left) and control (right) analyzed samples.

When plant endogenous sRNAs recovered from infected and healthy plants were analyzed by pairwise alignment against the cucumber transcript database, we observed that the sRNAs derived from 45S ribosomal RNA were the most differentially accumulated population of sRNAs in viroid-infected plants (Fig. 1*B*). The accumulation of 45S- rRNAs-derived sRNAs (rb-sRNAs) was at least 4-fold higher in infected (27.4 %) compared to control (6.8%) plants. This difference slightly increased (24.2% and 4.9%, respectively) when considering only sRNAs with expected DCL canonical sizes ranging from 21 to 24 nts (Fig. 1*C*). In contrast, negligible differences were found when considering the levels of the unexpected size (<21 - >24 nts in length) reads (Fig. 1*D*). Consistently with the global sRNAs population (Fig. 1*A*), the rb-sRNAs of 21 nt and 24 nt were respectively up- and down recovered from the HSVd-infected dataset in comparison to control cucumber reads (Fig. 1*E*). To examine the distribution of the rb-sRNA set, all the potentially DCL-processed sequences (21 to 24 nt) recovered from the healthy and HSVd-infected cucumber plants were mapped on the 45S-rRNA transcriptional unit (Fig. 2*A*). Despite both sRNAs populations displayed a relatively heterogeneous distribution pattern along the rRNA sequence (Fig. 2*B*), the total number of sequences matching throughout the rRNA gene significantly increased in infected plants as compared to the reads recovered from mock-inoculated cucumbers (Fig. 2*C*; parametric *t*-test: arithmetic means of 37.6 and 9.4, for infected and mock-inoculated plants respectively, $P < 2.2 \times 10^{-16}$). Moreover, we noticed two considerable differences between rb-sRNAs profiles in both analyzed samples. First in the infected plants, the differentially recovered rb-sRNAs are predominantly mapping to two homologous regions of 300 nt located in the Intergenic Spacer Region (IGS) and the 3´end of the 25s rRNA (Fig. 2*B*). Indeed, the Northern blot analyses, using a probe corresponding to this specific IGS region, revealed a remarkable accumulation of rb-sRNAs in the infected plants (Fig. 2*D*). Second, a major proportion of rb-sRNAs complementary to the rRNA transcripts from both polarities was recovered from the HSVd-infected plants (Fig. 2*E* and *F* and Fig. S1), suggesting that the over-accumulation of rb-sRNAs observed in infected plants might originate from the rRNA-derived double stranded RNAs processed in sRNAs.

Interestingly, the accumulation of sRNAs derived from 5S rRNA transcripts (5S-sRNAs) was also increased in HSVd-infected (0.17%) compared to control (0.06%) plants (Fig. S2*A*). Consistently with the observed in the 25S small RNAs population, the 5S-sRNAs of 21 nt and 24 nt were respectively up- and down regulated in the HSVd-infected plants, and a major proportion of sRNAs complementary to 5S transcripts was recovered from the infected cucumber plants (Fig. S2*B* and *C*). When the 5S-sRNAs were mapped onto their transcriptional unity, we observed that in the infected plants, the 5S-sRNAs are heterogeneously distributed along the 5S-rRNA sequence (Fig. S2*D*). However, the 5S-sRNAs recovered from mock control disproportionately (72% of the analyzed reads) match to a region adjacent to the

transcription start site. Importantly the totality of these sRNAs was 24 nt in length. All together, these results support that in cucumber, HSVd-infection is associated with a drastic alteration of rRNA-derived sRNAs processing, mainly characterized by an increase in the accumulation of 21 nt in length sRNAs (potential products of the processing of ds-rRNAs) and a significant decreasing of ribosomal-specific 24 nt sRNAs (assumed to be involved in maintenance of methylation status).

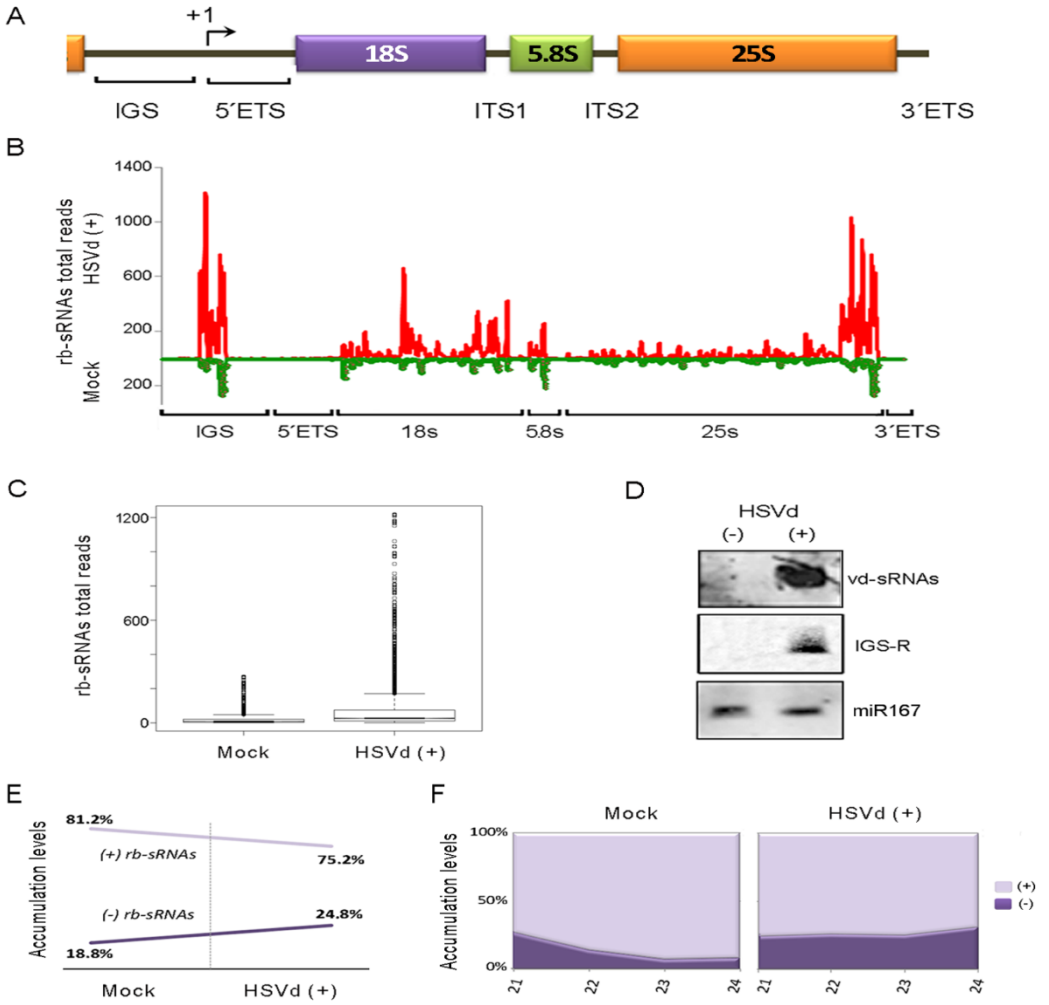

Figure 2. Analysis of ribosomal-derived sRNAs differentially expressed in infected cucumber plants. (*A*) Diagram (no scale) of the rRNA gene unit. The rRNA gene repeats are arranged in long tandem arrays of 45S rRNA genes, each including the region for the 18S, 5.8S and 25S rRNAs, and separated from adjacent units by an Intergenic spacer (IGS). The transcription start site is indicated by +1. The external (ETS) and internal (ITS) transcribed spacers are removed during rRNA processing. (*B*) The rb-sRNAs recovered from the infected (above the X-axis) or the non-inoculated plants (below the X-axis) were plotted according to the position of their 5´-end onto the cucumber rRNA sequence. The values on the Y-axis represent the number of total reads in each library. The nucleotide positions -115 to +15 of the 45S- rRNA analyzed region are represented on the X-axis. (*C*) Comparison of the accumulation of the rb-sRNAs that map along the rRNA transcriptional unit between both the infected and control plants as shown in the box-plot (boxes represent the medians, and the first and third quartiles of the dataset; circles refer to the data whose value is beyond the quartiles. Comparison of the means of the boxes showed significant differences between both samples using a parametric t-test: arithmetic means for mock and infected are 9.49 and 37.66, respectively; $t = 27.11$; $P < 2.2 \times 10^{-16}$). (*D*) The hyper-accumulation in the infected samples of the rb-sRNAs derived from a ~300 nt region of the IGS (IGS-R) was validated by Northern blot assays. The miR167 equally recovered from both analyzed sRNAs dataset was used as a load control. Hybridization with a probe against the HSVd-derived sRNAs (vd-sRNAs) was used as a positive control. (*E*) The relative accumulation of total rb-sRNAs complementary to rRNA transcripts increased in the HSVd-infected plants (left). A similar result was obtained when individually analyzing the expected canonical size of the rb-sRNAs (right).

27S-rRNA precursors accumulate differentially during viroid infection

In *Arabidopsis*, the 45S rRNA genes (Fig. 2*A*) are tandemly arrayed by hundreds at the chromosomal loci known as Nucleolus Organizers (NORs) (42). RNA polymerase I (Pol I) transcribes primary transcripts (called pre-rRNAs) that are then extensively processed into 18S, 5.8S and 25S rRNAs by the sequential deletion of external and internal transcribed spacers (ETS and ITS, respectively) (43). Each rRNA gene is separated from its adjacent one by an Intergenic spacer (IGS) and its expression is regulated at several levels according to the physiological need for ribosomes, with one such level being the epigenetic on/off switch that controls the number of active rRNA genes (44). A deficiency in this regulatory mechanism, which controls rRNA transcriptional activity, has been recently associated with overproduction of rb-sRNAs in *Arabidopsis* mutants (45-46). In order to determine if an alteration in the transcriptional activity of rRNA genes can be linked to the substantial accumulation of rb-sRNAs in HSVd-infected cucumber plants, we analyzed the accumulation of pre-rRNAs at specific points (T1: 10 dpi and T3: 30 dpi) during viroid infection. The RT-PCR assay was used to compare the pre-RNA levels, analyzing specifically two regions in the 27S rRNA transcription unit (Fig. 3*A*). Two different primers complementary to the 3´ end of 25S rRNA (25s-A) and ITS2 (ITS2-A) were used to generate the cDNA template. The pair 5.8s-Fw/5.8s-Rv was used to differentially amplify by PCR the unprocessed rRNAs. Significant differences in the pre-rRNA transcripts accumulation levels were found in viroid-infected plants in comparison to mock-inoculated controls at infection time T3 when using both the 25s-A and the ITS2-A primers for RT (Fig. 3*B*, panels *B*1 and *B*2, respectively). In the analysis performed at T1 (10dpi), we observed only a selective accumulation of pre-rRNAs when the PCR was done from the ITS2-A-generated cDNA. This slight incongruence, however, can be attributed to poorer efficiency in the generation of sufficiently long cDNA templates when using the 25s-A primer, instead of ITS2-A, in the RT reaction. The differential accumulation of pre-rRNAs in infected plants at infection time T3 was corroborated by Northern blot assays of 27S pre-RNA levels (Fig. 3*C*). The finding that HSVd-infection is associated with an increase in the pre-rRNAs levels suggests that the regulation of the transcriptional activity of rRNA genes might be impaired in viroid-infected cucumber.

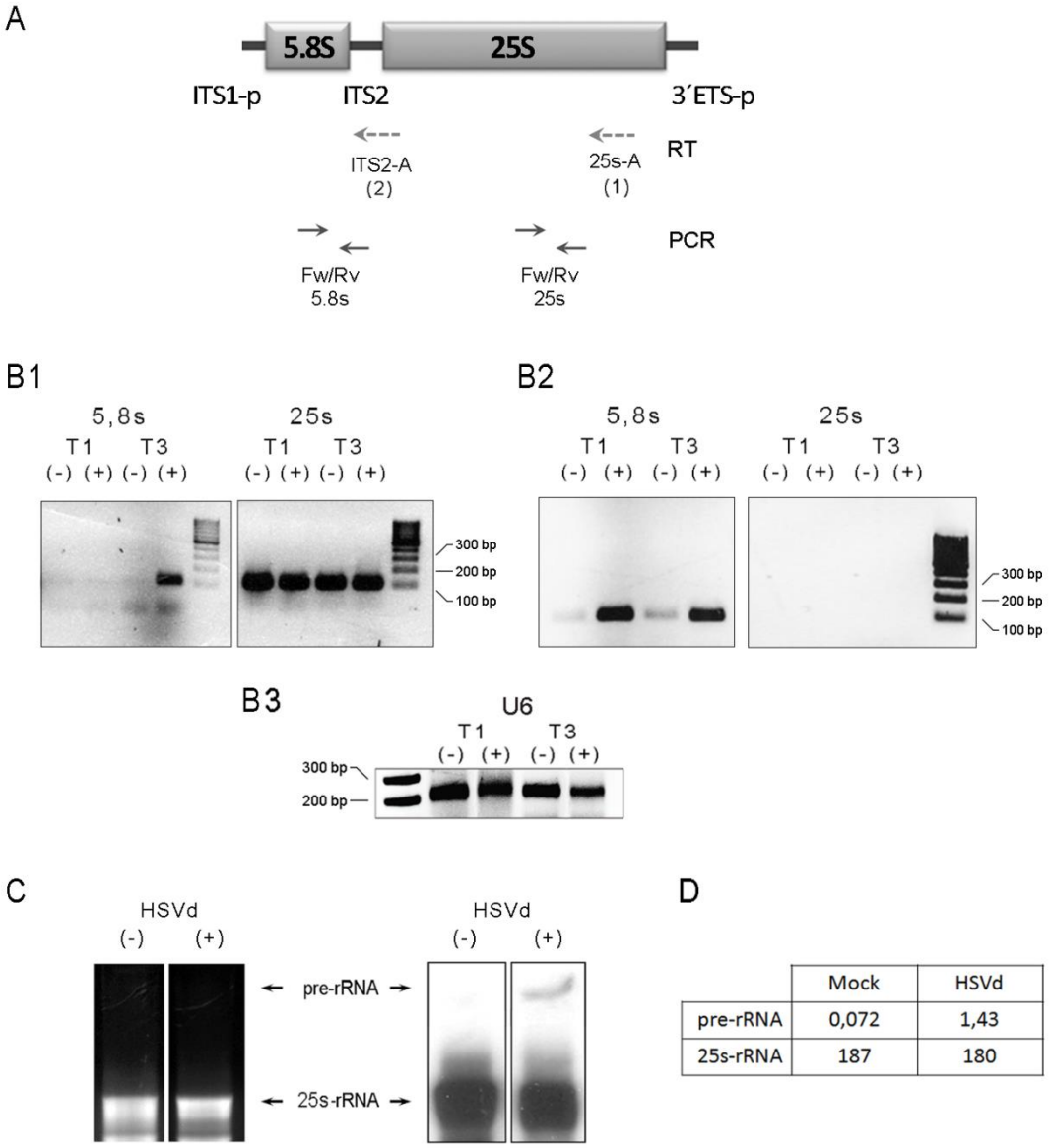

	Mock	HSVd
pre-rRNA	0,072	1,43
25s-rRNA	187	180

Figure 3. Precursor for rRNAs (pre-rRNAs) accumulates in infected plants. (*A*) Diagram (no scale) of the pre-27S rRNA (ITS1-p and 3´ETS-p refer to partially processed transcribed spacers). The dotted arrows below depict the oligos used for the RT reaction starting from the 25S 3`end (25s-A/ RT-1) and the ITS2 (ITS2-A/ RT-2) regions of the pre-rRNA. Solid arrows indicate the oligos used in the PCR amplification. (*B*) The RT-PCR analyses of the pre-rRNA expression in the HSVd-infected (+) and mock-inoculated (-) plants at 10 (T1) and 30 (T3) days post-inoculation. The initial cDNAs were transcribed using the 25s-A (B1) and ITS2-A (B2) oligos, respectively. (*B*3) RT-PCR amplification of U6 snoRNA served as control for RNA load. (*C*) The accumulation of the pre-rRNA (marked with arrows) in the infected plants was validated by Northern blot assays in the total RNAs extracted from plants at T3 using a probe complementary to the 3' end of the 25S rRNA. (*D*)The bands intensity was measured using the Image-J application http://www.imagej.en.softonic.com.

Viroid infection modifies dynamic rDNA methylation

During diverse phases of the plants life cycle, rRNA genes are presumably in excess and are consequently silenced. At present, it is well accepted that the silencing of rRNA genes is a self-reinforcing regulatory phenomenon mediated by siRNA-directed cytosine methylation and heterochromatin formation (44,47). To investigate whether the transcriptional deregulation of rRNA genes (revealed as pre-rRNA

accumulation) observed during viroid infection can be associated with reduced cytosine methylation, we analyzed by bisulfite sequencing, which identifies the position of methylated and unmethylated cytosines, a 131-bp region of genomic 45S-rDNA (Fig. 4*A*). Within this sequence, there were 9 symmetric (5 CG, 4 CHG) and 14 asymmetric (CHH) potential methylation sites (Fig. 4*B*).

The DNA extracted from leaves of HSVd-infected and mock-inoculated cucumber plants at 10 dpi (T1) and 30 dpi (T3) was treated with bisulfite reagent to convert unmethylated cytosines into uracil, followed by PCR to amplify a specific rDNA sequence of 131 nt comprised between positions -115 and +15. PCR products were cloned, and the sequences of 13-34 clones were compiled for each time point. Methylation analysis revealed that at T1 point, HSVd infection resulted in a decrease in the relative number of methylated cytosine residues (83%) when compared to control plants. However, comparable relative methylation levels between infected and healthy plants were observed at 30 dpi (T3) (Fig. 4*C*). When dynamic methylation was differentially analyzed for both symmetric and asymmetric pathways, we saw two different patterns. Symmetric methylation (CG/CHG) slightly decreased during infection and displayed lowered relative methylation levels between 10% and 12% at T1 and T3, respectively (Fig. 4*D* and *F*, Fig. S3). These results indicate that HSVd infection is linked to CG/CHG demethylation, which may contribute to the transcriptional activation of normally silenced rDNA units, and can consequently induce the accumulation of pre-rRNA during pathogenesis. Conversely in the asymmetric context (CHH), loss of relative methylation in infected plants at T1 was more significant than in the symmetric pathway, and a drastic increase in the relative methylation pattern of rDNA was observed at T3 of the HSVd-infected plants (Fig. 4*D* and *G*, Fig. S4). To provide a more accurate picture of the changes occurring in the CHH methylation during viroid infection, we next studied an intermediate point of the infective cycle, at 20dpi (T2), by bisulfite sequencing (Fig. S3). As shown in Fig. 4*E*, the level of asymmetric methylation progressively increased at the analyzed infection times, thus explaining the equilibrium in the total methylation level observed at point T3 when comparing the HSVd-infected and mock-inoculated plants (Fig. 4*C*). The alteration in the methylation levels of infected plants at T3 infection time was validated by combined bisulfite and restriction analysis (Fig. S5). Taken together, these results indicate that in the analyzed rDNA regions, while CG and CHG sites maintain a constant hypometylated status during infection, the CHH sites shown a dual scenario being hypometylated at T1 and actively hypermethylated during HSVd-infection development.

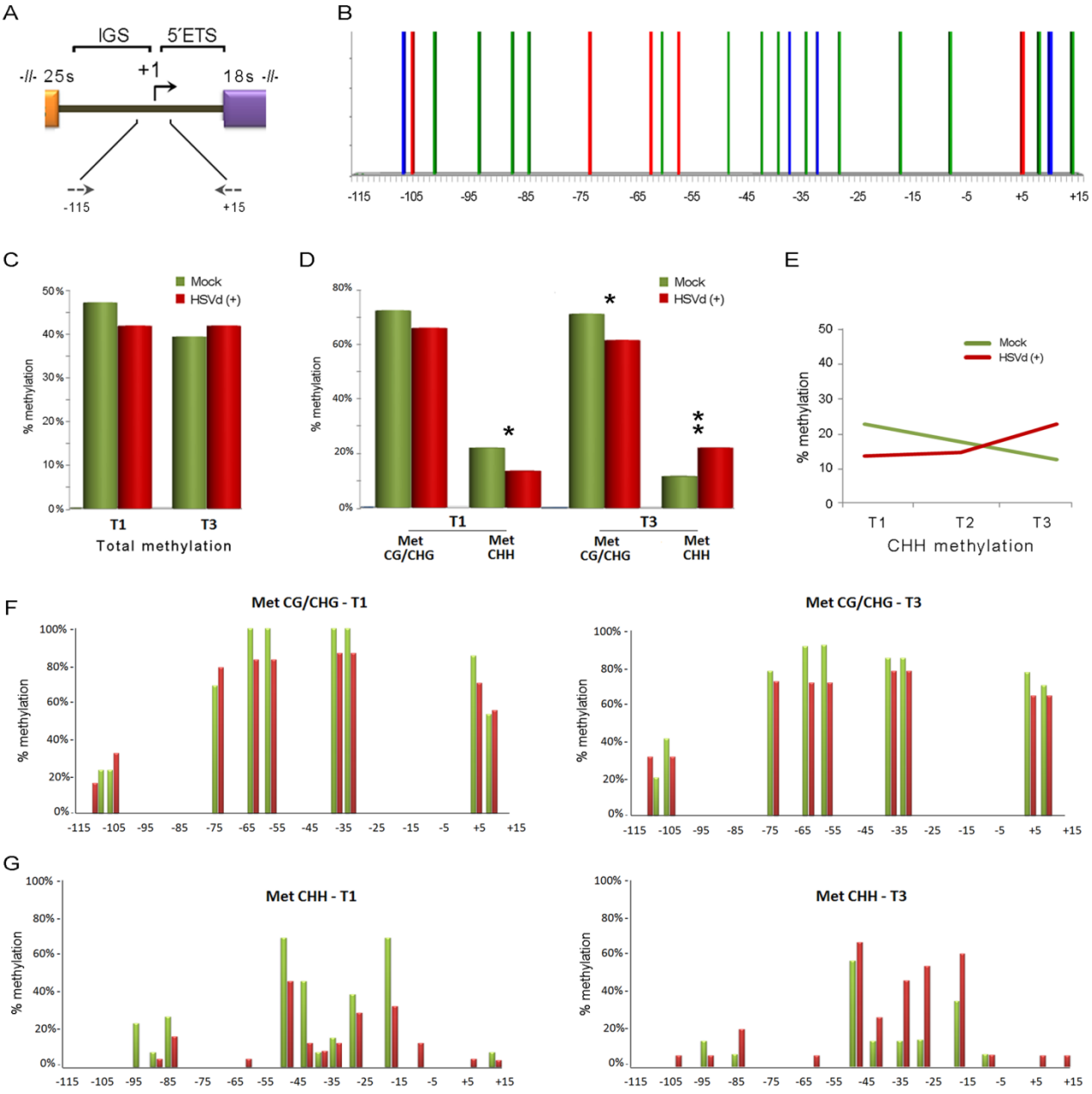

Figure 4. HSVd infection affects the methylation patterns in 45S-rRNA genes. (*A*) Diagram of the rRNA gene Intergenic region highlighting the promoter zone analyzed by bisulfite sequencing. The arrows represent the oligos used in the PCR assay and their relative position in the rRNA gene. (*B*) Graphic representation of the potential symmetric (CG – red bars - and CHG – blue bars) and asymmetric (CHH – green bars) positions predicted to exist within the analyzed region. (*C*) Histogram documenting the relative (HSVd/Mock) total DNA methylation levels at infection times T1 and T3. (*D*) Schematic representation of the differential analysis of both symmetric and asymmetric cytosine methylation at infection times T1 and T3 (Paired t-test values T1: means symmetric methylation (mock) 0.73, (infected) 0.67, t=1.604; means CHH methylation (mock) 0.22, (infected) 0.13, t=2.180; T3: means symmetric methylation (mock) 0.72, (infected) 0.64, t=2.481; means CHH methylation (mock) 0.11, (infected) 0.22, t=3.047; **P* < 0.05, ***P* < 0.01). (*E*) Evolution of the CHH methylation during HSVd infection in comparison to the level observed in the mock-inoculated plants. (*F*) Positions of methylcytosines in the analyzed regions displayed in the symmetric (CG and CHG) context. (*G*) Positions of methylcytosines in the analyzed regions displayed in the asymmetric context. The height of the bar represents the frequency at which cytosine was methylated at the analyzed infection times T1 (left) and T3 (right).

To obtain additional evidences supporting the influence of HSVd-infection on host-transcriptional activity, we also analyze by bisulfite sequencing a 149bp region of 5S rDNA (Fig. S6 *A* and *B*), another well established target transcriptionally regulated by DNA methylation in plants (48). Consistently with the observed for 45S-rRNA, sequence analysis revealed that HSVd infection is also associated with alterations in the methylation status of the 5S-rDNA. Methylation analysis revealed that at initial states of the infectious cycle (T1) the methylation levels observed in the analyzed region of the 5S rDNA were comparable for both analyzed samples (Fig. S6*C*). However, HSVd infection resulted in a significant reduction in the relative number of methylated cytosine residues in infected plants (53.6%) compared with mock-inoculated controls (62.4%) at T3 analyzed infection time (Fig. S6*D*). The loss of relative methylation in infected plants at T3 was comparable for cytosine restudies at both symmetric and asymmetric sequence context (Fig. S6*D*, *E* and *F*). Collectively our results provide unprecedented insights into alterations in the dynamics of the host DNA methylation status in viroid-induced pathogenesis.

DISCUSSION

Increasing evidence supports the notion that the study of viroid-host interactions can shed light on the regulatory pathways directed by non-coding RNAs in plants (2,13). Within this framework, deciphering the molecular basis of the viroid pathogenesis processes emerges as a fundamental milestone to be fulfilled. Since the first viroid-induced disease was reported, diverse pathogenesis models have been proposed (3). The actual prevailing notion linking viroid pathogenesis and RNA silencing essentially considers the interference of viroid-derived sRNAs in endogenous RNA metabolism at post-transcriptional level (19-20). However, the possibility that the expression of plant symptoms could eventually be a consequence of specific alterations in host regulatory mechanisms at transcriptional level has also been envisioned (3,13,31-35). Interestingly, the data obtained in this work reveals that viroid-induced pathogenesis is also associated with transcriptional host alterations.

The initial observation that HSVd-infected cucumber plants show an unexpected hyper-accumulation of rb-sRNAs prompted us to speculate about the possibility that, during infection, HSVd (as previously observed for a symptomatic variant of PLMVd (49) could interfere in a yet undetermined manner in the rRNA maturation process, and that the rb-sRNAs highly recovered from infected plants could be a product of the DCL-mediated degradation of aberrantly processed rRNAs. Nonetheless, the observation that mature forms of rRNAs, such as 25S, accumulate at comparable levels in both healthy and infected plants (Fig. 3*B* and *C*) was incongruent with this supposition. Consequently, we explored an alternative option that of rb-sRNAs accumulation in infected plants could be the result of the viroid-induced transcriptional

deregulation of rRNAs, resembling that recently observed in *Arabidopsis* where rb-sRNAs overproduction has been linked to deficiencies in the on/off switch controlling the number of active rRNA genes (46). Increased accumulation of 27S pre-rRNA in infected plants, in parallel to the maintenance of equivalent levels of processed rRNA forms (i.e., 25S), strongly suggests that, during infection, HSVd may induce the up-regulation of some of the normally inoperative rRNA transcriptional units.

Bisulfite sequencing clearly correlated HSVd infection with dynamic DNA methylation changes taking place in the analyzed regulatory region (-115 / +15) of 45S- rDNA. The symmetrical cytosine methylation progressively decreased during infection whereas the asymmetric *de novo* cytosine methylation also decreased at initial infection-time, being however actively increased throughout infection development. Interestingly, it has been previously reported in *Arabidopsis* that changes in the expression of rRNAs transcripts are related with the activation of silenced 45S-rRNAs genes and correlate with reduced CG and CHG methylation in the position flanking the rRNA gene transcription initiation site (44,46). Accordingly, we favour the idea that 27S pre-rRNA over-accumulation in HSVd-infected plants can result from activation of otherwise generally repressed rRNAs genes by loss in maintenance of the methylation status in both symmetric and asymmetric motifs. Additional bisulfite sequencing approaches focussed to analyze the methylation status of 5S rDNA unities (region -143 / +5) revealed that HSVd-infection also induce hypomethylation at both symmetric and asymmetric context in this rDNA family, thus reinforcing the biological relevance of this HSVd-induced phenomenon. In this point it is important to emphasize that our data were obtained from HSVd-agroinfected and not from transgenic plants constitutively expressing viroid-RNAs. Consequently we cannot exclude the possibility that the analyzed tissues could represent a mix of infected and non-infected cells, thus underestimating the effects of viroid infection on host-DNA methylation. Our novel and unexpected result for the HSVd-pathogenesis process is consistent with that previously reported for plant-bacteria interactions, where 5S rRNA repeats were demethylated at a significant level in response to infection (50). Furthermore, dynamic changes in DNA methylation patterns have been recently described during antibacterial defence in rice (51), tobacco (52) and *Arabidopsis* (23,50). Finally, in a recent study using transgenic *N. benthamiana* plants expressing the replication-associated protein (Rep) of a Geminivirus it was proposed that this type of plant DNA viruses can induce a substantial reduction in the levels of host-DNA methylation at CG sites in infected plants (53). Interestingly, the geminiviruses have, as HSVd do, a nuclear replication.

Speculations on the nature of the molecular mechanism regulating this active change in rDNA methylation during HSVd infection seem premature at this stage. Intriguingly, however, a similar scenario to that observed in infected cucumber plants has been described in *Arabidopsis* when a mutant for histone

deacetylase 6 (HDA6), a key regulator of gene silencing that displays a complex interrelationship with DNA methylation, was analyzed (46). Earley et al reported that *hda6* mutants lose the maintenance of symmetric methylation in 45S-rRNA promoter regions in parallel with a gain of *de novo* CHH methylation. Unexpectedly, and in concert with our results, increasing CHH methylation in *hda6* mutants, a typically repressive phenomenon, failed to suppress rRNA over-transcription. In addition, the siRNAs derived from the 45S-IGS region hyper-accumulated in the *hda6* mutant, resembling at least in part, that found in viroid-infected cucumber plants (Fig. 2*B* and *C*). Interestingly, it was also showed that the lost of HDA6 activity, induced a decrease of the symmetrical methylation of 5S rDNA and leads to the release of 5S rDNA silencing in mutant *Arabidopsis* plants (54). On the other hand, it was also proposed that spurious transcription of ribosomal genes by Pol II can be associated with the elimination of the repressive modification regulating the rRNA expression in *Arabidopsis* (46). By bearing this in mind, it is important to consider that, during infection, HSVd reprograms Pol II activity to transcribe viroid-RNA instead of the DNA template (55), which perhaps favours the spurious transcription of rRNAs in infected plants. Further studies are required to explore if there is some interrelation between the observed herein and the rRNA silencing of the rRNA genes mediated by HDA6 and Pol II in *Arabidopsis*. Moreover, we cannot rule out the possibility that viroid infection may induce changes in widespread dynamic DNA methylation, resembling what was observed in other pathogen-plant interactions (23,50-52). Broader analyses of DNA methylome on viroid-infected plants would help define the impact of viroid infection on DNA demethylation and host-gene transcription.

In summary, the data shown here support that during its pathogenesis process, HSVd induces changes in the DNA methylation of inactive rRNA genes, a previously non described mechanism linked to viroid (or any other pathogenic RNA) infection in plants. Moreover, our findings provide new insights into aspects of the host alterations associated with the HSVd infectious cycle and constitute additional support to the emerging notion that viroid pathogenesis can be a consequence of a multilayered process involving diverse pathogen-host interactions at both the post-transcriptional and transcriptional levels.

MATERIAL AND METHODS

Plant Material

Cucumber (*Cucumis sativus Cv Marketer)* plants were agroinoculated with *Agrobacterium tumefaciens* strain C58C1 transformed with a binary pMOG800 vector carrying a head-to-tail infectious dimeric HSVd cDNA (Y09352) (36), as previously described (21) (Supplementary Materials). Mock-inoculated cucumber plants were used as a negative control. Plants were maintained in growing chambers at 30°C for 16 h with

fluorescent light and at 25 °C for 8 h in darkness. To collect cucumber pollen grains, we used a paintbrush to gently brush the pollen from the anthers into an *Eppendorf* tube. This procedure was repeated for 150 and 117 flowers recovered from HSVd-infected and control plants respectively.

Small RNA library information

The sRNA sequences used in this work were obtained from a library generated by starting from an sRNAs population recovered from leaves and phloem exudates of healthy and *Hop stunt viroid*-infected cucumber (*C. sativus*) plants and sequenced by 454 Life Science Technology (Lifesequencing, Branfor, CT, USA; www.lifesequencing.com) ((37) - NCBI/SRA accession code SRP001408). The viroid derived sRNAs, recovered from infected plants, were filtered out from this analysis.

RNA isolation

Total RNA was extracted from the leaves (~0.1 g) of different infected and healthy cucumber plants using the TRI reagent (SIGMA, St. Louis, MO, USA) according to the manufacturer's instructions. The low-molecular weight RNA (<200 nt) fraction was enriched from total RNA using MIRACLE (miRNA isolation Kit, STRATAGENE) according to the manufacturer's instructions (Supplementary Materials).

Northern blot assays

Total RNA was analyzed by electrophoresis under denaturing conditions in 1% agarose gels with 0.25 x TBE and 8 M urea (38). The RNA was blotted on nylon membranes (ROCHE Diagnostics GmbH, Mannheim, Germany) and was hybridized as previously described (11). Approximately 25 µg of low-molecular weight RNA was loaded onto 20% polyacrylamide gels with 0.25 x TBE and 8 M urea. RNA was transferred to a nylon membrane (ROCHE Diagnostics-GmbH, Mannheim, Germany). Hybridization was performed as previously described (39).

Bisulfite Conversion and Sequencing

Total genomic DNA was extracted from the leaves (~0.1 g) of different infected and healthy cucumber plants (Supplementary Material – Supplementary Fig. S7*A* and *B*) (40). Bisulfite treatment was performed using the EpiTec Bisulfite kit (Quiagen) (Supplementary Material). Modified DNA was amplified by PCR and was cloned (Supplemental Material – Fig. S7*C*). Between 13 and 24 clones were sequenced for each analyzed time in both the infected and mock-treated plants

ACKNOWLEDGMENTS

We thank Drs. M. Fares and J. Forment (Bioinformatics Service of IBMCP) for his valuable contribution in the statistical analysis of the data and the sRNA sequence analysis, respectively.

FUNDING

This work was supported by grant BIO2011-25018 from the Spanish granting agency Direccion General de Investigacion Cientifica and from the *Prometeo* program 2011/003 from the Generalitat Valenciana. GM is the recipient of a *Marie Curie* IOF fellowship.

REFERENCES

1. Ding, B. (2009) The biology of viroid-host interactions. *Annu Rev Phytopathol*, **47**, 105-131.
2. Ding, B. (2010) Viroids: self-replicating, mobile, and fast-evolving noncoding regulatory RNAs. *Wiley Interdiscip Rev RNA*, **1**, 362-375.
3. Navarro, B., Gisel, A., Rodio, M.E., Delgado, S., Flores, R. and Di Serio, F. (2012) Viroids: how to infect a host and cause disease without encoding proteins. *Biochimie*, **94**, 1474-1480.
4. Zhao, Y., Owens, R.A. and Hammond, R.W. (2001) Use of a vector based on Potato virus X in a whole plant assay to demonstrate nuclear targeting of Potato spindle tuber viroid. *J Gen Virol*, **82**, 1491-1497.
5. Gomez, G. and Pallas, V. (2012) Studies on subcellular compartmentalization of plant pathogenic noncoding RNAs give new insights into the intracellular RNA-traffic mechanisms. *Plant Physiol*, **159**, 558-564.
6. Navarro, J.A., Vera, A. and Flores, R. (2000) A chloroplastic RNA polymerase resistant to tagetitoxin is involved in replication of avocado sunblotch viroid. *Virology*, **268**, 218-225.
7. Nohales, M.A., Flores, R. and Daros, J.A. (2012) Viroid RNA redirects host DNA ligase 1 to act as an RNA ligase. *Proc Natl Acad Sci U S A*, **109**, 13805-13810.
8. Nohales, M.A., Molina-Serrano, D., Flores, R. and Daros, J.A. (2012) Involvement of the chloroplastic isoform of tRNA ligase in the replication of viroids belonging to the family Avsunviroidae. *J Virol*, **86**, 8269-8276.
9. Zhong, X. and Ding, B. (2008) Distinct RNA motifs mediate systemic RNA trafficking. *Plant Signal Behav*, **3**, 58-59.
10. Gomez, G. and Pallas, V. (2004) A long-distance translocatable phloem protein from cucumber forms a ribonucleoprotein complex in vivo with Hop stunt viroid RNA. *J Virol*, **78**, 10104-10110.
11. Gomez, G. and Pallas, V. (2001) Identification of an in vitro ribonucleoprotein complex between a viroid RNA and a phloem protein from cucumber plants. *Mol Plant Microbe Interact*, **14**, 910-913.
12. Owens, R.A., Blackburn, M. and Ding, B. (2001) Possible involvement of the phloem lectin in long-distance viroid movement. *Mol Plant Microbe Interact*, **14**, 905-909.
13. Gomez, G. and Pallas, V. (2013) Viroids: a light in the darkness of the lncRNA-directed regulatory networks in plants. *New Phytol*, **198**, 10-15.
14. Diener, T.O. (1981) Are viroids escaped introns? *Proc Natl Acad Sci U S A*, **78**, 5014-5015.
15. Haas, B., Klanner, A., Ramm, K. and Sanger, H.L. (1988) The 7S RNA from tomato leaf tissue resembles a signal recognition particle RNA and exhibits a remarkable sequence complementarity to viroids. *EMBO J*, **7**, 4063-4074.

16.Visvader, J.E. and Symons, R.H. (1985) Eleven new sequence variants of citrus exocortis viroid and the correlation of sequence with pathogenicity. *Nucleic Acids Res*, **13**, 2907-2920.
17.Schnolzer, M., Haas, B., Raam, K., Hofmann, H. and Sanger, H.L. (1985) Correlation between structure and pathogenicity of potato spindle tuber viroid (PSTV). *EMBO J*, **4**, 2181-2190.
18.Papaefthimiou, I., Hamilton, A., Denti, M., Baulcombe, D., Tsagris, M. and Tabler, M. (2001) Replicating potato spindle tuber viroid RNA is accompanied by short RNA fragments that are characteristic of post-transcriptional gene silencing. *Nucleic Acids Res*, **29**, 2395-2400.
19.Wang, M.B., Bian, X.Y., Wu, L.M., Liu, L.X., Smith, N.A., Isenegger, D., Wu, R.M., Masuta, C., Vance, V.B., Watson, J.M. *et al.* (2004) On the role of RNA silencing in the pathogenicity and evolution of viroids and viral satellites. *Proc Natl Acad Sci U S A*, **101**, 3275-3280.
20.Gomez, G., Martinez, G. and Pallas, V. (2009) Interplay between viroid-induced pathogenesis and RNA silencing pathways. *Trends Plant Sci*, **14**, 264-269.
21.Gomez, G., Martinez, G. and Pallas, V. (2008) Viroid-induced symptoms in Nicotiana benthamiana plants are dependent on RDR6 activity. *Plant Physiol*, **148**, 414-423.
22.Navarro, B., Gisel, A., Rodio, M.E., Delgado, S., Flores, R. and Di Serio, F. (2012) Small RNAs containing the pathogenic determinant of a chloroplast-replicating viroid guide the degradation of a host mRNA as predicted by RNA silencing. *Plant J*, **70**, 991-1003.
23.Dowen, R.H., Pelizzola, M., Schmitz, R.J., Lister, R., Dowen, J.M., Nery, J.R., Dixon, J.E. and Ecker, J.R. (2012) Widespread dynamic DNA methylation in response to biotic stress. *Proc Natl Acad Sci U S A*, **109**, E2183-2191.
24.Law, J.A. and Jacobsen, S.E. (2010) Establishing, maintaining and modifying DNA methylation patterns in plants and animals. *Nat Rev Genet*, **11**, 204-220.
25.Matzke, M., Kanno, T., Daxinger, L., Huettel, B. and Matzke, A.J. (2009) RNA-mediated chromatin-based silencing in plants. *Curr Opin Cell Biol*, **21**, 367-376.
26.Zhang, X., Henderson, I.R., Lu, C., Green, P.J. and Jacobsen, S.E. (2007) Role of RNA polymerase IV in plant small RNA metabolism. *Proc Natl Acad Sci U S A*, **104**, 4536-4541.
27.Haag, J.R. and Pikaard, C.S. (2011) Multisubunit RNA polymerases IV and V: purveyors of non-coding RNA for plant gene silencing. *Nat Rev Mol Cell Biol*, **12**, 483-492.
28.Gong, Z., Morales-Ruiz, T., Ariza, R.R., Roldan-Arjona, T., David, L. and Zhu, J.K. (2002) ROS1, a repressor of transcriptional gene silencing in *Arabidopsis*, encodes a DNA glycosylase/lyase. *Cell*, **111**, 803-814.
29.Nuthikattu, S., McCue, A.D., Panda, K., Fultz, D., Defraia, C., Thomas, E.N. and Slotkin, R.K. (2013) The Initiation of Epigenetic Silencing of Active Transposable Elements Is Triggered by RDR6 and 21-22 Nucleotide Small Interfering RNAs. *Plant Physiol*, **162**, 116-131.

30.Wassenegger, M., Heimes, S., Riedel, L. and Sanger, H.L. (1994) RNA-directed de novo methylation of genomic sequences in plants. *Cell*, **76**, 567-576.

31.Itaya, A., Matsuda, Y., Gonzales, R.A., Nelson, R.S. and Ding, B. (2002) Potato spindle tuber viroid strains of different pathogenicity induces and suppresses expression of common and unique genes in infected tomato. *Mol Plant Microbe Interact*, **15**, 990-999.

32.Owens, R.A., Tech, K.B., Shao, J.Y., Sano, T. and Baker, C.J. (2012) Global analysis of tomato gene expression during Potato spindle tuber viroid infection reveals a complex array of changes affecting hormone signaling. *Mol Plant Microbe Interact*, **25**, 582-598.

33.Tessitori, M., Maria, G., Capasso, C., Catara, G., Rizza, S., De Luca, V., Catara, A., Capasso, A. and Carginale, V. (2007) Differential display analysis of gene expression in Etrog citron leaves infected by Citrus viroid III. *Biochim Biophys Acta*, **1769**, 228-235.

34.Herranz, M.C., Niehl, A., Rosales, M., Fiore, N., Zamorano, A., Granell, A. and Pallas, V. (2013) A remarkable synergistic effect at the transcriptomic level in peach fruits doubly infected by prunus necrotic ringspot virus and peach latent mosaic viroid. *Virol J*, **10**, 164.

35.Lison, P., Tarraga, S., Lopez-Gresa, P., Sauri, A., Torres, C., Campos, L., Belles, J.M., Conejero, V. and Rodrigo, I. (2013) A noncoding plant pathogen provokes both transcriptional and posttranscriptional alterations in tomato. *Proteomics*, **13**, 833-844.

36.Gomez, G. and Pallas, V. (2006) Hop stunt viroid is processed and translocated in transgenic Nicotiana benthamiana plants. *Mol Plant Pathol*, **7**, 511-517.

37.Martinez, G., Donaire, L., Llave, C., Pallas, V. and Gomez, G. (2010) High-throughput sequencing of Hop stunt viroid-derived small RNAs from cucumber leaves and phloem. *Mol Plant Pathol*, **11**, 347-359.

38.Pallas, V., Navarro, A. and Flores, R. (1987) Isolation of a viroid-like RNA from hop different from hop stunt viroid. *Journal of General Virology*, **68**, 3201-3205.

39.Gomez, G. and Pallas, V. (2007) Mature monomeric forms of Hop stunt viroid resist RNA silencing in transgenic plants. *Plant J*, **51**, 1041-1049.

40.Dellaporta, S.L., Wood, J. and Hicks, J.B. (1983) A plant DNA minipreparation: version II. *Plant molecular biology reporter*, **1**, 19-21.

41.Martinez, G., Forment, J., Llave, C., Pallas, V. and Gomez, G. (2011) High-throughput sequencing, characterization and detection of new and conserved cucumber miRNAs. *PLoS One*, **6**, e19523.

42.Long, E.O. and Dawid, I.B. (1980) Repeated genes in eukaryotes. *Annu Rev Biochem*, **49**, 727-764.

43.Henras, A.K., Soudet, J., Gerus, M., Lebaron, S., Caizergues-Ferrer, M., Mougin, A. and Henry, Y. (2008) The post-transcriptional steps of eukaryotic ribosome biogenesis. *Cell Mol Life Sci*, **65**, 2334-2359.

44.Pontvianne, F., Blevins, T., Chandrasekhara, C., Feng, W., Stroud, H., Jacobsen, S.E., Michaels, S.D. and Pikaard, C.S. (2012) Histone methyltransferases regulating rRNA gene dose and dosage control in *Arabidopsis*. *Genes Dev*, **26**, 945-957.

45.Preuss, S. and Pikaard, C.S. (2007) rRNA gene silencing and nucleolar dominance: insights into a chromosome-scale epigenetic on/off switch. *Biochim Biophys Acta*, **1769**, 383-392.

46.Earley, K.W., Pontvianne, F., Wierzbicki, A.T., Blevins, T., Tucker, S., Costa-Nunes, P., Pontes, O. and Pikaard, C.S. (2010) Mechanisms of HDA6-mediated rRNA gene silencing: suppression of intergenic Pol II transcription and differential effects on maintenance versus siRNA-directed cytosine methylation. *Genes Dev*, **24**, 1119-1132.

47.Tucker, S., Vitins, A. and Pikaard, C.S. (2010) Nucleolar dominance and ribosomal RNA gene silencing. *Curr Opin Cell Biol*, **22**, 351-356.

48.Layat, E., Cotterell, S., Vaillant, I., Yukawa, Y., Tutois, S. and Tourmente, S. (2012) Transcript levels, alternative splicing and proteolytic cleavage of TFIIIA control 5S rRNA accumulation during *Arabidopsis* thaliana development. *Plant J*, **71**, 35-44.

49.Rodio, M.E., Delgado, S., De Stradis, A., Gomez, M.D., Flores, R. and Di Serio, F. (2007) A viroid RNA with a specific structural motif inhibits chloroplast development. *Plant Cell*, **19**, 3610-3626.

50.Yu, A., Lepere, G., Jay, F., Wang, J., Bapaume, L., Wang, Y., Abraham, A.L., Penterman, J., Fischer, R.L., Voinnet, O. *et al.* (2013) Dynamics and biological relevance of DNA demethylation in *Arabidopsis* antibacterial defense. *Proc Natl Acad Sci U S A*, **110**, 2389-2394.

51.Sha, A.H., Lin, X.H., Huang, J.B. and Zhang, D.P. (2005) Analysis of DNA methylation related to rice adult plant resistance to bacterial blight based on methylation-sensitive AFLP (MSAP) analysis. *Mol Genet Genomics*, **273**, 484-490.

52.Boyko, A., Kathiria, P., Zemp, F.J., Yao, Y., Pogribny, I. and Kovalchuk, I. (2007) Transgenerational changes in the genome stability and methylation in pathogen-infected plants: (virus-induced plant genome instability). *Nucleic Acids Res*, **35**, 1714-1725.

53.Rodriguez-Negrete, E., Lozano-Duran, R., Piedra-Aguilera, A., Cruzado, L., Bejarano, E.R. and Castillo, A.G. (2013) Geminivirus Rep protein interferes with the plant DNA methylation machinery and suppresses transcriptional gene silencing. *New Phytol*, **199**, 464-475.

54.Vaillant, I., Tutois, S., Cuvillier, C., Schubert, I. and Tourmente, S. (2007) Regulation of *Arabidopsis* thaliana 5S rRNA Genes. *Plant Cell Physiol*, **48**, 745-752.

55.Muhlbach, H.P. and Sanger, H.L. (1979) Viroid replication is inhibited by alpha-amanitin. *Nature*, **278**, 185-188.

56. Li, L.C. and Dahiya, R. (2002) MethPrimer: designing primers for methylation PCRs. *Bioinformatics*, **18,** 1427-1431.

SUPPLEMENTAL DATA

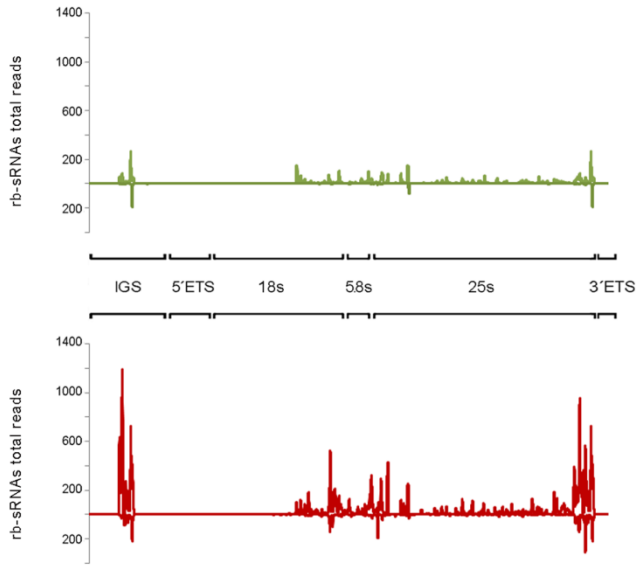

Figure S1. Analysis of ribosomal-derived sRNAs differentially expressed in infected cucumber plants. The rb-sRNAs recovered from mock inoculated (green lines) or infected (red lines) plants were plotted according the position of their 5´-extrem onto the sequence of the cucumber rRNA in either sense (above the X-axis) or antisense (below the X-axis) configuration. The values in the Y-axis represent the number of total reads in each library

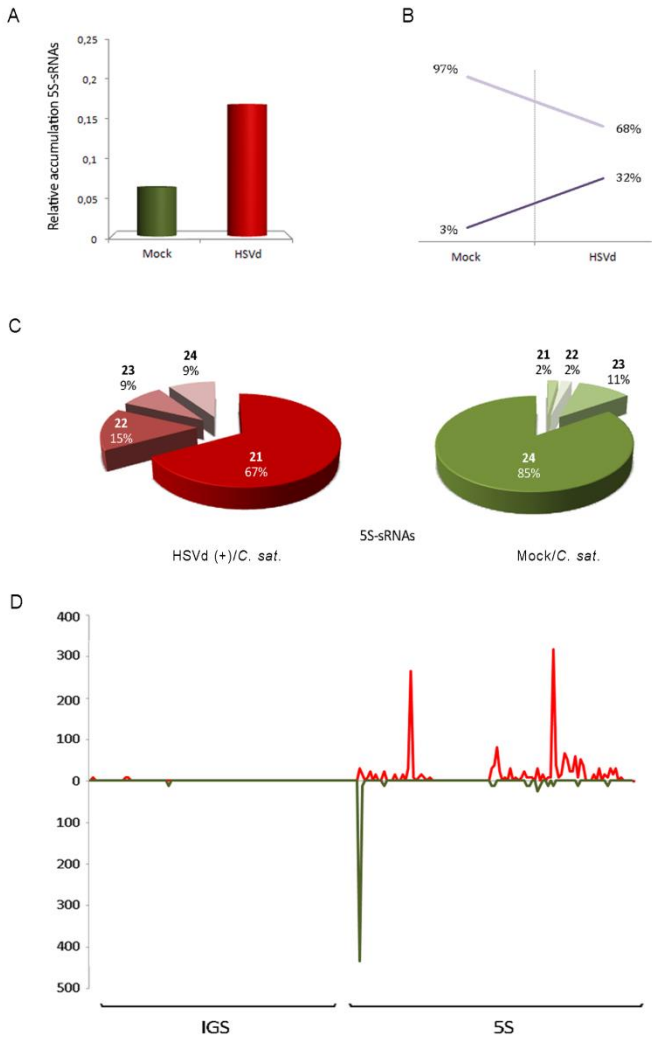

Figure S2. Analysis of the 5SrRNA-derived small RNAs recovered from cucumber leaves by deep sequencing. (*A*) Differential recovering of 5S derived sRNAs (5S-sRNAs) from infected and healthy tissues. The accumulation of 5S-sRNAs is expressed as the percentage of total 5S-sRNAs from the overall sRNAs in the library. (*B*) The relative accumulation of total 5S-sRNAs complementary to rRNA transcripts increased in the HSVd-infected plants (left). *C*) Graphic representation of the distribution of the total reads of 5S-sRNAs (ranging between 21 and 24 nt) recovered from both the HSVd-infected (left) and control (right) analyzed samples. (*D*) The 5S-sRNAs recovered from the infected (above the X-axis) or the mock-inoculated plants (below the X-axis) were plotted according to the position of their 5´-end onto the cucumber 5S-rRNA sequence. The values on the Y-axis represent the number of total reads/million in each library. The nucleotide positions -143 to +5 of the rRNA analyzed region are represented on the X-axis.

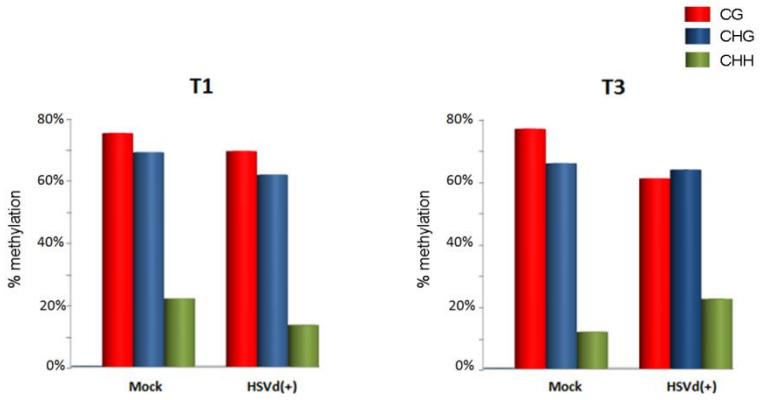

Figure S3. Histograms documenting the detailed analysis of the cytosine methylation in the CG (red bars), CHG (blue bars) and CHH (green bars) sequence context in Mock-inoculated and HSVd-infected cucumber plants at both T1 (10 dpi) and T3 (30 dpi) infection times.

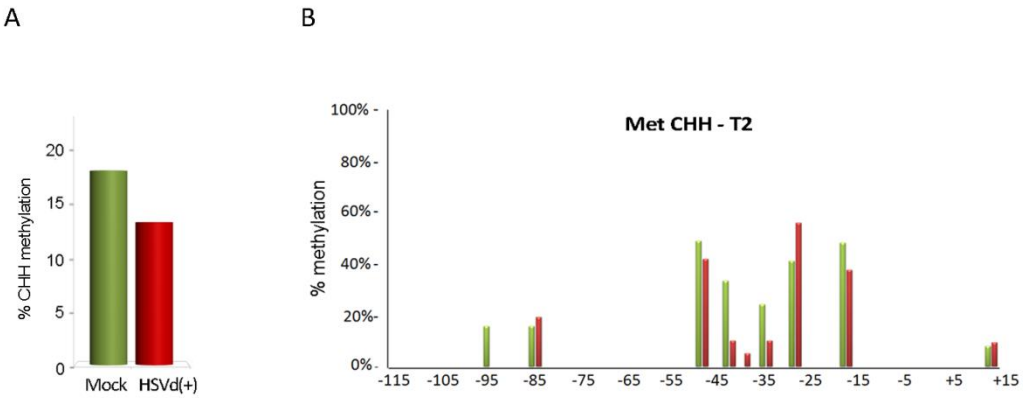

Figure S4. Methylation in the CHH sequence context at T2 infection point (*A*) Schematic representation of the cytosine methylation levels observed in mock inoculated (green bars) and HSVd-infected (red bars) plants. (*B*) Positions of methylcytosines in the analyzed regions displayed in the asymmetric context. The height of the bar represent the frequency at which cytosine is methylated.

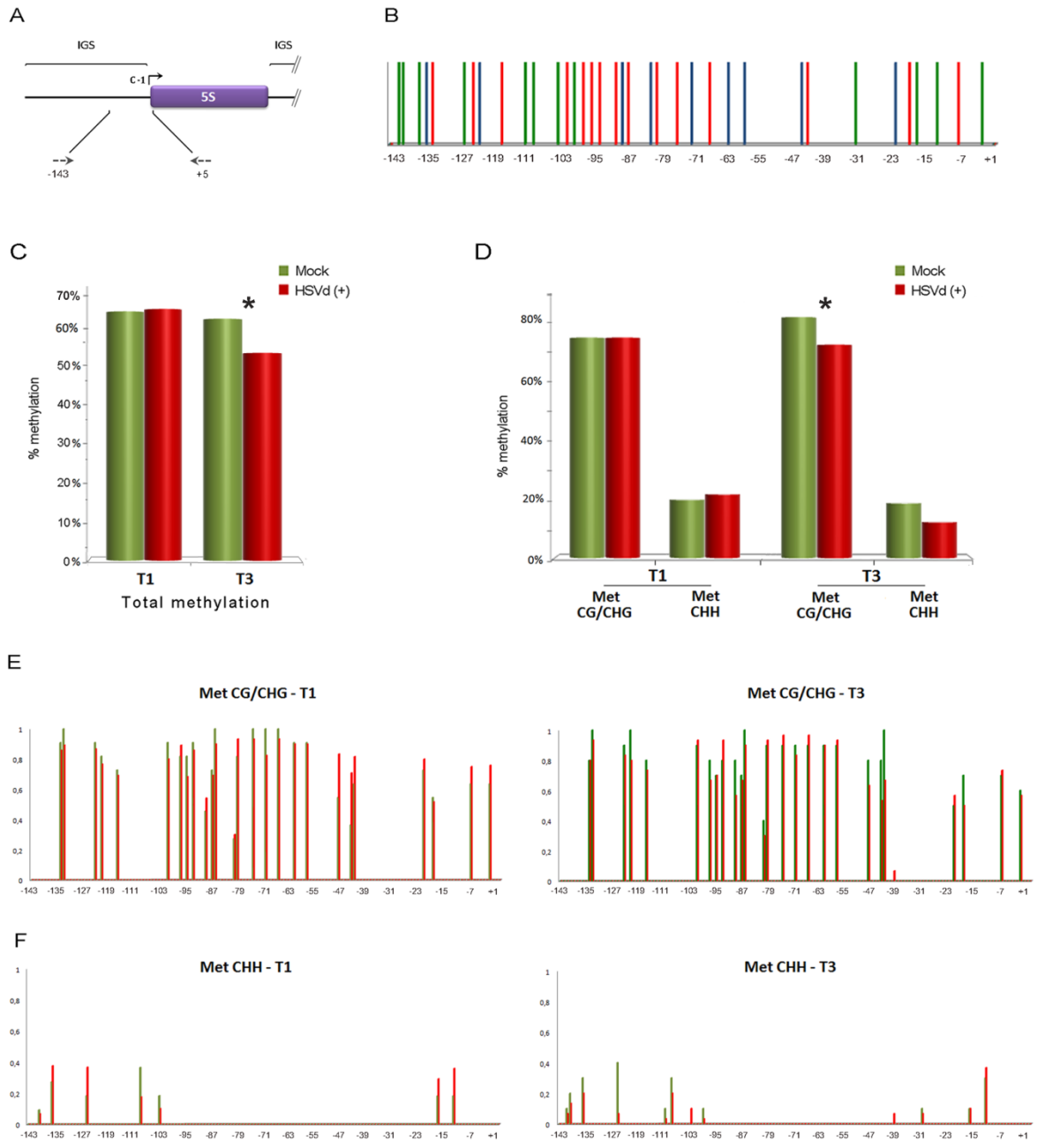

Figure S5. HSVd infection affects the methylation patterns in 5S-rRNA genes. (*A*) Diagram of the 5S-rRNA gene highlighting the zone analyzed by bisulfite sequencing. The arrows represent the oligos used in the PCR assay and their relative position in the 5S-rRNA gene. (*B*) Graphic representation of the potential symmetric (CG – red bars - and CHG – blue bars) and asymmetric (CHH – green bars) positions predicted to exist within the analyzed region. (*C*) Histogram documenting the relative (HSVd/Mock) DNA methylation levels at infection times T1 (means total methylation: mock, 0.642; infected 0.648) and T3 (Paired t-test values T3: means total methylation (mock) 0.624, (infected) 0.536, t=4.6837; **P* < 0.0005). (*D*) Schematic representation of the differential analysis of both symmetric and asymmetric cytosine methylation at infection times T1 (means symmetric methylation (mock) 0.762, (infected) 0.762; means CHH methylation (mock) 0.206, (infected) 0.243) and T3 (Paired t-test values T3: means symmetric methylation (mock) 0.811, (infected) 0. 727, t=4.294; means CHH methylation (mock) 0.181, (infected) 0.120, t=1.79; **P* < 0.0005). (*E*) Positions of methylcytosines in the analyzed regions displayed in the symmetric (CG and CHG) context. (*F*) Positions of methylcytosines in the analyzed regions displayed in the asymmetric context. The height of the bar represents the frequency at which cytosine was methylated at the analyzed infection times T1 (left) and T3 (right).

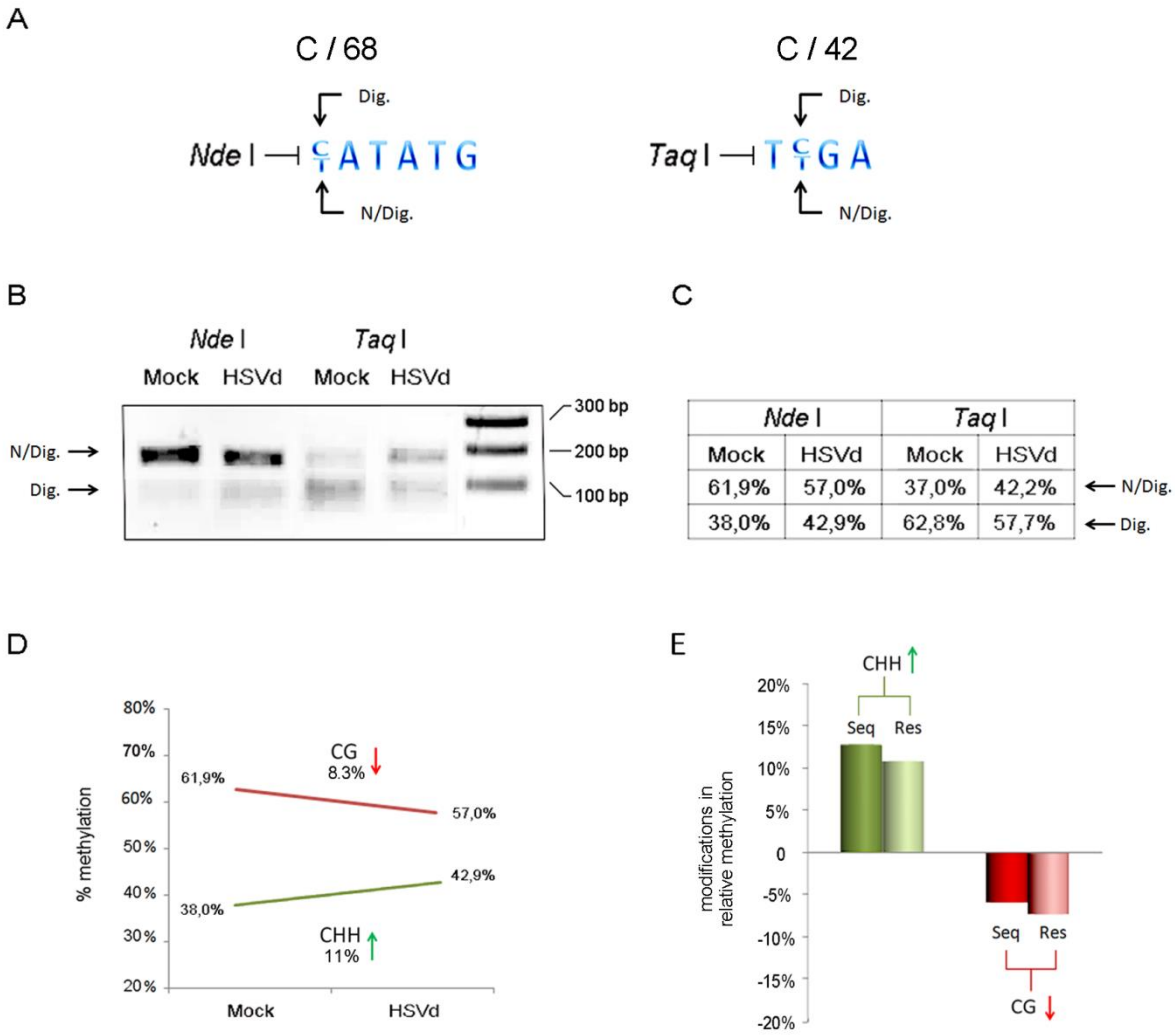

Figure S6. Combined bisulfite and restriction analysis of the methylation alterations induced by HSVd-infection in 45S-rDNA. (*A*) Graphic representation of the *Nde* I and *Taq* I analyzed restriction sites showing the possible presence of C or T according methylation status in both analyzed asymmetric and symmetric sequence contexts C/68 (CHH) and C/48 (CG) respectively. (*B*) Electrophoresis in 1.5% agarose gel of PCR products amplified from 45S-rRNA digested with *Nde* I and *Taq* I restriction enzymes. Dig and N/Dig refers to digested and non-digested DNA respectively. (*C*) Values for relative pixel intensity observed for each analyzed band. (*D*) Histogram documenting the alterations in the relative (HSVd/Mock) DNA methylation levels (in the C/68 and C/42) at infection times T3 determined by restriction analysis. (*E*) Comparative analysis of the alterations induced by HSVd-infection in the methylation levels (in cytosine residues in position C/68 and c/42) estimated by bisulfite sequencing (Seq) and restriction analysis (Res).

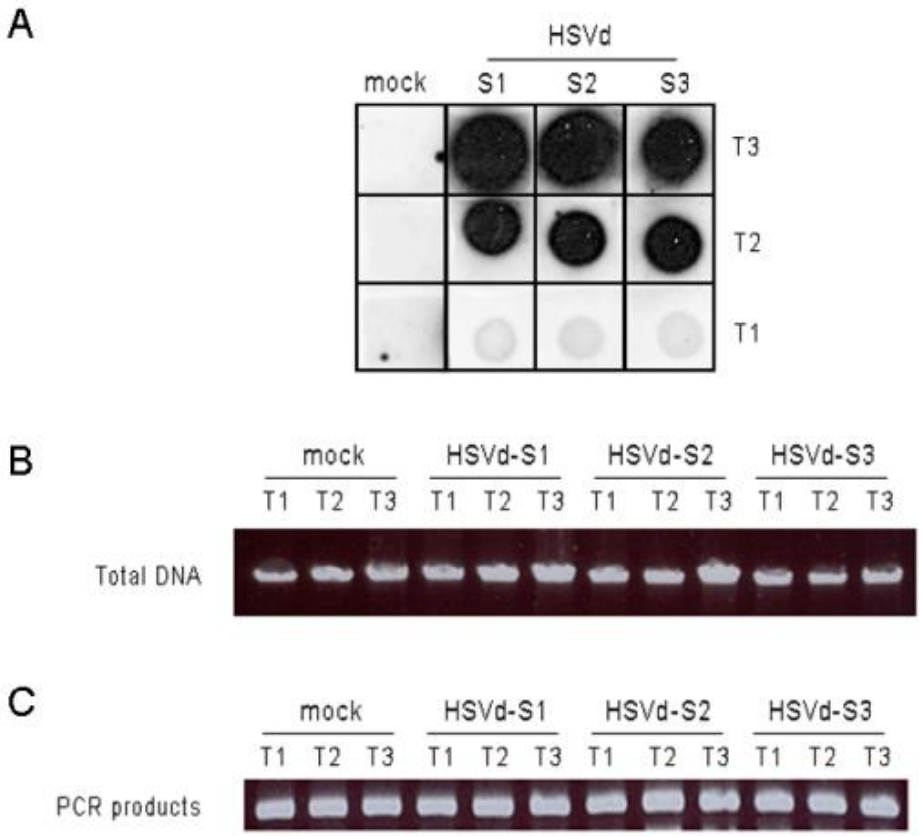

Figure S7. Selection of the HSVd infected cucumber plants. (*A*) Total RNAs extracted from leaves of a pool (six) of mock-inoculated and three HSVd-infected cucumber plants (S1, S2 and S3) used in this work, were analyzed by Dot-blot assays (using a HSVd-specific probe) at T1 (10 dpi), T2 (20dpi) and T3 (30 dpi) infection times. (*B*) Electrophoresis in 1% Agarose gel of the total DNA extracted from mock-inoculated and HSVd-infected plants. (C) DNA extracted from mock-inoculated and infected plants was treated with bisulfite and amplified by PCR using specific primers for rRNA transcriptional unity.

SUPPLEMENTARY MATERIAL

Plant Material

Twelve days-old cucumber (*Cucumis sativus Cv* Suyo*)* plants were agro-inoculated with *Agrobacterium tumefaciens* strain C58C1 transformed with a binary pMOG800 vector carrying a head-to-tail infectious dimeric HSVd cDNA (Y09352) (36) or an empty vector, in both cotyledons. Plants were maintained in growing chambers at 30°C for 16 h with fluorescent light and at 25 °C for 8 h in darkness, and analyzed at 10 (T1), 20 (T2) and 30 (T3) days post infiltration. In each analyzed point (T1, T2 and T3) we collect the third leaf below apical end in both infected and mock-inoculated plants. Leaves of three similarly infected cucumber plants were used in this analysis (Fig. S7*A*). A pool of six different mock inoculated plants was used as control.

RNA extraction and Northern blot analysis

Total RNA were extracted using TRI reagent (SIGMA, St. Louis, MO, USA) according to the manufacturer instructions. Briefly, 500 mg of leaves from HSVd-infected and control plants were ground in 2ml of TRI reagent, 400 µl of chloroform was then added and the sample was vigorously vortexed, followed by centrifugation. The supernatant was recovered and the totals RNA were precipitated with isopropanol. The RNA pellet was resuspended in sterile water and phenol-chloroform extracted. The supernatant was recovered and total RNAs were precipitated (1/10 volume 3 M sodium acetate, 2 volume ethanol) and resuspended in 50 µl of sterile water. The total RNAs preparations were quantified by spectrometry and their concentration equalled.

To detect the rRNAs, serial dilution of total RNAs pooled from the three HSVd-infected and mock-inoculated plants at 30 dpi (T3) were loaded on denaturing 1% agarose-formaldehyde gel in 1x MOPS buffer. The gel was run at 100 V for 1 h and then the RNA was transferred to positively charged Nylon membranes (ROCHE Diagnostics GmbH, Manneiheim, Germany). Hybridization was performed at 68°C for 14–16 h, using as probe, Digoxigenin-labelled strand-specific for 3´end of the cucumber 25S-rRNA.

To detect the small RNAs, 200 ng of small RNA enriched total RNA were loaded on 15% polyacrylamide gel, 0,25 x TBE, 8 M urea. The gel was run at 100 V for 2 h and then the RNA was transferred to positively charged Nylon membranes (ROCHE Diagnostics GmbH, Manneiheim, Germany). Hybridization was performed at 35°C for 14–16 h, using as probe, Digoxigenin-labelled strand-specific for HSVd-RNA, IGS-r of the rRNA and csat-miR367. The membranes were washed with 2x SSC, 0.1% SDS for 15 min at 35ºC and 0.1x SSC, 0.1% SDS for 15 min at 37°C. In both hybridization assays chemiluminescent detection was performed as previously described (39).

Bisulfite Conversion and Sequencing

Total genomic DNA was extracted from HSVd-infected and mock-inoculated leaves using previously described protocol (40) (Fig. S7*B*). Total DNA (1ug) was diluted en into 20 µL of water and further subjected to bisulfite treatment using the EpiTect Bisulfite kit (Qiagen), according to the manufacturer instructions. The rRNA region to be analyzed and the corresponding oligos were determined using the MethPrimer software http://www.urogene.org/cgi-bin/methprimer (56). PCRs were performed using Taq DNA polymerase (Promega) and analyzed in 1.5% agarose gel (Fig. S7*C*). PCR products were purified from gel extraction and cloned using the pTz cloning kit (Fermentas). Thirteen to 24 clones were sequenced from each analyzed point from mock-treated and HSVd-infected samples. Three independent biological replicates were analyzed for each analysis point in HSVd-infected plants. A pool of six different mock inoculated plants was used as control.

Combined bisulfite and restriction analysis

45S-derived PCR products amplified from total DNA (extracted at T3) subjected to bisulfite treatment (250 ng) were digested with *Nde* I and *Taq* I to corroborate the methylation levels determined by sequencing in the positions C/68 and C/42 respectively. The digestion products were analyzed in 1.5% agarose gel and digitalized (Fig. S6*B*). The bands intensity was measures using the Image-J application http://www.imagej.en.softonic.com/ (Fig. S6*C*). The methylation level in each position was estimated as the relative signal intensity in the digested DNA.

Estimation of the cucumber 45S-rRNAand 5S-rRNA sequence

The 45S-rRNA sequence used in this work was constructed by assembling and overlapping of partial rRNA sequences recovered from the gene bank (accessions: X07991, AF017157, AM981112 and X51542). The *C. Sativus* 5S-rRNA sequence used for sRNAs alignment was obtained from the gene bank (accession: AY424363.1)

Supplementary refrences

56. Li, L.C. and Dahiya, R. (2002) MethPrimer: designing primers for methylation PCRs. *Bioinformatics*, **18,** 1427-1431.

CAPÍTULO SEGUNDO

Este capítulo ha dado lugar a la siguiente publicación:

Castellano, M., Martínez, G., Pallas, V. and Gómez, G. (2015).

Alterations in host DNA methylation in response to constitutive expression of Hop stunt viroid RNA in Nicotiana benthamiana plants. *Plant Pathology*.

64: 1247-1257. Doi: 10.111/ppa.12358

Title:

Alterations in host-DNA methylation in* response to constitutive expression of *Hop stunt viroid RNA* in *Nicotiana benthamiana plants

Authors:

M. Castellano[1], G. Martinez[1,2], V. Pallas[1] and G. Gomez[1]*

Authors Address:

[1] Instituto de Biología Molecular y Celular de Plantas (IBMCP), Consejo Superior de Investigaciones Científicas (CSIC)-UPV, CPI, Edificio 8 E, Av. de los Naranjos s/n, 46022 Valencia, Spain.

[2] Present addresses: Center for RNA Biology. The Ohio State University, Columbus, OH 43210, USA.

Running title:

Viroid and host epigenetic response

Keywords:

1- Viroid pathogenesis

2- Epigenetic response to infections

3- Pathogenic noncoding RNAs

4- Viroid-host interactions

SUMMARY

Increasing evidence points to the epigenetic regulation of the transcriptional activity as a general mechanism controlling host-response to pathogen-infection. Recent results revealed that cucumber plants infected with *Hop stunt viroid* (HSVd) showed alterations in the DNA methylation-pattern of usually silenced rRNA-genes that are consequently transcriptionally reactivated during infection. These results indicated that, at least in cucumber, HSVd-pathogenesis could be associated to disruptions in the transcriptional mechanisms regulated by epigenetic modifications of host-DNA. To determine if this disorder in host-regulatory activity can be a common phenomenon that can occur in other viroid-host combinations, here we analyze the transcriptional activity in transgenic *N. benthamiana* constitutively expressing HSVd. We observed that the HSVd-RNA accumulation in *N. benthamiana* mimics the alteration induced by the viroid-infection in cucumber, promoting the unbalance in the accumulation of ribosomal-derived sRNAs. Bisulfite sequencing demonstrates that this phenomenon is linked to a loss of symmetric cytosine methylation and correlates with an increasing accumulation of rRNAs precursors in *HSVd/Nb* plants. Our data supports that the interference of this pathogenic-*lncRNA* in the epigenetic mechanisms (associated to rDNA-methylation) controlling plant-gene expression is not restricted to a specific host, suggesting that may constitute a more general phenomenon able to occur in other viroid-plant interactions.

INTRODUCTION

Viroids, proposed survivors of the ancient RNA-based world (Flores *et al*., 2014), are plant-pathogenic noncoding RNAs (*ncRNAs*) composed of a circular single-stranded molecule ranging from 240 to 400 nt in length (Ding 2010; Navarro B *et al.,* 2012; Palukaitis 2014). They are classified into two families: *Pospiviroidae*, (with nuclear replication), and *Avsunviroidae*, (that replicate in chloroplasts of infected cells) (DiSerio *et al*., 2014). Lacking protein-coding activity, viroids are compelled to hijack endogenous *ncRNA*-directed regulatory routes to complete their life cycle in the infected cell. Consequently, the study of viroid interactions with cellular factors can help to decipher the regulatory networks mediated by ncRNAs in plants (Gomez & Pallas, 2013).

A large body of experimental evidence obtained in the last years has contributed to elucidate basics steps of viroid life-cycle in the infected cell such as compartmentalization (Gomez & Pallas, 2012; Zao *et al.,* 2001), replication (Navarro *et al.,* 2000; Nohales *et al.,* 2012; a and b) and movement (Gomez & Pallas, 2001 and 2004; Owens *et al.,* 2001; Zhong & Ding, 2008). However, the plant-regulatory pathways subverted by these ncRNAs to promote symptoms expression in infected hosts remains yet, to be completely deciphered.

Viroids trigger a RNA silencing response on their hosts inducing the production of sRNAs termed viroid derived-sRNAs (vd-sRNAs). This interaction with the RNA silencing pathways highlights the idea that there could exist a close link between functional alterations associated to viroid-infection and RNA silencing. In this aspect, it was initially proposed that vd-sRNAs could down-regulate *in trans*, host mRNAs with which they would share a high degree of complementarity (Gomez & Pallas, 2009; Papaefthimiou *et al*., 2001; Wang *et al*., 2004). This hypothesis was confirmed by the observation that the expression of host symptoms is associated with post-transcriptional RNA silencing in members of both *Pospiviroidae* (Eamens *et al.,* 2014; Gomez *et al.,* 2008) and *Avsunviroidae* (Navarro *et al.,* 2012) families. However, although the interaction between viroids and RNA silencing has been partially well characterized, the possibility that in some viroid-host interactions additional ncRNA-dependent regulatory mechanisms could be disrupted by infection, involving alterations in plant gene-expression at transcriptional levels is stills plausible. This emerging notion correlates for example, with the observed in bacterial infection where host-response at both post-transcriptional (Navarro *et al.,* 2006) and transcriptional (Dowen *et al*., 2012; Yu *et al*., 2013) levels, was described. In line with this possibility, host transcriptional alterations were reported in diverse plant-viroid pathogenic interactions (Fussi *et al.,* 2013; Herranz *et al.,* 2013; Itaya *et al.,* 2002; Lison *et al.,* 2013; Owens *et al*., 2012; Tessitori *et al*., 2007).

Increasing evidence points to the epigenetic regulation of the transcriptional activity as a general regulatory mechanism controlling the host responses to pathogen infection. Indeed, an epigenetic regulation of host-genomes has been confirmed for bacteria (Dowen *et al*., 2012; Yu *et al*., 2013) virus (Raja *et al*., 2008; Rodriguez-Negrete *et al*., 2013; Yang *et al*., 2013) and viroid (Martinez *et al*., 2014) infections.

In the case of viroids, it has been shown that cucumber plants infected with *Hop stunt viroid* (HSVd) accumulated high levels of ribosomal-derived sRNAs with this accumulation linked to an increase in the transcription of rRNAs precursors (Martinez *et al.*, 2014). The higher transcription of rRNA-genes was correlated with an alteration in the dynamics of DNA methylation in their promoter region revealing that some rRNA-genes are demethylated and transcriptionally reactivated during infection. The data obtained in this study supports the idea that, at least in the model HSVd-cucumber, viroid-induced pathogenesis could be associated with disruptions in the biogenesis of endogenous sRNAs and/or transcriptional mechanism regulated by epigenetic modifications of the repetitive host-DNA. However, this evidence is not sufficient to assume that the alterations in host-transcriptional activity can be a general phenomenon in other viroid-pathogenic combinations. In addition, the lack of natural mutants in cucumber together with the difficulty to transform this species limits the potential of the interaction HSVd-cucumber to be used as experimental resource to attempt elucidating the molecular basis of this phenomenon. Remarkably, transgenic-based models (expressing viroid RNA) have been a valuable tool used to understand several aspects of viroid infectivity (Wassenegger *et al*., 1994), processing (Daros & Flores, 2004; Gas *et al*., 2007) resistance of mature forms to RNA silencing (Gomez & Pallas, 2007) and pathogenesis (Gomez *et al.,* 2008 and 2009; Wang *et al*., 2004). One of these transgenic models systems consists on *N. benthamiana* plants carrying a dimeric sequence of HSVd (*HSVd/Nb*) (Gomez & Pallas, 2006). These plants process, accumulate and systemically transport biological forms of the viroid, providing evidences that basics-steps of HSVd life-cycle occurs in this model.

Here, we report the use of the transgenic model *HSVd/Nb* to analyze if the alteration at transcriptional level observed in infected cucumber plants can take place in other HSVd-host. We used high-throughput sRNA sequencing to characterize the sRNA profiles of viroid-derived and host-endogenous sRNAs. This analysis showed that the accumulation of HSVd-RNA in *N. benthamiana,* mimics the alteration induced by the natural viroid-infection in cucumber. Moreover, we confirm that in this host, HSVd promotes the unbalance in the accumulation of ribosomal-derived sRNAs. Further analysis of the cytosine-methylation level of rRNA gene indicated that it is linked to a loss of symmetric cytosine methylation. Finally, it was demonstrated that this phenomenon correlates with an increasing accumulation of rRNAs precursors in *HSVd/Nb* plants.

RESULTS

The analysis of sRNAs recovered from the *HSVd/Nb* libraries revealed that 1.23% of the total reads were 100% complementary to the HSVd. These sRNAs were considered vd-sRNAs and used for subsequent analysis. The nucleotides contained in the vd-sRNAs represent 62.3 fold the length of the HSVd-genome, indicating that our data set constitutes a representative landscape of vd-sRNAs biogenesis in *N. benthamiana*. The distribution of vd-sRNAs over the HSVd-genome, confirmed that, as for previous reports, vd-sRNAs virtually cover the totality of the viroid molecule (Figure 1a). Sequences with expected DCL canonical sizes (21 to 24 nt) comprising the 96.9% of the total vd-sRNAs were used for further analysis (Fig. 1b). The sizes of vd-sRNAs were mainly 22 (50.23%), 21 (33.6%) and 24 (9.86%) nt in length (Fig. 1c). This profile of vd-sRNAs was slightly different to the previously reported for HSVd-sRNAs in cucumber and grapevine plants where the 21 nt in length was the predominant class (53% and 43% respectively). Considering their polarity, a comparable proportion of sense (54%) and antisense (46 %) vd-sRNAs species were similarly represented in the sequenced pool (Fig. 1d). Similar vd-sRNAs size and polarity distribution was observed when non-redundant sequences were analyzed (Fig. S3). To estimate their sequence complexity, non-redundant vd-sRNAs were plotted onto HSVd-RNA, as previously reported (Martinez *et al.,* 2010). This analysis revealed that the highest sequence complexity belonged to 22 nt vd-sRNAs, followed by 21, 24 and 23 nt in length (Fig. 1e). Altogether these results indicate that, as previously reported for HSVd-infected cucumber, *N. benthamiana* plants constitutively expressing HSVd equally accumulate plus and minus vd-sRNAs with no preference for any viroid-genome sequence or region.

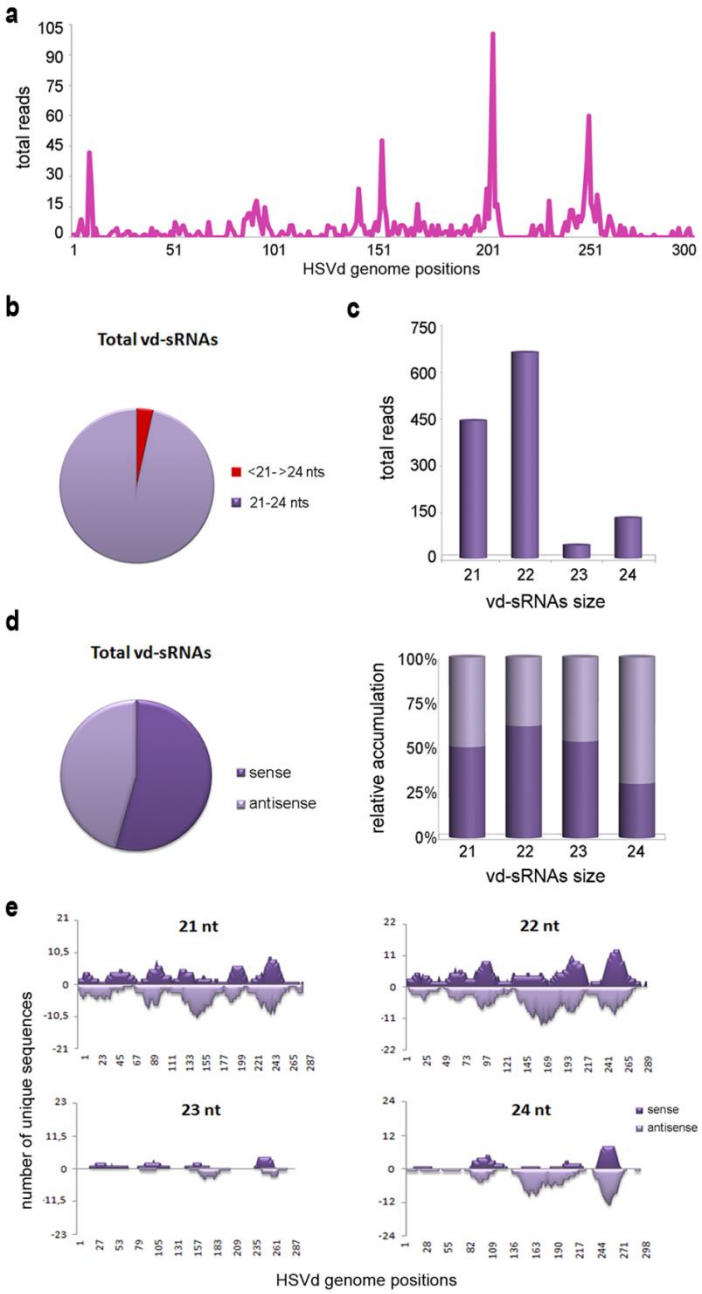

Figure 1: Characterization of vd-RNAs. a) Total vd-sRNAs were plotted according the position of their 5´-end onto the HSVd-sequence (Y09352). The values in the Y-axis represent the vd-sRNAs abundance in the library. In the X-axis are represented the HSVd-RNA nucleotide positions. b) vd-sRNAs with expected DCL canonical sizes representing the 95% of the total reads were used in subsequent analysis. c) Histogram illustrating the size distribution of the vd-sRNAs. d) Graphic representation of relative accumulation of sense and antisense vd-sRNAs, showed as total reads (left panel) or classified according size (right panel). e) View of HSVd-genome showing the number of plotted unique vd-sRNAs, according size class (21, 22, 23 and 24-nt). In the Y-axis are represented the times that a single HSVd nucleotide was present in a sense (above the X-axis) or antisense (below the X-axis) unique vd-sRNAs.

To estimate the potential alteration in the general profiles of endogenous sRNAs, induced by viroid accumulation in *N. benthamiana*, we compared the size distribution of the total reads (ranging 21-24 nt) recovered from untransformed (Fig. 2a) and *HSVd/Nb* plants (Fig. 2b). The 21 and 22 nt in length were the sRNAs with increased accumulation in *HSVd/Nb* plants, while the 24 nt size-class was relatively most abundant in the control (Fig. 2c). The 23 nt sRNAs showed equivalent accumulation levels in both analyzed populations. A comparable sRNA distribution was observed when non-redundant sequences recovered from both datasets were analyzed (Fig. S4), denoting that, in *N. benthamiana*, viroid accumulation correlates with alterations in the accumulation and diversity of endogenous sRNAs, being mainly the 21 nt and 24 nt the species showing respectively, up- and down-regulation.

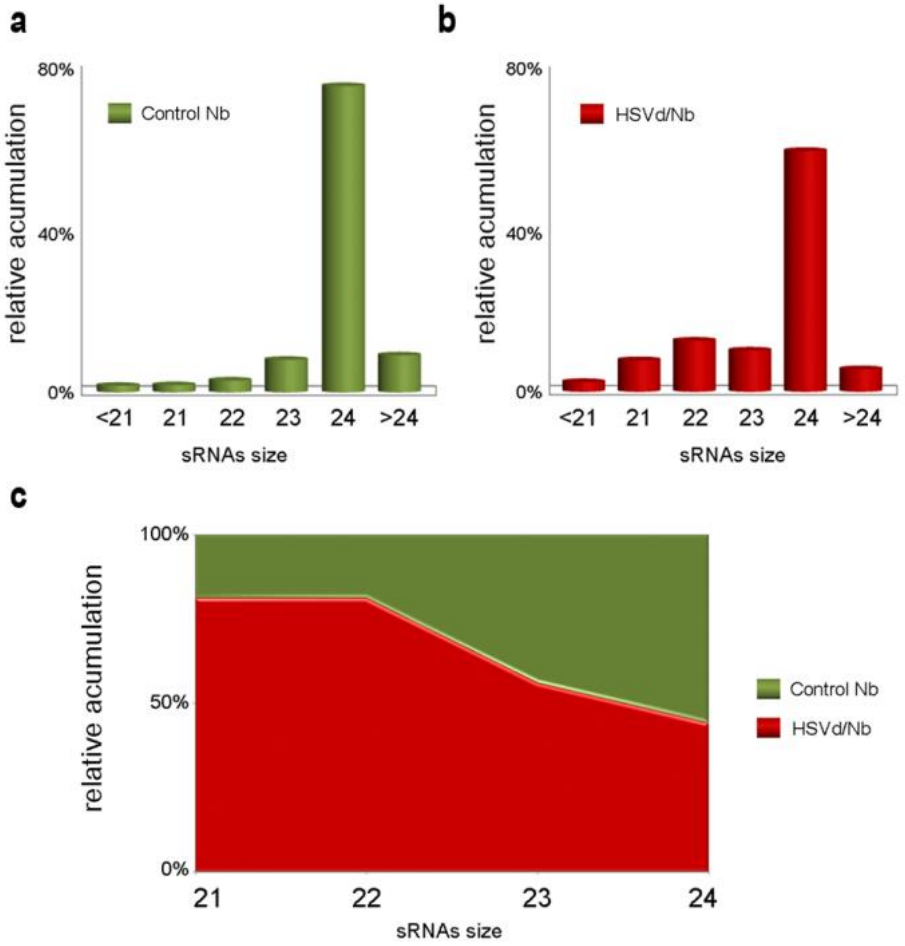

Figure 2. Characterization of the endogenous N. Benthamiana sRNAs. Graphic representation of the differential accumulation and distribution of the total reads of endogenous sRNAs recovered from both (a) the control and (b) HSVd/Nb samples. c) Comparative of the relative accumulation of total reads (ranging between 21 and 24 nt) recovered from both untransformed (gren) and HSVd/Nb (red) plants.

In order to determine if, as observed in cucumber, changes in the general profile of sRNAs induced by HSVd-infection is associated with alterations in the metabolism of ribosomal sRNAs in *N. benthamiana*, we compared by pairwise alignment against the 45S ribosomal genomic sequence, the sRNAs distribution for *HSVd/Nb* and control plants. In contrast with the observations in cucumber, the global accumulation of 45S rRNA-derived sRNAs (rb-sRNAs) ranging from 21 to 24 nt was comparable in both samples (Fig. 3a). However, a significant difference was observed when comparing the differential accumulation of rb-sRNAs according to size distribution. As shown in Figure 3b, rb-sRNAs of 21 and 24 nt were respectively up- and down recovered from the *HSVd/Nb* dataset in comparison to the control. This change in rb-sRNAs profile is not only with reference to total number of sequences (accumulation) but also to non-redundant sequences (diversity) (Fig. S5). Although these variations in accumulation of rb-sRNAs are consistent with the alteration in the global *N. benthamiana* sRNAs population, the increase/decrease of the rb-sRNAs in *HSVd/Nb* plants exceed the relative modification values observed when total sRNAs were analyzed (Fig. 3c).

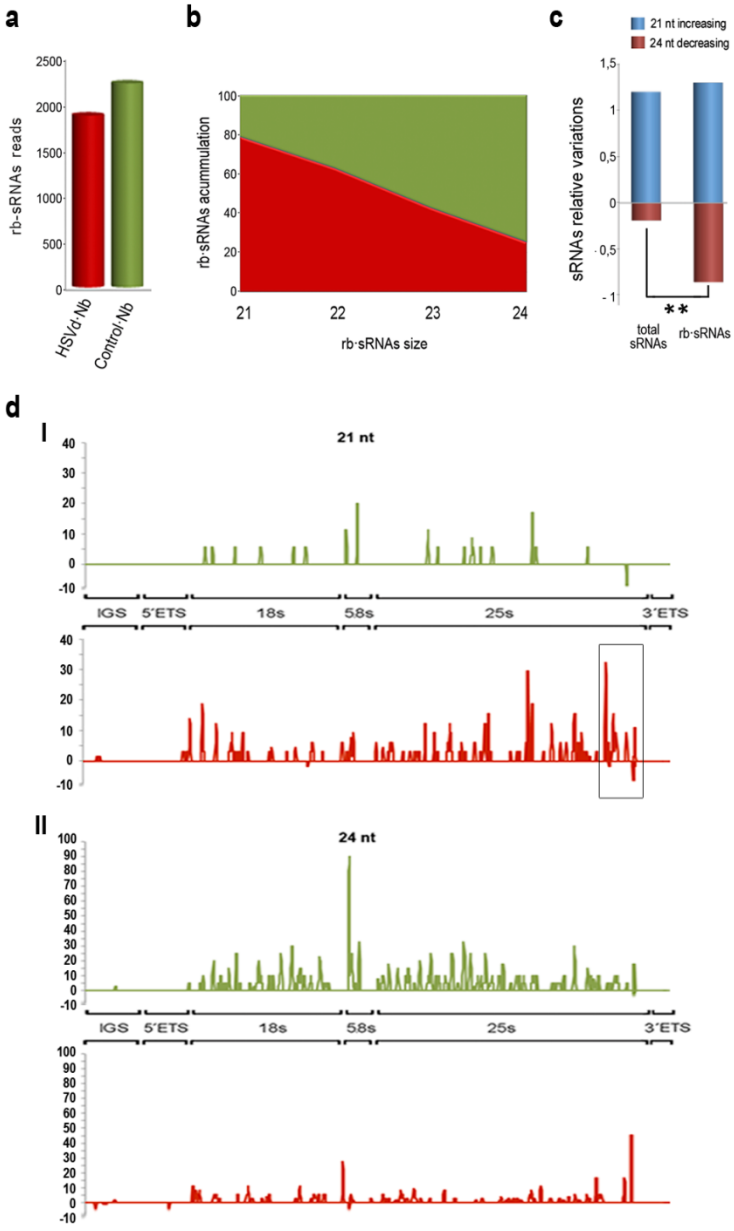

Figure 3. Differential recovering of rb-sRNAs from HSVd/Nb plants. a) The accumulation of normalized rb-sRNAs in HSVd/Nb and untransformed-Nb is expressed as total rb-sRNAs per 100.000 reads. b) Graphic representation of the distribution of the total rb-sRNAs (between 21 and 24 nt) recovered from both the control (green) and HSVd/Nb (red) samples, showing the increasing and decreasing of 21 and 24 nt rb-sRNAs respectively, in HSVd/Nb. c) Histogram representing the comparison between the relative alterations in the accumulation of normalized total and ribosomal-derived 21/24 nt in length sRNAs in HSVd/Nb plants compared to untransformed Nb. Significant difference in the decreasing of 24 nt rb-sRNAs in HSVd/Nb compared control plants estimated by Fisher´s exacts test, F= 0.482, ** p= 0,025. d) The 21 and 24 nt (panels I and II respectively) in length rb-sRNAs recovered from the HSVd/Nb (red bars) or the untransformed control plants (green bars) were plotted according to polarity (+ above and – below the X-axis) and position of their 5-end onto the rRNA sequence. The values on the Y-axis represent the number of normalized total reads in each library. The ≈ 300 bp region in the 3´-end of the rRNA transcripts containing hyper-accumulation of complementary 21 nt rb-sRNAs in HSVd/Nb plants is boxed in panel I.

When the rb-sRNAs were plotted onto rRNA sequence, we observed that the 21 nt rb-sRNAs recovered from *HSVd/Nb* showed a predominating accumulation hot spot (15.2% of the sRNAs) mapping in a region of 300 nt (3.7% of the total sequence) located between the position 6886 and 7186 of the 45S rRNA (Fig. 3d - panel I). No relevant differences in the distribution pattern of the 24 nt size-class were observed between the rb-sRNAs recovered from both samples (Fig. 3d – panel II). A similar rb-sRNA distribution characterized by increased recovery of 21 nt (potential products of the processing of ds-rRNAs) and decreased recovery of 24 nt rb-sRNAs (assumed to be involved in *de novo* methylation) has been recently associated with changes in the epigenetic regulation of the transcriptional activity of ribosomal genes in HSVd-infected cucumber (Martinez *et al*., 2014).

In plants, the 45S rRNA genes are transcribed by *RNA polymerase I* as rRNA precursor (pre-rRNA) that is subsequently processed into the different functional (18S, 5.8S and 25S) rRNAs (Fig. 4a). The transcriptional activity of these highly repetitive rRNA units is regulated by multilayered epigenetic mechanisms, one of then being the methylation of cytosine residues in the rDNA. To determine if the altered profiles of 24 nt rb-sRNAs observed in *HSVd/Nb* correlated with transcriptional deregulation of rDNA, we analyze the relative accumulation of pre-rRNAs in *HSVd/Nb* and control plants. Two primers complementary to specific regions of the ETS (Rv-1) and the 3´-end of 25S rRNAb (25S-Fw) (Fig. 4b) were used to detect by RT-PCR the unprocessed rRNA transcripts. As shown in Figure 4c and d, a significant increasing in the accumulation of pre-rRNAs transcripts was observed in *HSVd/Nb* in comparison to control plants. Considering that accumulation of mature rRNAs forms was comparable in both analyzed samples (Fig. S6), we assumed that differential accumulation of pre-rRNAs in *HSVd/Nb* is consequence of transcriptional deregulation of rRNA genes and not related to impairment of the pre-rRNA processing.

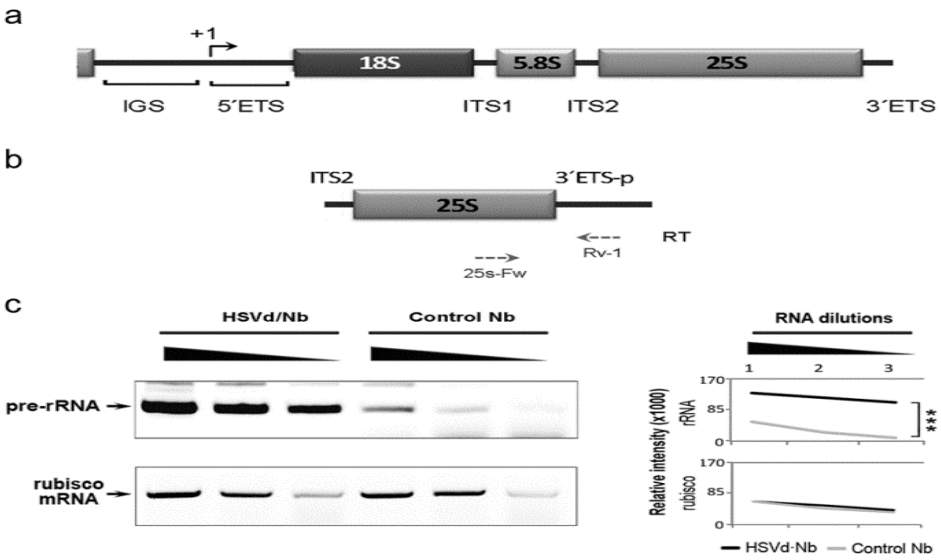

Figure 4: Pre-rRNAs accumulates differentially in HSVd/Nb plants. a) Diagram (no scale) of the rRNA gene. The rRNA gene repeats are arranged in long tandem arrays of 45S rRNA genes, each including the region for the 18S, 5.8S and 25S rRNAs, and separated from adjacent units by an IGS. The transcription start site is indicated by+1. The ETS and ITS are removed during rRNA processing. b) Diagram (no scale) of the analysed region of the pre-27S rRNA. The arrows below depict the primers used for the RT-PCR amplification. c) Representative analysis of the pre-rRNA expression in the HSVd/Nb and untransformed plants by RT-PCR amplification of serial dilutions of total RNAs. RT-PCR amplification of Rubisco mRNA served as control for RNA load. d) Relative accumulation of pre-rRNA and rubisco mRNA in analysed samples determined by measurement of band intensity. Significant increasing of pre-rRNAs in HSVd/Nb plants was determined by Fisher´s exacts test, F= 2.611, 4.38 and 10.46 for dilution 1, 2 and 3 respectively. ***P< $2.2x10^{-16}$. The band intensity was measured using the Image-J application http://www.imagej.en.softonic.com.

To determine if the alterations in rRNAs transcription observed in *HSVd/Nb* correlate with modifications in the cytosine methylation, a 474-bp region (comprised between the position –1 and +473) corresponding to the initial region of *N. benthamiana* 45S-rDNA gene was analyzed by bisulfite sequencing (Fig. 5a). Genomic DNA obtained from both transformed and control plants were bisulfite converted, amplified by PCR and cloned for sequencing. The sequences analysis revealed that viroid accumulation in *HSVd/Nb* plants resulted in a decrease (11.6%) in the relative number of total cytosine methylation in this region of the 45S rDNA (Fig. 5b). A deeper analysis considering both symmetric and asymmetric sequence contexts, revealed two different situations. The level of symmetric methylation showed a significant reduction (15.5%) in *HSVd/Nb* plants, however a slight increase in the relative values was observed when considering methylation at the asymmetric (CHH) sequence context (Fig. 5c). Our observations indicate that, in consonance with the described in infected cucumber, in *HSVd/Nb* plants, viroid accumulation induces an alteration in the dynamic methylation profiles promoting CG/CHG demethylation and CHH hypermethylation of the 45S rDNA. To obtain a more accurate picture of the interference of HSVd in the dynamic regulation of rRNA transcription in *N. benthamiana*, we also analyze the methylation status of 5S rDNA. Bisulfite sequencing assays of a 193-bp region of 5S rDNA showed that, the methylation pattern of these ribosomal transcriptional units is also significantly altered in *N. benthamiana* plants as consequence of HSVd accumulation (Fig. 6b). This alteration was observed in both symmetric and asymmetric sequence contexts (Fig. 6c). Altogether these results provide evidence supporting the existence, in *N. benthamiana*, of a functional link between methylation-dependent control of the rDNA transcription and persistent HSVd-accumulation.

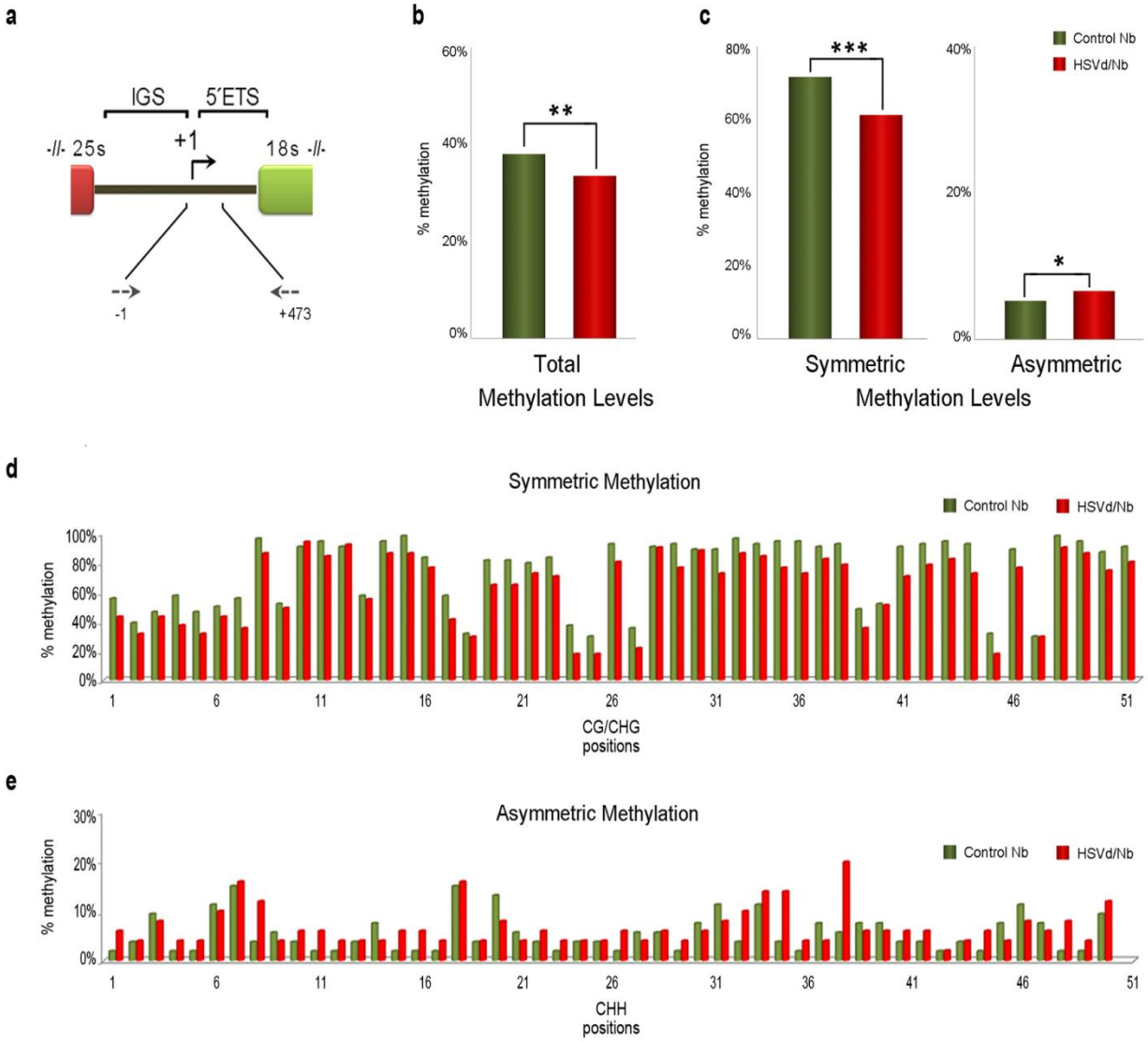

Figure 5: HSVd accumulation affects the methylation patterns in 45S rRNA genes. a) Diagram of the rRNA intergenic region highlighting the zone analyzed by bisulfite sequencing. The arrows represent the position of the primers used in the PCR assay. b) Histogram documenting the total DNA methylation levels in HSVd/Nb and control Nb plants (paired t-test values: means total methylation (control) 0.386, (HSVd/Nb) 0.340, t=5.879; **P<5x10^{-8}. c) Schematic representation of the differential analysis of both symmetric (CG and CHG) and asymmetric (CHH) cytosine methylation levels (paired t-test values: means symmetric methylation (control) 0.713, (HSVd/Nb) 0.609, t=11.555; means asymmetric methylation (control) 0.0529, (HSVd/Nb) 0.0658, t= -2.645; ***P<5x10^{-16}, *P<0.01). d) Positions of methylcytosines in the analyzed regions displayed in the symmetric (CG and CHG) context. e) Positions of methylcytosines in the analyzed regions displayed in the asymmetric context. The height of the bar represents the frequency at which cytosine was methylated in both control Nb (green) and HSVd/Nb (red) samples.

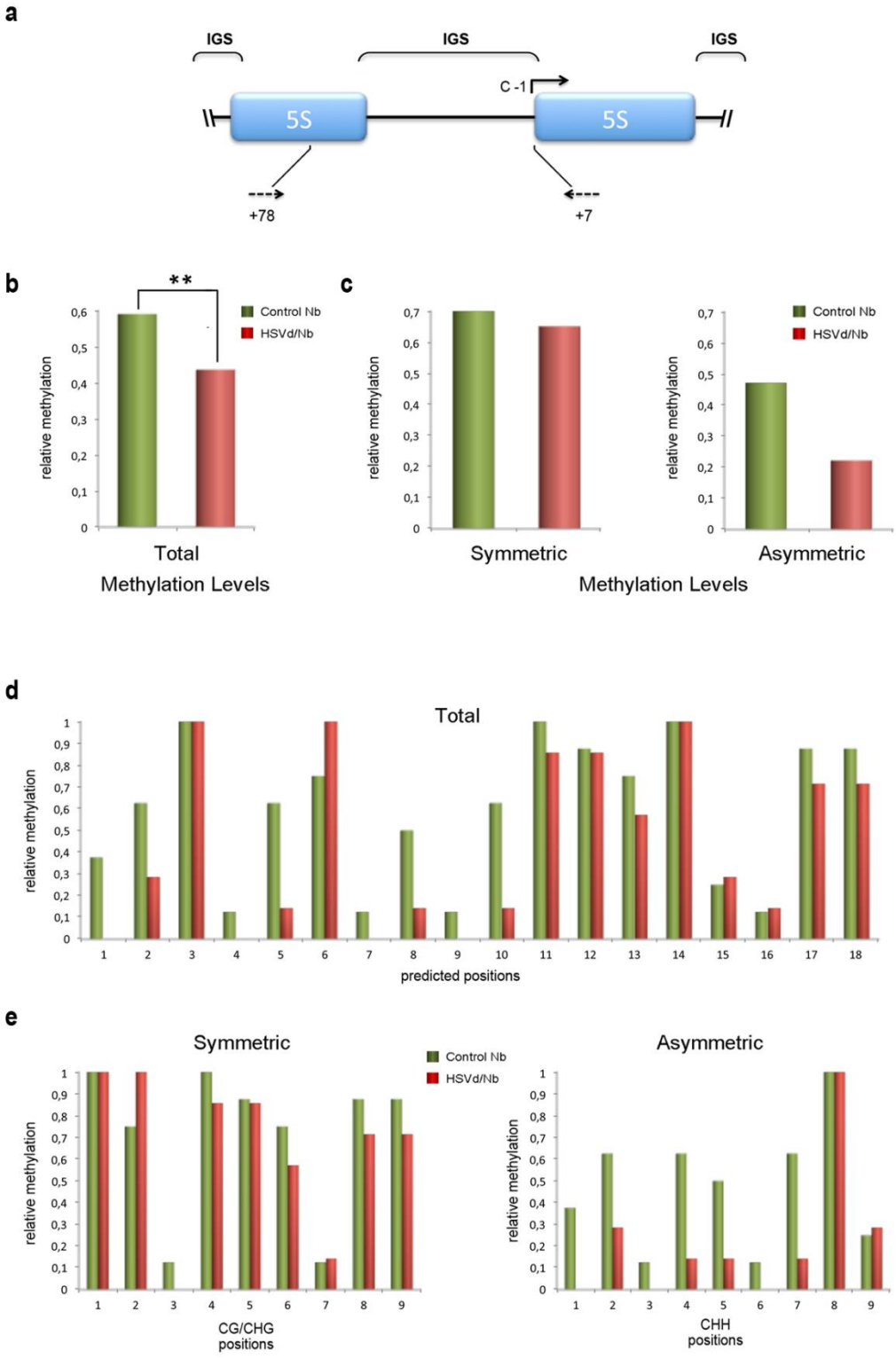

Figure 6: HSVd affects the methylation patterns in 5S rRNA genes. a) Diagram of the 5S rRNA transcriptional unit highlighting the zone analyzed by bisulfite sequencing. The arrows represent the primers used in PCR assay and their relative position in the rRNA gene. b) Histogram showing the total DNA methylation levels in HSVd-Nb and control Nb plants (paired t-test values: means total methylation (control) 0.590, HSVd/Nb) 0.436, **P<0,005). c) Analysis differential of both symmetric (CG and CHG) and asymmetric (CHH) cytosine methylation levels. d) Positions in the analyzed region, of the 18 cytosines suceptibles to be methylated. e) Levels of methylcytosines displayed in both symmetric (CG and CHG) and asymmetric contexts. The height of the bar represents the frequency al which cytosine was methylated in both control Nb (green) and HSVd/Nb (red) samples.

DISCUSSION

The potential interplay between viroid-pathogenesis and host-gene transcriptional regulation, was recently reinforced by the demonstration that HSVd disturbs the dynamic methylation of rRNAs genes in cucumber plants, promoting their transcriptional reactivation during infection (Martinez *et al*., 2014). Nevertheless, additional evidence is necessary to consider that this phenomenon can be common to other hosts. The observation that in *HSVd/Nb* plants, viroid accumulation mimics the pathogenic effects associated to conventional infection (Martinez *et al*., 2008), together with the demonstration that the profiles of vd-sRNAs recovered from *HSVd/Nb* plants are similar to that previously described in other HSVd-host interactions, prompted us to analyze the effects of viroid accumulation in transcriptional activity of *N. benthamiana* plants.

Our analysis revealed that *HSVd/Nb* showed a modified sRNA landscape, supporting the idea that viroid accumulation interferes with endogenous RNA silencing pathways in this alternative host. Considering that a similar profile of sRNAs was associated with alterations in the processing of rRNA-derived sRNAs (rb-sRNAs) in HSVd-infected cucumber, we analyzed the rb-sRNAs in *HSVd/Nb* plants. The obtained results indicated that, although the rb-sRNAs accumulation levels were equivalent in both analyzed samples, alterations in their size distribution were clearly observed for *HSVd/Nb* compared to control plants. An increase and decrease of 21 nt and 24 nt rb-sRNAs, respectively, characterized the rb-sRNAs map recovered from *HSVd/Nb* data set. These alterations were relatively higher to the observations in the global sRNA population, suggesting a biological relevance for this observation in the context of viroid-host interaction. Increased accumulation of unprocessed pre-rRNA in *HSVd/Nb* plants indicated that the predominance of 21 nt rb-sRNAs (potential products of the processing of rRNAs) could be consequence of an unbalance in transcriptional activity of ribosomal genes. Previous results demonstrated that *Potato spindle tuber viroid* (PSTVd)-infected tomato plants overexpressed ribosomal genes (Itaya *et al*., 2002) strongly suggesting that this rRNA reactivation could be a common phenomenon associated to viroid infection.

Finally, bisulfite sequencing demonstrates changes in DNA methylation in regulatory sequences of both 45S and 5S rDNA in *HSVd/Nb* plants. These alterations, mainly characterized by a selective hypomethylation in the symmetric (CG and CHG) sequence context are indicative of the activation of normally silenced rRNAs genes and explain the accumulation of rRNA transcripts in *HSVd/Nb*.

In summary, our results indicate that in *N. benthamiana*, the persistent accumulation of HSVd-RNA globally mimics the transcriptional alterations induced in cucumber during a conventional viroid infection. Thus, the interference of this pathogenic *ncRNA* in the epigenetic mechanisms (associated to DNA

methylation) controlling plant-gene expression is not restricted to a specific host, and suggesting that may constitute a more general phenomenon able to occur in other viroid-plant interactions.

MATERIAL AND METHODS

Plant Material

The HSVd/Nb plants used in this work carry a dimeric sequence of (HSVd). In previous works was demonstrated that HSVd/Nb accumulate monomeric circular and linear viroid-forms that are systemically translocated throughout grafts to untransformed scions (Gómez & Pallas, 2006), providing evidences that basics-steps of HSVd life-cycle occurs in this model. In addition, HSVd/Nb plants, develop phenotypic alterations similar to the characteristics symptoms of HSVd infection such as stunting, decrease in the leaf and flower size and reduced fertility (Martinez *et al*., 2008). Consequently, is a valuable tool to study diverse aspects of viroid pathogenesis (Gomez et al., 2009; Gomez, et al., 2008; Martinez, et al., 2008; Gomez and Pallas, 2007). In addition, in a recent study were used transgenic plants expressing partial sequences of a Geminivirus to propose that these plant-DNA viruses alter host-DNA methylation (Rodriguez-Negrete, et al., 2013). Thus, providing evidences that transgenic plants expressing pathogen-sequences can be used to study the relations between infection and host-DNA methylation.

Untransformed and HSVd/Nb plants were maintained in growing chambers for 6-7 weeks. For analysis we selected symptomatic HSVd/Nb plants with similar accumulation levels of both HSVd mature forms (circular and linear) and HSVd-derived sRNAs.

Small RNA library information

The sRNA sequences used in this work were obtained from a library generated by starting from an sRNAs population recovered from leaves of *HSVd/Nb* and untransformed *Nicotiana benthamiana* plants and sequenced by 454 Life Science Technology (Lifesequencing, Branfor, CT, USA; www.lifesequencing.com) as previously described (Martinez *et al.,* 2010) (NCBI/SRA accession code SRP044905). A detailed description of reads recovered from both analyzed libraries is shown in the Fig. S1.

Nicotiana benthamiana rDNA sequencing

Total genomic DNA extracted from the leaves of untransformed *N. benthamiana* plants was amplified by PCR with two different primers sets complementary to diverse regions of 45S and 5S rDNA. The

amplification products were cloned and sequenced to determine the entire sequence of the transcriptional units of both 45S and 5Ss rRNAs in *N. benthamiana* (provisional accession code ID 1768724).

RNA isolation

Total RNA was extracted from the leaves (~0.1 g) of different HSVd/Nb and untransformed control plants using the TRI reagent (SIGMA, St. Louis, MO, USA) according to the manufacturer's instructions.

Bisulfite Conversion and Sequencing

Total genomic DNA was extracted from the leaves of five-pooled HSVd/Nb and untransformed control plants. Bisulfite treatment was performed as previously (Martinez et al., 2014) using the EpiTec Bisulfite kit (Qiagen). Modified DNA was amplified by PCR and cloned. The relative position of the primers used to PCR amplification (45s-Fw GTATATAAGGGGGGTAGAGGTG (position -1 to +21) and 45S-Rv AATGCCANACACAACCCACATC (position +452 to +473) and (5S-Fw GTAGTACTAGGATGGGTGAC - position +71 to +90, and 5S-Rv CTTAGTGCTGGTATGATCGCA - position -11 to +9) is show in Figures 4 and 6 respectively. We selected for sequencing 50 and 10 clones (obtained from two independent experiments), from 45S and 5S rDNA respectively, for each analysis in both the *HSVd/Nb* and untransformed control plants.

RT-PCR analysis

Total RNA extracted from the leaves of three-pooled HSVd/Nb and untransformed control plants was treated with DNase in order to avoid DNA contaminations. The depletion of genomic DNA was confirmed by PCR amplification of rDNA using the primers (Fw-25S and Rv-25S) described below (Fig. S2). RT-PCR analysis of serial dilutions (500ng, 100 ng and 20 ng) of total RNAs obtained from HSVd/Nb and control/Nb was performed using the SuperScript® III One-Step RT-PCR System with Platinum® Taq DNA Polymerase [Invitrogen Corporation, Carlsbad, CA, USA] according to the manufacturer's instructions. The relative sequence position of the specific primers used for the RT-PCR amplification of rRNA precursors (Fw 25s : CACCAATAGGGAACGTGAGCTG and Rv 25s : CCTCTTTTCGGAAAAGTTAGAAATTG) flanking a region (~500 nt) of pre-rRNA is shown in the Figure 4. RT-PCR conditions (45ºC 30 min.), 95ºC/15s, 55ºC/30s, 72ºC/30s (30 cycles). The primers Rub-Dir (5´ TACTTGAACGCTACTGCAG) and Rub-Rev (5´ CTGCATGCATTGCACGGTG) flanking a region (~180 nt) of Rubisco mRNA, were used to amplify this mRNAs as load control. RT-PCR conditions (45ºC 30 min.), 95ºC/15s, 58ºC/20s, 72ºC/15s (30 cycles).

Three repetitions of this analysis were performed. To discard the possible amplification of residual genomic rDNA, 100 ng of total RNAs were analyzed by PCR using the primers (Fw-25S and Rv-25S).

Acknowledgments

We thank Drs. M. Fares and J. Forment (Bioinformatics-service IBMCP) for their contribution in the statistical analysis of the data and the sRNA sequence analysis, respectively. Work supported by grants BIO2011-25018 (VP) and AGL2013-47886-R (GG) from Spanish Granting Agency (Direccion General Investigacion Cientifica) and PROMETEO program 2011/003 (Generalitat Valenciana). MC and GM are recipients of MINECO and Marie-Curie IOF fellowships respectively.

References

Daròs JA, Flores R, 2004. *Arabidopsis* thaliana has the enzymatic machinery for replicating representative viroid species of the family Pospiviroidae. *Proceedings of the National Academy of Science,* USA **101,** 6792-7.

Di Serio F, Flores R, Verhoeven JT, *et al*., 2014. Current status of viroid taxonomy. *Archives of Virology* doi.org/10.1007/s00705-014-2200-6.

Ding B 2010. Viroids: self-replicating, mobile, and fast-evolving noncoding regulatory RNAs. *Wiley Interdisciplinary Review* RNA **1**, 362-75.

Dowen RH, Pelizzola M, Schmitz RJ, *et al*., 2012. Widespread dynamic DNA methylation in response to biotic stress. *Proceedings of the National Academy of Science,* USA **109**, 2183-91.

Eamens AL, Smith NA, Dennis E, *et al*., 2014. In Nicotiana species, an artificial microRNA corresponding to the virulence modulating region of Potato spindle tuber viroid directs RNA silencing of a soluble inorganic pyrophosphatase gene and the development of abnormal phenotypes. *Virology* **450**, 266-77.

Flores R, Gago-Zachert S, Serra P, *et al*., 2014. Viroids: survivors from the RNA world? *Annual Review Microbiology* **8**, 395-414.

Füssy Z, Patzak J, Stehlík J, Matoušek J, 2013. Imbalance in expression of hop (Humulus lupulus) chalcone synthase H1 and its regulators during hop stunt viroid pathogenesis. *Journal Plant Physiology* **170**, 688-95.

Gas ME, Hernández C, Flores R, Daròs JA 2007. Processing of nuclear viroids in vivo: an interplay between RNA conformations. *PLoS Pathogens* **3**(11):e182

Gómez G, Martínez G, Pallás V, 2008. Viroid-induced symptoms in *N. benthamiana* plants are dependent on *RDR6* activity. *Plant Physiology* **148,** 414-23.

Gómez G, Pallas V, 2001. Identification of an in vitro ribonucleoprotein complex between a viroid RNA and a phloem protein from cucumber plants. *Molecular Plant Microbe Interactions* **14**, 910–13.

Gómez G, Pallas V, 2004. A long-distance translocatable phloem protein from cucumber forms a ribonucleoprotein complex in vivo with Hop stunt viroid RNA. *Journal of Virology* **78**, 10104-10.

Gómez G, Pallas V, 2006. Hop stunt viroid is processed and translocated in transgenic Nicotiana benthamiana plants. *Molecular Plant Pathology* **7**, 511–7.

Gomez, G, Pallas V, 2007. Mature monomeric forms of Hop stunt viroid resist RNA silencing in transgenic plants. *Plant Journal* **51**, 1041-9.

Gómez G, Pallas V, 2012. Studies on subcellular compartmentalization of plant pathogenic noncoding RNAs give new insights into the intracellular RNA-traffic mechanisms. *Plant Physiology* **159**, 558–64.

Gómez G, Pallas V, 2013. Viroids: a light in the darkness of the lncRNA-directed regulatory networks in plants. *New Phytologist* **198**, 10-15.

Gómez G, Martinez G, Pallás V, 2009. Interplay between viroid-induced pathogenesis and RNA silencing pathways. *Trends in Plant Science* **14,** 264-9

Herranz MC, Niehl A, Rosales M, *et al*., 2013. A remarkable synergistic effect at the transcriptomic level in peach fruits doubly infected by prunus necrotic ringspot virus and peach latent mosaic viroid. *Virology Journal* **10**, 164.

Itaya A, Matsuda Y, Gonzales RA, *et al*., 2002. Potato spindle tuber viroid strains of different pathogenicity induces and suppresses expression of common and unique genes in infected tomato. *Molecular Plant Microbe Interactions* **15**, 990–9.

Lison P, Tarraga S, Lopez-Gresa P, *et al*., 2013. A noncoding plant pathogen provokes both transcriptional and posttranscriptional alterations in tomato. *Proteomics* **13**, 833–44.

Martinez G, Castellano M, Tortosa M, *et al*., 2014. A pathogenic non-coding RNA induces changes in dynamic DNA methylation of ribosomal RNA genes in host plants. *Nucleic Acids Research* **42**, 1553-62.

Martinez G, Donaire L, Llave C, *et al*., 2010. High-throughput sequencing of Hop stunt viroid-derived small RNAs from cucumber leaves and phloem. *Molecular Plant Pathology* **11**, 347-59.

Martinez G, Pallás V, Gómez G, 2008. Analysis of Symptoms Developed in N. Benthamiana expressing HSVd dimeric forms. *Journal of Plant Pathology* **90**, 121-4.

Navarro B, Gisel A, Rodio ME, *et al*., 2012. Small RNAs containing the pathogenic determinant of a chloroplast-replicating viroid guide the degradation of a host mRNA as predicted by RNA silencing. *Plant Journal* **70**, 991–1003.

Navarro B, Gisel A, Rodio ME, *et al*., 2012. Viroids: how to infect a host and cause disease without encoding proteins. *Biochimie* **94**, 1474–80.

Navarro JA, Vera A, Flores R, 2000. A chloroplastic RNA polymerase resistant to tagetitoxin is involved in replication of avocado sunblotch viroid. *Virology* **268**, 218–25.

Navarro L, Dunoyer P, Jay F, *et al*., 2006. A plant miRNA contributes to antibacterial resistance by repressing auxin signaling. *Science* **312**, 436-9.

Nohales MA, Flores R, Daros JA, 2012. Viroid RNA redirects host DNA ligase 1 to act as an RNA ligase. *Proceedings of the National Academy of Science,* USA. **109**, 13805-10.

Nohales MA, Molina-Serrano D, Flores R, *et al*., 2012. Involvement of the chloroplastic isoform of tRNA ligase in the replication of viroids belonging to the family Avsunviroidae. *Journal of Virology* **86,** 8269–76.

Owens RA, Blackburn M, Ding B, 2001. Possible involvement of the phloem lectin in long-distance viroid movement. *Molecular Plant Microbe Interactions* **14**, 905–9.

Owens RA, Tech KB, Shao JY, *et al*., 2012. Global analysis of tomato gene expression during Potato spindle tuber viroid infection reveals a complex array of changes affecting hormone signaling. *Molecular Plant Microbe Interactions* **25**, 582–98.

Palukaitis P, 2014. What has been happening with viroids? *Virus Genes* **49**, 175-84

Papaefthimiou I, Hamilton A, Denti M, *et al*., 2001. Replicating potato spindle tuber viroid RNA is accompanied by short RNA fragments that are characteristic of post-transcriptional gene silencing. *Nucleic Acids Research* **29**, 2395–400.

Raja P, Sanville BC, Buchmann RC, *et al*., 2008. Viral genome methylation as an epigenetic defense against geminiviruses. *Journal of Virology* **82,** 8997-9007.

Rodriguez-Negrete E, Lozano-Duran R, Piedra-Aguilera A, *et al*., 2013. Geminivirus Rep protein interferes with the plant DNA methylation machinery and suppresses transcriptional gene silencing. *New Phytologist* **199**, 464-75.

Tessitori M, Maria G, Capasso C, *et al*., 2007. Differential display analysis of gene expression in Etrog citron leaves infected by Citrus viroid III. *Biochimica et Biophysica Acta* **1769**, 228–35.

Wang MB, Bian XY, Wu LM, *et al*., 2004. On the role of RNA silencing in the pathogenicity and evolution of viroids and viral satellites. *Proceedings of the National Academy of Science,* USA **101,** 3275–80.

Wassenegger M, Heimes S, Riedel L, *et al*., 1994. RNA-directed de novo methylation of genomic sequences in 120 plants. *Cell* **76**, 567–76.

Yang LP, Fang YY, An CP, *et al*., 2013. C2-mediated decrease in DNA methylation, accumulation of siRNAs, and increase in expression for genes involved in defense pathways in plants infected with beet severe curly top virus. *Plant Journal* **73,** 910-7.

Yu A, Lepere G, Jay F, *et al*., 2013. Dynamics and biological relevance of DNA demethylation in *Arabidopsis* antibacterial defense. *Proceedings of the National Academy of Science,* USA. **110**, 2389-94.

Zhao Y, Owens RA, Hammond RW, 2001. Use of a vector based on potato virus X in a whole plant assay to demonstrate nuclear targeting of potato spindle tuber viroid. *Journal of General Virology* **82**, 1491–7.

Zhong X, Ding B, 2008. Distinct RNA motifs mediate systemic RNA trafficking. *Plant Signaling and Behavior* **3**, 58–9.

SUPPLEMENTAL DATA

HSVd-Nb library nt size	Total redas	Total %	Unique reads	Unique %
20	619	0,873861791	525	0,902635696
21	5474	7,727818169	3399	5,843921393
22	8860	12,50794099	6205	10,66829428
23	7169	10,12070304	6499	11,17377027
24	41641	58,78591092	37419	64,33471451
25	1923	2,714759653	1646	2,829977821
26	507	0,715747865	364	0,625827416
27	337	0,475753512	206	0,354177054
28	321	0,453165808	205	0,352457748
29	281	0,396696548	142	0,244141465
30	556	0,784922708	136	0,233825628
	67688	95,55728101	56746	97,56374327

Wt-Nb library nt size	Total redas	Total %	Unique reads	Unique %
20	188	0,519150581	156	0,495222374
21	648	1,789412642	405	1,285673471
22	1049	2,896749786	819	2,599917463
23	2873	7,933615	2575	8,174343672
24	26973	74,48430122	24142	76,63883686
25	1785	4,929169083	1434	4,552236437
26	659	1,819788474	515	1,634868734
27	442	1,220556154	276	0,876162662
28	187	0,516389142	137	0,434906828
29	123	0,339657029	92	0,292054221
30	72	0,198823627	48	0,152376115
	34999	96,64761274	30599	97,13659884

nt size	Total redas	Total %	Unique reads	Unique %
20	619	0,873861791	525	0,902635696
21	5474	7,727818169	3399	5,843921393
22	8860	12,50794099	6205	10,66829428
23	7169	10,12070304	6499	11,17377027
24	41641	58,78591092	37419	64,33471451
	63763	90,01623491	54047	92,92333614

nt size	Total redas	Total %	Unique reads	Unique %
20	188	0,519150581	156	0,495222374
21	648	1,789412642	405	1,285673471
22	1049	2,896749786	819	2,599917463
23	2873	7,933615	2575	8,174343672
24	26973	74,48430122	24142	76,63883686
	31731	87,62322923	28097	89,19399384

Figure Suplementary 1. Detail of total (upper panel) and unique (low panel) reads recovered from sRNAs libraries arising from both Wt-Nb and HSVd/Nb plants.

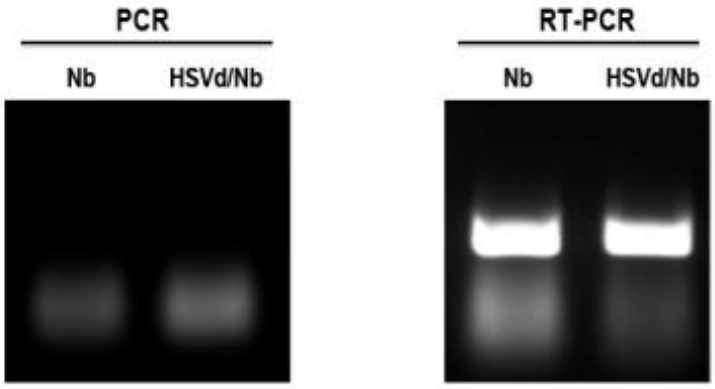

Figure Supplementary 2. Total RNA (100ng) extracted from the leaves of three-pooled HSVd/Nb and untransformed control plants was treated with DNase in order to avoid DNA contaminations. The depletion of genomic DNA was confirmed by PCR amplification (left panel) of rDNA using the primers (Fw-25S and Rv-25S) described in the text. PCR conditions 95°C/15s, 55°C/30s, 72°C/30s (30 cycles).The primers Rub-Dir and Rub-Rev specific for Rubisco mRNA, were used to amplify mRNAs as load control (right panel).RT-PCR conditions (45°C 30 min), 95°C/15s, 58°C/20s, 72°C/15s (30 cycles). Serial dilutions of these RNA samples were used to estimate by semi-quantitative RT-PCR the accumulation of pre-rRNAs (Figure 4).

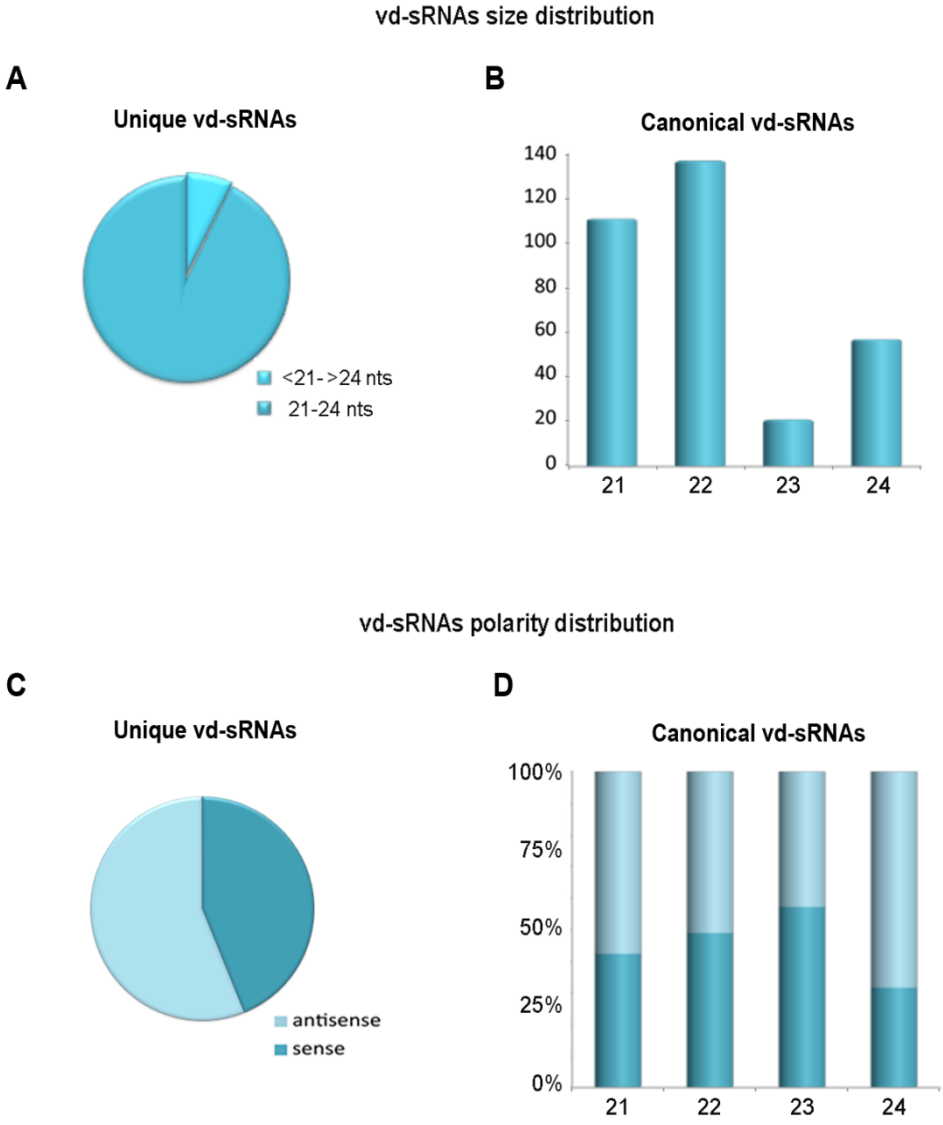

Supplementary Figure 3. Characterization of uniques vd-sRNAs.

A).Graphic showing the proportion of non-redundant vd-sRNAs with expected DCL canonical sizes (93% of the total reads). These sequences were used in subsequent analysis. B). Histogram illustrating the size distribution of the canonical uniques vd-sRNAs sequenced in this work. Graphic representation of relative accumulation of sense and antisense vd-sRNAs reads recovered from our dataset showed as total vd-sRNAs (C) or classified according size (D).

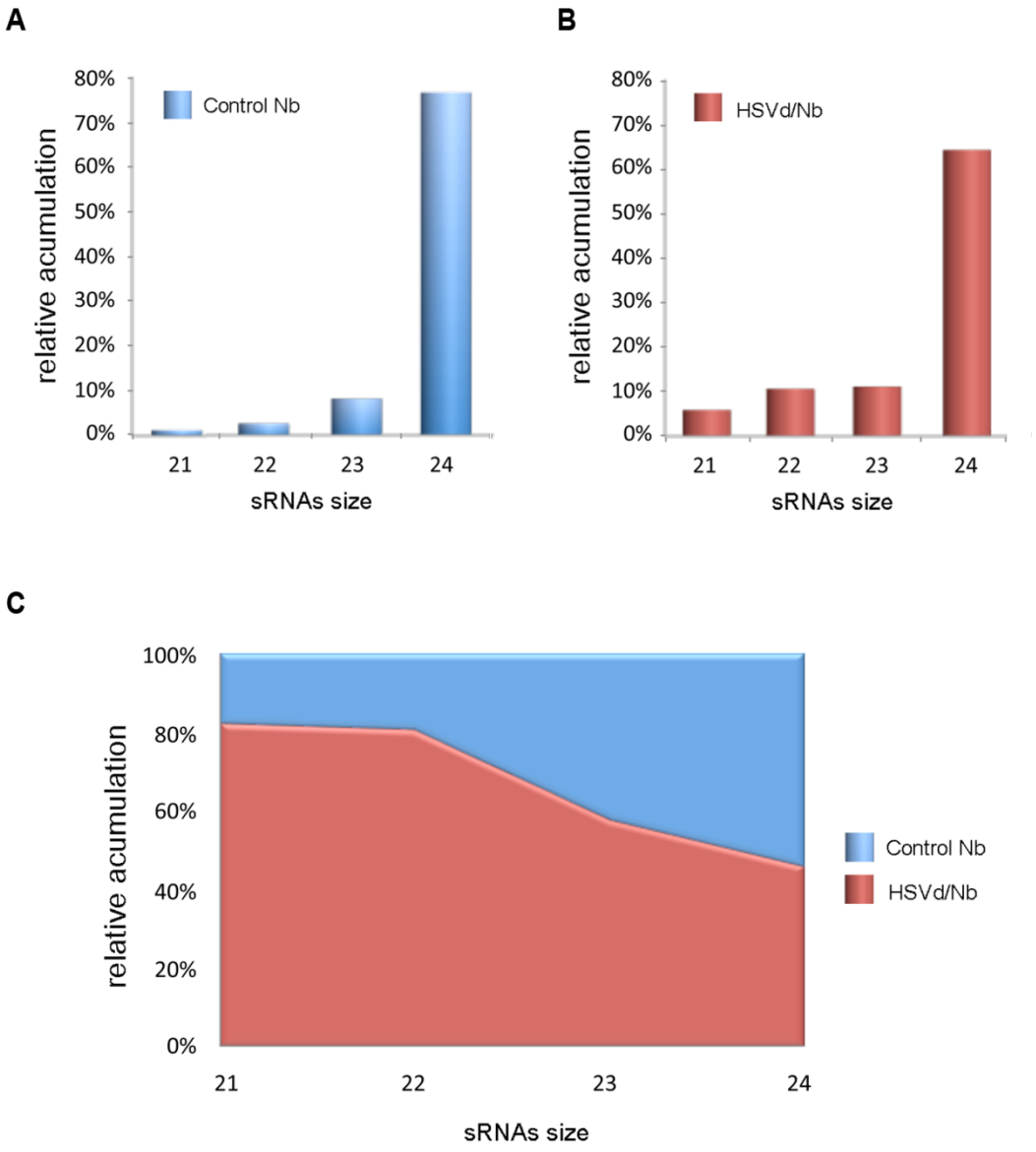

Supplementary Figure 4. Characterization of uniques endogenous sRNAs.

Histograms showing the differential accumulation and distribution of the non-redundant reads of endogenous sRNAs recovered from both the control (A) and HSVd-Nb samples (B). C) Comparative of the relative accumulation of total reads (ranging between 21 and 24nt) recovered from both untransformed control (blue) and HSVd-Nb (red) plants.

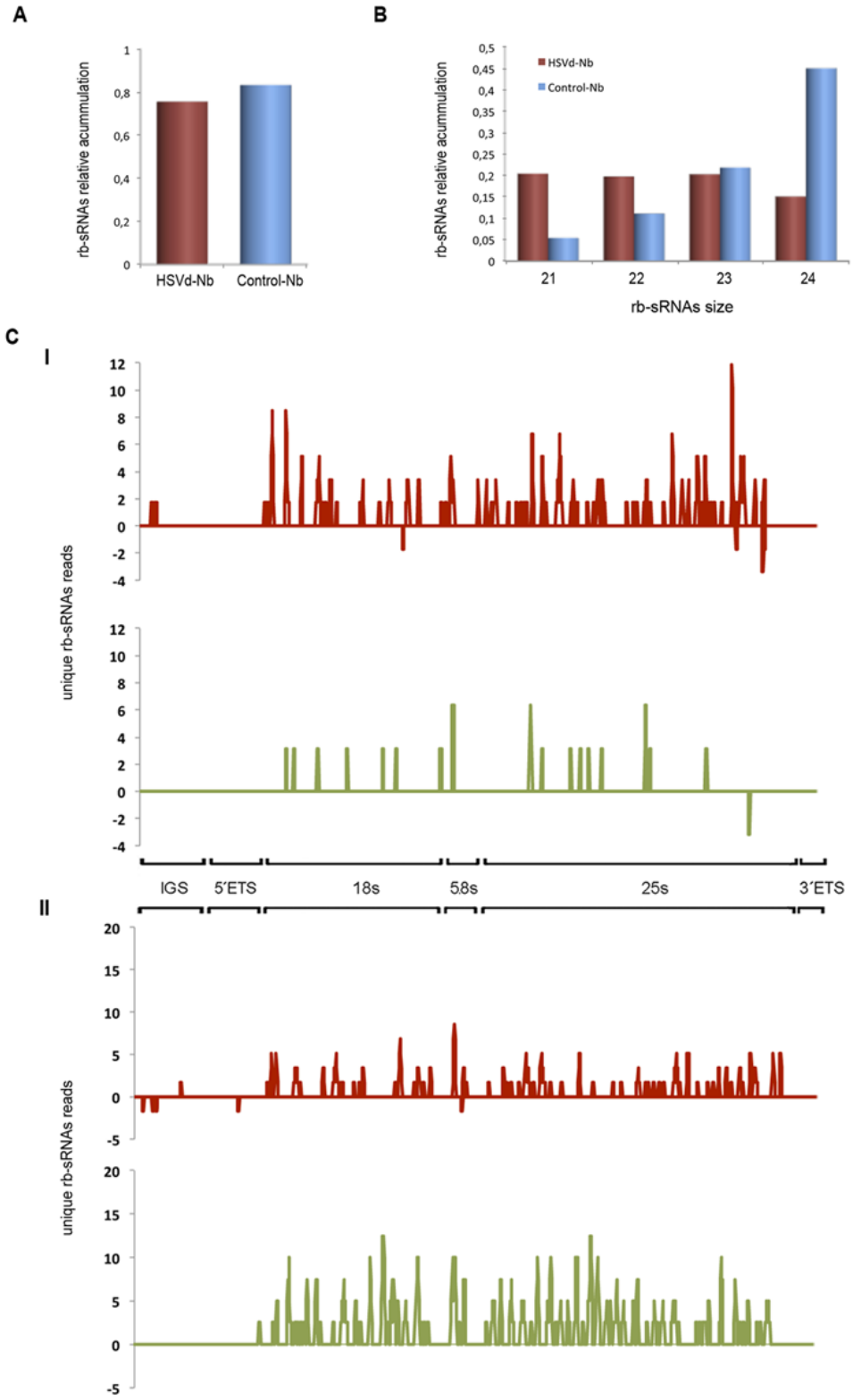

Supplementary Figure 5. Differential accumulation of uniques rb-sRNAs in HSVd-Nb plants.

A). The accumulation of rb-sRNAs is expressed as the percentage of total rb-sRNAs from the overall non-redundant sRNAs in the library. B) Graphic representation of the distribution of the uniques reads of rb-sRNAs (ranging between 21 and 24 nt) recovered from both the control (blue) and HSVdNb (red) plants. C) The 21 and 24 nt (panels I and II respectively) in length rb-sRNAs recovered from the HSVd/Nb (red bars) or the untransformed control plants (green bars) were plotted according to polarity (+above and – below the X-axis) and position of their 5-end onto the rRNA sequence. The values on the Y-axis represent the number of normalized uniques reads in each library.

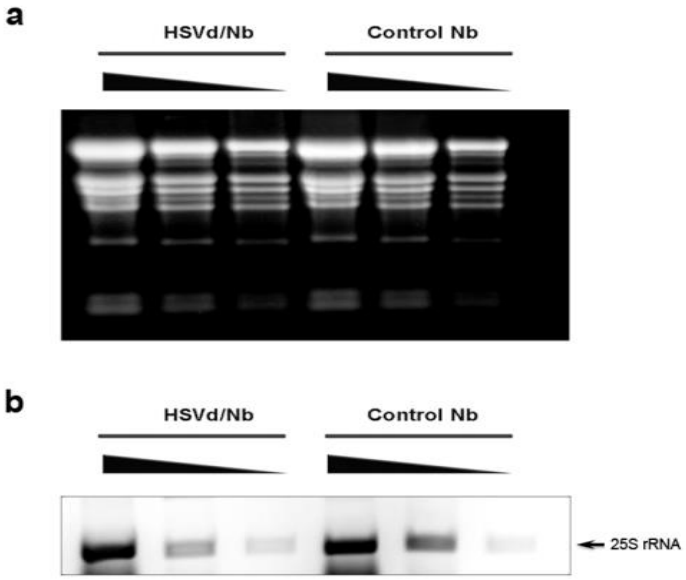

Supplementary Figure 6. Mature rRNAs accumulate comparably in HSVd/Nb and Nb plants. a) Analysis of the mature rRNA accumulation by electrophoresis in denaturing agarose gel of serial dilutions (2 ug, 1 ug and 500 ng) of total RNAs obtained fromHSVd/Nb and untransformed plants. b) RT-PCR analysis of serial dilutions (100ng, 20 ng and 4 ng) of total RNAs obtained from HSVd/Nb and control/Nb was performed using the SupeScript® III One-Step RT-PCR System with Platinum® Taq DNA Polymerase (Invitrogen Corporation, Carlsbad, CA, USA) according to the manufacturer's instructions. The primers FW- TATATAAGGGGGGTAGAGGTGTTG and Rv-GGTTGTTGTGAGTTGTGTTTGGCAT flanking a 473 bp region of 3' end of 25S mature rRNA were employed. RT-PCR conditions (45°C 30 min), 95°C/15s, 55°C/30s, 72°C/30s (20 cycles).Two repetition of both analysiswere performed.

CAPÍTULO TERCERO

Este capítulo ha dado lugar a la siguiente publicación:

Castellano, M., Pallas, V. and Gómez, G. (2016).

A pathogenic long non-coding RNA redesigns the epigenetic landscape of the infected cells by subverting host Histone Deacetylase 6 activity.

New Phytologist. 4:1311-1322. Doi: 10.1111/nph.14001

A pathogenic long non-coding RNA redesigns the epigenetic landscape of the infected cells by subverting host Histone Deacetylase 6 activity

Mayte Castellano, Vicente Pallas and Gustavo Gomez*

Instituto de Biología Molecular y Celular de Plantas (IBMCP), Consejo Superior de Investigaciones Científicas (CSIC)-Universidad Politecnica de Valencia (UPV), CPI, Edificio 8 E, Av. de los Naranjos s/n, 46022 Valencia, Spain.

Key words:

Viroid-host interaction; DNA methylation; Viroid-induced pathogenesis; Epigenetic plant-response to infections; Viroid-protein interactions.

Word count

Total:	5250
Introduction:	928
Mat. & Meth:	1700
Results:	1406
Discussion:	1189
Acknowledgements:	27

Figures:	5
Supplementary ***Fig:***	8

SUMMARY

- **Viroids, ancient plant-pathogenic long noncoding-RNAs, have developed a singular evolutionary strategy based on reprogramming specific phases of host-metabolism to ensure that their infection cycle can be completed in infected-cells. However, the molecular aspects governing this trans-regulatory phenomenon remain elusive.**

- **Here, we use immunoprecipitation assays and bisulfite sequencing of rDNA to shown that, in infected cucumber and *N. benthamina* plants, *Hop stunt viroid* (HSVd) recruits and functionally subverts the Histone Deacetylase 6 (HDA6) to promote host-epigenetic alterations that trigger the transcriptional alterations observed during viroid-pathogenesis.**

- **This notion is supported by the demonstration that, during infection, the HSVd-HDA6 complex occurs *in vivo* and that endogenous HDA6 expression is increased in HSVd-infected cells. Moreover, transient overexpression of recombinant HDA6 reverts the hypomethylation status of rDNA observed in HSVd-infected plants and reduces viroid accumulation. We hypothesize that the host-transcriptional alterations induced as a consequence of viroid-mediated HDA6 recruitment favor spurious recognition of HSVd-RNA as an RNA Pol II template, thereby improving viroid replication.**

- **Our results constitute the first description of a physical and functional interaction between a pathogenic-RNA and a component of the host RNA silencing mechanism, providing novel evidence of the potential of these pathogenic lncRNAs to physically redesign the host-cell environment and reprogram their regulatory mechanisms.**

INTRODUCTION

Viroids are a class of sub-viral plant pathogenic long noncoding RNAs (lncRNAs) composed of a circular single-stranded (240–400 nt in length) molecule (Flores *et al*., 2014; Palukaitis *et al*., 2014; Katsarou *et al*., 2015). Limited by their nature as obligated intracellular parasites, viroids must optimize their minimum non-protein-coding genome to ensure autonomous proliferation within infected hosts (Ding, 2010). To overcome this challenge, these lncRNAs have evolved through their adaptive history into versatile molecules that are able to subvert specific plant cell components and/or mechanisms at different functional levels (Navarro *et al*., 2012; Gago-Zachert, 2016). A representative example of this ability can be observed in the generation of their progeny. Replication of viroids in the nucleus (for members of the family *Pospiviroidae*) or chloroplasts (for members of the family *Avsunviroidae*) is a sequential process that involves transcription, cleavage and circularization of RNA strands. An increasing body of evidence has demonstrated that, besides recruiting cellular mechanisms commonly involved in host RNA metabolism (Navarro *et al*., 2000; Gas *et al*., 2007; Nohales *et al*., 2012), viroids are able to subvert and redirect DNA-dependent factors such as DNA-dependent RNA Polymerase II (RNA Pol II) (Flores & Semancik, 1982; Mühlbach & Sänger, 1997) and/or DNA ligase 1 (Nohales *et al*., 2012b) during progeny generation to promote their accumulation in infected cells. However, the strategy used by these pathogenic lncRNAs to reprogram the activity of the cellular components involved in host RNA and/or DNA processing is currently unknown.

The functional alterations induced by viroids in infected plants, more commonly recognized as symptoms, represent another aspect of the infection cycle that is intimately associated with the ability of viroids to interfere with host cell homeostasis. Although the basis of viroid pathogenesis remains to be fully deciphered, this process can be envisioned as the product of diverse disruptions in plant gene expression generated by viroid interference in ncRNA-directed regulatory networks (Owens & Hammond, 2009; Navarro *et al*., 2012; Gomez & Pallas, 2013; Palukaitis *et al*., 2014; Gago-Zachert, 2016). In recent years, several studies have provided evidence for the existence of a close interplay between viroid-induced pathogenesis and RNA silencing. The idea that viroid-derived sRNAs (vd-sRNAs) can trigger the post-transcriptional cleavage of host mRNAs and induce the expression of plant symptoms (Papaefthimiou *et al*., 2001; Wang *et al*., 2004; Gomez *et al*., 2009) was experimentally validated for viroids that replicate in the nucleus (Gomez *et al*., 2008; Eamens *et al*., 2014; Adkar-Purushothama *et al*., 2015) and chloroplasts (Navarro *et al*., 2012b). However, the recent observation that *Hop stunt viroid* (HSVd) infection is associated with decreased levels of methylation for normally silenced host genes (Martinez *et al*., 2014; Castellano *et al*., 2015) opened the door to the notion that the viroid interference of plant gene expression is a multilayered process, which may also include epigenetic alterations in host gene expression (Castellano *et al*., 2015; Dalakouras *et al*., 2015).

Experiments in two different hosts (cucumber -*Cucumis sativus*- and *Nicotiana benthamiana*) have shown that HSVd-infected plants over-accumulate ribosomal-derived sRNAs (rb-sRNAs) as a consequence of increased transcriptional activity of rRNA precursors. This phenomenon correlated with a significant reduction in the methylation levels of ribosomal DNA (rDNA) promoter regions, providing evidence that specific rRNA genes commonly silenced by cytosine methylation are transcriptionally reactivated during viroid infection (Martinez *et al*., 2014; Castellano *et al*., 2015). These results suggest that HSVd infection could be associated with alterations of the epigenetic pathways that regulate the transcription of repetitive rDNA. Intriguingly, the regulatory disorders observed in viroid-infected plants display certain similarities to those previously described in *Arabidopsis* mutants for Histone Deacetylase 6 (HDA6). The *hda6* mutants lose the maintenance of symmetric methylation of 45S rRNA promoter regions, which increases their transcriptional activity in parallel with massive overproduction of rb-sRNAs (Earley *et al*., 2010), resembling, at least in part, the observations in HSVd-infected plants. In *Arabidopsis,* HDA6, a class I RPD3-like HDAC, is recognized as a component of the plant-specific gene silencing mechanism called RNA-directed DNA methylation (RdDM) (Dalakouras & Wassenegger, 2013). Increasing evidence indicates that HDA6 is an epigenetic regulator involved in the maintenance and *de novo* DNA methylation of Transposable Elements (TEs), rRNA genes and transgenes (Aufsatz *et al*., 2002; Probst *et al*., 2004; May *et al*., 2005; To *et al*., 2011; Liu *et al*., 2012 and 2012b; Hristova *et al*., 2015) via interactions with Methyltransferase 1 (MET1). The similarity between the regulatory disturbances observed in HSVd-infected plants and *hda6* mutants prompted us to speculate that viroid-induced interferences in the regulatory pathways mediated by HDA6 could be linked to the epigenetic alterations observed in HSVd-infected plants.

To provide experimental evidence to support this hypothesis, we analyzed the possible interrelation between HSVd infection and HDA6 in both cucumber and *N. benthamiana* plants. Our results reveal that viroid infection is associated with over-accumulation of HDA6 in the natural HSVd-host cucumber. In parallel, we demonstrate that HSVd RNA is able to bind HDA6 *in vitro* and confirmed that this interrelation also occurs *in vivo* during viroid infection. Regarding the functional aspects of the interaction between HSVd and HDA6, the data obtained by bisulfite sequencing demonstrated that transient overexpression of recombinant HDA6 in infected plants reversed the hypomethylation of the ribosomal genes induced by viroid infection, directly linking viroid-mediated recruitment of HDA6 and loss of methylation maintenance. Moreover, we provide evidence of an inverse correlation between transient expression of HDA6 and HSVd accumulation in both cucumber and *N. benthamiana* hosts, suggesting that the recruitment of this protein to the HSVd-HDA6 complex, which we observed *in vivo*, may play a crucial role in viroid accumulation in infected plants.

RESULTS

Cucumber HDA6 is a nuclear protein that is overexpressed during HSVd infection

To characterize the putative HDA6 protein in cucumber, we first retrieved the predicted HDA6 sequence from GenBank (accession no. XM_004168847.1). Next, starting from a total RNA preparation, we used RT-PCR to amplify the full-length cDNA corresponding to the cucumber HDA6 ORF and cloned the sequence into a plasmid to express a recombinant version of the protein with an amino-terminal His6 tag in *Escherichia coli*. Recombinant HDA6 was purified by affinity chromatography using a nickel column (Supplementary Fig. 1a) and used to generate a polyclonal antiserum (HDA6-As) in rabbit (Supplementary Fig. 1b). To evaluate whether the cucumber HDA6 exhibits nuclear localization, like *Arabidopsis* HDA6, we generated a vector expressing the complete HDA6 ORF fused to GFP under the control of the 35S promoter. The HDA6-GFP DNA was cloned into a binary vector to be transformed into *Agrobacterium* and was used for the analysis of transient expression by means of agro-infiltration. Observation of the infiltrated leaves using confocal microscopy revealed that, unlike the free GFP used as a control (detected in the cytosol and the nucleus), the HDA6-GFP was mainly localized in the nuclei of the cucumber (Fig. 1a) and *N. benthamiana* (Supplementary Fig. 2) cells. It is important to note that the predicted size of HDA6-GFP (81 kDa) exceeds the size exclusion limit (40 to 60 kDa) for passive diffusion of proteins through nuclear pores (Raikhel, 1992). Moreover, specific detection of HDA6 in nuclear fractions recovered from untreated cucumber plants by western blot assays (Fig. 1c) provided additional evidence supporting that endogenous cucumber HDA6 accumulates in the nucleus. Similar results were obtained in immunological assays performed with nuclear extracts of *N. benthamiana* plants transiently expressing recombinant HDA6 (Supplementary Fig. 3), reinforcing the confocal microscopy observations and demonstrating that recombinant cucumber HDA6 can accumulate in the nuclei of *N. benthamiana* cells. Next, we reasoned that, as stated in the introduction, a close interaction might occur between HSVd and HDA6 during infection; viroid pathogenesis may be accompanied by alteration in the pattern of HDA6 accumulation in infected cucumber cells. To address this issue, we analyzed the levels of endogenous HDA6 in the nuclear extracts of HSVd-infected and control plants by western blot. As shown in Fig. 1d and Supplementary Fig. 4, viroid infection was associated with increased accumulation of HDA6 in the nuclei of infected cucumber cells, providing evidence of a functional link between HSVd infection and HDA6 metabolism.

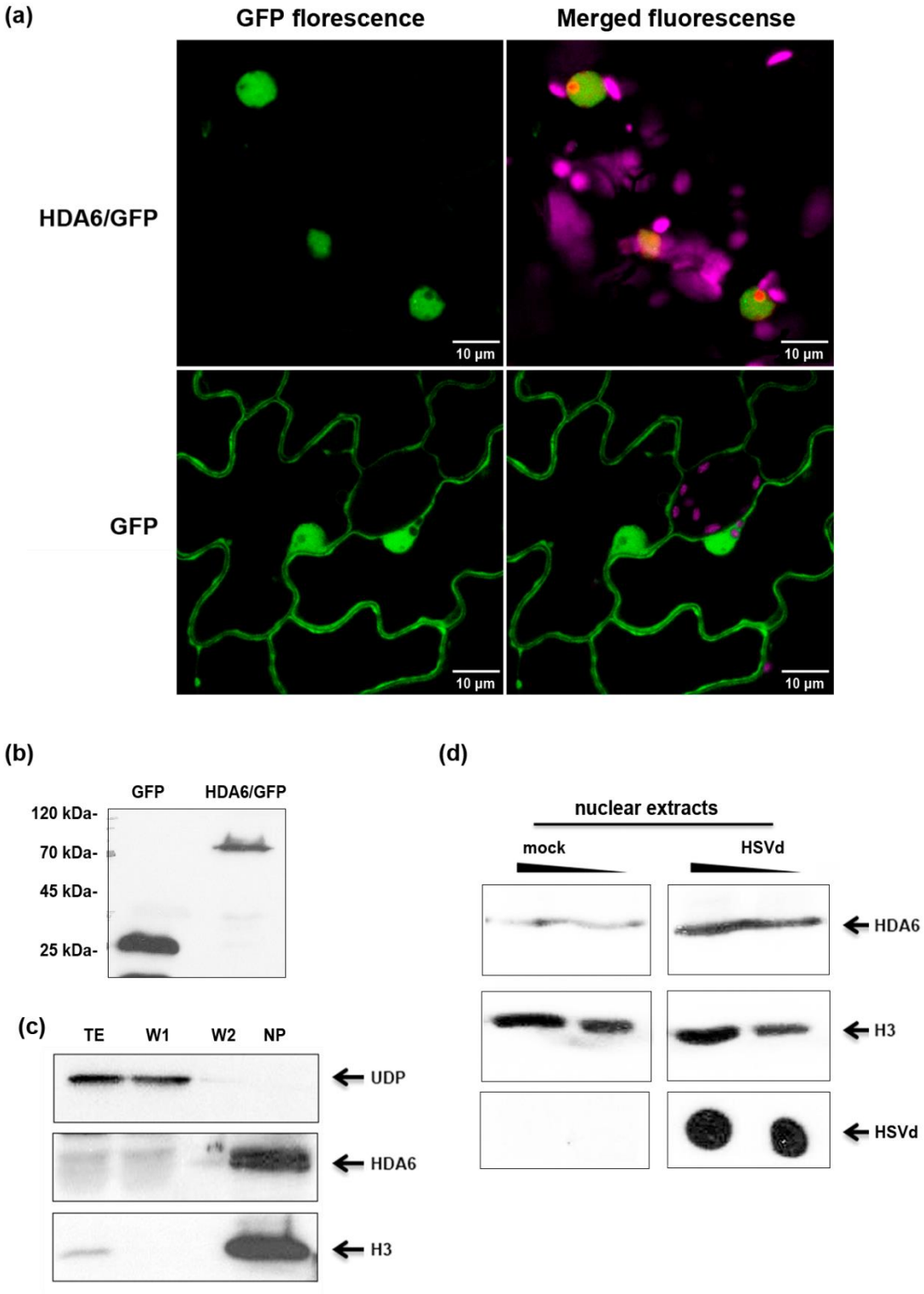

Figure 1: Cucumber HDA6 is a nuclear protein that is overexpressed during HSVd infection. a) Confocal microscopy imaging of cucumber leaves expressing HDA6/GFP (upper panels) and unmodified GFP (lower panels). As can be observed, HDA6/GFP mainly accumulates in the cell nucleus. Fibrillarin fused to RFP was used as a nucleolar marker. Cell chloroplasts are shown in magenta. **b**) The correct expression of the recombinant HDA6/GFP protein in the infiltrated tissues was established by western blotting using anti-GFP. **c)** Serological detection (using HDA6-As) of endogenous HDA6 in nuclear extracts of cucumber leaves (middle panel). Histone 3 (H3) (lower panel) and UDP-glucose pyrophosphorylase (UDP) (upper panel) were used as well-established markers of the nuclear and cytoplasmic fractions, respectively. TE: total extract, W1 and W2: Wash 1 and 2, respectively, NP: nuclear pellet. **d**) Differential detection of endogenous HDA6 in two dilutions (1:1 and 1:2) of nuclear extracts from mock-inoculated and HSVd-infected leaves. Accumulation of H3 was assessed as a loading control. The presence of viroid in the infected leaves was confirmed by dot blot hybridization using HSVd-specific probes.

HSVd RNA binds to HDA6 *in vitro* and *in vivo*

Keeping in mind that it is generally accepted that viroids use direct interaction as a general mechanism to recruit and subvert host cell factors, we performed *in vitro* assays to determine whether cucumber HDA6 possesses potential HSVd RNA binding activity. Northwestern blot analysis (Gomez *et al*., 2005) indicated that HDA6 efficiently bound to full-length HSVd transcripts with both plus and minus polarity (Fig. 2a). To complement these data with *in vivo* approaches in a heterologous system, recombinant HDA6 was expressed by agro-infiltration in transgenic *N. benthamiana* plants accumulating HSVd (*HSVd-Nb*) (Gomez & Pallas; 2007). Nuclear extracts were purified from the infiltrated leaves and subjected to capture assays for recombinant HDA6 (carrying an amino-terminal His6 tag) by affinity chromatography using a nickel column. Western blot analysis of the eluates confirmed that recombinant HDA6 could be efficiently recovered from infiltrated leaves (Supplementary Fig. 5a). The RNAs extracted from the different eluates were subjected to RT-PCR assays to detect viroid RNA and demonstrate that HSVd could be amplified from the eluates containing the HDA6 protein (Supplementary Fig. 5b). No amplification of HSVd RNA was observed in the eluates recovered from control *HSVd-Nb* leaves infiltrated with *Agrobacterium* carrying the empty vector (Supplementary Fig. 5b). To provide more robust *in vivo* evidence of the HSVd-HDA6 interaction, we next performed canonical IP assays in infected cucumber plants using the polyclonal antiserum generated against cucumber HDA6 protein (HDA6-As). Immunoprecipitation studies were carried out starting from nuclear extracts (Fig. 2b). When the immunoprecipitates were electrophoresed on SDS-PAGE and analyzed by western blot assays, we observed that HDA6 was specifically recovered (Fig 2c). In contrast, no protein bands were detected in the immunoprecipitation control performed with antibody-free protein-A agarose beads (Fig. 2c). The presence of HSVd RNA in the immunoprecipitation extracts was confirmed by RT-PCR. A band of the expected size was only detected in the immunoprecipitation extract containing HDA6 and not in the IP-control lacking HDA6 (Fig. 2c – lower panel).

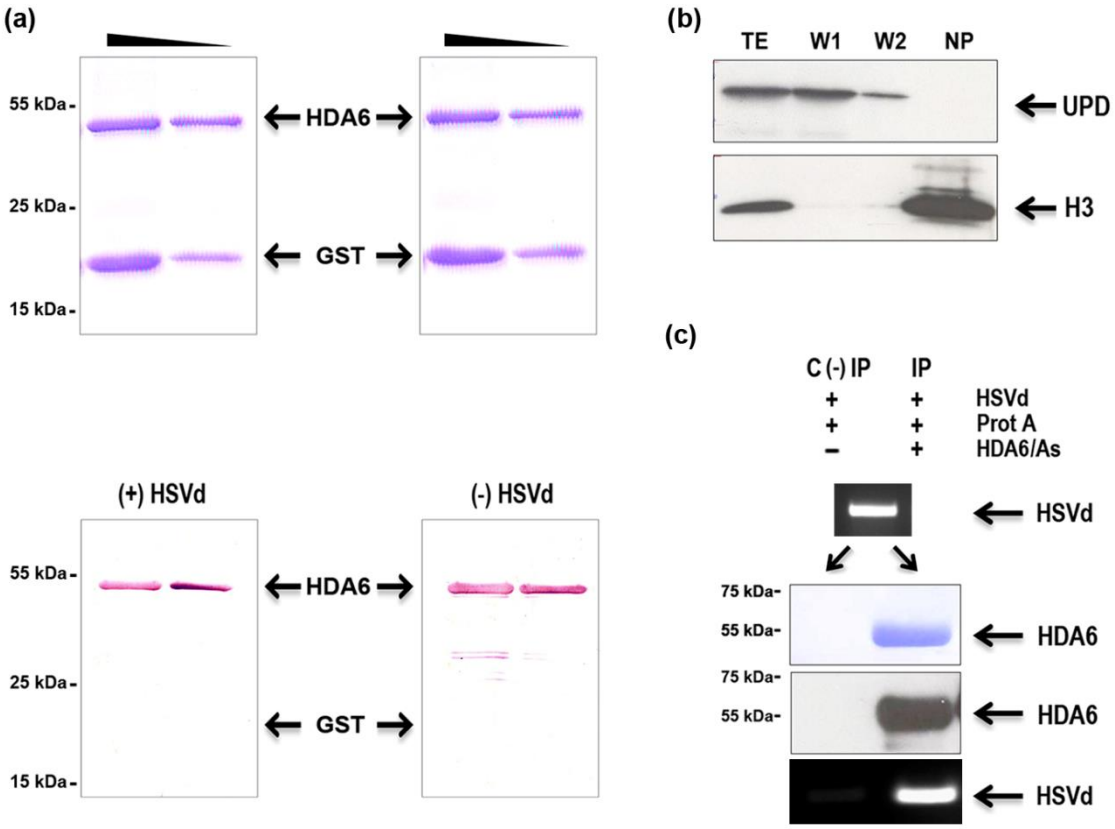

Figure 2: HSVd-HDA6 form a stable complex *in vitro* and *in vivo*. a) Two dilutions (1 μg and 0.5 μg) of recombinant HDA6 and glutathione S-transferase (GST, used as a control) were subjected to SDS-PAGE (upper panel), transferred to nitrocellulose membranes and analyzed by northwestern blot with HSVd probes in both (plus and minus) polarities (lower panel left and right, respectively). **b)** Purification of nuclear extracts from HSVd-infected cucumber plants. Selective accumulation of Histone 3 (H3) and UDP-glucose pyrophosphorylase (UDP) were used as indicators of enriched cytoplasmic and nuclear fractions (upper and lower panels, respectively). TE: total extract, W1 and W2: Wash 1 and 2, respectively, NP: nuclear pellet. **c)** Immunoprecipitation (IP) of HSVd-HDA6 complexes. The nuclear fraction, which was extracted from HSVd-infected plants, was divided into two identical parts. One part was incubated with Protein-A agarose and subjected to IP assays using polyclonal HDA6-As. An equivalent fraction was incubated without HDA6-As as a negative control $C^{(-)}$ IP. The IP of HDA6 was confirmed by SDS-PAGE analysis and serological detection by western blot (upper panels). Total RNAs extracted from IP fractions were subjected to RT-PCR analysis to confirm the specific recovery of HSVd RNA.

HDA6 overexpression reverses the hypomethylation induced by HSVd infection

Having confirmed that HSVd interacts directly with HDA6 in infected plants, we next attempted to establish whether this interaction exerts a functional effect on the alteration in the methylation of host DNA observed in HSVd-infected cucumber (Martinez *et al*., 2014) and *N. benthamiana* (Castellano *et al*., 2015) plants. First, the time-point at which viroid RNA could be detected in systemic leaves of HSVd-inoculated cucumber and *N. benthamiana* plants (Supplementary Fig. 6a) was determined. Next, we expressed recombinant HDA6 in the apical leaves 3 days prior to the time-point established for HSVd detection. After systemic infection was established, the leaves overexpressing recombinant HDA6 were collected and

processed to obtain total RNA and DNA (Supplementary Fig. 6 b and c). The recovered DNA was analyzed by bisulfite sequencing of a region of the cucumber 45S-rDNA promoter (Fig. 3a) containing 9 symmetric (5 CG, 4 CHG) and 14 asymmetric (CHH) potential methylation sites (Fig. 3b) that were previously demonstrated to be hypomethylated during HSVd infection (Martinez *et al*., 2014). Genomic cucumber DNA samples, obtained from HDA6-expressing and control plants, were bisulfite-converted, amplified by PCR and cloned for sequencing. Methylation analysis revealed that, as previously observed (Martinez *et al*., 2014), HSVd infection decreased the relative number of methylated cytosine residues in cucumber leaves not overexpressing HDA6 compared to non-infected control plants (Fig. 3c). Alterations in methylation were observed in both symmetric and asymmetric sequence contexts (Fig. 3 c and d). In contrast, a significant increase in the levels of total methylated cytosine was observed in HSVd-infected leaves overexpressing recombinant HDA6 in comparison with HSVd-infected leaves without exogenous HDA6 supplementation (Fig. 3c). A detailed analysis showed that this increase in the methylation level was maintained in both symmetric and asymmetric sequence contexts (Fig. 3d).

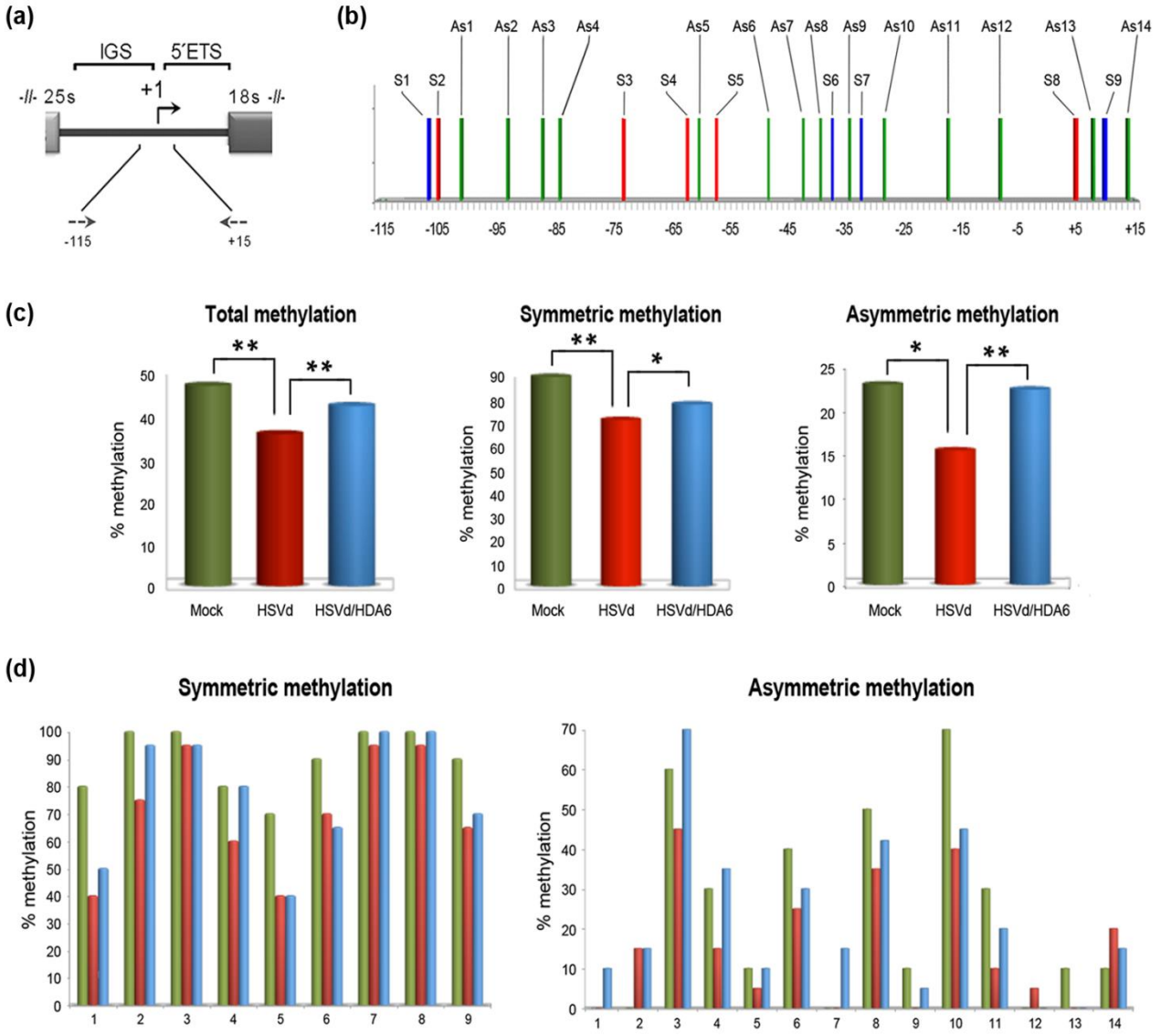

Figure 3: HDA6 reverses hypomethylation of the cucumber 45S rRNA gene induced by HSVd infection a) Diagram of the intergenic region of the 45S rRNA highlighting the area of the promoter region analyzed by bisulfite sequencing. The arrows represent the oligos used in the PCR assay and their relative positions in the rRNA. **b)** Graphic representation of the potential symmetric (S) and asymmetric (As) methylation positions predicted to exist within the analyzed region. **c)** Histogram illustrating the relative DNA methylation levels of the 45S rRNA promoter in cucumber plants: mock-inoculated (green bars), HSVd-infected (red bars) and HSVd-infected plants overexpressing recombinant HDA6 (blue bars). Total methylation (paired t-test values) means 0.50 (mock), 0.38 (HSVd) and 0.45 (HSVd/HDA6), ***P*<0.0005. Symmetric methylation (paired t-test values) means 0.88 (mock), 0.70 (HSVd) and 0.77 (HSVd/HDA6), **P*<0.025, ***P*<0.0025. Asymmetric methylation (paired t-test values) means 0.24 (mock), 0.16 (HSVd) and 0.23 (HSVd/HDA6), **P*<0.015, ***P*<0.0005. D) Positions of methylcytosines in the analyzed regions displayed in the symmetric (CG and CHG) and asymmetric (CHH) sequence context. The height of the bar represents the frequency at which cytosine was methylated in the three analyzed samples: mock-inoculated (green bars), HSVd-infected (red bars) and HSVd-infected plants overexpressing recombinant HDA6 (blue bars).

Comparable results regarding cytosine hypomethylation in symmetric sequence contexts were obtained when these assays were performed in conventionally HSVd-infected *N. benthamiana* plants but not in asymmetric sequence contexts (Supplementary Fig. 7).

HSVd accumulation is affected by HDA6

Our results support the idea that the hypomethylation status associated with HSVd infection could be a consequence of the viroid-mediated recruitment of HDA6 in infected cells, which would explain the disrupted transcriptional scenario observed in the host during HSVd infection (Martinez *et al*., 2014; Castellano *et al*., 2015). To clarify whether the HSVd-HDA6 interaction influences viroid accumulation, HSVd presence was analyzed in tissues overexpressing recombinant HDA6 using the RNA extracts obtained from the leaves described above (Supplementary Fig. 6).

A semi-quantitative RT-PCR assay was used to compare the levels of HSVd in viroid-infected cucumber and *N. benthamiana* plants (Fig. 4a, left and right, respectively). Our data clearly demonstrated that, unlike the endogenous RNAs used as controls, the HSVd accumulation estimated by RT-PCR amplification was significantly lower in viroid-infected cucumber (Fig. 4b left, blue bars) and *N. benthamiana* (Fig. 4b right, blue bars) leaves overexpressing exogenous HDA6 in comparison with mock-infiltrated HSVd-infected controls (red bars). The observation that viroid accumulation was significantly impaired in both hosts (Fig. 4c), by an excess of HDA6 in the nuclei of the infected cells suggests that recruitment of this host factor during the viroid infective cycle (demonstrated by IP assays) has an influence on the biological efficiency of HSVd.

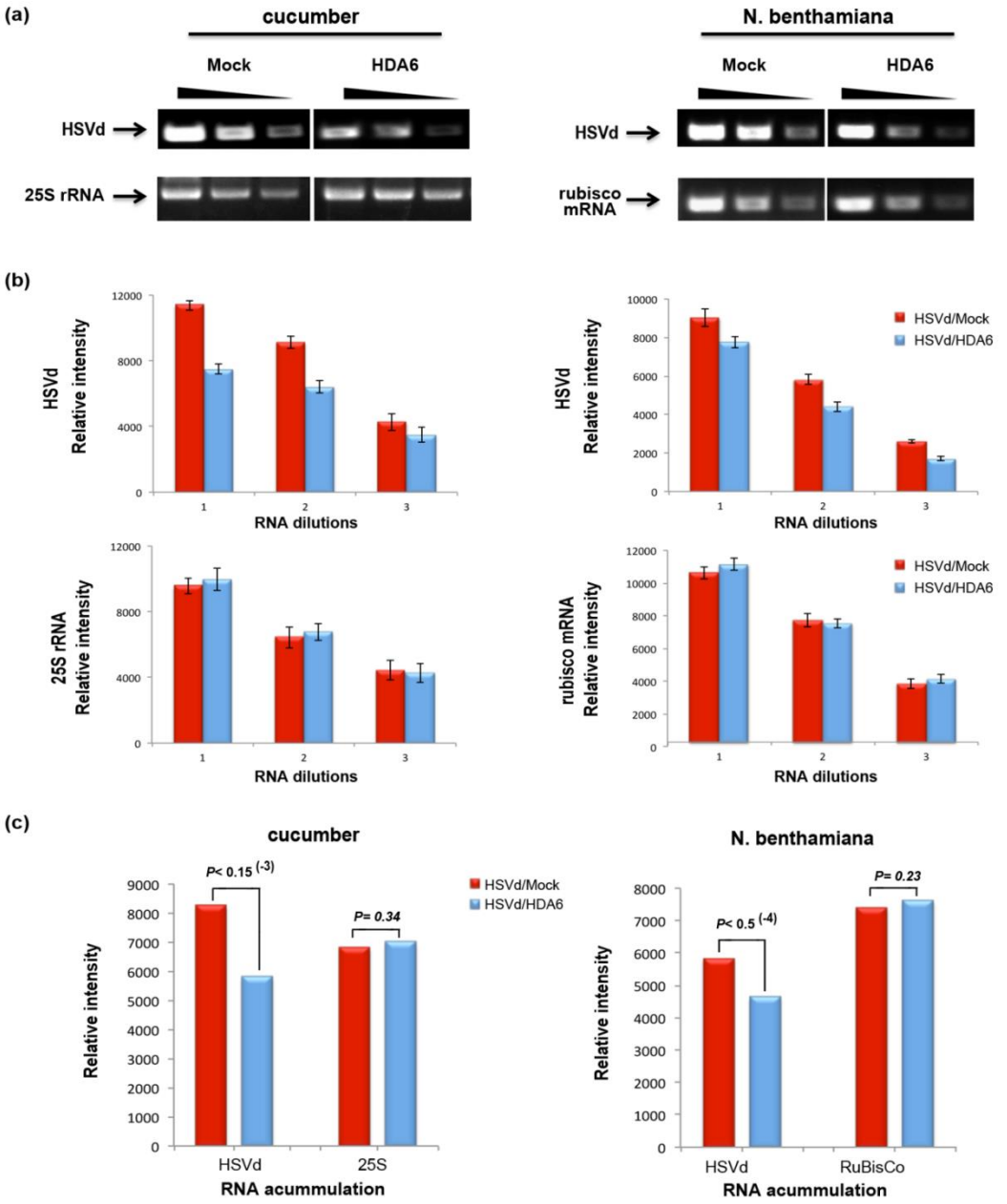

Figure 4. HSVd accumulation is negatively affected by HDA6 overexpression. a) Representative RT-PCR analyses of the viroid accumulation in serial dilutions of total RNAs extracted from HSVd-infected cucumber (left) and *N. benthamiana* (right) plants transiently overexpressing recombinant HDA6 or mock infiltrated with empty agrobacterium, as detailed in Supplementary Fig. 6. RT-PCR amplification of 25S rRNA (cucumber) and RuBisCo mRNA (*N. benthamiana*) served as RNA loading controls. **b)** Histogram showing the comparison between the relative intensity of the bands amplified by RT-PCR from the serial dilutions of the RNAs extracted from HSVd/Mock and HSVd/HDA6 plants. The lower panels show the values obtained when the RT-PCR products obtained for 25S and RuBisCo RNAs used as loading controls were analyzed. The bars (red for HSVd/Mock and blue for HSVd/HDA6) represent the means of 3 biological and 3 technical replicates for each event. Fine bars represent the standard error of the means. **c)** Graphical comparison of relative HSVd accumulation levels (estimated from the intensity of the RT-PCR products) in mock-infiltrated and HDA6-overexpressing infected samples. Bars (red for HSVd/Mock and blue for HSVd/HDA6) represent the mean values obtained for HSVd RNA amplification expressed relative to the controls (25S rRNA for cucumber and RuBisCo mRNA for *N. benthamiana* plants). Paired t-test values cucumber: HSVd mean values 8258 (mock) and 5801 (HSVd/HDA6); 25 sRNA mean values 6812 (mock) and 7006 (HSVd/HDA6). Paired t-test values N. benthamiana: HSVd mean values 5822 (mock) and 4602 (HSVd/HDA6); RuBisCo mean values 7412 (mock) and 7615 (HSVd/HDA6). The *P* values are shown in the figure.

To provide additional evidence for the physiological relevance of the HSVd-HDA6 interaction, we infected cucumber cotyledons overexpressing (by *A. tumefaciens*-mediated transient transformation) a hairpin construct designed to silence the gene encoding cucumber HDA6 (Supplementary Fig. 8). Total RNA was purified from the infiltrated areas at 3 dpi and analyzed by semi-quantitative RT-PCR assay. The relative accumulation of HSVd was significantly higher in infected cotyledons expressing the HDA6 hairpin construct in comparison with the relative accumulation of HSVd observed in control plants infiltrated with the empty vector (Fig. 5a, b and c). RT-PCR analysis of cucumber HDA6 mRNA indicated a significant reduction at 4 dpi in tissues infiltrated with the hairpin construct relative to those infiltrated with the empty vector (Fig. 5d and e), correlating HDA6-silencing and increasing in HSVd accumulation.

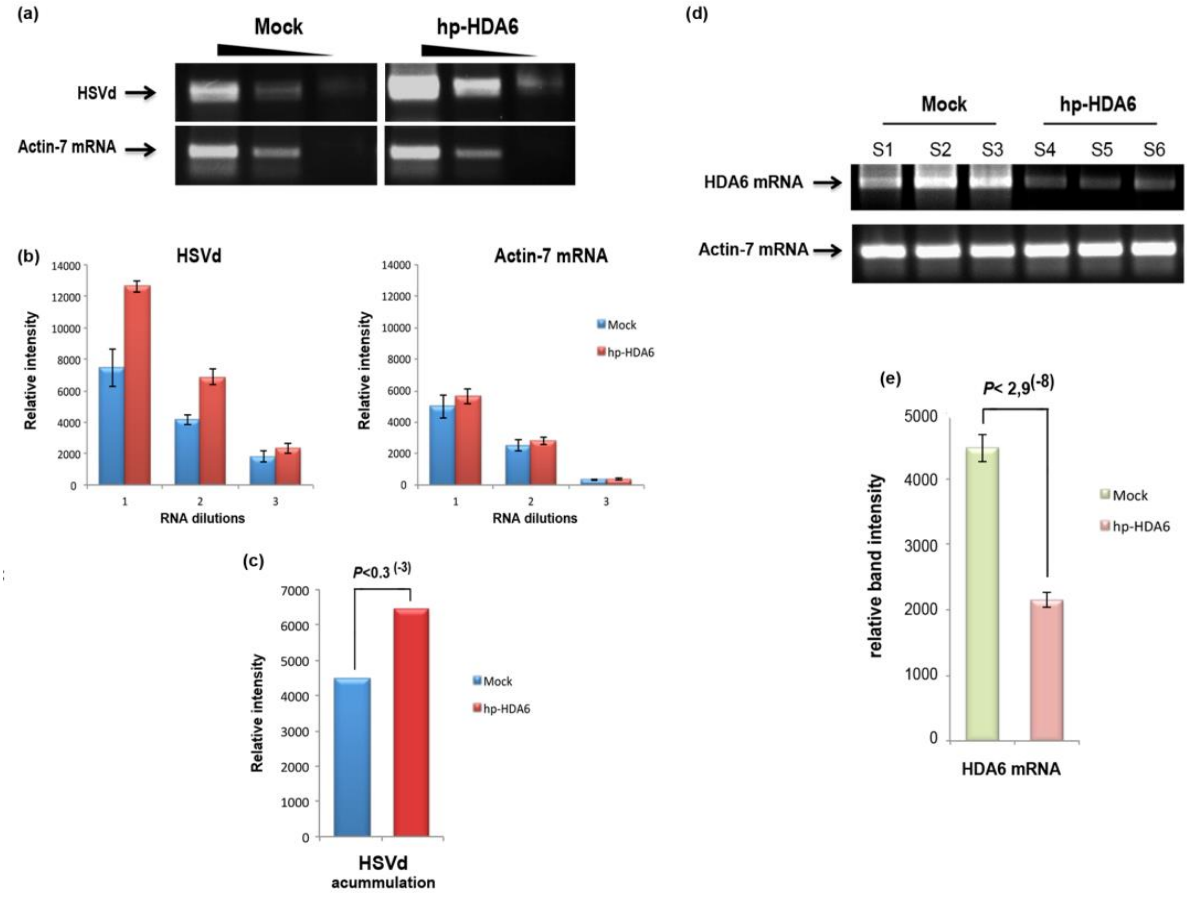

Figure 5: HSVd accumulation is increased in cucumber plants with reduced HDA6 expression. a) Representative RT-PCR analyses of the viroid accumulation in serial dilutions of total RNAs extracted from infected cotyledons overexpressing a hairpin construct designed to silence the gene encoding HDA6 (hp-HDA6) or mock infiltrated with empty vector. RT-PCR amplification of ubiquitin-40S ribosomal protein mRNA served as a RNA loading control. **b)** Histogram showing the comparison between the relative intensity of the bands amplified by RT-PCR from the dilutions of the RNAs extracted from infected plants infiltrated with hp-HDA6 and empty plasmid, respectively. The values obtained for the RT-PCR products of ubiquitin mRNA (control) were also analyzed. The bars (red for HSVd/hp-HDA6 and blue for HSVd/Mock) represent the means of 3 biological and 3 technical replicates. Fine bars represent the standard error of the means. **c)** Comparison of relative HSVd accumulation (estimated as in Figure 4) in HDA6-silenced and mock-infiltrated samples. Bars (red for HSVd/hp-HDA6 and blue for HSVd/Mock) represent the mean values obtained for HSVd RNA amplification expressed relative to control. Paired t-test values: HSVd mean values 4468 (HSVd/mock) and 6442 (HSVd/hp-HDA6). The *P* value is

shown in the figure. **d)** Representative RT-PCR analyses of the HDA6 mRNA levels in total RNAs extracted at 4 days post infiltration from 3 cucumber cotyledons infiltrated with *Agrobacterium* transformed with the vector hp-HDA6 (S4 to S6) and 3 mock-infiltrated controls (S1 to S3). RT-PCR amplification of actin 7 mRNA served as an RNA loading control. **e)** Histogram showing the comparison between the relative HDA6 mRNA levels estimated by RT-PCR in HDA6-silenced and mock-infiltrated samples. Bars (red for hp-HDA6 and green for mock) represent the mean values obtained for HDA6 mRNA amplification expressed relative to control. Paired t-test values: HDA6 mean values 4458 (mock) and 2146 (hp-HDA6). Fine bars represent the standard error. The *P* value is shown in the figure.

DISCUSSION

Conditioned by their incapacity to encode proteins, it is well established that viroids are strictly dependent on close interactions with host cellular components and functional mechanisms to complete their infection cycle. Considered to be a standardized and unique RNA, viroids have at least two (sequence- and structure-dependent) concomitant flexible ways to interact with plant regulatory machinery. This dual nature provides these lncRNAs the extraordinary potential to subvert plant cell developmental networks at multiple functional levels to increase their biological efficiency (Gomez & Pallas, 2013). Previous observations revealed that HSVd-infected cucumber and *N. benthamiana* plants exhibited an unexpected decrease in the cytosine methylation levels of the ribosomal gene promoters, demonstrating that HSVd can interfere with specific host methylation pathways during infection in a similar manner as that observed for other plant pathogens (Raja *et al*., 2008; Dowen *et al*., 2012; Rodriguez Negrete *et al*., 2013; Yang *et al*., 2013; Yu *et al*., 2013). The similarities between the observations in HSVd-infected plants (hyper-accumulation of 21-nt rb-sRNAs, loss of symmetric methylation and increased ribosomal gene transcription) (Martinez *et al*., 2014; Castellano *et al*., 2015) and in mutant *Arabidopsis* plants that fail to express HDA6 (Earley *et al*., 2010) provide experimental evidence supporting the possibility that a close interrelation between HSVd and HDA6 could occur during the pathogenesis process. Our first data supporting this idea was the observation that HDA6 accumulation increases in the nuclei of HSVd-infected cucumber cells, thus establishing a functional connection between viroid pathogenesis and HDA6 metabolism in infected plants. Next, *in vitro* assays demonstrated that HSVd RNA could bind recombinant cucumber HDA6, fulfilling the first characteristics essential for the existence of a direct interaction. In this regard, it is important to emphasize that co-compartmentalization of both HSVd-RNA and HDA6 in the nucleus provides a spatial scenario to permit this interaction *in vivo*. Furthermore, the observation that the HDA6-HSVd complex occurred *in vivo* in the heterologous *HSVd-Nb* system provided additional evidence for this interaction. Finally, recovery of the HSVd-HDA6 complex in immunoprecipitation assays of viroid-infected leaves confirmed that HSVd recognizes and recruits endogenous cucumber HDA6 during the pathogenesis process.

Having established the existence of the HSVd-HDA6 complex *in vivo*, we attempted to determine whether this complex possesses a functional relationship with the hypomethylation of rDNA observed during viroid infection (Martinez *et al*., 2014; Castellano *et al*., 2015). Bisulfite sequencing of DNA obtained from viroid-infected cucumber plants infiltrated with empty vectors clearly correlated the HSVd infection with reduced cytosine methylation in a key promoter region of cucumber 45S rDNA, reinforcing our previous observation that HSVd infection and hypomethylation of ribosomal genes occur in parallel in this viroid host. However, a significant increase in the methylation levels of this regulatory rDNA region was observed when recombinant HDA6 was overexpressed in the leaves of these same HSVd-infected plants. Furthermore, the modifications in the methylation levels of cytosine residues in the symmetric sequence context were also observed when cucumber HDA6 was transiently overexpressed in viroid-infected *N. benthamiana* plants. The demonstration that overexpression of exogenous cucumber HDA6 could reverse, at least in part, the dynamic changes in rDNA methylation induced by viroid infection in cucumber and *N. benthamiana* cells suggests that the alterations in cytosine methylation observed in the HSVd-infected plants may be associated with viroid interferences in the HDA6-dependent pathways responsible for the maintenance of rDNA methylation (Earley *et al*., 2010). We can speculate that the interaction between HSVd and HDA6 interferes with the formation of the HDA6-MET1 complex that is required to regulate maintenance of DNA methylation in symmetric sequence contexts (To *et al*., 2011; Liu *et al.* 2012 and 2012b). Further studies will be necessary to determine whether viroid-mediated recruitment of HDA6 also affects cytosine methylation in alternative HDA6 targets, such as repetitive DNA encoding transposable elements (Liu *et al.* 2012).

Altogether, these data support that HSVd is able to recruit and functionally inactivate host HDA6 during infection, consequently inducing changes in the methylation status of rDNA and causing transcriptional reactivation of normally silenced rRNA genes. Moreover, and in response to this functional interaction, there is increased accumulation of HDA6 in the nuclei of infected cells during the first steps of the infectious process. These findings support the view that epigenetic regulation of host transcriptional activity constitutes a regulatory mechanism associated with the plant response to viroid infection, as was previously shown for the pathogenesis processes induced by bacteria (Dowen *et al*., 2012; Yu *et al*., 2013) and viruses (Raja *et al*., 2008; Rodriguez Negrete *et al*., 2013; Yang *et al*., 2013).

However, a fundamental question remains unanswered: does the interaction between HSVd and HDA6 provide any adaptive advantage for viroids? Analysis of the HSVd accumulation estimated by RT-PCR revealed that viroid levels were significantly reduced when exogenous HDA6 was transiently overexpressed in infected cucumber and *N. benthamiana* plants. This suggests that an excess of free HDA6 in the nuclei of infected cells negatively affects the accumulation of HSVd, providing evidence of a

functional link between HDA6 activity and viroid biological efficiency. This idea was reinforced by the observation that transient silencing of cucumber HDA6 favors HSVd accumulation in infected plants.

Speculations regarding the functional nature of the HSVd-HDA6 complex during viroid infection seem premature at this point. However, it is opportune to consider that, although it is well established that members of the *Pospiviroidae* family recruit and re-direct RNA Pol II to transcribe the viroid RNA instead of the host DNA template (Flores & Semancik, 1982; Mühlbach & Sänger, 1997; Bojic *et al*., 2012), the strategy used by these pathogenic lncRNAs to reprogram RNA Pol II activity remains a conundrum. Interestingly, it was previously shown in *Arabidopsis hda6* mutants that, in addition to hypomethylation, loss of HDA6 activity was associated with spurious Pol II transcription of non-conventional rDNA templates (normally transcribed by RNA Pol I) (Earley *et al*., 2010). Based on these observations, we envision a hypothetical scenario in which, subsequent to cell invasion and once localized in the nucleus, HSVd RNA recruits and functionally inactivates endogenous HDA6 to promote spurious RNA Pol II activity, as indicated by the over-accumulation of pre-rRNAs and rb-sRNAs in infected plants (Martinez *et al*., 2014; Castellano *et al*., 2015). This favorable transcriptional environment may promote RNA Pol II to recognize and spuriously transcribe non-canonical templates (viroid RNA) in a manner similar to that observed for rDNA intergenic regions in *Arabidopsis hda6* mutants (Earley *et al*., 2010). Further studies assessing the stability of the HSVd-RNA Pol II complex in relation to HDA6 accumulation in viroid-infected plants are required to shed light on this possibility.

In summary, the data reported herein reveal that HSVd is able to recruit and subvert host HDA6 during infection, providing novel evidence regarding the potential of viroids to redesign the host cell environment and reprogram host regulatory mechanisms to ensure that their infectious cycle can be fulfilled. Furthermore, this study provides additional support to the emerging idea that the study of viroids as regulatory elements capable to alter host cell homeostasis can contribute to interpret the poorly understood pan-regulatory pathways directed by lncRNAs in plants (Ding, 2010; Gomez & Pallas, 2013; Katsarou *et al*., 2015; Liu *et al*., 2015; Gago-Zachert, 2016).

MATERIALS AND METHODS

Plant Material

Twelve-day-old cucumber (*Cucumis sativus* L *Cv* Suyo*)* and twenty-day-old *Nicotiana benthamiana* Domin plants were agro-inoculated with the *Agrobacterium tumefaciens* strain C58C1 transformed with a binary pMOG800 vector carrying a head-to-tail infectious dimeric HSVd cDNA (Y09352) (Gomez & Pallas, 2006) or an empty vector in both cotyledons and basal leaves. Plants were maintained in growth chambers

at 28 °C for 16 h with fluorescent light and at 24 °C for 8 h in darkness. Plants were analyzed as described in the figure legends. The HSVd/Nb plants (Gomez & Pallas, 2006) used in this study that carry a dimeric sequence of HSVd are able to process, accumulate and systemically transport viroid mature forms. Untransformed and HSVd/Nb plants were maintained in growth chambers (16 h light/8 h dark, 28 °C day/24 °C night) for 6–7 weeks.

Expression and purification of recombinant HDA6

The putative cucumber HDA6 was amplified by RT-PCR using the SuperScript® III One-Step RT-PCR System with Platinum® Taq DNA Polymerase [Invitrogen Corporation, Carlsbad, CA, USA] according to the manufacturer's instructions. The primers HDA6-DIR: GGATCCATCCGACGACATTCACG and HDA6-REV: CTCGAGTAAGAAGTATGGCTTGATCCTAG carrying the *Bam*HI and *Xho*I restriction sites, respectively, were used for amplification. The amplified fragments were cloned and sequenced. After establishing the correct cucumber HDA6 sequence, HDA6-ORF was *Bam*HI and *Xho*I digested and cloned into the expression vector pETDue-1 (Novagen) to obtain a recombinant version of HDA6 including amino-terminal Met-Gly-Ser-Ser-His6 extensions. The recombinant protein was purified under denaturing conditions by chromatography using a 1-ml Ni-NTA Agarose column (NI-NTA Purification System, Invitrogen) according to the manufacturer's instructions. The purified recombinant HDA6 protein was used to generate polyclonal antiserum in rabbits as previously described (Gomez & Pallas, 2004) and to perform HSVd-RNA binding assays by northwestern blot.

Western blot assays

Protein extracts obtained from cucumber and *N. benthamiana* were fractionated by SDS-PAGE 12% and transferred to PVDF membranes. Membranes were treated for 1 h in blocking solution [TBS (500 mM NaCl, 20 mM Tris, pH 7.5), 5% defatted milk, 2% BSA, and 0.1% Triton X-100] and incubated overnight with the antiserum against cucumber HDA6 or Green Fluorescent Protein (GFP) accordingly. Membranes were washed (TBS, 0.5% Tween 20), incubated with anti-rabbit IgG linked to horseradish peroxidase whole antibody. The antibody-protein complex was detected by luminescence (ECL+Plus, Amersham-Pharmacia Biotech, UK) according to the manufacturer's instructions. The serological detection of nuclear and cytoplasmic protein-controls was performed with antisera against Histone 3 (H3) and UDP-glucose pyrophosphorylase (UDP) (Agrisera AB, Vannas, Sweden - AS10710 and AS05086, respectively) according to the manufacturer's instructions.

Northwestern blot assays

Recombinant HDA6 was denatured by heating for 5 min at 95°C, fractionated by SDS-PAGE 12% and transferred to nitrocellulose membranes (Bio-Rad). Northwestern assays were performed as previously described (Gomez *et al*., 2005). Briefly, membranes were incubated in RN Buffer (10 mM Tris-HCl pH 7.5, 1 mM EDTA, 100 mM NaCl, 0.05% Triton X-100, and 1x Denhardt's reagent) for 2 h at room temperature followed by a 3-h incubation in RN buffer in the presence of DIG-labeled HSVd-RNAs (25-50 ng/ml). The detection of hybrid RNA-protein was performed using a colorimetric method.

Nuclei isolation

The enriched fraction of nuclear proteins was obtained starting from nuclei isolated as previously described (Sikorskaite *et al*., 2013), with minor modifications. Briefly, tissue extracts were clarified and treated with Triton X-100 to lyse membranes (according to the original protocol). Next, nuclei were collected by centrifugation through 2.5 M sucrose cushion solution (Nuclei Pure Prep Nuclei Isolation Kit, SIGMA). In immunoprecipitation (IP) assays, prior to nuclei isolation, the *N. benthamiana* and cucumber leaves were vacuum infiltrated with 1% formaldehyde to reversibly crosslink the RNA-protein complexes (Ricardi *et al*., 2010).

Immunoprecipitation assays

Two complementary assays were performed to detect the HDA6-HSVd complexes *in vivo* in *N. benthamiana* and cucumber plants.

N. benthamiana: Recombinant HDA6 (carrying an amino-terminal His6 tag) was transiently expressed by agro-infiltration in the leaves of transgenic *N. benthamiana* plants constitutively expressing dimeric HSVd transcripts (HSVd/Nb). Three days after infiltration, the leaves overexpressing HDA6 were treated with 1% formaldehyde to reversibly crosslink the RNA-protein complexes and were used to obtain purified nuclei as described above. The HDA6-HSVd complexes were captured by affinity chromatography with a nickel column (NI-NTA Purification System, Invitrogen) according to the manufacturer's instructions. Eluates were analyzed by western blot and RT-PCR to detect recombinant HDA6 and HSVd RNA, respectively.

Cucumber: Nuclear extracts obtained from the leaves of HSVd-infected plants (at 30 days post inoculation) as described above were subjected to conventional IP assays with HDA6-As and agarose-conjugated protein A (Roche Diagnostics, Mannheim, Germany) according to the manufacturer's instructions as previously described (Gomez & Pallas, 2004). Immunoprecipitated extracts were analyzed by western blot and RT-PCR to detect recombinant HDA6 and HSVd-RNA, respectively.

RNA extraction and northern blot analysis

Total RNAs were extracted using TRI reagent (SIGMA, St. Louis, MO, USA) according to the manufacturer instructions. Briefly, 500 mg of leaves from HSVd-infected and control plants were ground in 2 ml of TRI reagent. Then, 400 µl of chloroform was added, and the sample was vigorously vortexed and subsequently centrifuged. The supernatant was recovered, and the total RNAs were precipitated with isopropanol and resuspended in sterile water. The total RNA preparations were quantified by spectrometry and their concentrations were equalized. To analyze the circular and linear forms of HSVd-RNA by northern blot analysis, 1.5 µg of the total RNA preparations were electrophoresed under denaturing conditions in a 5% polyacrylamide mini-gel, with 0.25 x TBE and 8 M urea. After electrophoresis, the RNAs were blotted onto positively charged nylon membranes and hybridized as previously described (Gomez & Pallas, 2006).

Bisulfite conversion and sequencing

Total genomic DNA was extracted from HSVd-infected and mock-inoculated cucumber and *N. benthamiana* leaves using a previously described protocol (Martinez *et al*., 2014). Total DNA (1 µg) was diluted into 20 µL of water and subjected to bisulfite treatment using the EpiTect Bisulfite kit (Qiagen) according to the manufacturer's instructions. The rRNA region to be analyzed and the corresponding oligos were determined using MethPrimer software http://www.urogene.org/cgi-bin/methprimer (Li & Dahiya, 2002). PCRs were performed using Taq DNA polymerase (Promega) and analyzed in 1.5% agarose gels. PCR products were purified by gel extraction and cloned using the pTz cloning kit (Fermentas). Twenty to 25 clones were sequenced from each analyzed point from mock-treated and HDA6-expressing HSVd-infected samples. Two independent biological replicates were analyzed for HSVd-infected and mock-inoculated plants.

Agro-infiltration

N. benthamiana and cucumber plants were infiltrated with the HDA6/GFP or unmodified GFP constructs as previously described (Gomez & Pallas, 2007) and maintained at 28 °C with 14 h of light. GFP expression in plants was analyzed at 72 h after agro-infiltration using a TCS SL confocal laser scanning microscope (Leica), with excitation at 488 nm and emission at 510–560 nm. The nuclear localization of the HDA6/GFP was established using Red Fluorescent Protein (RFP) fused to a nucleolar-specific peptide as a reference. The GFP- and HDA6/GFP-expressed proteins were also detected by western blot using GFP-specific antibodies, as previously described (Gomez & Pallas, 2007).

In transient HDA6 silencing assays, eleven-day-old cucumber plants were infiltrated with *Agrobacterium* transformed with the vector hp-HDA6 or empty vector (control) in both cotyledons. At one day post agro-

infiltration (dpa), the distal part of the cotyledons was inoculated with *Agrobacterium* transformed with a vector carrying a dimeric HSVd cDNA. At three days post HSVd inoculation (dpi), the HSVd-inoculated area was eliminated, and total RNAs were extracted from the remaining parts of the cotyledons. The RNA was used to determine HSVd accumulation and HDA6 mRNA levels by RT-PCR.

Analysis of GFP expression

GFP expression was analyzed using a Leica MZ 16 F fluorescence stereomicroscope equipped with filters DSR, GFP2 and V (Leica). Tissue sections were also observed using a TCS SL confocal laser scanning microscope (Leica), with excitation at 488 nm and emission at 510–560 nm. GFP was also detected by western blot using GFP-specific antibodies, as previously described.

Plasmid Constructs for RNA Silencing Assays

A fragment of the cucumber HDA6 sequence between positions 369 and 868 (GenBank accession XM_004138046.2) was inserted in sense orientation between the XhoI and KpnI sites and in reverse orientation between the XbaI and HindIII sites of pHANNIBAL (GenBank accession no. AJ311872) to produce a hairpin expression cassette, which included a CaMV 35S promoter and an *A. tumefaciens* ocs terminator. This cassette, flanked by two NotI restriction sites, was inserted into the unique NotI site of the binary plasmid pMOG. The empty pHANNIBAL NotI cassette was also inserted into the binary plasmid pMOG to produce the control plasmid. Both plasmids were electroporated into *A. tumefaciens* C58C1.

RT-PCR analysis

Total RNA was extracted from the leaves of the HSVd-infected and mock-inoculated plants using TRI reagent (Sigma, St. Louis, MO, USA) according to the manufacturer's instructions. RT-PCR analysis was performed using the SuperScript® III One-Step RT-PCR System with Platinum® Taq DNA Polymerase [Invitrogen Corporation, Carlsbad, CA, USA] according to the conditions described below.

HSVd amplification: Primers Dir-1 (GGTTCGCTCCAACCTGCTTTTG) and Rev-1 (CCCCGGGGCTCCTTTCTCAGGT) flanking an ~150 bp region of HSVd RNA. Assay conditions: RT (30 min at 50 °C and 3 min at 95 °C); 25 PCR cycles at (95 °C/15 s, 55 °C/20 s, and 70 °C/15 s).

25S rRNA amplification: Primers 25S-Fw (TATATAAGGGGGGTAGAGGTGTTG) and 25S-Rv (ATRCCAAACACAACTCACAACAACC) flanking an ~500 bp region of rRNA. Assay conditions: RT (30 min at 50°C and 3 min at 95 °C); 20 PCR cycles at (95 °C/15 s, 55 °C/20s, and 70 °C/30s).

RuBisCO mRNA amplification: Primers Rub-Dir (TACTTGAACGCTACTGCAG) and Rub-Rev (CTGCATGCATTGCACGGTG) flanking a region (~180 nt) of RuBisCO mRNA were used to amplify this mRNA as a loading control. RT-PCR conditions 45 °C for 30 min, followed by 30 cycles of 95 °C/15 s, 58 °C/20 s, and 70 °C/15 s.

Primers H6-Dir (ATGTCCGACGACATTCACGGCG) and H6-Rev (TTTCGGGGCTGACGGAGGCGAG) flanking a region (~280 nt) of cucumber HDA6 mRNA were used to amplify this mRNA. RT-PCR conditions were 45 °C for 30 min, followed by 30 cycles of 95 °C/15 s, 62 °C/20 s, and 70 °C/24 s.

Primers Act-Dir (GGAGCTGAGAGATTCCGTTG) and Act-Rev (GGTGCAACGACCTTGATTTT) flanking a region (~270 nt) of cucumber Actin-7 mRNA (XM_004147305.2) were used to amplify this mRNA as a loading control. RT-PCR conditions were 45°C for 30 min, followed by 27 cycles of 95 °C/15s, 57 °C/20s, and 72 °C/20s.

ACKNOWLEDGMENTS

The authors thank Drs M. Fares for their contribution to the statistical analysis of the data and Dr G. Martinez for the critical reading ofthis manuscript. This work was supported by grants AGL2013-47886-R and BIO2014-61826-EXP (GG) and BIO2014-54862-R (VP) from the Spanish Granting Agency (Direccion General Investigacion Cientifica).

AUTHOR CONTRIBUTIONS

M.C. performed the experiments, discussed the results and revised the mansuscript. V.P. discussed the results and wrote the main manuscript text. G.G designed the experiments, discussed the results, prepared figures and wrote the main manuscript text.

REFERENCES

Adkar-Purushothama CR, Brosseau C, Giguère T, Sano T, Moffettb P, Perreault JP. 2015. Small RNA Derived from the Virulence Modulating Region of the Potato spindle tuber viroid Silences callose synthase Genes of Tomato Plants. *The Plant Cell* **27**: 2178-2194.

Aufsatz W, Mette M, der Winden van J, Matzke M, Matzke AJ. 2002. HDA6, a putative histone deacetylase needed to enhance DNA methylation induced by double-stranded RNA. *EMBO Journal* **21:** 6832-6841.

Bojic T, Beeharry Y, Zhang DJ, Pelchat M. 2012. Tomato RNA polymerase II interacts with the rod-like conformation of the left terminal domain of the potato spindle tuber viroid positive RNA genome. *Journal of General Virology* **93:** 1591-1600.

Castellano M, Martinez G, Pallás V, Gómez G. 2015. Alterations in host DNA methylation in response to constitutive expression of Hop stunt viroid RNA in Nicotiana benthamiana plants. *Plant Pathology* **64:** 1247–1257.

Dalakouras A, Dadami E, Bassler A, Zwiebel M, Krczal G, Wassenegger M. 2015. Replicating Potato spindle tuber viroid mediates de novo methylation of an intronic viroid sequence but no cleavage of the corresponding pre-mRNA. *RNA Biology* **12:** 268-275.

Dalakouras A, Wassenegger M. 2013. Revisiting RNA-directed DNA methylation. *RNA Biology* **10:** 453-455.

Ding B. 2010. Viroids: self-replicating, mobile, and fast-evolving noncoding regulatory RNAs. *Wiley Interdisciplinary Reviews: RNA* **1**: 362-375.

Dowen R, Pelizzola M, Schmitz R, Lister R, Dowen JM, Nery JR, Dixon JE, Ecker JR. 2012. Widespread dynamic DNA methylation in response to biotic stress. *Proceedings of the National Academy of Sciences USA* **109:** 2183-2191.

Eamens AL, Smith N, Dennis E, Wassenegger M, Wang MB. 2014. In Nicotiana species, an artificial microRNA corresponding to the virulence modulating region of Potato spindle tuber viroid directs RNA silencing of a soluble inorganic pyrophosphatase gene and the development of abnormal phenotypes. *Virology* **450:** 266-277.

Earley KW, Pontvianne F, Wierzbicki AT, Blevins T, Tucker S, Costa-Nunes P, Pontes O, Pikaard CS. 2010. Mechanisms of HDA6-mediated rRNA gene silencing: suppression of intergenic Pol II transcription

and differential effects on maintenance versus siRNA-directed cytosine methylation. *Genes Development* **24:** 1119-1132.

Flores R, Gago Zachert S, Serra P, Sanjuán R, Elena SF. 2014. Viroids: survivors from the RNA world? *Annual Review of Microbiology* **68**: 395-414.

Flores R, Semancik JS. 1982. Properties of a cell-free system for synthesis of citrus exocortis viroid. *Proceedings of the National Academy of Sciences USA* **79:** 6285-6288.

Gago-Zachert S. 2016. Viroids, infectious long non-coding RNAs with autonomous replication. *Virus Research* **212:** 12-24.

Gas ME, Hernández C, Flores R, Daròs JA. 2007. Processing of nuclear viroids in vivo: interplay between RNA conformations. *PLoS Pathogens* 3: e182.

Gomez G, Martinez G, Pallas V. 2008. Viroid-induced symptoms in Nicotiana benthamiana plants are dependent on RDR6 activity. *Plant Physiology* **148:** 414-423.

Gomez G, Martinez G, Pallas V. 2009. Interplay between viroid-induced pathogenesis and RNA silencing pathways. *Trends in Plant Science* **14:** 264-269.

Gomez G, Pallas V. 2004. A long-distance translocatable phloem protein from cucumber forms a ribonucleoprotein complex in vivo with Hop stunt viroid RNA. *Journal of Virology* **78:** 10104-10110.

Gomez G, Pallas V. 2007. Mature monomeric forms of Hop stunt viroid resists RNA silencing in transgenic plants. *Plant Journal* **51:** 1041-1049 (2007).

Gomez G, Pallas V. 2013. Viroids: a light in the darkness of the lncRNA-directed regulatory networks in plants. *New Phytologist* **198:** 10-15.

Gomez G, Torres H, Pallás V. 2005. Identification of translocatable RNA-binding phloem proteins from melon, potential components of the long-distance RNA transport system. *Plant Journal* **41:** 107–116.

Gomez, G, Pallas V. 2006. Hop stunt viroid is processed and translocated in transgenic Nicotiana benthamiana plants. *Molecular Plant Pathology* **7:** 511-517.

Hristova E, Fal K, Klemme L, Windels D, Bucher E. 2015. HDA6 controls gene expression patterning and DNA methylation-independent euchromatic silencing. *Plant Physiology* **168:**1298-1308.

Katsarou K, Rao AL, Tsagris M, Kalantidis K. 2015. Infectious long non-coding RNAs. *Biochimie* **117:** 37-47.

Li LC, Dahiya R. 2002. MethPrimer: designing primers for methylation PCRs. *Bioinformatics* **18:** 1427-1431.

Liu X, Hao L, Li D, Zhu L, Hu S. 2015. Long Non-coding RNAs and Their Biological Roles in Plants. *Genomics Proteomics Bioinformatics* **13:**137-147.

Liu X, Luo M, Wu K. 2012. Epigenetic interplay of histone modifications and DNA methylation mediated by HDA6. *Plant Signaling Behavior* **7:** 633-635.

Liu X, Yu C, Duan J, Luo M, Wang K, *et al*. 2012b. HDA6 directly interacts with DNA methyltransferase MET1 and maintains transposable element silencing in *Arabidopsis*. *Plant Physiology* **158:** 119-129.

Martinez G, Castellano M, Tortosa M, Pallas V, Gomez G. 2014. A pathogenic non-coding RNA induces changes in dynamic DNA methylation of ribosomal RNA genes in host plants. *Nucleic Acids Reseach* **42:** 1553-1562.

May B, Lippman Z, Fang Y, Spector D, Martienssen RA. 2005. Differential regulation of strand-specific transcripts from *Arabidopsis* centromeric satellite repeats. *PLoS Genetics* **1**: e79. doi:10.1371/journal.pgen.0010079.

Mühlbach HP, Sänger HL. 1997. Viroid replication is inhibited by alpha-amanitin. *Nature* **278:** 185-188 (1997).

Navarro B, Gisel A, Rodio ME, Delgado S, Flores R, Di Serio F. 2012. Viroids: how to infect a host and cause disease without encoding proteins. *Biochimie* **94**: 1474-1480.

Navarro B, Gisel A, Rodio M, Delgado S, Flores R, Di Serio F. 2012b. Small RNAs containing the pathogenic determinant of a chloroplast-replicating viroid guide the degradation of a host mRNA as predicted by RNA silencing. *Plant Journal* **70:** 991-1003.

Navarro JA, Vera A, Flores RA. 2000. Chloroplastic RNA polymerase resistant to tagetitoxin is involved in replication of avocado sunblotch viroid. *Virology* **268:** 218-225.

Nohales MA, Molina Serrano D, Flores R, Daros JA. 2012. Involvement of the chloroplastic isoform of tRNA ligase in the replication of viroids belonging to the family Avsunviroidae. *Journal of Virology* **86**: 8269-8276.

Nohales MA, Flores R, Daros JA. 2012b. Viroid RNA redirects host DNA ligase 1 to act as an RNA ligase. *Proceedings of the National Academy of Sciences USA* **109**, 13805-13810.

Owens RA, Hammond RW. 2009. Viroid pathogenicity: One process, many faces. *Viruses* **1:** 298-316.

Palukaitis P. 2014. What has been happening with viroids? *Virus Genes* **49:** 175-184.

Papaefthimiou I, Hamilton A, Denti M, Baulcombe D, Tsagris M, Tabler M. 2001. Replicating potato spindle tuber viroid RNA is accompanied by short RNA fragments that are characteristic of post-transcriptional gene silencing. *Nucleic Acids Research* **29:** 2395-2400.

Probst A, Fagard M, Proux F, Mourrain P, Boutet S, Earley K, Lawrence RJ, Pikaard CS, Murfett J, Furner I, Vaucheret H, Mittelsten-Scheid O. 2004. *Arabidopsis* Histone Deacetylase HDA6 is required for maintenance of transcriptional gene silencing and determines nuclear organization of rdna repeats. *Plant Cell* **16:** 1021-1034.

Raikhel N. 1992. Nuclear targeting in plants. *Plant Physiology* **100:** 1627-1632.

Raja P, Sanville BC, Buchmann R. 2008. Viral genome methylation as an epigenetic defense against geminiviruses. *Journal of Virology* **82:** 8997–9007.

Ricardi M, González RM, Iusem ND. 2010. Protocol: fine-tuning of a Chromatin Immunoprecipitation (ChIP) protocol in tomato. *Plant Methods* **9:** 6-11.

Rodriguez Negrete E, Lozano Duran R, Piedra Aguilera A, Cruzado L, Bejarano E, Castillo AG. 2013. Geminivirus Rep protein interferes with the plant DNA methylation machinery and suppresses transcriptional gene silencing. *New Phytologist* **199:** 464-475.

Sikorskaite S, Rajamäki ML, Baniulis D, Stanys V, Valkonen JP. 2013. Protocol: Optimised methodology for isolation of nuclei from leaves of species in the Solanaceae and Rosaceae families. *Plant Methods* **26:** 9-31.

To T, Kim J, Matsui A, Kurihara Y, Morosawa T, Ishida J, Tanaka M, Endo T, Kakutani T, Toyoda T, *et al.* 2011. *Arabidopsis* HDA6 regulates jocus-directed heterochromatin silencing in cooperation with MET1. *PLoS Genetics* **7**(4): e1002055.

Wang MB, Bian XY, Wu LM, Lium LX, Smith N, Isenegger D, Wu RM, Masuta C, Vance VB, Watson JM. *et al*. 2004. On the role of RNA silencing in the pathogenicity and evolution of viroids and viral satellites. *Proceedings of the National Academy of Sciences USA* **101:** 3275-3280.

Yang LP, Fang Y, An CP. 2013. C2-mediated decrease in DNA methylation, accumulation of siRNAs, and increase in expression for genes involved in defense pathways in plants infected with beet severe curly top virus. *Plant Journal* **73:** 910-917.

Yu A, Lepere G, Jay F, Wang J, Bapaume L, Wang Y, Abraham AL, Penterman J, Fischer RL, Voinnet O, *et al*. 2013. Dynamics and biological relevance of DNA demethylation in *Arabidopsis* antibacterial defence. *Proceedings of the National Academy of Sciences USA* **110:** 2389-2394.

SUPPORTING FIGURES

Figure S1: Purification of recombinant cucumber HDA6 and production of polyclonal antiserum.

Figure S2: HDA6-GFP accumulates specifically in the nucleus of *N. benthamiana* cells.

Figure S3: Recombinant cucumber HDA6 is detected in nuclear extracts of *N. benthamiana* plants.

Figure S4: Differential detection of endogenous HDA6 in HSVd-infected plants.

Figure S5: Cucumber HDA6 binds HSVd-RNA in HSVd-expressing transgenic *N. benthamiana* plants.

Figure S6: Schematization of combined agro-infiltration assays in infected cucumber and *N. benthamiana* plants.

Figure S7: Recombinant cucumber HDA6 reverts the hypomethylation induced by HSVd infection in N. benthamiana 45S rRNA genes.

Figure S8: Schematization of transient HDA6 silencing assays in HSVd-infected cucumber plants.

ADDITIONAL INFORMATION:

Author contribution

MC: performed the experiments, discussed the results and revised the manuscript. VP: discussed the results and wrote the main manuscript text. GG: has designed the experiments, discussed the results, prepared figures and wrote the main manuscript text.

SUPPLEMENTAL DATA

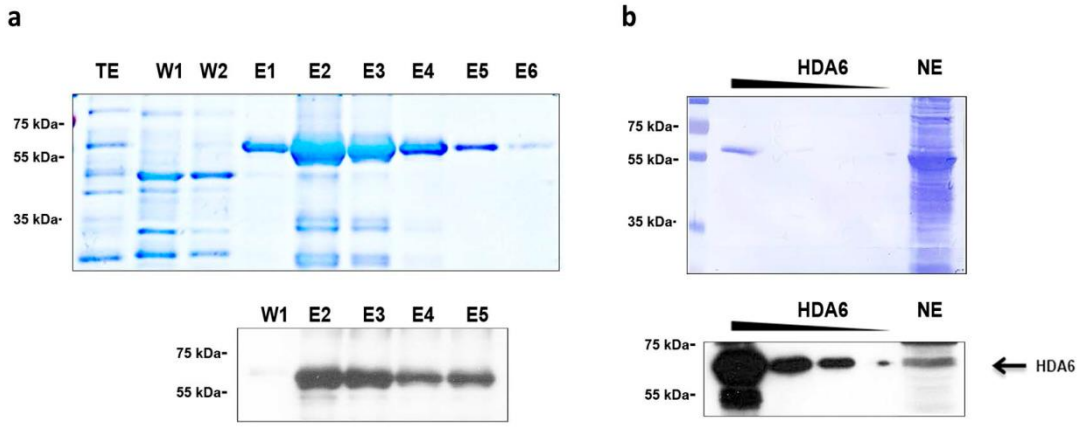

Fig. S1: Purification of recombinant cucumber HDA6 and production of polyclonal antiserum. a) A recombinant version of HDA6 was expressed in *E. coli* and purified by affinity chromatography in a nickel column. Proteins in the *E. coli* crude extract (TE), wash eluates (W1 and W2) and sequential fractions eluted with 0.5 M imidazole (E1 to E6) were fractionated by SDS/PAGE, and the gel was stained with Coomassie Blue to analyze the recovered protein (upper panel). The W1 and E2 to E5 fractions were arbitrarily selected for confirmation by western blot (with H6-As) for the specific enrichment of recombinant cucumber HDA6 (lower panel). b) Purified recombinant HDA6 was used to raise polyclonal antibodies in rabbit. Subcutaneous doses (~ 7.5 µg) were injected weekly over a 4-week period, and blood was collected. Serial dilutions of recombinant HDA6 were fractionated by SDS-PAGE and transferred to PVDF membranes for serological analysis with the polyclonal antiserum raised against cucumber HDA6 (diluted 1/10000) (upper and lower panels, respectively). An extract of nuclear enriched proteins (NE) was used as a control.

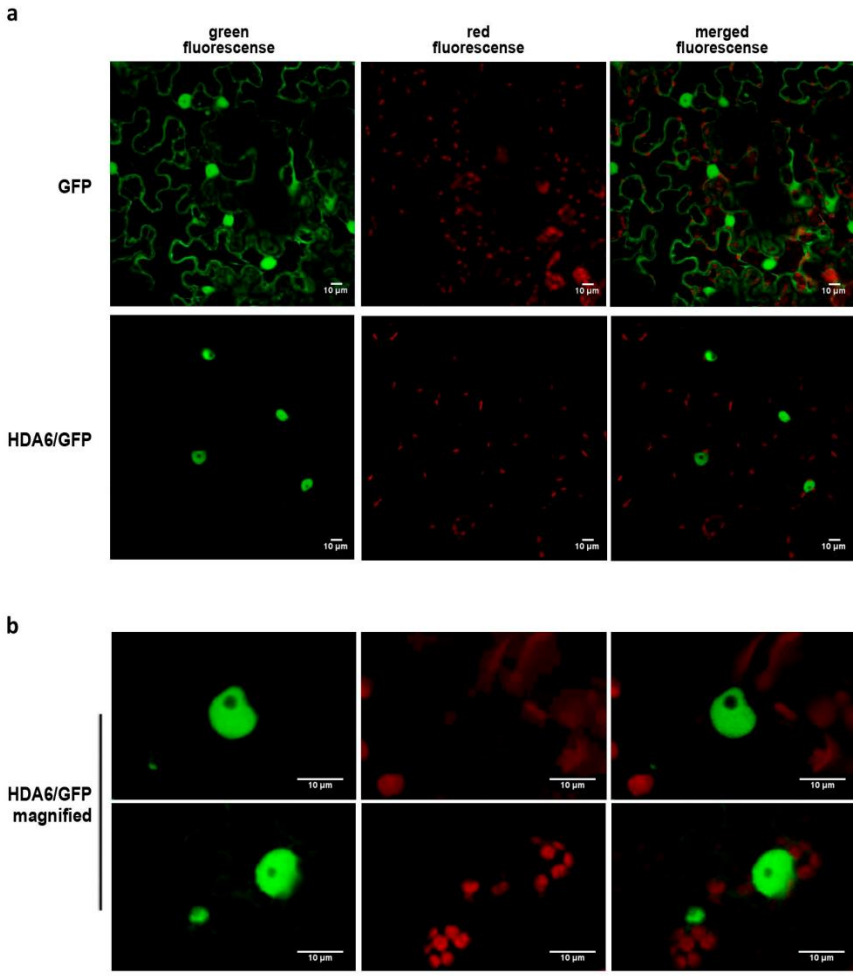

Fig. S2: HDA6-GFP accumulates specifically in the nucleus of *N. benthamiana* cells. a) Confocal microscope observation of NB leaves transiently expressing free GFP (upper panels) and HDA6/GFP (lower panels). As can be observed, HDA6/GFP mainly accumulates in the cell nucleus, in contrast to the free GFP used as a control, which is indistinctly detected in the cytosol and the nucleus. Chloroplasts are shown in red. b) Magnified images confirming the specific nuclear localization of HDA6/GFP in NB cells. Chloroplasts are shown in red.

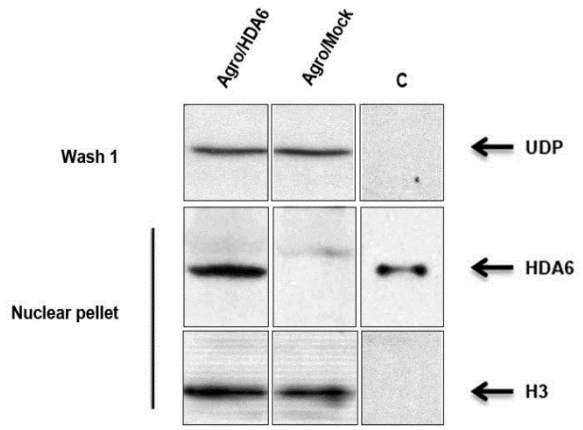

Fig. S3: Recombinant cucumber HDA6 is detected in nuclear extracts of *N. benthamiana* plants. Specific detection by western blot assays of cucumber HDA6 (using HDA6-As) in nuclear fractions recovered from nuclear extracts of *N. benthamiana* plants transiently expressing recombinant HDA6 or agro-infiltrated with empty vector (middle panel). Histone 3 (H3) (lower panel) and UDP-glucose pyrophosphorylase (UDP) (upper panel) were used as well-established markers of nuclear and cytoplasmic fractions, respectively. Purified recombinant HDA6 was used as a control.

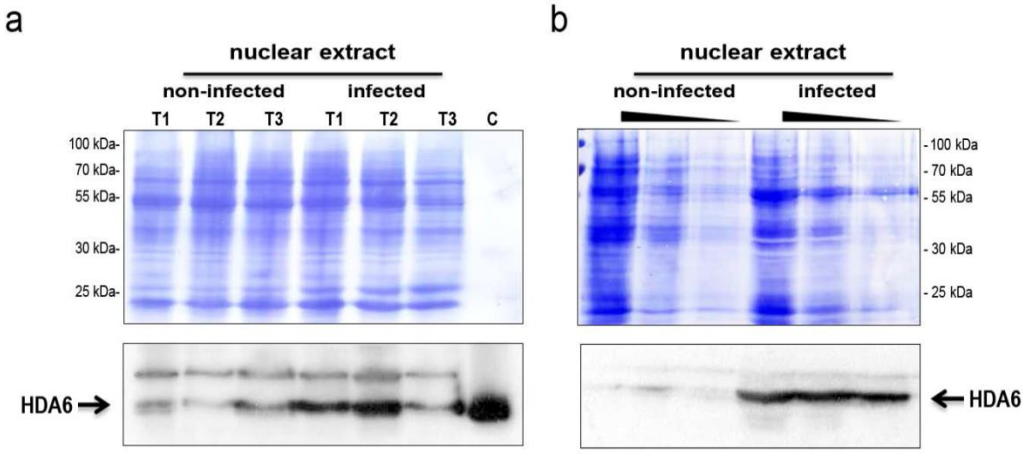

Fig. S4: Differential detection of endogenous HDA6 in HSVd-infected plants. a) Proteins obtained from nuclear extracts recovered from infected and mock-inoculated cucumber leaves at 18 (T1), 25 (T2) and 32 dpi were fractionated in SDS-PAGE (upper panel) and transferred to PDVF membranes for serological analysis with HDA6-As (lower panel). A notable increase in the expression of endogenous HDA6 is observed in the HSVd-infected cucumber plants at 18 and 25 dpi. b) Similar assays were performed with serial dilutions of proteins recovered from nuclear extracts of infected and mock-inoculated cucumber leaves at 25 dpi (T2) to confirm the differential expression of cucumber HDA6 in the extracts of infected cucumber leaves.

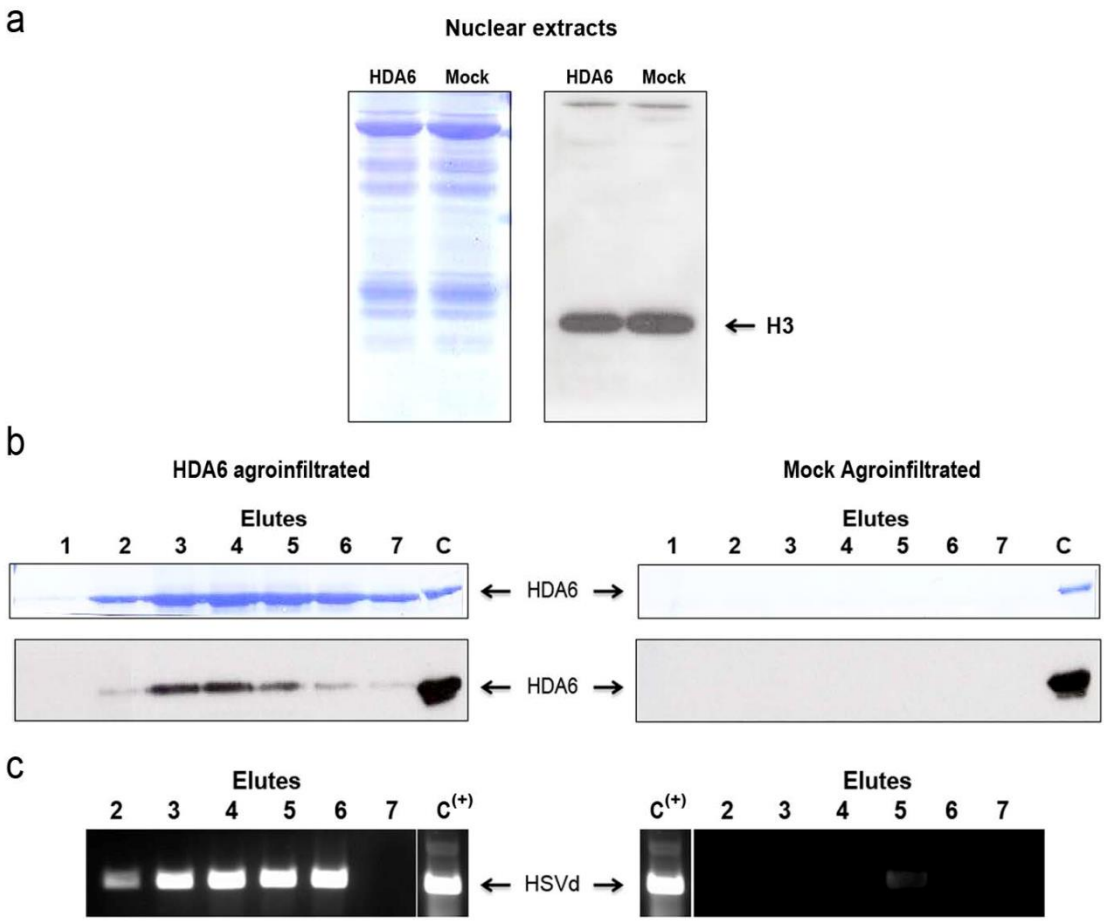

Fig. S5: Cucumber HDA6 binds HSVd-RNA in HSVd-expressing transgenic *N. benthamiana* plants. a) Nuclear extracts obtained from HSVd/Nb leaves transiently expressing recombinant cucumber HDA6 and mock-treated with *Agrobacterium* carrying an empty vector (60 h post agro-infiltration) were subjected to SDS-PAGE (left panel). Specific serological detection of Histone 3 (H3) was used as a control to guarantee equivalent nuclear protein accumulation in both samples analyzed (right panel). b) Proteins recovered from nuclear extracts were subjected to affinity chromatography in a nickel column to specifically recover recombinant cucumber HDA6. Sequential fractions eluted with 0.5 M imidazole (E1 to E7) were fractionated by SDS/PAGE, and the gel was stained with Coomassie Blue to analyze the recovered protein (upper panel). Eluates (E1 to E7) were next analyzed by western blot (with H6-As) to confirm the specific enrichment of recombinant cucumber HDA6 (lower panel). Purified recombinant HDA6 was used as a control. c) Total RNAs extracted from recombinant HDA6-enriched fractions (E2-E7) were subjected to RT-PCR analysis to confirm the specific recovery of HSVd-RNA. C^+ lines show a duplication of the RT-PCR control.

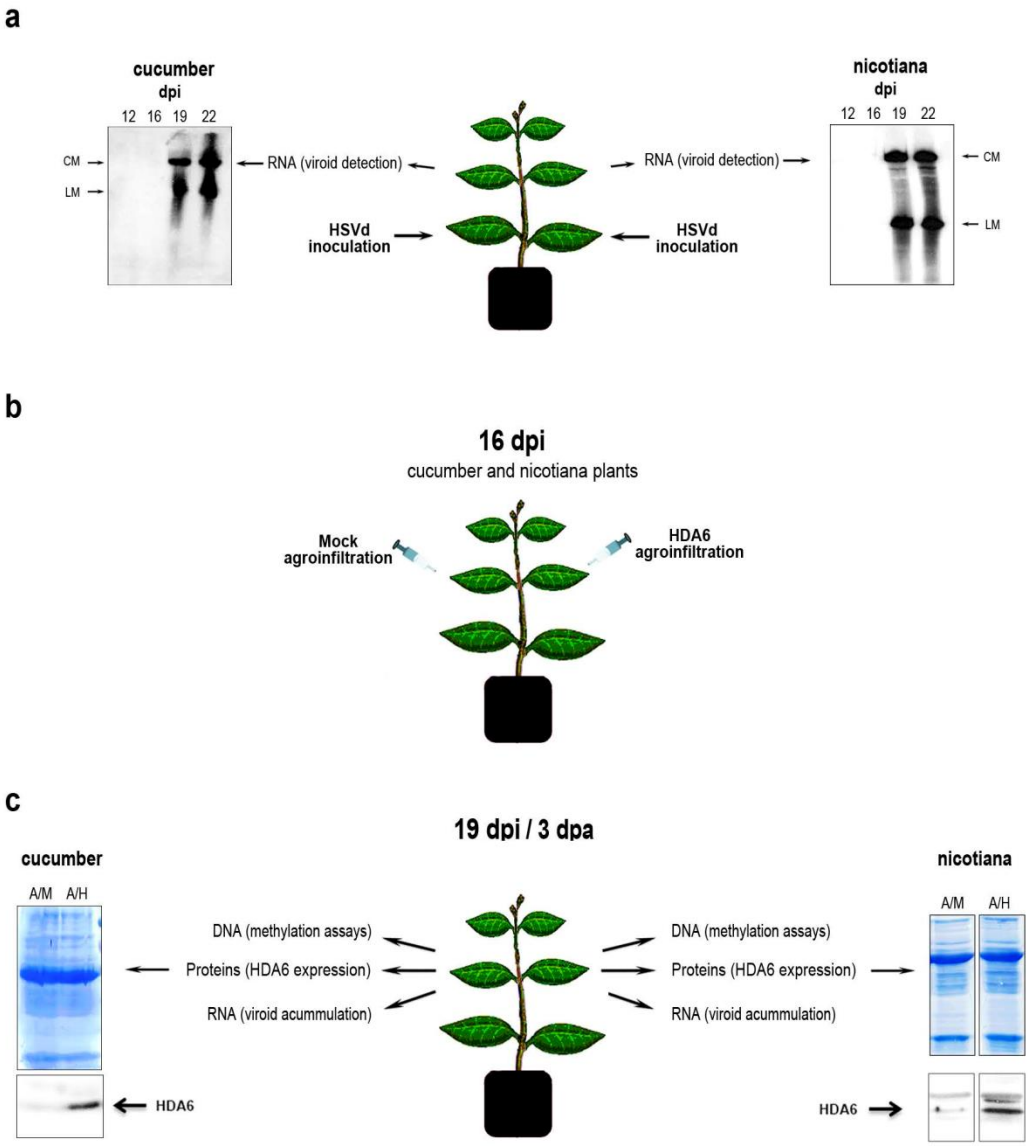

Fig. S6: Schematization of combined agro-infiltration assays in infected cucumber and *N. benthamiana* plants. a) Twelve-day-old cucumber and twenty-day-old *N. benthamiana* plants were inoculated with *Agrobacterium* transformed with a vector carrying a dimeric HSVd cDNA in both cotyledons and basal leaves. Total RNAs extracted from apical leaves were analyzed (at 12, 16, 19 and 22 dpi) by northern blot assays to detect circular (CM) and linear (LM) mature forms of HSVd. b) After establishing that HSVd is detected in systemic leaves at 19 dpi, we infiltrated (at 16 dpi) the opposite leaves of HSVd-infected cucumber and *N. benthamiana* plants with *Agrobacterium* transformed with a vector containing HDA6-ORF or empty vector as a control. c) At 3 days post agro-infiltration (dpa), infiltrated leaves were collected and used to extract proteins (to confirm the transient expression of recombinant HDA6), DNA (to perform the methylation analysis by bisulfite sequencing) and RNAs (to determine HSVd accumulation by RT-PCR). Proteins obtained from nuclear extracts recovered from HDA6-expressing and mock-infiltrated cucumber (left) and *N. benthamiana* (right) leaves were fractionated by SDS-PAGE (upper panel) and transferred to PDVF membranes for serological analysis with H6-As (in cucumber) and HDA6-As (in *N. benthamiana*) to confirm the overexpression of recombinant HDA6 in the analyzed tissues. A/M: Agro-Mock; A/H: Agro-HDA6.

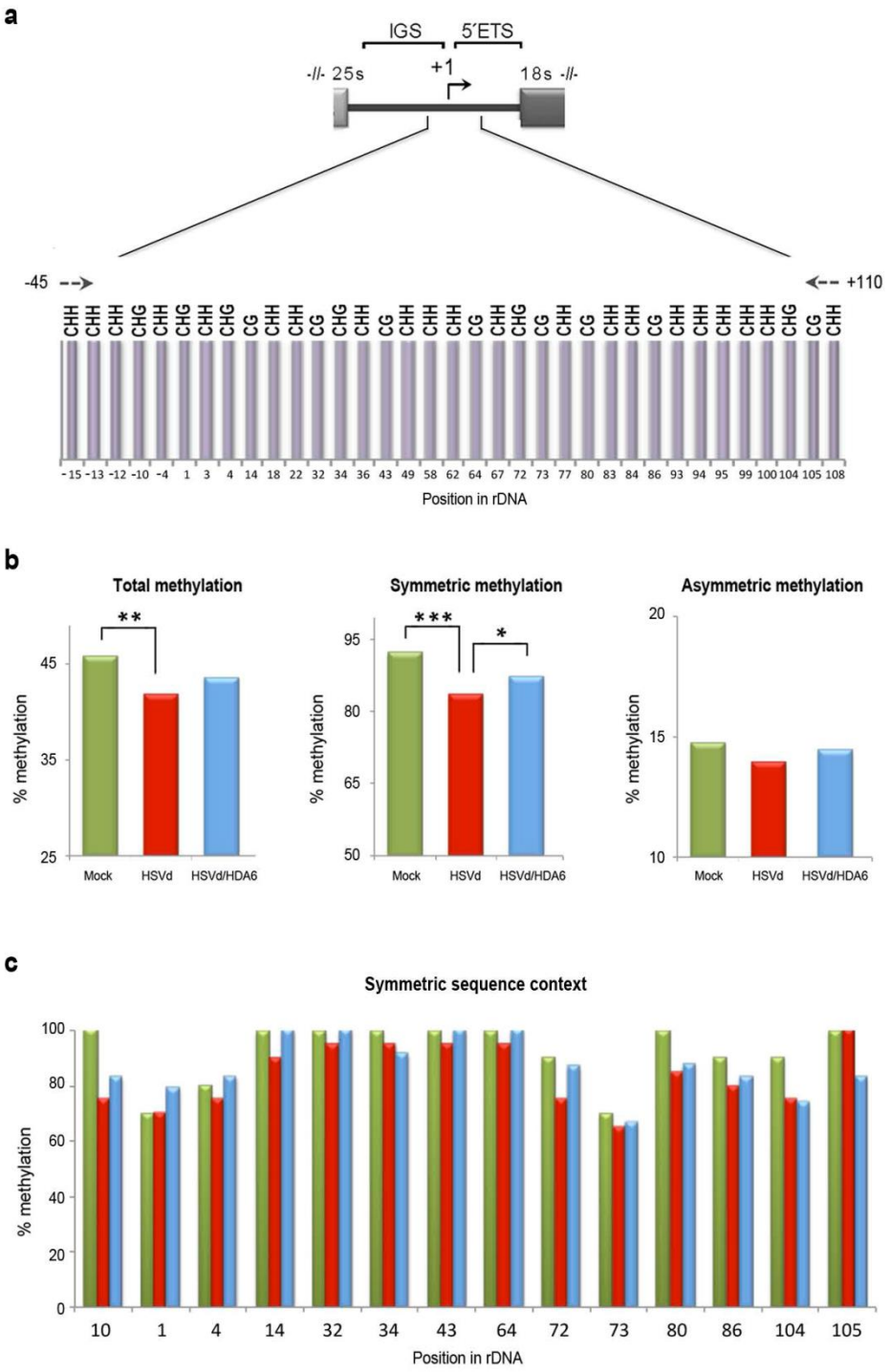

Fig. S7: Recombinant cucumber HDA6 reverts the hypomethylation induced by HSVd infection in N. benthamiana 45S rRNA genes. a) Diagram of the *N. benthamiana* rRNA intergenic region highlighting the promoter zone analyzed by bisulfite sequencing including a graphic representation of the 35 potential symmetric (8-CG and 6-CHG) and asymmetric (21-CHH) sites predicted to exist within this region. The arrows represent the relative positions in the rRNA gene of the oligos used in the PCR assay. b) Histogram documenting the relative DNA methylation levels in *N. benthamiana* plants: Mock-inoculated (green bars), HSVd-infected (red bars) and HSVd-infected plants overexpressing recombinant cucumber HDA6 (blue bars). Total methylation (paired t-test values) means 0.45 (mock), 0.41 (HSVd) and 0.43 (HSVd/HDA6), $^{**}P<0.015$. Symmetric methylation (paired t-test values) means 0.92 (mock), 0.83 (HSVd) and 0.87 (HSVd/HDA6), $^{*}P<0.05$, $^{***}P<0.00025$. Asymmetric methylation (paired t-test values) means 0.14 (mock), 0.13 (HSVd) and 0.14 (HSVd/HDA6). c) Positions of methylcytosines in the analyzed regions displayed in the symmetric (CG and CHG) sequence context. The height of the bar represents the frequency at which cytosine was methylated in the three analyzed samples: Mock-inoculated (green bars), HSVd-infected (red bars) and HSVd-infected plants overexpressing recombinant HDA6 (blue bars).

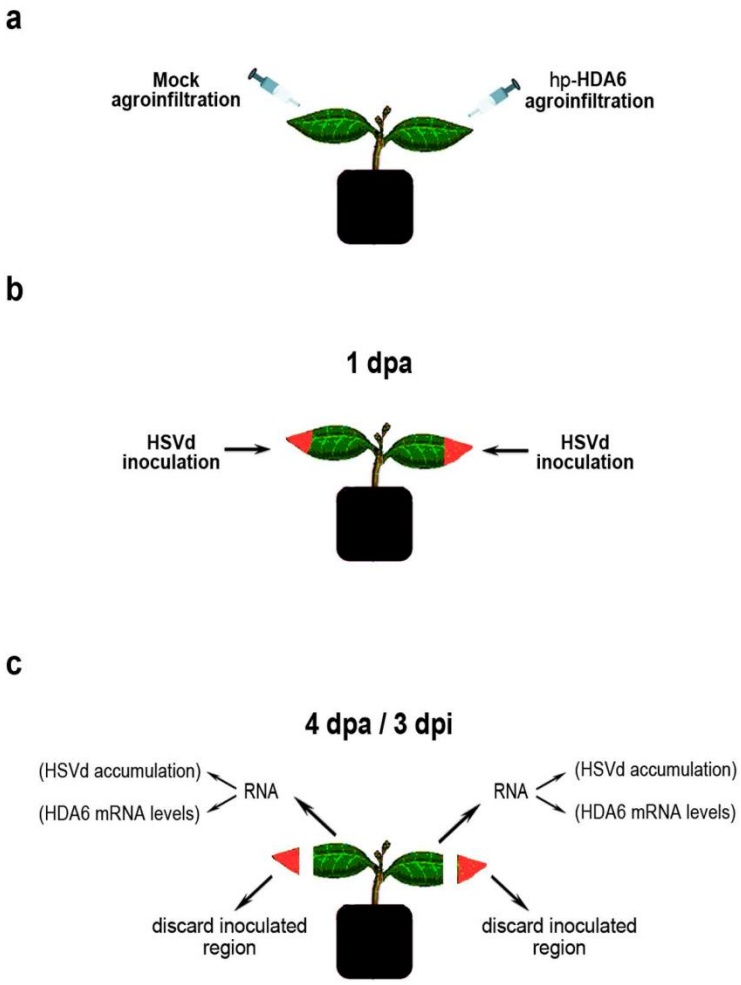

Fig. S8: Schematization of transient HDA6 silencing assays in HSVd-infected cucumber plants. a) Eleven-day-old cucumber plants were infiltrated with *Agrobacterium* transformed with the vector hp-HDA6 or empty vector (control) in both cotyledons. b) At one day post agro-infiltration (dpa), the distal part of the cotyledons (in red) was inoculated with *Agrobacterium* transformed with a vector carrying a dimeric HSVd cDNA. c) At 3 days post HSVd inoculation (dpi), the HSVd-inoculated area was eliminated, and total RNAs were extracted from the remaining parts of the cotyledons. The RNA was used to determine HSVd accumulation and HDA6 mRNA levels by RT-PCR.

CAPÍTULO CUARTO

Este capítulo ha dado lugar a la siguiente publicación:

Castellano, M., Martínez, G., Marques, MC., Moreno-Romero, J., Köhler, C., Pallas, V. and Gómez, G. (2016).

Changes in the DNA methylation pattern of the host male gametophyte of viroid-infected cucumber plants. *Journal of Experimental Botany.*

19:5857-5868. Doi: 10.1093/jxb/erw353

Changes in the DNA methylation pattern of the host male gametophyte induced by a pathogenic long non-coding RNA

Running Title:

Viroids modulate transcriptional scenario in pollen

Authors:

Mayte Castellano[1], German Martinez[2], Jordi Moreno-Romero-[2], Claudia Köhler[2], Vicente Pallas[1] and Gustavo Gomez[1*]

[1]Instituto de Biología Molecular y Celular de Plantas (IBMCP), Consejo Superior de Investigaciones Científicas (CSIC)-Universidad Politecnica de Valencia (UPV), CPI, Edificio 8 E, Av. de los Naranjos s/n, 46022 Valencia, Spain.

[2]Department of Plant Biology, Swedish University of Agricultural Sciences and Linnean Center for Plant Biology, SE-750 07 Uppsala, Sweden

Highlights

Here we shown that a nuclear-viroid reprogram the epigenetic-landscape of the pollen-grain opening the door to the possibility that hypomethylation induced during infection could be inherited to the next generation

ABSTRACT

Eukaryotic organisms exposed to adverse conditions are impelled to favor a certain degree of transcriptional plasticity to cope with stress. Epigenetic regulation of the genome is a key regulatory mechanism allowing dynamic changes of the transcriptional status in plant-response to stress. The *Hop stunt viroid* (HSVd) induces the demethylation of *ribosomal RNA* (*rRNA*) promoter-regions in vegetative tissues of cucumber (*Cucumis sativus*) plants, leading to increasing transcription rates of *rRNA*. In addition to the clear alterations in vegetative tissues, HSVd infection is associated with drastic changes in gametophyte development. To illuminate the basis of viroid-induced alterations in reproductive tissues, we have analyzed the cellular and molecular

consequences of HSVd infection in the male gametophyte of cucumber plants. Our results indicate that in the pollen grain, HSVd-RNA accumulation induces a decondensation of the generative nucleus that correlates with a dynamic demethylation of repetitive regions in the cucumber genome that include rRNA genes and transposable elements (TEs). We propose that HSVd infection impairs the epigenetic control of rRNA genes and TEs in gametic cells of cucumber, a phenomenon thus far unknown to occur in this reproductive tissue as a consequence of pathogen infection.

Key words: viroid-plant interactions, cucumber, viroid-induced pathogenesis, viroids and DNA methylation, Hop stunt viroid, Epigenetic inheritance.

INTRODUCTION

Maintenance of genome stability is a constant in living beings. At the same time, organisms must ensure that a certain level of genome plasticity is available in order to allow genome rearrangements and mutations that could introduce beneficial traits to cope with stresses. In the case of plants, due to their sessile nature, they are constantly exposed to different biotic and abiotic stresses that very often affect genome stability at both somatic and meiotic cells (Boyko and Kovalchuk, 2011; Zhu et al., 2016). Viroids are pathogenic long non-coding RNAs (lncRNAs), able to infect and systemically invade herbaceous and ligneous plants (Flores et al., 2005; Ding, 2009; Gomez and Pallas, 2013). Coerced by their small (250-400 nts) and non-protein-coding genome, viroids have evolved into versatile nucleic acids that subvert the plant-cell machinery at diverse functional levels to guarantee that their life cycle could be completed within the infected host (Ding, 2009). Although some pathogen-host interactions occur without visible plant-alterations (latent diseases), viroid infection is frequently associated with phenotypic changes recognized as symptoms.

Because these pathogenic RNAs lack protein-coding activity, it was initially assumed that viroid-induced symptoms resulted from a direct interaction between specific structural elements of the viroid RNA-genome and certain host-factors (proteins or nucleic acids) (Ding, 2009; Navarro et al., 2012). However, in the last years an increasing number of experimental data has evidenced the existence of other potential pathogenic mechanisms, for example the close interplay between viroid-induced pathogenesis and RNA silencing. The initially proposed idea that certain viroid-derived small RNAs (vd-sRNAs) can down-regulate *in trans* host mRNAs promoting symptoms expression (Papaefthimiou et al., 2001; Wang et al., 2004; Gomez et al., 2009), was experimentally validated for members of both *Pospiviroidae* (Gomez et al., 2008; Eamens et al., 2014; Adkar-Purushothama et al., 2015) and *Avsunviroidae* (Navarro et al., 2012) families. The observation that the Cucumber mosaic virus Y-satellite RNA uses a similar mechanism to alter host-gene expression (Shimura et al., 2011; Smith et al., 2011) suggests that this pathogenesis strategy is not exclusive for

viroids. Finally, and at a different functional level, it is recognized that beside viroids, viruses, bacteria, nematodes and aphids could alter the miRNA (Ruiz-Ferrer and Voinnet, 2009; Garcia and Pallas, 2015) or sRNA-metabolism (Cao et al., 2014) of their host-plants.

Recent studies have evidenced global changes of the host-genome epigenetic regulation upon viroid infection. The analysis of the interaction of *Hop stunt viroid* (HSVd) with two different hosts (cucumber -*Cucumis sativus*- and *Nicotiana benthamiana*) showed that viroid-accumulating plants exhibit an increased *rRNA* transcription rate. This altered transcription was associated with reduced cytosine methylation of rDNA promoter regions, revealing that some –normally silenced- *rRNA* genes are transcriptionally reactivated during HSVd infection (Martinez et al., 2014; Castellano et al., 2015). However, induction of changes in the host-epigenome is not exclusive for viroid infection. Indeed, dynamic changes in host-DNA methylation patterns occur during antibacterial or antiviral defence in rice (Sha et al., 2005), tobacco (Boyko et al., 2007) and *Arabidopsis* (Dowen et al., 2012; Yu et al., 2013). Furthermore, overexpression of the replication-associated protein (Rep) of a geminivirus induces hypomethylation of host-DNA in *N. benthamiana* plants (Rodriguez-Negrete et al., 2013). Altogether, these observations support the notion that host DNA demethylation may be part of a common plant-induced immune response (Alvarez et al., 2010; Zhu et al., 2016).

In viroid-cucumber interactions DNA demethylation has been connected with HSVd recruiting and functionally subverting the host HISTONE DEACETYLASE 6 (HDA6) (Castellano et al., 2016). In *Arabidopsis* HDA6 confers an epigenetic memory of the silent state (Blewins et al., 2014) and is furthermore involved in the maintenance and *de novo* CG and CHG (were H is A, T or C) methylation of TEs, *rRNA* genes and transgenes via its interaction with DNA METHYLTRANSFERASE 1 (MET 1) and the RNA-directed DNA methylation (RdDM) pathway (Aufsatz et al., 2002; Probst et al., 2004; Earley et al., 2010; Liu et al., 2012; Hristova et al., 2015). Viroids are pathogenic long non-coding RNAs (lncRNAs) that subvert endogenous lncRNA-directed regulatory routes to complete their life cycle in the infected cell (Gomez and Pallas, 2013). Remarkably, endogenous lncRNAs are able to function as epigenetic modulators by binding to chromatin-modifying proteins and recruit their catalytic activity to specific sites in the genome, thereby modulating chromatin states and impacting gene expression (Mercer and Mattick, 2013).

HSVd is a polyphagous pathogenic lncRNA able to infect a wide range of hosts (cucumber, grapevine, citrus, plum, peach, etc.) causing diverse symptoms (Pallas et al., 2003; Sano, 2003). In cucumber, HSVd infection induces –beside plant-stunting- severe alterations in reproductive organs that are frequently associated with reduced fertility (Singh et al., 2003; Martinez et al., 2008). Although HSVd is poorly

transmitted through seeds and pollen, seed transmission may play a role for its survival in certain hosts such as grapevine (Wah and Symons, 1999). The molecular mechanism underlying the structural and functional alterations in host reproductive organs associated to viroid infection, are currently unsolved.

Having established that HSVd alters the DNA methylation in vegetative cells, here we addressed the question whether the epigenetic changes induced by viroid-infection were also present in the male gametophyte. Pollen grains are known to transmit other members of *Pospiviroidae* family (Singh, 1970; Kryczyński et al., 1988; Barba et al., 2007; Card et al., 2007). Our results reveal that both HSVd mature forms and vd-sRNAs could be recovered from pollen grains of infected cucumber plants. Moreover, viroid accumulation was associated with an increased pollen germination level and heterochromatin decondensation in the generative nucleus. Analysis of DNA methylation in rDNA and TE repeats revealed a significant reduction in the symmetric cytosine methylation context, which was associated with a transcriptional increase of their RNAs. In summary, our results reveal that the previously observed epigenetic changes in vegetative tissues are maintained in male gametes and thus passed on to the next generation

RESULTS

Cucumber reproductive tissues are affected as consequence of HSVd-infection

A characteristic symptom related to HSVd infection is the alteration of fertility that triggers deficiencies in flower size (Sano, 2003; Martinez et al., 2008), fruit quality and seed viability (Singh et al., 2003; Martinez et al., 2008). In order to precisely determine the level of phenotypic effects induced by HSVd-infection in reproductive organs of cucumber plants, we analyzed diverse morphological aspects of male and female flowers. As shown in the Figure 1a flowers obtained from HSVd-infected plants exhibited a significant reduction (close to 50%) of the corolla-size as previously observed in the HSVd-*N. benthamiana* interaction (Martinez et al., 2008). Morphological studies evidenced that HSVd did not induce alterations in pollen grain size (Figure 1b). However, DAPI staining of pollen revealed a significant size increase of the generative cell nucleus (Figure 1c), suggesting alteration of chromatin structure under viroid infection. To determine if this alteration is associated with physiological changes, we performed germination assays. As shown in Figure 1d, pollen grains derived from HSVd-infected plants had a higher germination rate than pollen collected from control plants, suggesting that regulatory processes associated with pollen germination are affected during HSVd-infection.

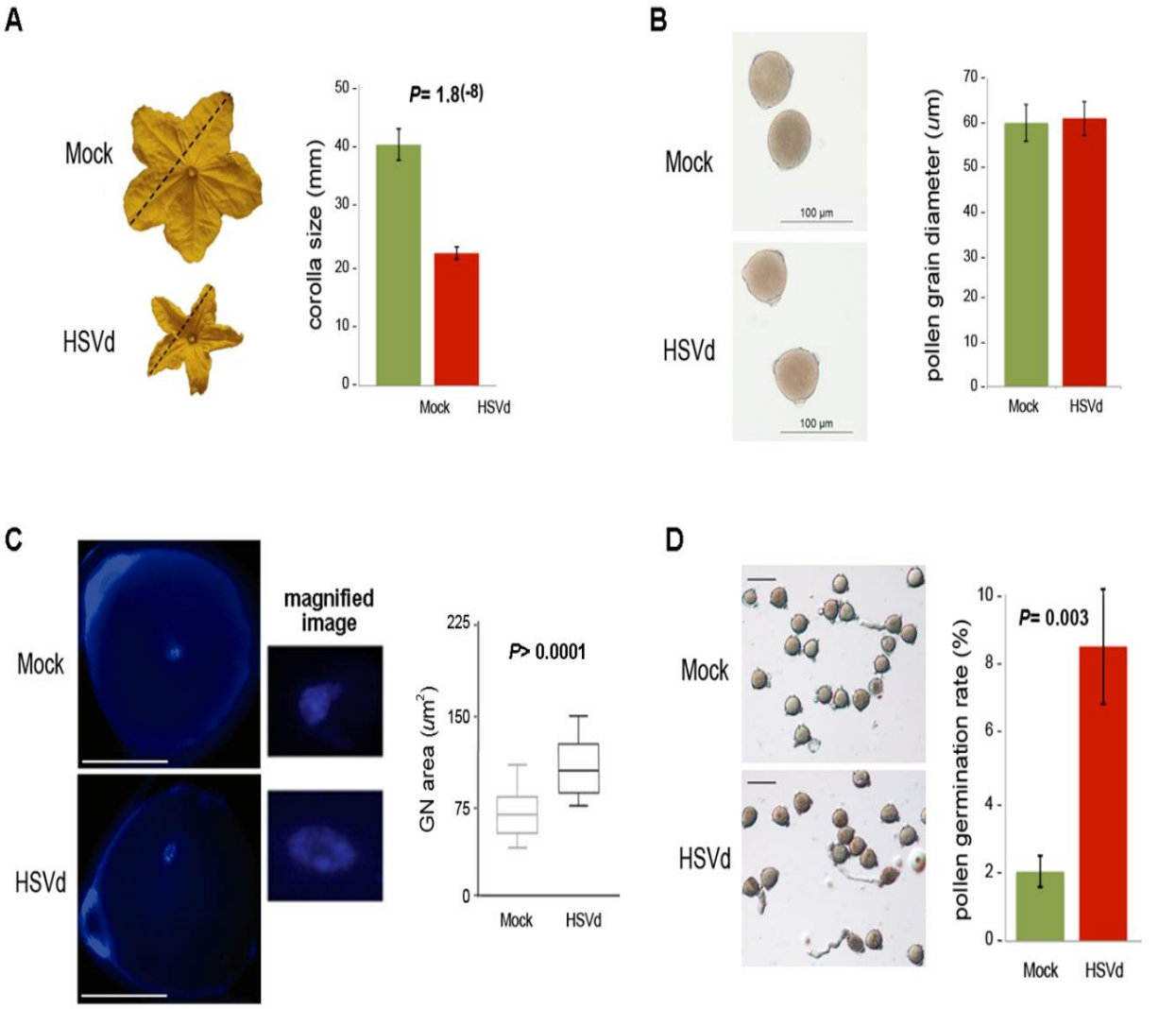

Figure 1: Cucumber reproductive tissues are affected in response to HSVd-infection. (A**)** Flowers obtained from HSVd-infected and mock-inoculated cucumber plants were measured as indicated by the dotted-line (left). Diagram shows mean values of 750 (HSVd-infected) and 650 (control) flowers (right). Statistical significance was tested using a paired t-test. **(B)** Microphotography of representative pollen grains recovered from HSVd-infected and mock-inoculated cucumber plants (left). Diagram showing the mean diameter of 200 pollen grains recovered from infected and control plants (right). Statistical significance was tested using a paired t-test. No significant differences were observed. **(C)** Representative images of DAPI stained pollen grains from non-infected and HSVd-infected plants and magnifications of their respective generative cells nuclei (GN). Scale bar 30 µm. Box plots show the distribution of the area values of the GN of more than 100 pollen grains. Statistical significance was tested using a paired t-test with Welch's correction. **(D)** Representative images of germinated pollen grains recovered from mock and HSVd-infected plants (left). The right panel shows the quantification of the germination rate of infected pollen grains in comparison with control samples. 1200 pollen grains were analysed for each sample in 6 independent replicates. Statistical significance was tested using a paired t-test. In all panels, error bars represent standard error. Only significant *P* values are shown in the figure.

HSVd accumulates in pollen grains of infected plants

Having established that HSVd induces structural and functional alterations in the pollen of infected plants, we attempted to determine if viroid molecules could be detected in mature dehiscent pollen grains. RT-PCR assays demonstrated that genomic HSVd-RNA accumulated in the pollen grains obtained from infected plants (Figure 2a), indicating that HSVd is able to invade pollen of infected cucumber plants as has

been shown for *Potato spindle tuber viroid* (PSTVd) in potato (Singh et al., 1993) and petunia plants (Matsushita and Tsuda, 2014). We did not detect HSVd on the surface of the pollen grain (Figure 2a) providing robustness to this affirmation.

Considering that in cucumber vegetative tissues genomic HSVd-RNA accumulation is associated with the presence of vd-sRNAs (Martinez et al., 2010), we prepared sRNA libraries from pollen grains derived from mock-inoculated and HSVd-infected plants. A total of 4,918,251 and 4,566,866 raw sequences (ranging 18 to 36 nt) were obtained from HSVd-infected and control pollen grains sRNA libraries respectively. Sequences ranging from 20 to 25 nts (2,888,088 for infected-pollen and 2,523,747 for control data set) were used for further analysis. When sRNAs recovered from infected and non-infected pollen-grains were analysed by pairwise alignment against the HSVd genome, we observed that a total of 18,900 sequences (0,68 %) (ranging 20 to 25 nts in length) recovered from the infected pollen were perfectly

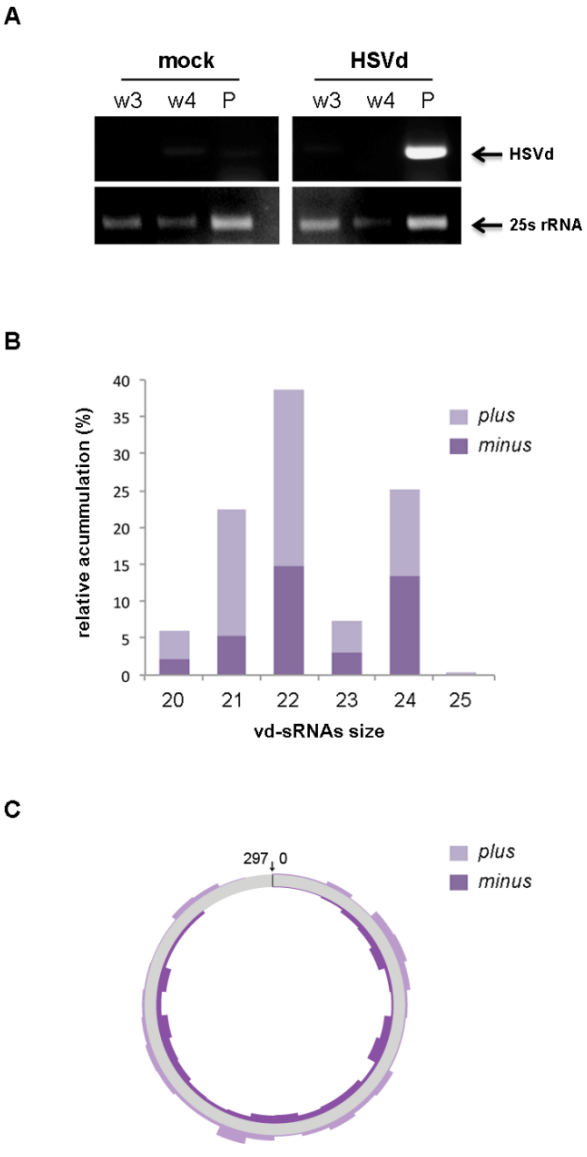

Figure 2: HSVd accumulates in pollen grains of infected cucumber plants. **(A)** Detection of HSVd-RNA by RT-PCR in pollen grains (P) recovered from infected plants. Total RNA extracted from successive washing of pollen grains (w3 and w4) was analysed by RT-PCR in order to discard contamination with HSVd-RNA of non- pollen-specific plant-tissue. **(B)** Diagram showing size distribution and polarity of canonical (20 to 25 nts) fully homologous total viroid-derived sRNAs (vd-sRNAs) recovered from infected pollen library. The values on the Y-axis represent the abundance of vd-sRNAs in the library. **(C)** The vd-sRNAs were plotted onto the circular sequence of the HSVd-RNA, in either sense (plus) or antisense (minus) configuration. The arrow indicates the position of the nucleotides 1 and 297 in the circular HSVd-RNA.

complementary to HSVd and considered as vd-sRNAs. Importantly, no HSVd perfectly matching sequences were recovered from the control cucumber pollen, confirming the integrity of the RNA samples. Analysis of polarity distribution indicated that sRNAs derived from the sense strand were slightly biased (60%) in comparison to sRNAs derived from the antisense strand (40%) (Figure 2b). This vd-sRNA landscape is different to that previously described in cucumber vegetative tissues where HSVd-derived sRNAs of both polarities were recovered at comparable levels (Martinez et al., 2010).

Categorized by size vd-sRNAs were mainly of 22 nt (34.1%) and 24 nt (22.1%) and 21 nt (19.9%), whereas vd-sRNAs of 20, 23 and 25 nt accumulated under the 6% of the total vd-sRNAs (Fig. 2b). As previously observed in infected leaves, sense and antisense vd-sRNAs spreading along the entire HSVd genome showed a heterogeneous distribution pattern (Fig. 2c). In summary, pollen grains of HSV infected plants accumulate HSVd RNA and vd-sRNAs.

Endogenous sRNA profile is altered in HSVd-infected pollen

In vegetative cells of cucumber HSVd infection induces, a drastic change in the accumulation profile of rRNA-derived sRNAs that is associated with changes in the epigenetic regulation of those repeats (Martinez et al., 2014; Castellano et al., 2015; Castellano et al., 2016). In order to evaluate whether HSVd infection induced global alterations in the epigenetic regulation of pollen, we analysed endogenous sRNAs from pollen of infected and non-infected plants (Figure 3a). Viroid-derived sRNAs, recovered from infected-pollen, were filtered out from this analysis. In HSVd-infected pollen there was a considerable increase of 21, 23, 24 and 25 nt sRNAs(Figure 3b). In contrast, 22 nt sRNAs were present at similar frequencies. These results indicate that HSVd accumulation in pollen grains causes changes in endogenous sRNAs, resembling -at least in part- those observed in HSVd-infected cucumber vegetative tissues.

When endogenous sRNAs recovered from infected and healthy pollen-grains were analysed by pairwise alignment against different *Cucumis sativus* transcript categories (Li et al., 2011), we observed that ribosomal and TE-derived sRNAs were significantly over-accumulated in HSVd-infected pollen-grains (Fig. 3c, Supplementary Figures 2 and 3). In contrast, no significant differences were obtained when sRNAs derived from coding and terminal repetitive cucumber sequences were analysed (Fig 3c). A more detailed analysis of up-regulated sRNAs classes showed that their over-accumulation in infected samples was detectable in all size classes (21 to 25 nts) (Fig. 3d). Together, these results indicate that HSVd accumulation in pollen grains is associated with alterations in endogenous sRNA levels, mainly affecting the accumulation of sRNAs derived from repetitive regions of the genome.

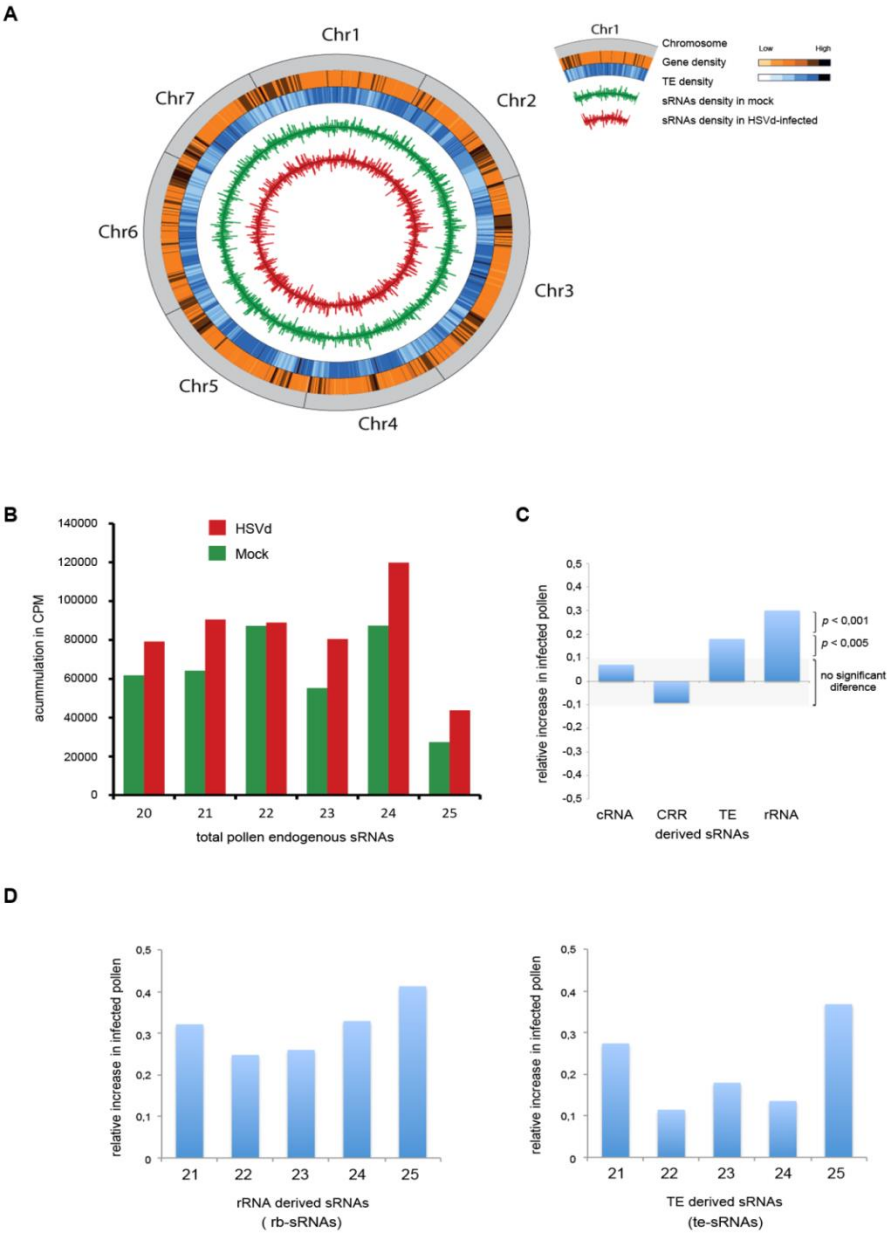

Figure 3: Characterization of the small RNAs recovered from cucumber pollen grains by deep sequencing. (A) Whole-genome distribution of sRNA density in control and HSVd-infected pollen grains. Outermost to innermost tracks depicting: *C. sativus* chromosomes (Chr 1 to 7); heat map of gene density (low density clear orange, high density black); heat map of transposable element density (low density clear blue, high density black) and sRNA density in mock (green) and HSVd-infected (red) pollen grains. **(B)** Diagram showing the differential accumulation and distribution of the total reads of endogenous cucumber sRNAs ranging between 21 and 25 nt recovered from both the control and HSVd-infected analysed samples. **(C)** Relative increase of ribosomal-derived sRNAs (rb-sRNAs) and TE-derived sRNAs (te-sRNAs) in infected pollen. sRNAs derived from coding-transcripts (cRNA) and centromeric regions (CRR), exhibit no significant alterations in both analysed samples. The ratio of reads obtained in infected pollen compared to the control library is shown. **(D)** Relative increase of rb-sRNAs (left panel) and te-sRNAs (right panel) in infected pollen compared to non-infected pollen based on sRNAs-length.

Viroid infection modifies cytosine methylation of repetitive regions in pollen

To investigate if the increase in sRNAs derived from rDNA and TEs observed in infected-pollen could be linked to alterations in the host epigenetic landscape, we analysed the methylation pattern of representative regions of the repetitive pollen-DNAs exhibiting sRNA-derived over-accumulation. Specifically, we analysed the rRNA promoter region previously described (Martinez et al., 2014) and a TE region that had the highest increase in sRNA accumulation. The genomic DNA extracted from pollen grains of HSVd-infected and mock-inoculated cucumber plants was bisulfite-converted and subjected to PCR to amplify specific regions of rDNAs and TE DNA.

We analysed a specific promoter sequence of 201 nt located between positions -80 and +121 of the 45S-rDNA containing 16 symmetric (12 CG, 4 CHG) and 23 asymmetric (CHH) potential methylation sites (Figure Supplementary 4a and b). PCR products were cloned, and the sequences of 51 and 44 clones were compiled for control and infected samples, respectively. Methylation analysis revealed that HSVd infection resulted in a significant decrease in the relative number of total methylated cytosine residues when compared to the control (Figure 4a). Hypomethylation was restricted to symmetric (CG/CHG) sequence contexts (Figure 4b and c), and not detected at asymmetric (CHH) positions (Figure 4b). We furthermore analysed a 236 bp region of a TE with homology to a Copia element (termed *cuc_reannotTE.Scaffold000159.7* in the reannotation of TEs from Li et al. 2012) containing 20 symmetric (9 CG, 11 CHG) and 41 asymmetric (CHH) potential methylation sites (Figure Supplementary 5a). Similar as for the 45S-rDNA locus, HSVd infection resulted in a significant reduction in the relative number of methylated cytosine residues of this transposable DNA compared to mock-inoculated controls. This drastic hypomethylation affected both, symmetric and asymmetric sequence contexts (Figure 4e and f) Hypomethylation of the Copia element in symmetric sequence context was also observed in vegetative tissues of HSVd-infected cucumber plants (Figure Supplementary 5b and c), revealing that this effect was not restricted to pollen. Taken together, these results indicate that in pollen grains, similar as in vegetative tissues rDNA and TEs lose DNA methylation in response to viroid infection, reinforcing the close interplay suggested to exist between HSVd-pathogenesis and host-epigenetic alterations in these class of repetitive DNAs.

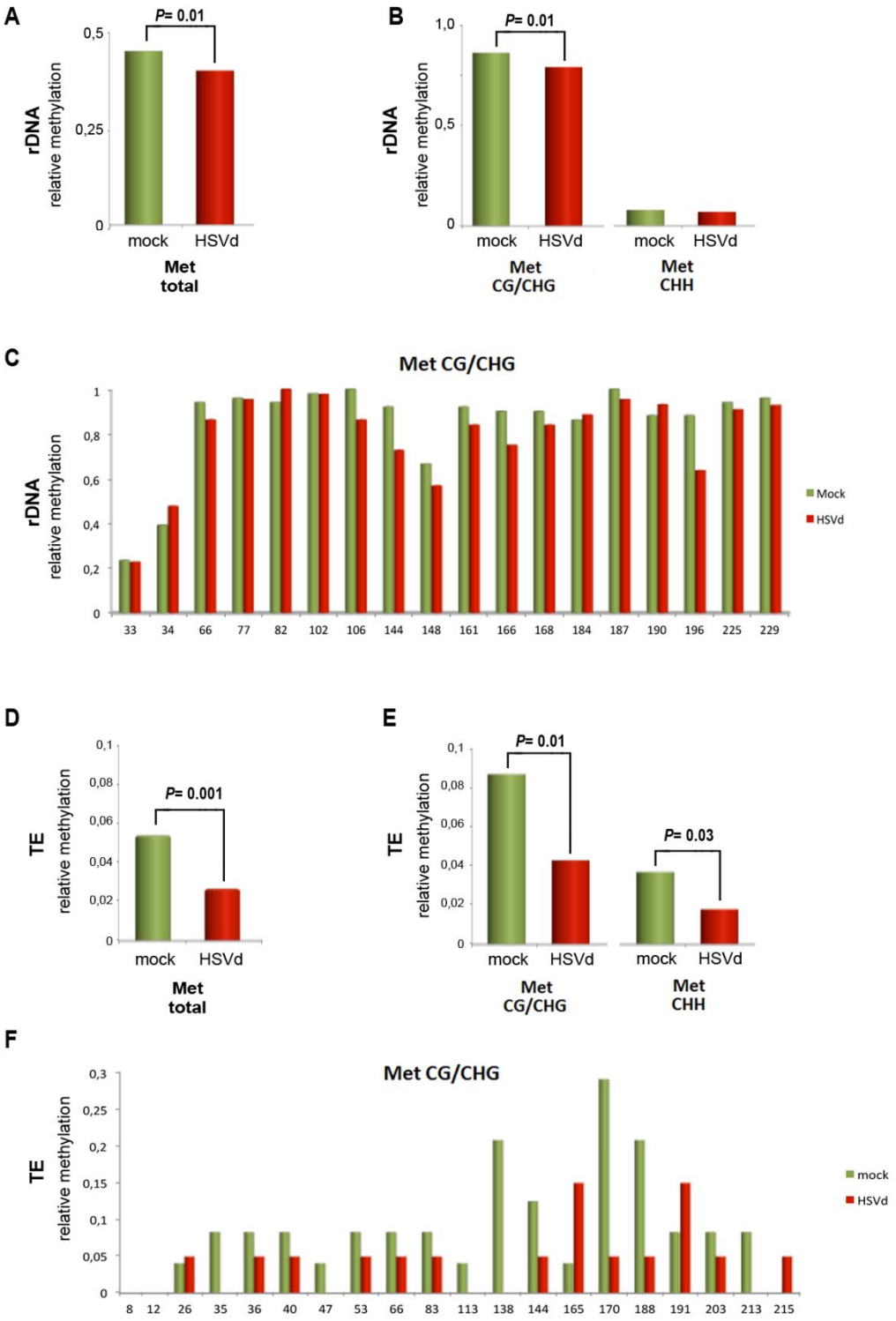

Figure 4. HSVd infection affects the methylation patterns of rRNA genes and TE in pollen grains. **(A)** Diagram showing the relative (HSVd/Mock) total rDNA methylation levels. **(B)** Analysis of symmetric and asymmetric cytosine methylation levels in analysed rDNA. **(C)** Position-specific relative methylation levels in CG and CHG context in the analysed rDNA. **(D)** Relative (HSVd/Mock) total TE methylation. **(E)** Analysis of symmetric and asymmetric cytosine methylation in analysed TE. **(F)** Position-specific relative methylation levels in CG and CHG context in the analyzed TE. In panels a, b, d and e statistical significance was tested using a paired t-test. Only significant *P* values are shown in all figure panels.

HSVd infection promotes transcriptional alterations in the pollen grain

Silencing of repetitive DNA is a self-reinforcing transcriptional regulatory phenomenon mediated by siRNA-directed cytosine methylation and heterochromatin formation (Slotkin and Martienssen, 2007; Law and Jacobsen, 2010) that is dynamically regulated during plant development and stress (Martinez and Slotkin, 2012). To investigate whether the observed increase of sRNAs derived from rRNA and TEs and DNA-hypomethylation could be associated with alterations in the host transcriptional activity, we analysed the accumulation of transcripts derived from these regions.

For this, a primer complementary to the 3´ end of the internal transcribed spacer 2 (ITS2-A) of the 45S rRNA transcription unit (Figure Supplementary 4c) was employed to generate the cDNA template. The pair 5.8s-Fw/5.8s-Rv was used to differentially amplify by PCR the unprocessed rRNA. We observed significantly increased levels of pre-rRNA and TE-derived transcripts in pollen-RNA from viroid-infected plants compared to mock-inoculated controls (Figure 5a and b). We thus conclude that HSVd-infection promotes increased transcriptional activity of the analysed repetitive DNAs in pollen, revealing that the viroid-induced hypometylation causes changes of the transcriptional status in cucumber reproductive tissues.

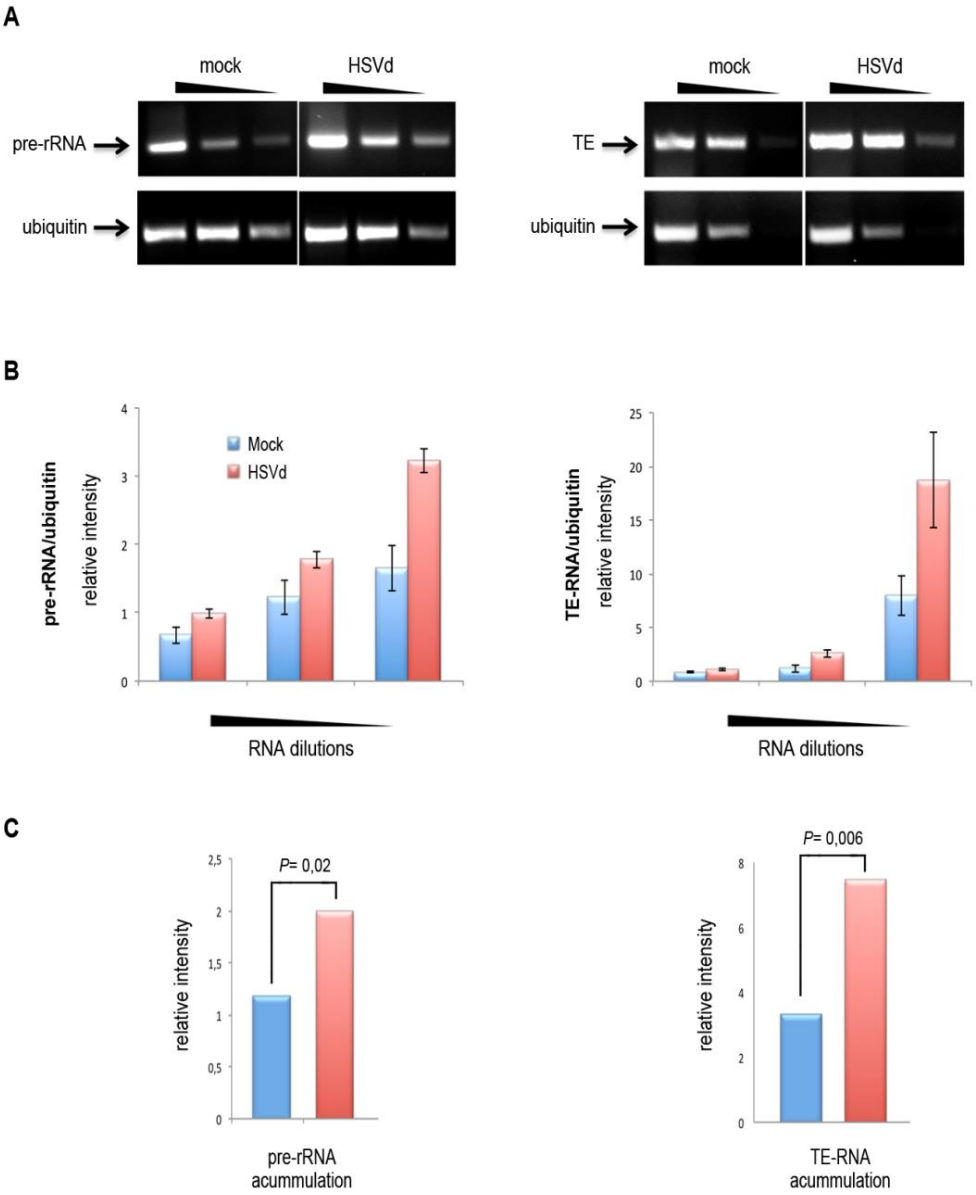

Figure 5: Differential accumulation of the precursor for rRNAs (pre-rRNAs) and TE-derived transcripts in infected pollen. **(A)** Representative RT-PCR analysis of the pre-rRNA (left panel) and TE (right panel) expression in serial dilutions (500ng, 100 ng and 20 ng) of HSVd-infected and control total RNAs. RT-PCR amplification of ubiquitin mRNA served as normalization control. **(B)** Diagram showing the relative accumulation (in relation to ubiquitin expression) of pre-rRNA (left) and TE-derived transcripts (right) in serial dilutions analysed in (A), determined by measurement of band intensity. The band intensity was measured using the Image-J application http://www.imagej.en.softonic.com. Error bars represent standard error. **(C)** Comparison of relative pre-RNA and TE transcript accumulation (estimated from the sum of the intensity of the RT-PCR products) in control and infected pollen grains. Bars (red for HSVd-infected and blue for mock samples) represent means values obtained for pre-rRNA and TE amplification relative to the normalization control ubiquitin. Statistical significance was tested using a paired t-test. Only significant *P* values are shown in the figure.

DISCUSSION

Drastic alterations of the epigenome in response to pathogen attack have been described for both, plants (Agorio and Vera, 2007; Boyko et al., 2007; Boyko et al., 2010; Lopez et al., 2011; Dowen et al., 2012; Luna and Ton, 2012; Yu et al., 2013) and animals (Tang et al., 2011). These observations support the notion that epigenetic reprogramming of transcriptional activity is a general mechanism controlling the host response to pathogen infection (Zhu et al., 2016). Consistent with this idea, HSVd accumulation in vegetative tissues causes hypomethylation of the promoter region of rRNA genes, leading to significant alterations in rRNA transcription (Martinez et al., 2014; Castellano et al., 2015). In this study we show that both, viroid-mature forms and vd-sRNAs accumulate in pollen grains of HSVd-infected plants, indicating that during the pathogenesis process the viroid is able to invade this reproductive cell. We furthermore demonstrate that general sRNA profiles are altered in this reproductive tissue, in particular we observed increased sRNAs derived from rRNA and TE transcripts. Increased levels of ribosomal RNA-derived sRNAs (rb-sRNAs) was previously reported to occur in leaves of cucumber and *N. benthamiana* plants infected by HSVd, reinforcing the close interplay between viroid-induced pathogenesis and host rRNA metabolism. Importantly, the observation that sRNAs derived from TE (te-sRNAs), are also over-accumulated in infected tissue, suggests that the viroid-induced transcriptional alteration is a more general phenomenon not restricted only to rRNA repeats. In line with this possibility, bisulfite sequencing clearly correlated HSVd infection with changes in DNA methylation –in symmetric sequence context- in both rDNA and TE.

The hypomethylated status of the analysed rDNA regions is consistent with the significant size increase of the nucleolus in the generative nucleus of HSVd infected pollen. Nucleolus are mainly composed by active and inactive rDNA (Lam and Trinkle-Mulcahy, 2015), consequently is reasonable suppose that changes in nucleolar morphology (Fig 1D) can be associated to alterations in the rRNA transcriptional activity observed, in pollen grains, during viroid infection (Fig. 5). Thus resembling -at least in part- the observed in soybean plants grown at low temperature where different condensation state of nucleololar chromatin -in response to stress - correlated with changes in DNA methylation levels and transcriptional activity (Stepinski, 2013). Moreover and considering that nucleus heterochromatin is mostly occupied by TEs and other repetitive DNAs (Lippman et al., 2004), it seems likely that HSVd infection causes a general reduction of DNA methylation at repeat regions. Interestingly, decondensation of centromeric regions and rDNA loci also occurs in response to heat stress (Pecinka et al., 2010), suggesting a general stress response on heterochromatin. Whether this is connected to increased metabolic activities that require increased ribosome production remains to be investigated. Interestingly, we observed that HSVd infected

pollen had an increased germination rate compared to pollen from mock infected plants, which may be a consequence of increased ribosomal activity.

Together, our data support the idea that HSVd accumulation in pollen grains, promotes host-epigenetic alterations evidenced by drastic changes on rDNA and TE expression. Although the molecular basis of this phenomenon remains to be completely elucidated, it was recently shown that in infected leaves HSVd-RNA is able to bind and functionally subvert host-HDA6, promoting rDNA hypo-methylation (Castellano et al., 2016). HDA6 acts as an epigenetic regulator required to confer memory of the silent state and to maintain DNA methylation (Aufsatz et al., 2002; Probst et al., 2004; Earley et al., 2010; Liu et al., 2012; Blevins et al., 2014; Hristova et al., 2015). As we observed similar changes in DNA methylation in pollen and vegetative tissues suggests that also in pollen HSVd impairs function of HDA6. Nevertheless, in contrast to HSVd-infected cucumber leaves where 21 nt and 24 nt rb-sRNAs were respectively up and down regulated, the methylation loss in pollen grains was accompanied by a general increase of sRNAs in all size classes. Increase of 21 nt TE or rRNA-derived sRNAs is a known trademark of Pol II transcription of repetitive regions upon downregulation of epigenetic factors such as DDM1 or HDA6 (Earley et al., 2010; McCue et al., 2012). Consequently, our results suggest that although the altered epigenetic-scenario is similar in both, vegetative and reproductive tissues, specific aspects of the HDA6-dependent regulatory mechanisms underlying this phenomenon differ. Regarding this issue, recent data have demonstrated that DNA methylation can also be modulated by DCL-independent siRNAs (Yang et al., 2015; Dalakouras et al., 2016; Ye et al., 2016). These siRNAs (ranging 20 to 60 nt in length) are mainly derived from repetitive sequences and loaded in AGO4 to direct DNA methylation (Ye et al., 2016). Further studies are needed in order to determine if this non-canonical regulatory pathway could be also affected in HSVd-infected pollen grains.

It will furthermore be important to test whether epigenome changes in response to HSVd infection will have functional consequences in the next generation of plants. Thus far, transgenerational effects of stress are rather questionable (Pecinka and Scheid, 2012); however, our data show a stress response affecting the chromatin status of the generative nucleus, suggesting that these changes will be potentially inherited to the next generation.

In summary, we have shown that HSVd infection induces hypomethylation of rRNA genes and TEs in pollen grains, providing the first example of epigenome changes in reproductive cells upon pathogen infection.

MATERIAL AND METHODS

Plant Material

Cucumber (*Cucumis sativus Cv Marketer)* plants (six) were agroinoculated with *Agrobacterium tumefaciens* strain C58C1 transformed with a binary pMOG800 vector carrying a head-to-tail infectious dimeric HSVd cDNA (Y09352) (Gomez and Pallas, 2006), as previously described (Gomez et al., 2008). Mock-inoculated cucumber plants (three) were used as a negative control. Plants were maintained in growing chambers at 30°C for 16 h with fluorescent light and at 25 °C for 8 h in darkness until flowering. To collect cucumber pollen grains, a paintbrush was used to gently brush the pollen from the anthers into an *Eppendorf* tube. This procedure was repeated for approximately 750 and 650 mature flowers recovered from HSVd-infected and control plants respectively, between 80 and 110 days post-infiltration.

RNA isolation

As previously described (Aparicio et al., 1999), 20 mg of pollen grains were suspended in 1.5 ml of phosphate saline-Tween polyvinylpyrrolidone buffer, pH 7.4, vigorously shaken for 1 min, and centrifuged at 3,000 rpm for 5 min. This procedure was repeated three times, followed by an additional washing with 1.5 ml of 1% sodium dodecyl sulphate (SDS) to remove particles firmly bound to the pollen grains. Aliquots from the four supernatants were phenol extracted and the aqueous phase was ethanol precipitated and resuspended in sterile water. Washed pollen was homogenized for total RNA extraction. Total RNA was extracted from polled pollen grains (~0.1 g) recovered from infected and control cucumber plants using the TRI reagent (SIGMA, St. Louis, MO, USA) according to the manufacturer's instructions. The low-molecular weight RNA (<200 nt) fraction was enriched from total RNA using MIRACLE (miRNA isolation Kit, STRATAGENE) according to the manufacturer's instructions. Supernatants and washed pollen were analysed for the presence of HSVd by RT-PCR as described (Martinez et al., 2010).

Small RNA library information

The sRNA sequences used in this work were obtained from an sRNAs population recovered from pollen of mock-inoculated and *Hop stunt viroid*-infected cucumber plants. The libraries were sequenced by HIseq 2500 (Illumina Technology).

Bisulfite Conversion and Sequencing

Total genomic DNA was extracted from the pollen grains (~0.1 g) recovered from different infected and healthy cucumber plants (Dellaporta et al., 1983). Bisulfite treatment was performed using the EpiTec Bisulfite kit (Qiagen). The DNA regions to be analyzed and their corresponding oligos were determined

using the MethPrimer software http://www.urogene.org/cgi-bin/methprimer (Li and Dahiya, 2002). Modified DNA was amplified by PCR using Taq DNA polymerase (Promega). The primers (45s-Fw ATCATAGATTTTTYGAGGGT (position -80 to -61) – 45s-Rv ATGACGACRTAAACATCCCAA (position +101 to +121) (according sequence X51542.1) and TE-Fw: TAGTTTTTTGAYAGGGGAAATA (position 545 to 566) – TE-Rv: CATTCATAAACTTRCTTTCTCA (position 760 to 781) (according TE cucumber predicted sequence: cuc_reannotTE.Scaffold000159.7) (Li et al., 2011), were used to amplify by PCR specific regions of rDNA and TE respectively. Obtained amplicons were cloned using the InsTAclone PCR cloning Kit (Thermo Scientific). We selected for sequencing sixteen to fifty clones (obtained from two independent replicates), from rDNA and TE respectively, for each analysis in both the HSVd-infected and control pollen.

RT-PCR analysis

Total RNA, extracted from pollen grains collected from HSVd-infected and control plants, was treated with DNase in order to avoid DNA contaminations. RT-PCR analysis of serial dilutions (500ng, 100 ng and 20 ng) of total RNAs obtained from HSVd-infected and control pollen was performed using the SuperScript® III One-Step RT-PCR System with Platinum® Taq DNA Polymerase [Invitrogen] according to the manufacturer's instructions. The sequence and relative position of the specific primers used to amplify by RT-PCR a region (~160 nt) of rRNA precursor is detailed un the Figure Sup 1c. RT-PCR conditions (45ºC/30 min.), 95ºC/15s, 51ºC/30s, 72ºC/20s (30 cycles).

To amplify TE transcripts we use the oligos (TE-Dir: TAGCTTTCTGACAGGGGAAATACC and TE-Rv: GCATTCATGAACTTGCTTTCTCAGC) flanking a region of (~240bp) of an annotated TE cucumber sequence (cuc_reannotTE.Scaffold000159.7) (Li et al., 2011). RT-PCR conditions (45ºC/30 min.), 95ºC/15s, 62ºC/30s, 72ºC/15s (30 cycles). The primers Ub-Dir (5´ CACCAAGCCCAAGAAGATC) and Ub-Rev (5´ TAAACCTAATCACCACCAGC) flanking a region (~220 nt) of ubiquitin mRNA (AN: NM-001282241.1), were used to amplify this mRNA as a load control. RT-PCR conditions (45ºC/30 min.), 95ºC/15s, 57ºC/20s, 72ºC/20s (27 cycles). Three repetitions of this analysis were performed. To discard the possible amplification of residual genomic rDNA, 100 ng of total RNAs were analyzed by PCR using the primers pairs (Fw-25s: CACCAATAGGGAACGTGAGCTG - Rv-25s: GCGCAATGACCAATTGTGCG) flanking a region (~130 bp) of 25s-rRNA and (TE-Dir – TE-Rv) detailed above (Figure Supplementary 1).

Real-Time Quantitative PCR assays

Total RNAs were extracted from pollen grains as described above. First-strand cDNA was synthetized by pulsed RT (Varkonyi-Gasic et al., 2007) using a RevertAid cDNA Synthesis Kit (Thermo Scientific TM) as follows. Initial step at 16ºC for 10 minutes followed by 45 cycles of 16ºC for 2 minutes, 42 ºC for 1

minute and 50ºC for 1 second, including a final denaturing step at 85ºC for 5 minutes. qRT-PCR assays were performed using PyroTaq EvaGreen mix Plus –ROX- (CulteK Molecular Bioline) according to the manufacturer's instructions. Ubiquitin mRNA (AN: NM-001282241.1) was used to normalize samples.

Small RNAs detection was performed starting from low molecular weight RNA (<200 nt) fractions obtained as described above. Stem-loop-specific reverse transcription for sRNAs detection was performed as previously described (Czimmerer et al., 2013) using a RevertAid cDNA Synthesis Kit (Thermo Scientific). Cucumber miR159 with stable expression in both analyzed samples according sequencing data was used to normalization. All analysis, were performed by triplicates on ABI 7500Fast-Real Time qPCR instrument (Applied Biosystems) using a standard protocol. The efficiency of PCR amplification was derived from a standard curve generated by four 5-fold serial dilution points of cDNA mixed by the two samples. Gene expression was quantified by the comparative ΔCt method. The primers, used for cDNA synthesis and qRT-PCR, are described above or listed in the supplementary Table S1 and S2.

Author contribution

MC: has performed the experiments, discussed the results, prepared figures and revised the manuscript. GM: performed the experiments, discussed the results, prepared figures and wrote the main manuscript text. JR: has collaborated in confocal analysis. CK and VP: discussed the results and revised the main manuscript text. GG: has designed the experiments, discussed the results, prepared figures and wrote the main manuscript text.

ACKNOWLEDGMENTS

The authors thank Drs A. Monforte for their collaboration in pollen-grains collection. This work was supported by grants AGL2013-47886-R and BIO2014-61826-EXP (GG) and BIO2014-54862-R (VP) from the Spanish Granting Agency (Direccion General Investigacion Cientifica).

REFERENCES

Adkar-Purushothama CR, Brosseau C, Giguere T, Sano T, Moffett P, Perreault JP (2015) Small RNA Derived from the Virulence Modulating Region of the Potato spindle tuber viroid Silences callose synthase Genes of Tomato Plants. Plant Cell **27:** 2178-2194

Agorio A, Vera P (2007) ARGONAUTE4 is required for resistance to Pseudomonas syringae in *Arabidopsis*. Plant Cell **19:** 3778-3790

Alvarez ME, Nota F, Cambiagno DA (2010) Epigenetic control of plant immunity. Mol Plant Pathol **11:** 563-576

Aparicio F, Sanchez-Pina MA, Sanchez-Navarro JA, Pallas V (1999) Location of prunus necrotic ringspot ilarvirus within pollen grains of infected nectarine trees: evidence from RT-PCR, dot-blot and in situ hybridisation. European Journal of Plant Pathology **105:** 623-627

Aufsatz W, Mette MF, van der Winden J, Matzke M, Matzke AJM (2002) HDA6, a putative histone deacetylase needed to enhance DNA methylation induced by double-stranded RNA. Embo Journal **21:** 6832-6841

Barba M, Ragozzino E, Faggioli F (2007) Pollen transmission of Peach latent mosaic viroid. Journal of Plant Pathology **89:** 287-289

Blevins T, Pontvianne F, Cocklin R, Podicheti R, Chandrasekhara C, Yerneni S, Braun C, Lee B, Rusch D, Mockaitis K, Tang H, Pikaard C (2014) A two-step process for epigenetic inheritance in *Arabidopsis*. Molecular Cell **54:** 30–42

Boyko A, Blevins T, Yao Y, Golubov A, Bilichak A, Ilnytskyy Y, Hollunder J, Meins F, Jr., Kovalchuk I (2010) Transgenerational adaptation of *Arabidopsis* to stress requires DNA methylation and the function of Dicer-like proteins. PLoS One **5:** e9514

Boyko A, Kathiria P, Zemp FJ, Yao Y, Pogribny I, Kovalchuk I (2007) Transgenerational changes in the genome stability and methylation in pathogen-infected plants: (virus-induced plant genome instability). Nucleic Acids Res **35:** 1714-1725

Boyko A, Kovalchuk I (2011) Genetic and epigenetic effects of plant-pathogen interactions: an evolutionary perspective. Mol Plant **4:** 1014-1023

Calarco JP, Borges F, Donoghue MT, Van Ex F, Jullien PE, Lopes T, Gardner R, Berger F, Feijo JA, Becker JD, Martienssen RA (2012) Reprogramming of DNA methylation in pollen guides epigenetic inheritance via small RNA. Cell **151:** 194-205

Cao MJ, Du P, Wang XB, Yu YQ, Qiu YH, Li WX, Gal-On A, Zhou CY, Li Y, Ding SW (2014) Virus infection triggers widespread silencing of host genes by a distinct class of endogenous siRNAs in

Arabidopsis. Proceedings of the National Academy of Sciences of the United States of America **111:** 14613-14618

Card SD, Pearson MN, Clover GRG (2007) Plant pathogens transmitted by pollen. Australasian Plant Pathology **36:** 455-461

Castellano M, Martinez G, Pallás V, Gómez G (2015) Alterations in host DNA methylation in response to constitutive expression of Hop stunt viroid RNA in Nicotiana benthamiana plants. Plant Pathology**:** n/a-n/a

Castellano M, Pallás V, Gómez G (2016) A pathogenic long non-coding RNA redesigns the epigenetic landscape of the infected cells by subverting host Histone Deacetylase 6 activity. New Phytologist (*in press*).

Dellaporta SL, Wood J, Hicks JB (1983) A plant DNA minipreparation: version II. Plant molecular biology reporter **1:** 19-21

Ding B (2009) The biology of viroid-host interactions. Annu Rev Phytopathol **47:** 105-131

Dowen RH, Pelizzola M, Schmitz RJ, Lister R, Dowen JM, Nery JR, Dixon JE, Ecker JR (2012) Widespread dynamic DNA methylation in response to biotic stress. Proc Natl Acad Sci U S A **109:** E2183-2191

Eamens AL, Smith NA, Dennis ES, Wassenegger M, Wang MB (2014) In Nicotiana species, an artificial microRNA corresponding to the virulence modulating region of Potato spindle tuber viroid directs RNA silencing of a soluble inorganic pyrophosphatase gene and the development of abnormal phenotypes. Virology **450:** 266-277

Earley KW, Pontvianne F, Wierzbicki AT, Blevins T, Tucker S, Costa-Nunes P, Pontes O, Pikaard CS (2010) Mechanisms of HDA6-mediated rRNA gene silencing: suppression of intergenic Pol II transcription and differential effects on maintenance versus siRNA-directed cytosine methylation. Genes & Development **24:** 1119-1132

Flores R, Hernandez C, Martinez de Alba AE, Daros JA, Di Serio F (2005) Viroids and viroid-host interactions. Annu Rev Phytopathol **43:** 117-139

Garcia JA, Pallas V (2015) Viral factors involved in plant pathogenesis. Current Opinion in Virology **11:** 21-30

Gomez G, Martinez G, Pallas V (2008) Viroid-induced symptoms in Nicotiana benthamiana plants are dependent on RDR6 activity. Plant Physiol **148:** 414-423

Gomez G, Martinez G, Pallas V (2009) Interplay between viroid-induced pathogenesis and RNA silencing pathways. Trends Plant Sci **14:** 264-269

Gomez G, Pallas V (2006) Hop stunt viroid is processed and translocated in transgenic Nicotiana benthamiana plants. Mol Plant Pathol **7:** 511-517

Gomez G, Pallas V (2013) Viroids: a light in the darkness of the lncRNA-directed regulatory networks in plants. New Phytol **198:** 10-15

Hristova E, Fal K, Klemme L, Windels D, Bucher E (2015) HISTONE DEACETYLASE6 Controls Gene Expression Patterning and DNA Methylation-Independent Euchromatic Silencing. Plant Physiology **168:** 1298-1308

Kryczyński S, Paduch-Cichal E, Skrzeczkowski LJ (1988) Transmission of Three Viroids Through Seed and Pollen of Tomato Plants. Journal of Phytopathology **121:** 51-57

Law JA, Jacobsen SE (2010) Establishing, maintaining and modifying DNA methylation patterns in plants and animals. Nat Rev Genet **11:** 204-220

Li LC, Dahiya R (2002) MethPrimer: designing primers for methylation PCRs. Bioinformatics **18:** 1427-1431

Li Z, Zhang ZH, Yan PC, Huang SW, Fei ZJ, Lin K (2011) RNA-Seq improves annotation of protein-coding genes in the cucumber genome. Bmc Genomics **12**

Lippman Z, Gendrel AV, Black M, Vaughn MW, Dedhia N, McCombie WR, Lavine K, Mittal V, May B, Kasschau KD, Carrington JC, Doerge RW, Colot V, Martienssen R (2004) Role of transposable elements in heterochromatin and epigenetic control. Nature **430:** 471-476

Liu XC, Yu CW, Duan J, Luo M, Wang KC, Tian G, Cui YH, Wu KQ (2012) HDA6 Directly Interacts with DNA Methyltransferase MET1 and Maintains Transposable Element Silencing in *Arabidopsis*. Plant Physiology **158:** 119-129

Lopez A, Ramirez V, Garcia-Andrade J, Flors V, Vera P (2011) The RNA silencing enzyme RNA polymerase v is required for plant immunity. PLoS Genet **7:** e1002434

Luna E, Ton J (2012) The epigenetic machinery controlling transgenerational systemic acquired resistance. Plant Signal Behav **7:** 615-618

Martinez G, Castellano M, Tortosa M, Pallas V, Gomez G (2014) A pathogenic non-coding RNA induces changes in dynamic DNA methylation of ribosomal RNA genes in host plants. Nucleic Acids Res **42:** 1553-1562

Martinez G, Donaire L, Llave C, Pallas V, Gomez G (2010) High-throughput sequencing of Hop stunt viroid-derived small RNAs from cucumber leaves and phloem. Mol Plant Pathol **11:** 347-359

Martinez G, Pallas V, Gomez G (2008) Analysis of symptoms developed in Nicotiana benthamiana plants expressing dimeric forms of Hop stunt viroid. Journal of Plant Pathology **90:** 121-124

Martinez G, Slotkin RK (2012) Developmental relaxation of transposable element silencing in plants: functional or byproduct? Curr Opin Plant Biol **15:** 496-502

Matsushita Y, Tsuda S (2014) Distribution of Potato spindle tuber viroid in Reproductive Organs of Petunia During Its Developmental Stages. Phytopathology **104:** 964-969

McCue AD, Nuthikattu S, Reeder SH, Slotkin RK (2012) Gene expression and stress response mediated by the epigenetic regulation of a transposable element small RNA. PLoS Genet **8:** e1002474

Mercer TR, Mattick JS (2013) Structure and function of long noncoding RNAs in epigenetic regulation. Nature Structural & Molecular Biology **20:** 300-307

Navarro B, Gisel A, Rodio ME, Delgado S, Flores R, Di Serio F (2012) Viroids: how to infect a host and cause disease without encoding proteins. Biochimie **94:** 1474-1480

Onodera Y, Haag JR, Ream T, Nunes PC, Pontes O, Pikaard CS (2005) Plant nuclear RNA polymerase IV mediates siRNA and DNA methylation-dependent heterochromatin formation. Cell **120:** 613-622

Pallas V, Gomez G, Amari K, Cañizares MC, Candresse T (2003) Hop stunt viroid in apricot and almond. *In* A Hadidi, J Randles, J Semancik, R Flores, eds, Viroids. Science Publishers, St Paul, MN, USA, pp 168-170

Papaefthimiou I, Hamilton A, Denti M, Baulcombe D, Tsagris M, Tabler M (2001) Replicating potato spindle tuber viroid RNA is accompanied by short RNA fragments that are characteristic of post-transcriptional gene silencing. Nucleic Acids Res **29:** 2395-2400

Pecinka A, Dinh HQ, Baubec T, Rosa M, Lettner N, Scheid OM (2010) Epigenetic Regulation of Repetitive Elements Is Attenuated by Prolonged Heat Stress in *Arabidopsis*. Plant Cell **22:** 3118-3129

Pecinka A, Scheid OM (2012) Stress-induced chromatin changes: a critical view on their heritability. Plant Cell Physiology **53:** 801-808.

Pontes O, Costa-Nunes P, Vithayathil P, Pikaard CS (2009) RNA Polymerase V Functions in *Arabidopsis* Interphase Heterochromatin Organization Independently of the 24-nt siRNA-Directed DNA Methylation Pathway. Molecular Plant **2:** 700-710

Probst AV, Fagard M, Proux F, Mourrain P, Boutet S, Earley K, Lawrence RJ, Pikaard CS, Murfett J, Furner I, Vaucheret H, Scheid OM (2004) *Arabidopsis* histone deacetylase HDA6 is required for maintenance of transcriptional gene silencing and determines nuclear organization of rDNA repeats. Plant Cell **16:** 1021-1034

Rodriguez-Negrete E, Lozano-Duran R, Piedra-Aguilera A, Cruzado L, Bejarano ER, Castillo AG (2013) Geminivirus Rep protein interferes with the plant DNA methylation machinery and suppresses transcriptional gene silencing. New Phytol **199:** 464-475

Ruiz-Ferrer V, Voinnet O (2009) Roles of plant small RNAs in biotic stress responses. Annu Rev Plant Biol **60:** 485-510

Sano T (2003) Hop stunt viroid in cucumber. *In* A Hadidi, J Randles, J Semancik, R Flores, eds, Viroids. Science Publishers, St Paul, MN, USA, pp 134-136

Sha AH, Lin XH, Huang JB, Zhang DP (2005) Analysis of DNA methylation related to rice adult plant resistance to bacterial blight based on methylation-sensitive AFLP (MSAP) analysis. Mol Genet Genomics **273:** 484-490

Shimura H, Pantaleo V, Ishihara T, Myojo N, Inaba J, Sueda K, Burgyan J, Masuta C (2011) A Viral Satellite RNA Induces Yellow Symptoms on Tobacco by Targeting a Gene Involved in Chlorophyll Biosynthesis using the RNA Silencing Machinery. Plos Pathogens **7**

Singh RP (1970) Seed transmission of potato spindle tuber virus in tomato and potato. American Potato Journal **47:** 225-227

Singh RP, Boucher A, Somerville TH (1993) Interactions between a mild and a severe strain of potato spindle tuber viroid in doubly infected potato plants. American Potato Journal **70:** 85-92

Singh RP, Ready KF, Nie X (2003) Biology. *In* A Hadidi, J Randles, J Semancik, R Flores, eds, Viroids. Science Publishers, St Paul, MN, USA, pp 30-48

Slotkin RK, Martienssen R (2007) Transposable elements and the epigenetic regulation of the genome. Nat Rev Genet **8:** 272-285

Smith NA, Eamens AL, Wang MB (2011) Viral Small Interfering RNAs Target Host Genes to Mediate Disease Symptoms in Plants. Plos Pathogens **7**

Tang B, Zhao R, Sun Y, Zhu Y, Zhong J, Zhao G, Zhu N (2011) Interleukin-6 expression was regulated by epigenetic mechanisms in response to influenza virus infection or dsRNA treatment. Mol Immunol **48:** 1001-1008

Tessadori F, Chupeau MC, Chupeau Y, Knip M, Germann S, van Driel R, Fransz P, Gaudin V (2007) Large-scale dissociation and sequential reassembly of pericentric heterochromatin in dedifferentiated *Arabidopsis* cells. Journal of Cell Science **120:** 1200-1208

Wah YFWC, Symons RH (1999) Transmission of viroids via grape seeds. Journal of Phytopathology-Phytopathologische Zeitschrift **147:** 285-291

Wang MB, Bian XY, Wu LM, Liu LX, Smith NA, Isenegger D, Wu RM, Masuta C, Vance VB, Watson JM, Rezaian A, Dennis ES, Waterhouse PM (2004) On the role of RNA silencing in the pathogenicity and evolution of viroids and viral satellites. Proc Natl Acad Sci U S A **101:** 3275-3280

Yu A, Lepere G, Jay F, Wang J, Bapaume L, Wang Y, Abraham AL, Penterman J, Fischer RL, Voinnet O, Navarro L (2013) Dynamics and biological relevance of DNA demethylation in *Arabidopsis* antibacterial defense. Proc Natl Acad Sci U S A **110:** 2389-2394

Zhu QH, Shan WX, Ayliffe MA, Wang MB (2016) Epigenetic Mechanisms: An Emerging Player in Plant-Microbe Interactions. Mol Plant Microbe Interact **29:** 187-196

SUPPLEMENTAL DATA

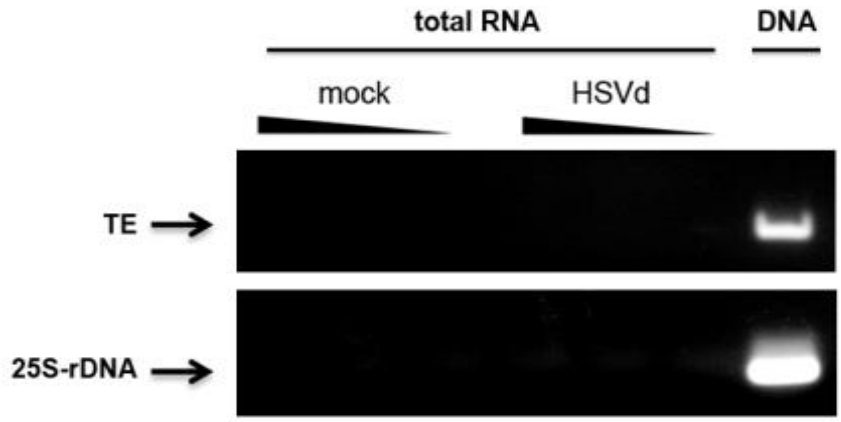

Figure Supplementary 1: Representative PCR analysis in serial dilutions of HSVd-infected and control total RNA extracts to corroborate the absence of DNA in RNA samples used to analysis of pre-rRNA and TE-derived transcripts expression. Extracts of total DNAs were used as positive amplification controls.

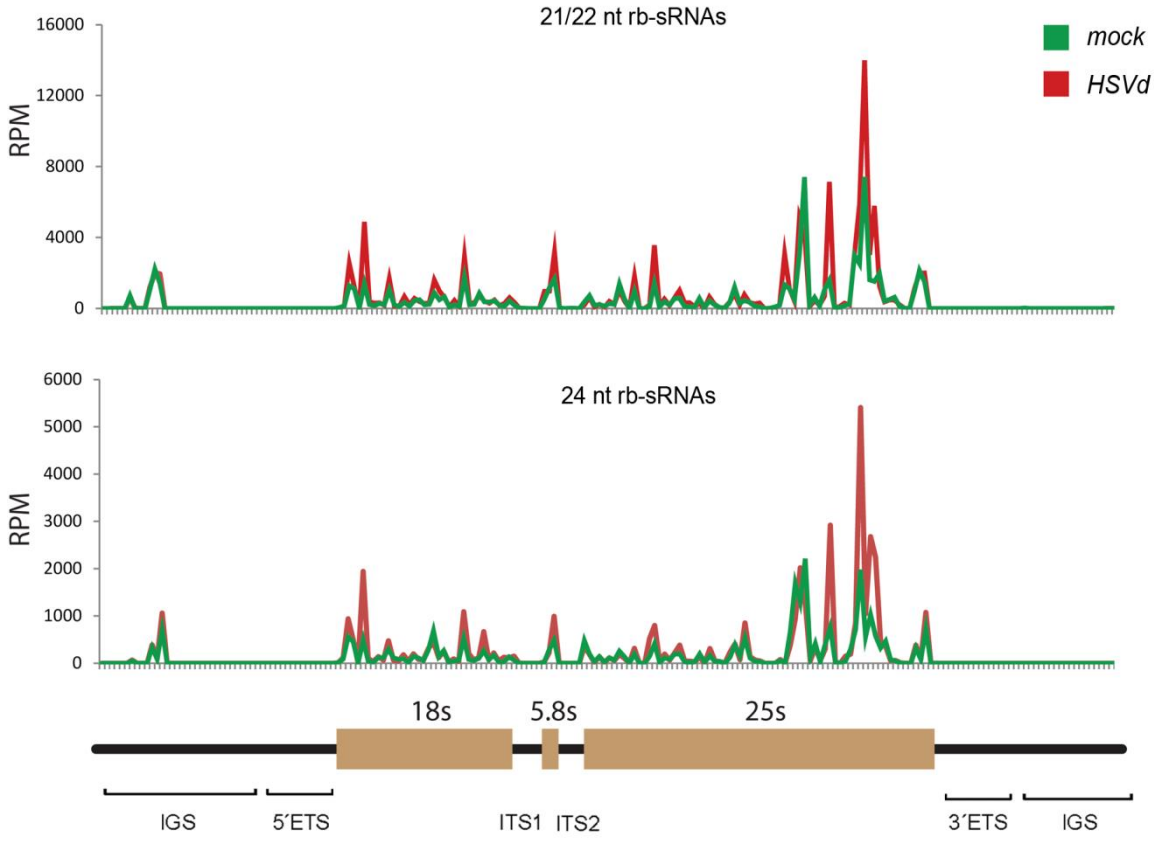

Figure Supplementary 2: Analysis of differentially expressed ribosomal-derived sRNAs in infected pollen grains. The rb-sRNAs (21/22 nt lengh upper, and 24 nt lower panel) recovered from the infected (red lines) or the mock-inoculated plants (green lines) were plotted according to the position of their 5´-end onto the cucumber rRNA sequence. The values on the Y-axis represent the number of normalized reads in each library. Diagram (no scale) of the rRNA unit. IGS (Non transcribed intergenic spacer). The external (ETS) and internal (ITS) transcribed spacers are removed during rRNA processing.

A

cuc_reannotTE.Scaffold000159.7

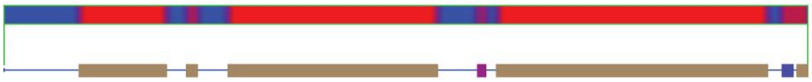

Name	From	To	Name	From	To	Class	Dir	Sim	Pos/Mm:Ts	Score
31229.tmp/data.ori	472	1024	Copia-74_GM-I	171	723	LTR/Copia	d	0.6435	1.9767	650
31229.tmp/data.ori	1152	1218	Copia-56_VV-I	861	926	LTR/Copia	d	0.7612	2.5000	257
31229.tmp/data.ori	1406	2722	Copia-34_NN-I	1157	2473	LTR/Copia	d	0.6927	1.9205	2620
31229.tmp/data.ori	2975	3023	DNA-8-1_DR	394	453	DNA	d	0.8462	1.6667	219
31229.tmp/data.ori	3094	4788	Copia-34_NN-I	2824	4524	LTR/Copia	d	0.7264	2.0145	5510
31229.tmp/data.ori	4876	4946	X1_LINE	234	310	NonLTR/CR1	c	0.7333	1.4545	229
31229.tmp/data.ori	4975	5039	Copia-15_GR-LTR	263	323	LTR/Copia	d	0.7969	1.6000	237

B

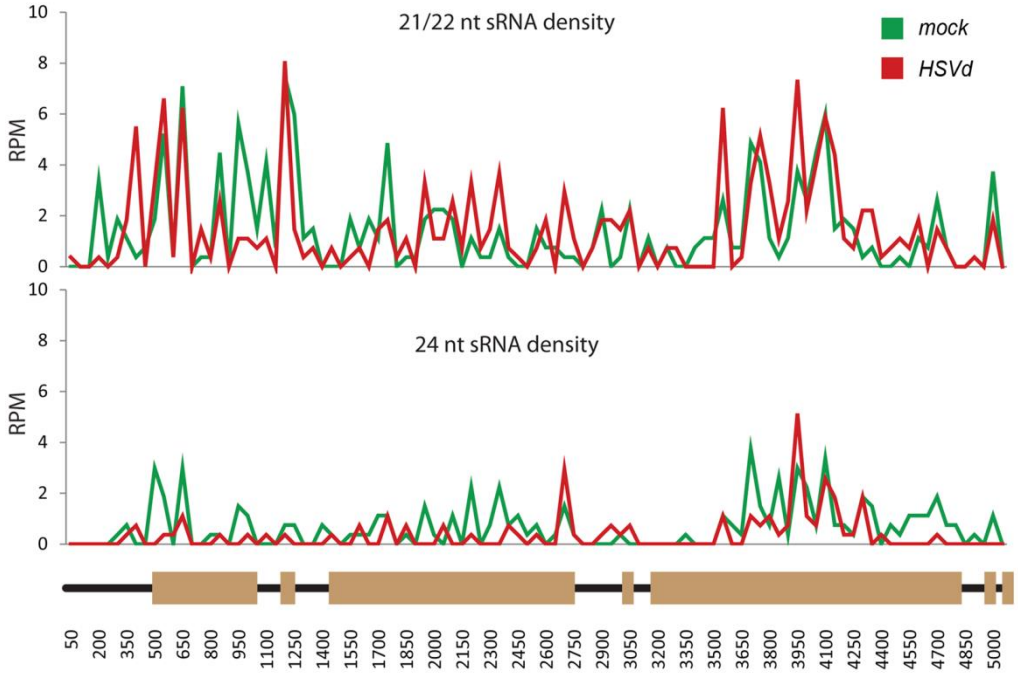

Figure Supplementary 3: Analysis of TE-derived sRNAs differentially expressed in infected cucumber pollen grains. **(A)** Screenshot of the CENSOR (http://www.girinst.org/censor/index.php) sequence homology analysis of the TE cuc_reannotTE.Scaffold000159.7. The analysis reveals homology of the element with different members of the Copia family. **(B)** sRNA accumulation profile over the TE cuc_reannotTE.Scaffold000159.7 in mock-inoculated (green line) and HSVd-infected (red line) pollen grains. Densities of 21/22 (upper panel) and 24 (lower panel) nt sRNAs are shown. Reads were normalized to reads per million (RPM).

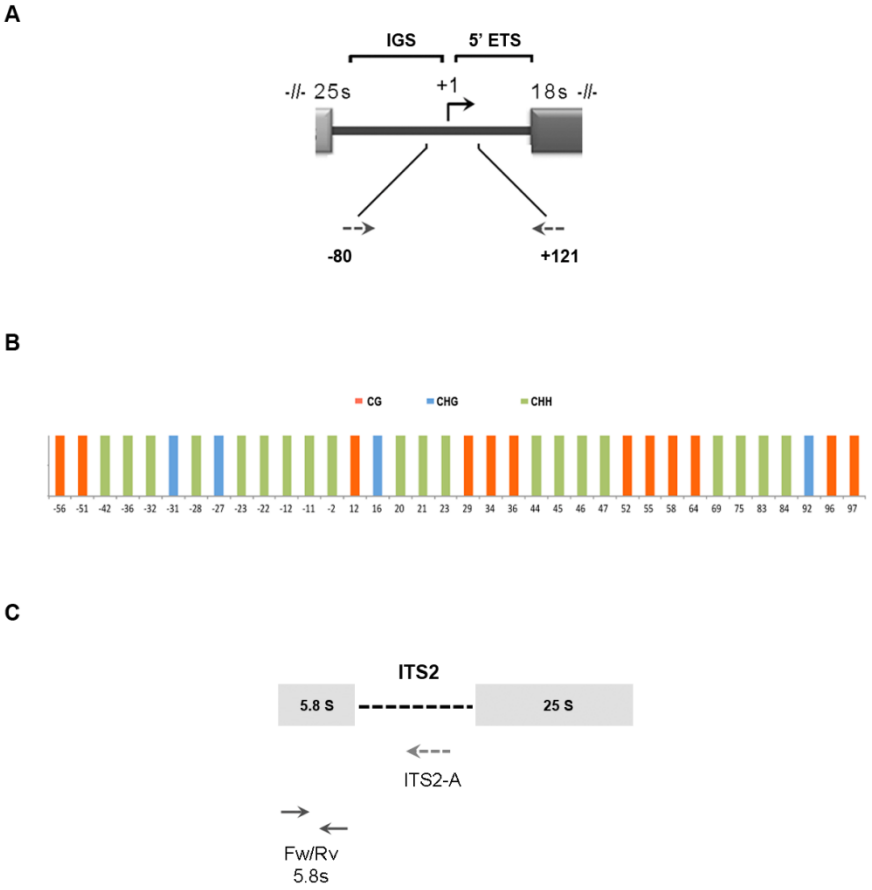

Figure Supplementary 4: (A) Diagram (no scale) of the rDNA intergenic region highlighting the promoter zone analyzed by bisulfite sequencing. The arrows represent the oligos used in the PCR assay and their relative position in the rDNA. IGS: Intergenic spacer, ETS: external transcribed spacer. +1 represent the transcription initiation site. **(B)** Graphic representation of the potential symmetric (CG – red bars - and CHG – blue bars) and asymmetric (CHH – green bars) positions predicted to exist within the analyzed rDNA region. **(C)** Diagram (no scale) of the partial pre-27S rRNA (ITS2 refer to unprocessed internal transcribed spacers). The dotted arrow below depicts the oligo used for the RT reaction starting from the ITS2 region of the pre-rRNA. Solid arrows indicate the oligos used in the PCR amplification.

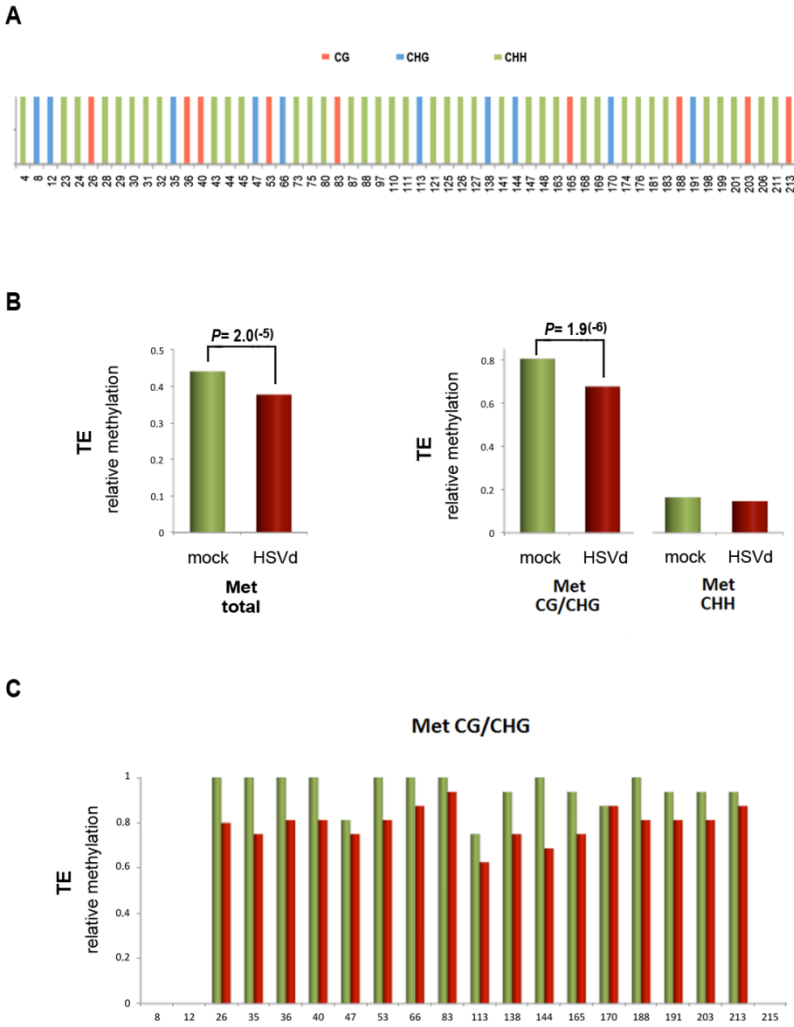

Figure Supplementary 5: HSVd infection affects the methylation patterns of TE DNA in cucumber leaves. **(A)** Graphic representation of the potential symmetric (CG – red bars - and CHG – blue bars) and asymmetric (CHH – green bars) positions predicted to exist within the analyzed TE DNA region. **(B)** *left panel:* Histogram documenting the total methylation levels in TE DNA obtained from mock and HSVd-infected cucumber leaves. *Right panel:* Schematic representation of both symmetric and asymmetric cytosine methylation levels in analysed TE DNA. Statistical significance was tested using a paired t-test. Only significant *P* values are shown in the figure. **(C)** Positions of methylcytosines in the analysed TE DNA, displayed in symmetric (CG and CHG) context. The height of the bar represents the frequency at which a cytosine was methylated.

DISCUSIÓN GENERAL

Los viroides son patógenos de plantas formados por RNA circulares de simple cadena, capaces de infectar e inducir enfermedades en un gran número de especies vegetales, tanto herbáceas como leñosas. No poseen capacidad para codificar proteínas. Todas las fases de su ciclo vital son estrictamente dependientes del huésped, por lo que los viroides se consideran organismos modelo para el estudio de las interacciones entre patógenos de RNA y plantas (Ding y Itaya, 2007). Además, debido a su simplicidad molecular, constituyen sistemas modelo excepcionales para el estudio de los mecanismos de regulación mediados por RNA no codificantes en plantas (Gómez y Pallás, 2013; Gago-Zachert, 2016).

En general, cuando se produce una infección viroidal se ha observado que, entre otras respuestas, se activa la maquinaria del silenciamiento de RNA a dos niveles. El primero es mediante la producción de sRNAs derivados del genoma del patógeno (Itaya *et al*., 2001; Wang y Waterhouse, 2002), y, el segundo, mediante la modificación del patrón de sRNAs celulares, alterando la expresión de reguladores o efectores de las rutas de defensa del hospedador (Ruiz-Ferrer y Voinnet, 2009).

Un gran número de observaciones recientes apoyan la idea de que las interacciones viroide-huésped podrían estar asociadas a las vías de regulación dirigidas por RNA no codificante (Ding, 2010; Gómez y Pallás, 2013). Un objetivo fundamental de este emergente escenario es descifrar las bases moleculares que intervienen en los distintos mecanismos que constituyen el proceso de patogénesis asociado a viroides.

Desde que se informó de la primera enfermedad inducida por viroides, se han propuesto diversos modelos sobre los mecanismos que regulan la patogénesis viroidal (Navarro *et al*., 2012). En lo que respecta a la expresión de síntomas, la idea que prevalece es la que establece una estrecha relación entre estas alteraciones en el huésped y el silenciamiento de RNA, además considera esencial a los siRNAs derivados del viroide que actúan en el metabolismo de RNA endógeno de la planta a nivel post-transcripcional (Wang *et al*., 2004; Gómez *et al*., 2009). Asimismo, diversos aspectos del proceso de patogénesis podrían ser consecuencia de las alteraciones específicas en los mecanismos de regulación a nivel transcripcional (Navarro *et al*., 2012; Gómez y Pallás, 2013; Itaya *et al*., 2002; Owens *et al*., 2012; Tessitori *et al*., 2007; Herranz *et al.,* 2013; Lison *et al*., 2013).

Así pues, a la vista de los resultados que se habían obtenido hasta entonces, en la presente tesis se quiso ahondar por un lado, acerca del conocimiento de cómo los viroides (ncRNAs) eran capaces de modificar la maquinaria transcripcional del huésped y obtener por ello beneficio, y, por otro, en la identificación de los componentes celulares que son alterados en la planta como consecuencia de esta infección viroidal. Por tanto, en este trabajo se ha abordado la interacción planta-viroide tanto desde el

punto de vista del viroide como desde el punto de vista de los cambios que experimenta la planta al ser infectada por un patógeno de RNA no codificante.

UN PATÓGENO DE RNA NO CODIFICANTE PRODUCE CAMBIOS DINÁMICOS EN LA METILACIÓN DE GENES RIBOSOMALES DEL HUÉSPED.

Al inicio de este trabajo se desconocía si algunos aspectos de la interacción viroide-huésped, podrían estar relacionados con la desregulación de sRNAs endógenos implicados en procesos fisiológicos fundamentales de la planta. Para abordar esta posibilidad, en el primer capítulo de la tesis utilizamos el sistema biológico HSVd-pepino, un huésped natural del viroide de interés agronómico.

Inicialmente se analizaron dos librerías de sRNAs en las que se comparó la población de sRNAs de plantas sanas e infectadas, observándose una hiperacumulación de sRNAs en plantas de pepino infectadas por HSVd derivados del RNA ribosomal (rRNA). Esta observación nos llevó a la posibilidad de que, durante la infección, este viroide (como ya se había descrito para una variante de PLMVd (Rodio *et al*., 2007)) pudiera estar interfiriendo, de manera aún desconocida, en el proceso de maduración y procesado del rRNA. Además, al analizar un gran número de sRNAs procedentes de esta región, sospechamos que podría deberse a la degradación del rRNA aberrante. Esta suposición se descartó al observar que las formas maduras del rRNA (25s) se acumulaban a niveles comparables en ambas muestras (Capítulo 1 Fig 3B y 3C). La posibilidad de que la acumulación de estos rb-sRNAs en plantas infectadas pudiera ser el resultado de la desregulación transcripcional de los rRNAs asociada a la infección por HSVd resultaba consistente con el fenómeno descrito en *Arabidopsis*. En este huésped se relacionó la sobreacumulación de rb-sRNAs con deficiencias en el mecanismo de encendido/apagado que controlaba el número de genes de rRNA activos (Earley *et al*., 2010).

Mediante análisis RT-PCR a partir de regiones intergénicas del DNA ribosomal de plantas sanas e infectadas, se detectó un significativo aumento de la acumulación de formas precursoras de rRNA (pre-rRNAs) en las plantas enfermas, sugiriendo que el HSVd podría inducir la desregulación de alguna de las unidades transcripcionales de rRNA, normalmente inoperativas.

Con el objeto de determinar si el aumento de la transcripción de los pre-rRNAs, observado en plantas infectadas, pudiera estar relacionado con cambios en los niveles de metilación del DNA analizamos, mediante secuenciación de DNA bisulfitado, los niveles de metilación de la región promotora de rDNA 45s. Este estudio puso de manifiesto que el nivel de metilación de citosinas en contexto simétrico (CG y CHG) y

asimétrico (CHH) variaba durante la infección. En el caso del contexto simétrico se observó una disminución; sin embargo la metilación asimétrica, a pesar de mostrar un comportamiento similar en una primera fase, aumentaba de forma significativa durante el desarrollo de la infección. Se obtuvieron resultados similares cuando analizamos los niveles de metilación de las regiones promotoras del rDNA 5s. Este fenómeno había sido previamente descrito en *Arabidopsis* (Pontivianne *et al*., 2012; Earley *et al.,* 2010). Con estos antecedentes especulamos que la sobreacumulación del pre-rRNA de las plantas infectadas podría ser consecuencia de la activación, asociada a alteraciones en la metilación, de genes ribosomales del huésped.

Estos resultados fueron consistentes con otros trabajos previos. En ellos observaron una asociación entre la alteración de la metilación y los mecanismos de respuesta a una infección por bacterias en arroz (Sha *et al*., 2005), tabaco (Boyko *et al., 2007*) y *Arabidopsis* (Dowen *et al*., 2012; Yu *et al*., 2013). Además, en un estudio realizado con plantas transgénicas de *N. benthamiana* que expresaban una proteína asociada a la replicación (Rep) de un *Gemenivirus*, se propuso que este tipo de virus de DNA podría inducir una reducción sustancial de los niveles de metilación del DNA del huésped (Rodriguez-Negrete *et al*., 2013). Esta suma de observaciones, nos permitió establecer una hipótesis; la alteración de los patrones de metilación del huésped podría constituir una repuesta clave durante la interacción planta-patógeno.

Una vez determinado el fenómeno epigenético asociado a la infección por HSVd, quisimos conocer su mecanismo molecular. En mutantes de *Arabidopsis* deficientes para la HISTONA DEACETILASA 6 (HDA6) se había descrito un escenario similar. Esta histona es un regulador del silenciamiento de RNA íntimamente relacionado con la metilación del DNA (Earley *et al*., 2010). De este trabajo se dedujeron tres eventos que mostraban un gran paralelismo con lo observado en las plantas de pepino infectadas con HSVd. Por un lado, los mutantes *hda6* sufrían hipometilación simétrica en las regiones promotoras del 45s del DNA ribosomal acompañada de una hipermetilación del contexto asimétrico. Por otro lado**,** este aumento de metilación asimétrica (un fenómeno típicamente represivo) no reprimía el exceso de transcripción de rRNA. Y, por último, esta alteración estaba asociada a la hiperacumulación de los sRNAs derivados del rRNA 45S; resultados que habíamos observado en las plantas de pepino infectadas. Los autores propusieron una posible relación entre la transcripción espuria de genes ribosomales mediada por Pol II y la disminución del nivel de metilación del rDNA observado en los mutantes *hda6* (Earley *et al*., 2010).

En este punto es importante tener en cuenta que durante la infección los viroides nucleares necesitan alterar la fidelidad transcripcional de Pol II para ser transcritos, al reconocer como molde cadenas de RNA

(del genoma del viroide) en lugar de DNA (Muhlbach *et al*., 1979). Por lo que se podría pensar que en un escenario transcripcionalmente alterado se favoreciera la acumulación del HSVd en el huésped. Son necesarios estudios más detallados sobre las funciones de este mecanismo para determinar las relaciones existentes entre la alteración transcripcional de los rRNAs y el ciclo de vida de los viroides con replicación nuclear.

En resumen, los datos presentados en el primer capítulo ponen de manifiesto que durante el proceso de patogénesis HSVd induce en su huésped cambios en el patrón de metilación del rDNA, un fenómeno que no había sido descrito anteriormente en infecciones ocasionadas por viroides (o por cualquier otro RNA patogénico). Por otro lado, nuestros resultados proporcionan nuevos conocimientos sobre las alteraciones que se producen en el huésped asociadas con el ciclo infeccioso del HSVd. Además, constituyen un apoyo adicional a la idea emergente de que la interacción viroide - huésped puede ser un proceso complejo que implica alteraciones en la planta tanto a nivel transcripcional como post-transcripcional.

ASOCIACIÓN ENTRE PATOGÉNESIS Y REGULACIÓN TRASCRIPCIONAL EN UN HUÉSPED DIFERENTE.

A continuación quisimos estudiar si la asociación entre la infección viroidal y la desregulación transcripcional de los genes del huésped era un fenómeno general o, por el contrario, estaba restringido específicamente a la interacción HSVd-pepino.

En ese momento, en el laboratorio se disponía de plantas de *N. benthamiana* transgénicas que sobreacumulaban de manera constitutiva la secuencia dimérica del HSVd (HSVd-*Nb*) (Gómez y Pallás, 2007). Estas plantas imitaban los efectos patogénicos asociados a la infección convencional (Gómez *et al*., 2008). Además, los perfiles vd-sRNAs recuperados fueron similares a los previamente descritos en otras interacciones HSVd-huésped, por lo que se consideró un modelo adecuado para analizar los efectos de la acumulación del HSVd sobre la actividad transcripcional.

Teniendo en cuenta que detectamos un incremento en la acumulación de sRNAs derivados del RNA ribosomal (rb-sRNAs) en las muestras de pepinos infectadas por HSVd, procedimos a analizar la acumulación de rb-sRNAs en plantas de HSVd/*Nb*. Los resultados que obtuvimos indicaron que había una clara diferencia en la distribución de estos sRNAs. Detectamos un aumento de la población de rb-sRNAs de 21nt y una significativa disminución de los de 24nt en las plantas transgénicas. Por otra parte, la

acumulación del viroide en las plantas de *N. benthamiana* estuvo también asociada con un incremento de la acumulación de los precursores del rRNA, como ya habíamos detectado en las plantas de pepino enfermas.

La observación de este hecho nos llevó a analizar la acumulación del pre-RNA no procesado en las plantas HSVd*/Nb*. Detectamos una mayor actividad transcripcional en ellas, que podría ser consecuencia de un desequilibrio en la actividad transcripcional de los genes ribosomales.

Además, algunos resultados previos demostraron que el viroide del tubérculo fusiforme de la patata (PSTVd) inducía la sobrexpresión de los genes ribosomales en plantas de tomate (Itaya *et al*., 2002). Datos que sugieren de forma robusta que la reactivación de rRNAs podría ser un fenómeno común asociado a la infección por viroides.

A continuación estudiamos, mediante secuenciación de DNA bisulfitado, las posibles alteraciones en los patrones de metilación del rDNA. Los datos obtenidos evidenciaron que la acumulación del viroide en *N. benthamiana* estaba asociada a una significativa hipometilación tanto en las zonas promotoras del 45s como del 5s rDNA. De la misma forma que observamos en plantas de pepino, esta alteración de los patrones de metilación se caracterizó por una selectiva hipometilación del contexto simétrico (CG y CHG) de los genes ribosomales. Este hecho nos permitió explicar la sobreacumulación de transcritos precursores de rRNA presentes en las plantas HSVd*/Nb.*

En definitiva, nuestros resultados indicaron que las plantas de *N.benthamiana* que expresaban de forma constitutiva el RNA viroidal, mostraban alteraciones transcripcionales comparables a las observadas en pepino durante una infección convencional. Por tanto, la interacción de este patógeno con los mecanismos epigenéticos (asociados a la metilación del DNA) que controlan la expresión génica en plantas, no estaría restringido a un huésped específico, pudiendo constituir un fenómeno más general capaz de ocurrir en otras interacciones planta-viroide.

EL HSVd MODIFICA LA REGULACIÓN EPIGENÉTICA DEL HUÉSPED COMO CONSECUENCIA DEL CAMBIO DE ACTIVIDAD DE LA HISTONA DEACETILASA 6 (HDA6).

Los resultados obtenidos en los capítulos anteriores revelaron que las plantas de pepino y *N. benthamiana* infectadas por HSVd, mostraban una disminución de los niveles de metilación en las regiones promotoras de los genes ribosomales. Esta observación sugirió que el viroide podría interferir en las vías específicas de metilación del huésped. Además, las similitudes observadas entre las plantas infectadas con HSVd (hiperacumulación de sRNAs de 21 nucleótidos derivados de los rRNAs, pérdida de metilación simétrica y aumento de la transcripción de genes ribosomales) y el mutante hda6 de *Arabidopsis* (Earley *et al*., 2010), nos proporcionaron la argumentación experimental necesaria para pensar que podía existir, durante el proceso de infección, una estrecha relación entre el HSVd y la HISTONA DEACETILASA 6 (HDA6) del huésped.

Al comenzar a estudiar la posible interacción entre el viroide y la HDA6, lo primero que detectamos fue un incremento de la concentración de la proteína en los núcleos de células de pepino infectadas. Esta observación nos ayudó a establecer una primera conexión funcional entre HSVd y el metabolismo de HDA6 en las plantas infectadas. A continuación quisimos averiguar si la proteína y el viroide eran capaces de interaccionar físicamente. Mediante ensayos de unión *in vitro* comprobamos que existía una interacción entre el RNA viroidal y la proteína HDA6. En este sentido, es importante destacar que ambas moléculas se encuentran localizadas en el núcleo, compartiendo el mismo escenario espacial que haría posible la interacción *in vivo*. La demostración, mediante ensayos de inmunoprecipitación, de que el complejo HSVd-HDA6 ocurría también *in vivo*, nos permitió confirmar que este viroide era capaz de reconocer y reclutar la proteína HDA6 de pepino durante el proceso de infección.

Una vez demostrada la existencia del complejo HSVd-HDA6 *in vivo*, quisimos determinar si esta unión podía tener alguna relación funcional con los patrones de hipometilación que habíamos observado tanto en las plantas de pepino infectadas como en las plantas HSVd-*Nb*. Para ello secuenciamos el DNA bisulfitado obtenido a partir de hojas de plantas de pepino infectadas que, o habían sido agroinfiltradas con la secuencia dimérica del viroide, o, con plásmido vacío, tomadas estas últimas como muestras control. Se observó una correlación clara entre la infección producida por el viroide y una reducción de la metilación de las citosinas en la región promotora del 45S rDNA de pepino. Este resultado reforzó los datos que habíamos obtenido en los anteriores capítulos en los que se había observado una asociación entre la infección del viroide y la hipometilación de los genes ribosomales.

Con el objeto de determinar si la sobreacumulación de HDA6 en el tejido infectado era capaz de revertir las alteraciones inducidas por el viroide, se expresó mediante agroinfiltración la proteína HDA6 en hojas de

plantas infectadas con HSVd. Se observó que los niveles de metilación se restauraron a valores casi normales en plantas infectadas que sobreexpresaban HDA6; determinando de forma inequívoca que el complejo HSVd-HDA6 estaba relacionado con la hipometilación del rDNA. Esta demostración sugería que las alteraciones de la metilación de las plantas infectadas podrían ser debidas a las interferencias causadas por el viroide en las rutas de mantenimiento de la metilación del DNA mediadas por HDA6 (Earley *et al.,* 2010).

El fenómeno podría explicarse, entre otras opciones, a la interferencia de la formación del complejo HDA6-MET1 por la interacción entre HSVd y HDA6. Este complejo es necesario para la regulación del mantenimiento de la metilación de las secuencias de DNA repetitivas en contextos simétricos (Liu *et al*., 2012a y 2012b). De forma que, en este caso, se alterarían los procesos de metilación de sus dianas (en este caso la región promotora del RNA ribosomal) (Figura 1). Esta modificación en la vía de regulación sería la responsable del fenómeno de hipometilación observado en las plantas infectadas por el viroide. Es importante señalar que sería necesario determinar si este reclutamiento de la HDA6 propiciado por el viroide también podría afectar a la metilación de la citosina en otras dianas alternativas de HDA6, tales como Elementos Transponibles (TEs) o transgenes (Liu *et al*., 2012).

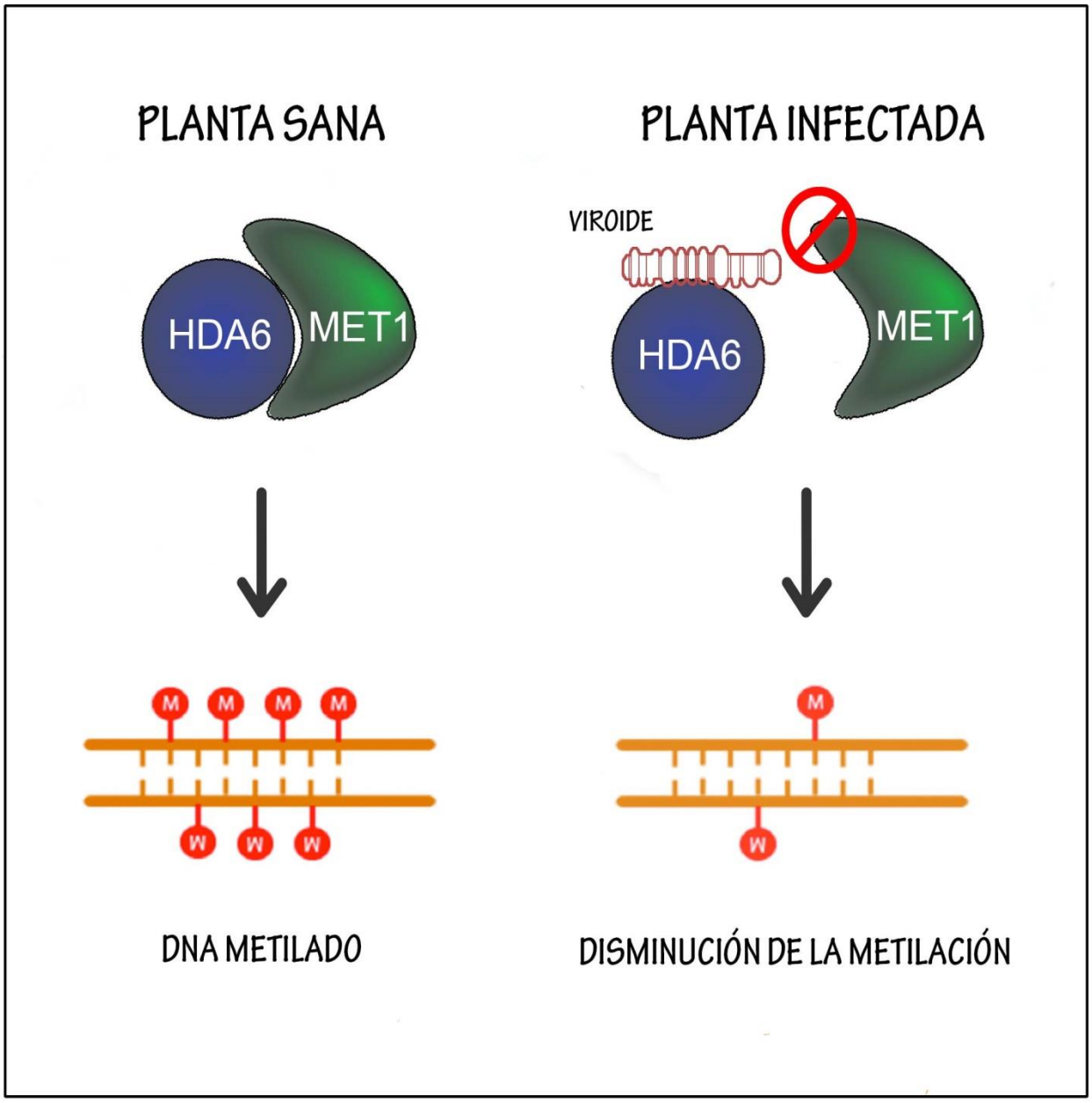

Figura 1. Representación de la interacción entre el viroide y la HISTONA DEACETILASA 6. Comparación de una planta sana y una infectada con HSVd observándose como la interacción del viroide con HDA6 dificulta la formación del complejo HDA6-MET1, provocando una disminución de la metilación del DNA (hipometilación de la zona promotora del RNA ribosomal).

En conjunto, estos datos sugieren que el HSVd es capaz de reclutar y bloquear en parte la función de la proteína HDA6 de pepino durante el proceso de infección y, por tanto, inducir cambios en el estado de metilación del DNA. Este fenómeno provoca la reactivación de la transcripción de genes ribosomales normalmente silenciados. Además, ponen de manifiesto que la regulación epigenética de la actividad transcripcional constituye un mecanismo de regulación asociado a la respuesta de la planta a la infección viroidal, tal y como se había demostrado previamente en los procesos de patogénesis inducidos por bacterias (Dowen *et al.,* 2012; Yu *et al.,* 2013) y virus (Raja *et al*., 2008; Rodriguez Negrete *et al*., 2013; Yang *et al*., 2013).

Sin embargo, y en lo que al ciclo de vida del viroide se refiere, una pregunta fundamental seguía aún sin resolver. No se sabía si la interacción HSVd-HDA6 podría proporcionar alguna ventaja adaptativa para el patógeno. Para tratar de discernirlo analizamos la acumulación del HSVd mediante RT-PCR semicuantitativa en hojas en las que la expresión de HDA6 estaba transitoriamente incrementada o disminuida. Los datos revelaron que los niveles de viroide se reducían de forma significativa en las hojas que sobreacumulaban HDA6, sugiriendo que un exceso de HDA6 libre en los núcleos de las células infectadas podría afectar de forma negativa a la acumulación de HSVd. Por el contrario, la acumulación del viroide se incrementaba significativamente cuando se silenció la expresión de HDA6 de manera transitoria. Estos resultados pusieron de manifiesto una relación directa entre los niveles de expresión de HDA6 y el grado de acumulación del HSVd.

Aunque parezcan prematuras las especulaciones acerca de la naturaleza funcional del complejo HSVd-HDA6 que se forma durante la infección, en este contexto es oportuno tener en cuenta que, a pesar de estar bien establecido que los miembros de la familia *Pospiviroidae* reclutan y redirigen la RNA Pol II para su transcripción (Flores y Semancik, 1982; Mühlbach y Sanger, 1997; Bojic *et al*., 2012), la estrategia empleada por estos patógenos para reprogramar la actividad de la RNA Pol II sigue siendo un enigma.

Como ya se ha mencionado, en un trabajo anterior se demostró que los mutantes hda6 de *Arabidopsis* sufrían claros procesos de hipometilación y que la pérdida de la actividad de la HDA6 observada en éstos se asoció con la transcripción espuria de Pol II de dianas de rDNA no convencionales (normalmente transcritas por RNA Pol I) (Earley *et al*., 2010). Basándonos en estas observaciones, propusimos un escenario hipotético que pudiera explicar y recapitular estos resultados. Tras producirse una infección viroidal, el patógeno entraría en el núcleo de la célula huésped, reclutando e inactivando funcionalmente la HISTONA DEACETILASA 6 al interactuar físicamente con la ella. Esta situación promovería un estado transcripcionalmente alterado que conduciría a la RNA Pol II a reconocer como molde las secuencias de RNA viroidal y transcribirlas de una manera similar a lo que ocurre con el DNA ribosomal en los mutantes hda6 de *Arabidopsis* (Earley *et al*., 2010) (Figura 2).

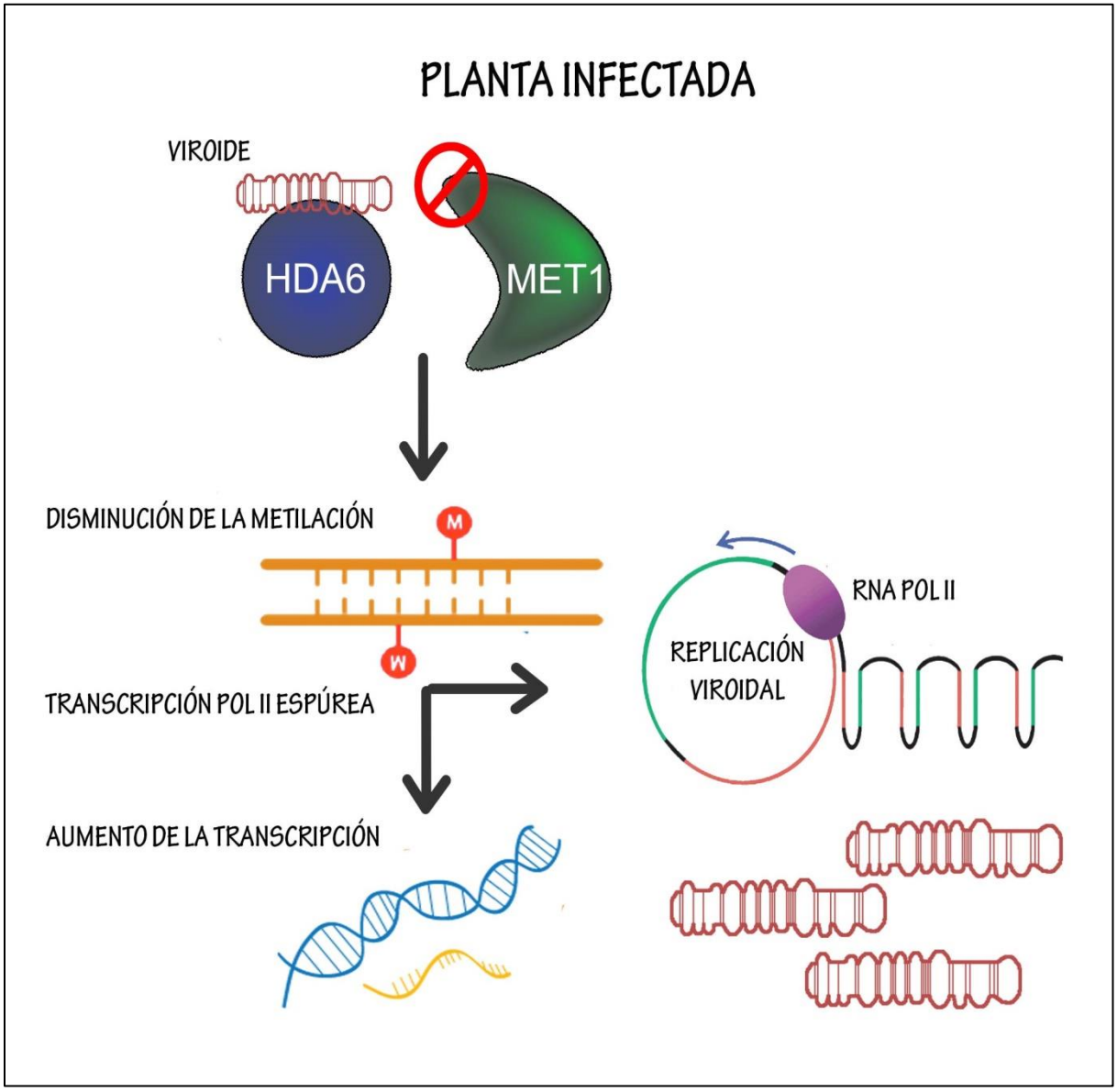

Figura 2. Representación gráfica del posible beneficio del viroide al interaccionar con la HISTONA DEACETILASA 6 (HDA6) del huésped. El viroide bloquearía la función de la HDA6 por su unión a ella, desencadenando procesos de hipometilación y transcripción activa que promoverá a la RNA Polimerasa II (Pol II) a reconocer como molde de forma errónea el RNA viroidal, aumentando el ratio de replicación del viroide y favoreciendo por tanto su infección a través de la planta.

En resumen, los datos presentados en el tercer capítulo revelan que durante la infección, el HSVd es capaz de reclutar y modificar las funciones de la proteína HDA6 del huésped. Este hecho proporciona nuevas evidencias sobre el potencial de estos agentes patogénicos para rediseñar estructural y funcionalmente el entorno de la célula huésped; además de reprogramar sus mecanismos de regulación con el fin de asegurarse el éxito de su ciclo infectivo (Ding, 2010; Gómez y Pallás, 2013; Katsarou *et al*., 2015; Liu *et al*., 2015; Gago-Zachert, 2016).

LA INFECCIÓN VIROIDAL PROVOCA CAMBIOS EN EL PATRÓN DE METILACIÓN DEL GAMETOFITO MASCULINO.

Hasta el momento se han descrito alteraciones drásticas del epigenoma en respuesta a patógenos tanto en plantas (Agorio y Vera, 2007; Boyko *et al*., 2010; López *et al*., 2011; Dowen *et al*., 2012; Luna y Ton, 2012; Yu *et al*., 2013) como en animales (Tang *et al*., 2011). Estas observaciones apoyan la idea de que la reprogramación epigenética de la actividad transcripcional es un mecanismo general que actúa durante la respuesta del huésped a la infección causada por un patógeno (Zhu *et al*., 2016). En consonancia con esta idea, a lo largo de este trabajo hemos descrito los efectos que tiene la infección del viroide HSVd sobre los mecanismos epigenéticos que controlan la transcripción de RNAs ribosomales del huésped. Considerando que todos nuestros datos habían sido obtenidos sobre tejido vegetativo (principalmente hoja), quisimos comprobar si este fenómeno también podría ocurrir en el tejido reproductivo de plantas de pepino infectadas por HSVd.

Para abordar este tema, primero tuvimos que determinar si ambas formas biológicas del viroide (RNA monomérico y vd-sRNAs) eran capaces de acumularse en los granos de polen de plantas infectadas. Mediante estudios de RT-PCR y secuenciación masiva fue posible determinar que ambas formas del RNA del HSVd se acumulaban eficientemente en este tipo de células reproductivas. Por otra parte, un estudio más detallado de los sRNAs, puso de manifiesto que el perfil general de acumulación de sRNAs endógenos también estaba alterado en el tejido reproductivo. En particular se observó un significativo aumento de sRNAs derivados de la transcripción de rRNA y de Elementos Transponibles (TEs).

Esta sobreacumulación de sRNAs procedente del RNA ribosomal (rb-sRNAs) coincidió con lo observado en tejido vegetativo de plantas infectadas por HSVd, reforzando la estrecha relación entre la patogénesis inducida por el viroide y el metabolismo del rRNA del huésped. También es importante destacar que la sobreacumulación de sRNAs derivados de TE (te-sRNAs) se detectó en ambos tejidos, tanto vegetativo como reproductivo, sugiriendo que la alteración transcripcional inducida por el viroide es un fenómeno más general para DNAs repetitivos y no sólo está restringido al rDNA.

En línea con esta posibilidad, observamos una clara correlación entre la infección producida por el viroide y los cambios de metilación (hipometilación) del DNA en contexto simétrico, tanto para el DNA ribosomal (rDNA) como para las secuencias de TEs analizadas. Dado que los resultados parecían seguir la misma tendencia que con el tejido vegetativo, quisimos comprobar si la transcripción de estos DNAs repetitivos se encontraba también alterada en polen. Los resultados que obtuvimos evidenciaron que los transcritos derivados de TEs y los precursores de rRNA se acumulaban diferencialmente en tejido

infectado, poniendo de manifiesto que la alteración del escenario transcripcional observado en hoja, se repetía también en este tipo de tejidos reproductivos.

Al observar los granos de polen teñidos con DAPI, pudimos detectar un aumento del tamaño del núcleo generativo y del nucleolo en granos de polen infectado, un fenómeno frecuentemente asociado a la descondensación de la heterocromatina (Pečinka *et al*., 2010). Teniendo en cuenta que la heterocromatina del grano de polen está constituida principalmente por DNA repetitivo (TEs y rDNA silenciado principalmente) (Lippman *et al*., 2004), parece probable que las alteraciones en el tamaño de núcleo y nucleolo sean consecuencia de la descondensación de la heterocromatina asociada a la hipometilación de estos DNAs repetitivos. Curiosamente, se ha descrito que la descondenación de regiones centroméricas y rDNAs también ocurre en respuesta a estrés por calor (Pečinka *et al*., 2010), lo que podría sugerir la existencia de un mecanismo general de respuesta a estrés asociado a la heterocromatina. Sin embargo, quedaría aún por determinar si esta descondensación está relacionada con un aumento de las actividades metabólicas que requieren incrementos de la producción de ribosomas, ya que también observamos una mayor tasa de germinación en el polen infectado; pudiendo ser consecuencia del aumento de la actividad ribosomal.

Como ya se ha demostrado anteriormente, en tejido vegetativo, el HSVd era capaz de secuestrar física y funcionalmente a la proteína HDA6, induciendo hipometilación del DNA ribosomal, dado que HDA6 actúa como un regulador necesario para mantener la memoria epigenética del rDNA (Aufsatz *et al*., 2002; Probst *et al*., 2004; Earley *et al*., 2010; Liu *et al*., 2012; Blevins *et al*., 2014; Hristova *et al*., 2015). Por tanto, es oportuno asumir que un fenómeno similar podría ser el responsable de las alteraciones transcripcionales en polen. Sin embargo, cuando analizamos detalladamente los patrones de acumulación de rb-sRNAs en este tejido reproductivo, no fue posible detectar el aumento especifico de sRNAs de 21 nt (todos los tamaños aumentaban de manera comparable) acompañado por el descenso de sRNAs de 24 nt, previamente observado en hoja infectada. Este tipo de alteraciones de los niveles de sRNAs derivados de rRNAs o de TEs, son una marca característica de la transcripción mediada por Pol II de regiones repetitivas regulada por factores tales como DDM1 o HDA6 (Earley *et al*., 2010; McCue *et al*., 2012). Por consiguiente, nuestros resultados permitirían especular que la alteración epigenética observada, si bien es similar en ambos tejidos, (vegetativo y reproductivo), el proceso de regulación de este fenómeno podría ser diferente. En este sentido serían necesarias aproximaciones experimentales más complejas (silenciamiento selectivo de genes, por ejemplo) para intentar elucidar las bases moleculares de estas diferencias de sRNAs.

Además, sería importante determinar si los cambios epigenéticos inducidos en respuesta a la infección por HSVd, podrían tener consecuencias funcionales en la siguiente generación de plantas dado que, hasta el momento, los efectos de estrés transgeneracionales son bastante cuestionables (Pečinka y Scheid, 2012). Nuestros datos muestran una respuesta de estrés que afecta al estado de la cromatina del núcleo generativo y nucléolo, sugiriendo que estos cambios podrían ser heredables a la siguiente generación.

Como resumen, en el cuarto y último capítulo hemos podido demostrar que la infección causada por HSVd induce hipometilación en los genes ribosomales y TE en los granos de polen, proporcionando la primera descripción de alteraciones del epigenoma de células reproductoras de un huésped asociadas a la infección por patógenos.

Para concluir podríamos decir que los resultados obtenidos en la presente tesis han contribuido a poner de manifiesto una nueva visión acerca de las alteraciones funcionales del huésped inducidas como consecuencia de la infección por un viroide. Mediante el estudio de las interacciones HSVd-pepino y HSVd-*N.benthamiana* se han podido detectar cambios transcripcionales en la planta infectada debidos a fenómenos de hipometilación. Posteriormente, demostramos que este fenómeno es consecuencia de la interacción directa del genoma del viroide con la proteína HDA6, responsable del mantenimiento de la metilación de zonas repetitivas del DNA, tales como genes ribosomales o TEs. Además, esta interacción HSVd-HDA6 contribuye a aumentar el ratio de replicación del viroide ya que, este ambiente transcripcionalmente activo facilitaría el reconocimiento espurio del genoma del viroide como molde por la RNA Pol II, aumentando así su tasa de replicación. Finalmente, y gracias a la demostración de que estas alteraciones epigenéticas observadas en hoja ocurren también en células reproductivas (polen), hemos puesto de manifiesto que la alteración del mapa de metilación asociada a la infección por HSVd es un fenómeno global, no solo restringido a tejido vegetativo. Este hecho proporciona un modelo de trabajo para intentar comprender cómo la información epigenética, asociada a la repuesta a estrés, puede transmitirse a sucesivas generaciones de plantas.

CONCLUSIONES

CONCLUSIONES

En el presente trabajo de tesis se han estudiado las alteraciones a nivel transcripcional que ocurren en el huésped como consecuencia de la infección con un viroide con replicación nuclear. Para ello se han utilizado como modelos experimentales las interacciones (planta-patógeno) pepino-HSVd y *N.benthamiana*-HSVd. En ambos sistemas biológicos se observó que la infección incrementaba la actividad transcripcional de regiones repetitivas de DNA (genes ribosomales y elementos transponibles) del huésped. Mediante la secuenciación del DNA bisulfitado se determinó que esta alteración en la transcripción era consecuencia de un estado de hipometilación de regiones específicas de estos DNAs. Posteriormente se demostró que esta alteración epigenética estaba inducida por la interacción (física y funcional) entre el RNA del viroide y la HISTONA DEACETILASA 6 (HDA6) del huésped, proteína responsable del mantenimiento de la metilación de la citosina de regiones repetitivas de DNA. Además, se detectó que esta interacción proteína-viroide contribuía a aumentar el ratio de acumulación del HSVd en la planta infectada. En base a estos resultados se propuso el siguiente modelo: el RNA viroidal se uniría a la proteína HDA6 inactivándola y provocando como consecuencia un escenario de hipometilación y activación de la transcripción. En este ambiente transcripcionalmente activo la RNA Pol II reconocería como molde de forma inespecífica el RNA viroidal, aumentando el ratio de replicación del viroide y favoreciendo por tanto su infección a través de la planta.

Por último, se determinó que estas alteraciones epigenéticas, además de producirse en tejidos vegetativos, ocurrían también en el tejido reproductivo (polen) de plantas infectadas. Esta observación puso de manifiesto que la alteración transcripcional del huésped durante una infección viroidal podría constituir un fenómeno más general, susceptible de ocurrir en diferentes regiones del genoma tanto a nivel vegetativo como reproductivo.

Las principales conclusiones que se pueden extraer de este trabajo son:

1- Se han identificado RNAs endógenos de las plantas de pepino y *N. benthamiana* cuya actividad transcripcional se encuentra alterada como consecuencia de la infección con HSVd.

2- Se ha comprobado que dicha alteración está asociada a modificaciones en los patrones de metilación (hipometilación) de citosinas en regiones específicas de DNA repetitivos del huésped (DNA ribosomal y elemento transponibles).

3- Se ha demostrado que durante el proceso de infección, el HSVd es capaz de interaccionar con la proteína HISTONA DEACETILASA 6 (HDA6) del huésped, un componente celular que interviene en el mantenimiento de la metilación del DNA repetitivo, y alterar su función.

4- Se ha identificado una vía de regulación de la transcripción que se encuentra alterada como consecuencia de la infección viroidal. La inactivación funcional de HDA6, como consecuencia de la interacción con el viroide, sería la responsable del estado de hipometilación del DNA de las plantas infectadas.

5- Los resultados obtenidos han permitido proponer un modelo que explica los fenómenos de alteración transcripcional y de hipometilación observados durante la infección como consecuencia de la interacción viroide-HDA6.

6- Respecto a la eficacia biológica del viroide, hemos demostrado que la inactivación funcional de HDA6 contribuye al incremento de la replicación del patógeno.

7- Se ha comprobado que los cambios transcripcionales que ocurren en tejidos vegetativos como consecuencia de la infección por HSVd también tienen lugar en el tejido reproductivo (polen) de plantas infectadas.

BIBLIOGRAFÍA

BIBLIOGRAFIA

Abraitiene A, Zhao Y, Hammond R, 2008. Nuclear targeting by fragmentation of the potato spindle tuber viroid genome. *Biochem. Biophys. Res. Commun* **368**, 470–475.

Agorio A, Vera P, 2007. ARGONAUTE4 is required for resistance to Pseudomonas syringae in *Arabidopsis*. *Plant Cell* **19**, 3778-90.

Alba MD, Castro MA, Clarke SM, Perdigon AC, 2003. NMR study of n-dodecane adsorbed on graphite. *Solid State Nucl Magn Reson* **23**, 174-81.

Allen E, Xie Z, Gustafson AM, Carrington JC, 2005. microRNA-directed phasing during trans-acting siRNA biogenesis in plants. *Cell* **121**, 207-21.

Amari K, Gomez G, Myrta A, Di Terlizzi B, Pallas V, 2001. The molecular characterization of 16 new sequence variants of Hop stunt viroid reveals the existence of invariable regions and a conserved hammerhead-like structure on the viroid molecule. *J Gen Virol* **82**, 953-62.

Ambros S, Flores R, 1998. In vitro and in vivo self-cleavage of a viroid RNA with a mutation in the hammerhead catalytic pocket. *Nucleic Acids Res* **26**, 1877-83.

Ambros S, Hernandez C, Desvignes JC, Flores R, 1998. Genomic structure of three phenotypically different isolates of peach latent mosaic viroid: implications of the existence of constraints limiting the heterogeneity of viroid quasispecies. *J Virol* **72**, 7397-406.

Arita K, Ariyoshi M, Tochio H, Nakamura Y, Shirakawa M, 2008. Recognition of hemi-methylated DNA by the SRA protein UHRF1 by a base-flipping mechanism. *Nature* **455**, 818-21.

Astruc N, Marcos J F, Macquaire G, Candresse T y Pallas V, 1996. Studies on the diagnosis of hop stunt viroid in fruit trees: Identification of new hosts and application of a nucleic acid extraction procedure based on non-organic solvents. *Plant Pathology* **102**, 837-846.

Aufsatz W, Mette MF, Van Der Winden J, Matzke M, Matzke AJ, 2002. HDA6, a putative histone deacetylase needed to enhance DNA methylation induced by double-stranded RNA. *EMBO J* **21**, 6832-41.

Aufsatz W, Stoiber T, Rakic B, Naumann K, 2007. *Arabidopsis* histone deacetylase 6: a green link to RNA silencing. *Oncogene* **26**, 5477-88.

Aukerman MJ, Sakai H, 2003. Regulation of flowering time and floral organ identity by a MicroRNA and its APETALA2-like target genes. *Plant Cell* **15**, 2730-41.

Ausin I, Greenberg MV, Simanshu DK*, et al.*, 2012. INVOLVED IN DE NOVO 2-containing complex involved in RNA-directed DNA methylation in *Arabidopsis*. *Proc Natl Acad Sci U S A* **109**, 8374-81.

Axtell MJ, 2013. Classification and comparison of small RNAs from plants. *Annu Rev Plant Biol* **64**, 137-59.

Axtell MJ, Jan C, Rajagopalan R, Bartel DP, 2006. A two-hit trigger for siRNA biogenesis in plants. *Cell* **127**, 565-77.

Baker CC, Sieber P, Wellmer F, Meyerowitz EM, 2005. The early extra petals1 mutant uncovers a role for microRNA miR164c in regulating petal number in *Arabidopsis*. *Curr Biol* **15**, 303-15.

Bartee L, Malagnac F, Bender J, 2001. *Arabidopsis* cmt3 chromomethylase mutations block non-CG methylation and silencing of an endogenous gene. *Genes Dev* **15**, 1753-8.

Bartova E, Krejci J, Harnicarova A, Galiova G, Kozubek S, 2008. Histone modifications and nuclear architecture: a review. *J Histochem Cytochem* **56**, 711-21.

Baulcombe D, 2002. RNA silencing. *Curr Biol* **12**, R82-4.

Baulcombe D, 2004. RNA silencing in plants. *Nature* **431**, 356-63.

Baumbusch LO, Thorstensen T, Krauss V*, et al.*, 2001. The *Arabidopsis* thaliana genome contains at least 29 active genes encoding SET domain proteins that can be assigned to four evolutionarily conserved classes. *Nucleic Acids Res* **29**, 4319-33.

Berger SL, 2007. The complex language of chromatin regulation during transcription. *Nature* **447**, 407-12.

Bernatavichute YV, Zhang X, Cokus S, Pellegrini M, Jacobsen SE, 2008. Genome-wide association of histone H3 lysine nine methylation with CHG DNA methylation in *Arabidopsis* thaliana. *PLoS One* **3**, e3156.

Bernstein E, Caudy AA, Hammond SM, Hannon GJ, 2001. Role for a bidentate ribonuclease in the initiation step of RNA interference. *Nature* **409**, 363-6.

Bies-Etheve N, Pontier D, Lahmy S*, et al.*, 2009. RNA-directed DNA methylation requires an AGO4-interacting member of the SPT5 elongation factor family. *EMBO Rep* **10**, 649-54.

Blevins T, Pontvianne F, Cocklin R*, et al.*, 2014. A two-step process for epigenetic inheritance in *Arabidopsis*. *Mol Cell* **54**, 30-42.

Bojic T, Beeharry Y, Zhang DJ, Pelchat M, 2012. Tomato RNA polymerase II interacts with the rod-like conformation of the left terminal domain of the potato spindle tuber viroid positive RNA genome. *J Gen Virol* **93**, 1591-600.

Bolduc F, Hoareau C, St-Pierre P, Perreault JP, 2010. In-depth sequencing of the siRNAs associated with peach latent mosaic viroid infection. *BMC Mol Biol* **11**, 16.

Bollman KM, Aukerman MJ, Park MY, Hunter C, Berardini TZ, Poethig RS, 2003. HASTY, the *Arabidopsis* ortholog of exportin 5/MSN5, regulates phase change and morphogenesis. *Development* **130**, 1493-504.

Bonfiglioli R, Webb D, Symons R**,** 1996. Tissue and intra-cellular distribution of coconut cadang cadang viroid and citrus exocortis viroid determined by in situ hybridization and confocal laser scanning and transmission electron microscopy. *Plant Journal* **9**, 457-465.

Borsani O, Zhu J, Verslues PE, Sunkar R, Zhu JK, 2005. Endogenous siRNAs derived from a pair of natural cis-antisense transcripts regulate salt tolerance in *Arabidopsis*. *Cell* **123**, 1279-91.

Boyko A, Blevins T, Yao Y*, et al.*, 2010. Transgenerational adaptation of *Arabidopsis* to stress requires DNA methylation and the function of Dicer-like proteins. *PLoS One* **5**, e9514.

Boyko A, Kathiria P, Zemp FJ, Yao Y, Pogribny I, Kovalchuk I, 2007. Transgenerational changes in the genome stability and methylation in pathogen-infected plants: (virus-induced plant genome instability). *Nucleic Acids Res* **35**, 1714-25.

Branch AD, Dickson E, 1980. Tomato DNA contains no detectable regions complementary to potato spindle tuber viroid as assayed by Southern hybridization. *Virology* **104**, 10-26.

Branch AD, Robertson HD, 1984. A replication cycle for viroids and other small infectious RNA's. *Science* **223**, 450-5.

Brodersen P, Sakvarelidze-Achard L, Bruun-Rasmussen M*, et al.*, 2008. Widespread translational inhibition by plant miRNAs and siRNAs. *Science* **320**, 1185-90.

Brodersen P, Voinnet O, 2006. The diversity of RNA silencing pathways in plants. *Trends Genet* **22**, 268-80.

Bussiere F, Ouellet J, Cote F, Levesque D, Perreault JP, 2000. Mapping in solution shows the peach latent mosaic viroid to possess a new pseudoknot in a complex, branched secondary structure. *J Virol* **74**, 2647-54.

Cañizares MC, Marcos JF y Pallás V ,1999. Molecular Characterization of an Almond Isolate of Hop Stunt Viroid (HSVd) and Conditions for Eliminating Spurious Hybridization in its Diagnosis in Almond Samples. *Plant Pathology* **105**,553-558.

Cao X, Aufsatz W, Zilberman D*, et al.*, 2003. Role of the DRM and CMT3 methyltransferases in RNA-directed DNA methylation. *Curr Biol* **13**, 2212-7.

Castel SE, Martienssen RA, 2013. RNA interference in the nucleus: roles for small RNAs in transcription, epigenetics and beyond. *Nat Rev Genet* **14**, 100-12.

Chan SW, Henderson IR, Jacobsen SE, 2005. Gardening the genome: DNA methylation in *Arabidopsis* thaliana. *Nat Rev Genet* **6**, 351-60.

Chan SW, Henderson IR, Zhang X, Shah G, Chien JS, Jacobsen SE, 2006. RNAi, DRD1, and histone methylation actively target developmentally important non-CG DNA methylation in *Arabidopsis*. *PLoS Genet* **2**, e83.
Chapman EJ, Carrington JC, 2007. Specialization and evolution of endogenous small RNA pathways. *Nat Rev Genet* **8**, 884-96.
Chen M, Lv S, Meng Y, 2010. Epigenetic performers in plants. *Dev Growth Differ* **52**, 555-66.
Chen X, 2004. A microRNA as a translational repressor of APETALA2 in *Arabidopsis* flower development. *Science* **303**, 2022-5.
Chen X, 2005. MicroRNA biogenesis and function in plants. *FEBS Lett* **579**, 5923-31.
Chen X, 2009. Small RNAs and their roles in plant development. *Annu Rev Cell Dev Biol* **25**, 21-44.
Chodavarapu RK, Feng S, Bernatavichute YV*, et al.*, 2010. Relationship between nucleosome positioning and DNA methylation. *Nature* **466**, 388-92.
Choi CS, Sano H, 2007. Abiotic-stress induces demethylation and transcriptional activation of a gene encoding a glycerophosphodiesterase-like protein in tobacco plants. *Mol Genet Genomics* **277**, 589-600.
Cigliano RA, Cremona G, Paparo R*, et al.*, 2013. Histone deacetylase AtHDA7 is required for female gametophyte and embryo development in *Arabidopsis*. *Plant Physiol* **163**, 431-40.
Cloos PA, Christensen J, Agger K, Helin K, 2008. Erasing the methyl mark: histone demethylases at the center of cellular differentiation and disease. *Genes Dev* **22**, 1115-40.
Cox KH y Golberg RB, 1988. Analysis of plant gene expression. *Plant Molecular Biology: A Practical Approach*(C. H. Shaw Ed.) 1-35.
Dagdemir A, Durif J, Ngollo M, Bignon YJ, Bernard-Gallon D, 2013. Histone lysine trimethylation or acetylation can be modulated by phytoestrogen, estrogen or anti-HDAC in breast cancer cell lines. *Epigenomics* **5**, 51-63.
Daros JA, Elena SF, Flores R, 2006. Viroids: an AriDNAe's thread into the RNA labyrinth. *EMBO Rep* **7**, 593-8.
Daros JA, Marcos JF, Hernandez C, Flores R, 1994. Replication of avocado sunblotch viroid: evidence for a symmetric pathway with two rolling circles and hammerhead ribozyme processing. *Proc Natl Acad Sci U S A* **91**, 12813-7.
Denti MA, Boutla A, Tsagris M, Tabler M, 2004. Short interfering RNAs specific for potato spindle tuber viroid are found in the cytoplasm but not in the nucleus. *Plant J* **37**, 762-9.
Di Serio F, Gisel A, Navarro B*, et al.*, 2009. Deep sequencing of the small RNAs derived from two symptomatic variants of a chloroplastic viroid: implications for their genesis and for pathogenesis. *PLoS One* **4**, e7539.
Di Serio F, Martinez De Alba AE, Navarro B, Gisel A, Flores R, 2010. RNA-dependent RNA polymerase 6 delays accumulation and precludes meristem invasion of a viroid that replicates in the nucleus. *J Virol* **84**, 2477-89.
Diener TO, 1972. Potato spindle tuber viroid. 8. Correlation of infectivity with a UV-absorbing component and thermal denaturation properties of the RNA. *Virology* **50**, 606-9.
Diener TO, Smith DR, Hammond RH, Albanese G, Larosa R y Davino M, 1988. Citrus-B viroid identified as a strain of hop stunt viroid. *Plant Disease* **72**,691-693
Diener TO, 1981. Are viroids escaped introns? *Proc Natl Acad Sci U S A* **78**, 5014-5.
Diener TO, 1989. Circular RNAs: relics of precellular evolution? *Proc Natl Acad Sci U S A* **86**, 9370-4.
Diener TO, 2001. The viroid: biological oddity or evolutionary fossil? *Adv Virus Res* **57**, 137-84.
Diener TO, 2003. Discovering viroids--a personal perspective. *Nat Rev Microbiol* **1**, 75-80.
Diener TO, 2016. Viroids: "living fossils" of primordial RNAs? *Biol Direct* **11**, 15.
Diener TO, Smith DR, 1971. Potato spindle tuber viroid. VI. Monodisperse distribution after electrophoresis in 20 per cent polyacrylamide gels. *Virology* **46**, 498-9.
Ding B, 2009. The biology of viroid-host interactions. *Annu Rev Phytopathol* **47**, 105-31.

Ding B, 2010. Viroids: self-replicating, mobile, and fast-evolving noncoding regulatory RNAs. *Wiley Interdiscip Rev RNA* **1**, 362-75.
Ding B, Itaya A, 2007. Viroid: a useful model for studying the basic principles of infection and RNA biology. *Mol Plant Microbe Interact* **20**, 7-20.
Ding B, Itaya A, Zhong X, 2005. Viroid trafficking: a small RNA makes a big move. *Curr Opin Plant Biol* **8**, 606-12.
Ding Y, Wang X, Su L*, et al.*, 2007. SDG714, a histone H3K9 methyltransferase, is involved in Tos17 DNA methylation and transposition in rice. *Plant Cell* **19**, 9-22.
Ding B, Kwon M.O, Hammond R, Owens R, 1997. Cell-to-cell movement of potato spindle tuber viroid. *Plant J*. **12**, 931-936.
Ding B, Wang Y, 2009. Viroids: uniquely simple and tractable models to elucidate regulation of cell-to-cell trafficking of RNAs. *DNA and Cell Biol*. **28**, 51-56.
Dowen RH, Pelizzola M, Schmitz RJ*, et al.*, 2012. Widespread dynamic DNA methylation in response to biotic stress. *Proc Natl Acad Sci U S A* **109**, E2183-91.
Earley K, Lawrence RJ, Pontes O*, et al.*, 2006. Erasure of histone acetylation by *Arabidopsis* HDA6 mediates large-scale gene silencing in nucleolar dominance. *Genes Dev* **20**, 1283-93.
Earley KW, Pontvianne F, Wierzbicki AT*, et al.*, 2010. Mechanisms of HDA6-mediated rRNA gene silencing: suppression of intergenic Pol II transcription and differential effects on maintenance versus siRNA-directed cytosine methylation. *Genes Dev* **24**, 1119-32.
Ebbs ML, Bender J, 2006. Locus-specific control of DNA methylation by the *Arabidopsis* SUVH5 histone methyltransferase. *Plant Cell* **18**, 1166-76.
Elbashir SM, Lendeckel W, Tuschl T, 2001a. RNA interference is mediated by 21- and 22-nucleotide RNAs. *Genes Dev* **15**, 188-200.
Elbashir SM, Martinez J, Patkaniowska A, Lendeckel W, Tuschl T, 2001b. Functional anatomy of siRNAs for mediating efficient RNAi in Drosophila melanogaster embryo lysate. *EMBO J* **20**, 6877-88.
Elena SF, Gomez G, Daros JA, 2009. Evolutionary constraints to viroid evolution. *Viruses* **1**, 241-54.
Engels WR, Johnson-Schlitz DM, Eggleston WB, Sved J, 1990. High-frequency P element loss in Drosophila is homolog dependent. *Cell* **62**, 515-25.
Enke RA, Dong Z, Bender J, 2011. Small RNAs prevent transcription-coupled loss of histone H3 lysine 9 methylation in *Arabidopsis* thaliana. *PLoS Genet* **7**, e1002350.
Eun C, Lorkovic ZJ, Sasaki T, Naumann U, Matzke AJ, Matzke M, 2012. Use of forward genetic screens to identify genes required for RNA-directed DNA methylation in *Arabidopsis* thaliana. *Cold Spring Harb Symp Quant Biol* **77**, 195-204.
Fadda Z, Daros JA, Fagoaga C, Flores R, Duran-Vila N, 2003. Eggplant latent viroid, the candidate type species for a new genus within the family Avsunviroidae (hammerhead viroids). *J Virol* **77**, 6528-32.
Fahlgren N, Howell MD, Kasschau KD*, et al.*, 2007. High-throughput sequencing of *Arabidopsis* microRNAs: evidence for frequent birth and death of MIRNA genes. *PLoS One* **2**, e219.
Feil R, Fraga MF, 2011. Epigenetics and the environment: emerging patterns and implications. *Nat Rev Genet* **13**, 97-109.
Finke A, Kuhlmann M, Mette MF, 2012. IDN2 has a role downstream of siRNA formation in RNA-directed DNA methylation. *Epigenetics* **7**, 950-60.
Fiore N , Zamorano A , Sánchez-Diana N , González X , Pallás V, Sánchez-Navarro J, 2016. First detection of Grapevine rupestris stem pitting-associated virus and Grapevine rupestris vein feathering virus, and new phylogenetic groups for Grapevine fleck virus and Hop stunt viroid isolates, revealed from grapevine field surveys in Spain. *Phytopathologia Mediterranea* **2**, 225−238.
Fire A, Xu S, Montgomery MK, Kostas SA, Driver SE, Mello CC, 1998. Potent and specific genetic interference by double-stranded RNA in Caenorhabditis elegans. *Nature* **391**, 806-11.
Flores R, Delgado S, Gas ME*, et al.*, 2004. Viroids: the minimal non-coding RNAs with autonomous replication. *FEBS Lett* **567**, 42-8.

Flores R, Gago-Zachert S, Serra P, Sanjuan R, Elena SF, 2014. Viroids: survivors from the RNA world? *Annu Rev Microbiol* **68**, 395-414.
Flores R, Hernandez C, Martinez De Alba AE, Daros JA, Di Serio F, 2005. Viroids and viroid-host interactions. *Annu Rev Phytopathol* **43**, 117-39.
Flores R, Minoia S, Carbonell A*, et al.*, 2015. Viroids, the simplest RNA replicons: How they manipulate their hosts for being propagated and how their hosts react for containing the infection. *Virus Res* **209**, 136-45.
Flores R, Semancik JS, 1982. Properties of a cell-free system for synthesis of citrus exocortis viroid. *Proc Natl Acad Sci U S A* **79**, 6285-8.
Furner IJ, Sheikh MA, Collett CE, 1998. Gene silencing and homology-dependent gene silencing in *Arabidopsis*: genetic modifiers and DNA methylation. *Genetics* **149**, 651-62.
Gago-Zachert S, 2016. Viroids, infectious long non-coding RNAs with autonomous replication. *Virus Res* **212**, 12-24.
Gao Z, Liu HL, Daxinger L*, et al.*, 2010. An RNA polymerase II- and AGO4-associated protein acts in RNA-directed DNA methylation. *Nature* **465**, 106-9.
Gas ME, Hernandez C, Flores R, Daros JA, 2007. Processing of nuclear viroids in vivo: an interplay between RNA conformations. *PLoS Pathog* **3**, e182.
Gomez G, Martinez G, Pallas V, 2008. Viroid-induced symptoms in Nicotiana benthamiana plants are dependent on RDR6 activity. *Plant Physiol* **148**, 414-23.
Gomez G, Martinez G, Pallas V, 2009. Interplay between viroid-induced pathogenesis and RNA silencing pathways. *Trends Plant Sci* **14**, 264-9.
Gomez G, Pallas V, 2006. Hop Stunt Viroid is processed and translocated in Nicotiana benthamiana plants. *Molecular Plant Pathology* **7**, 511-7.
Gomez G, Pallas V, 2007. Mature monomeric forms of Hop stunt viroid resist RNA silencing in transgenic plants. *Plant J* **51**, 1041-9.
Gómez G, Pallás V, 2012a. Studies on subcellular compartmentalization of plant pathogenic non coding RNAs give new insights into the intracellular RNA-traffic mechanisms. *Plant Physiol*. **159**, 558–564.
Gomez G, Pallas V, 2013. Viroids: a light in the darkness of the lncRNA-directed regulatory networks in plants. *New Phytol* **198**, 10-5.
Goodman TC, Nagel L, Rappold W, Klotz G, Riesner D, 1984. Viroid replication: equilibrium association constant and comparative activity measurements for the viroid-polymerase interaction. *Nucleic Acids Res* **12**, 6231-46.
Gora-Sochacka A, 2004. Viroids: unusual small pathogenic RNAs. *Acta Biochim Pol* **51**, 587-607.
Grativol C, Hemerly AS, Ferreira PC, 2012. Genetic and epigenetic regulation of stress responses in natural plant populations. *Biochim Biophys Acta* **1819**, 176-85.
Gross HJ, Domdey H, Lossow C*, et al.*, 1978. Nucleotide sequence and secondary structure of potato spindle tuber viroid. *Nature* **273**, 203-8.
Guo H, Ingolia NT, Weissman JS, Bartel DP, 2010. Mammalian microRNAs predominantly act to decrease target mRNA levels. *Nature* **466**, 835-40.
Guo HS, Xie Q, Fei JF, Chua NH, 2005. MicroRNA directs mRNA cleavage of the transcription factor NAC1 to downregulate auxin signals for *Arabidopsis* lateral root development. *Plant Cell* **17**, 1376-86.
Haag JR, Pikaard CS, 2011. Multisubunit RNA polymerases IV and V: purveyors of non-coding RNA for plant gene silencing. *Nat Rev Mol Cell Biol* **12**, 483-92.
Haag JR, Ream TS, Marasco M*, et al.*, 2012. In vitro transcription activities of Pol IV, Pol V, and RDR2 reveal coupling of Pol IV and RDR2 for dsRNA synthesis in plant RNA silencing. *Mol Cell* **48**, 811-8.
Hamilton A, Voinnet O, Chappell L, Baulcombe D, 2002. Two classes of short interfering RNA in RNA silencing. *EMBO J* **21**, 4671-9.

Hamilton AJ, Baulcombe DC, 1999. A species of small antisense RNA in posttranscriptional gene silencing in plants. *Science* **286**, 950-2.

Hammond SM, Bernstein E, Beach D, Hannon GJ, 2000. An RNA-directed nuclease mediates post-transcriptional gene silencing in Drosophila cells. *Nature* **404**, 293-6.
Hammond SM, Caudy AA, Hannon GJ, 2001. Post-transcriptional gene silencing by double-stranded RNA. *Nat Rev Genet* **2**, 110-9.
Harders J, Lukacs N, Robert-Nicoud M, Jovin TM, Riesner D, 1989. Imaging of viroids in nuclei from tomato leaf tissue by in situ hybridization and confocal laser scanning microscopy. *EMBO J* **8**, 3941-9.
He XJ, Chen T, Zhu JK, 2011. Regulation and function of DNA methylation in plants and animals. *Cell Res* **21**, 442-65.
He XJ, Hsu YF, Zhu S*, et al.*, 2009. A conserved transcriptional regulator is required for RNA-directed DNA methylation and plant development. *Genes Dev* **23**, 2717-22.
Herr AJ, Baulcombe DC, 2004. RNA silencing pathways in plants. *Cold Spring Harb Symp Quant Biol* **69**, 363-70.
Herr AJ, Jensen MB, Dalmay T, Baulcombe DC, 2005. RNA polymerase IV directs silencing of endogenous DNA. *Science* **308**, 118-20.
Herranz MC, Niehl A, Rosales M*, et al.*, 2013. A remarkable synergistic effect at the transcriptomic level in peach fruits doubly infected by prunus necrotic ringspot virus and peach latent mosaic viroid. *Virol J* **10**, 164.
Hristova E, Fal K, Klemme L, Windels D, Bucher E, 2015. HISTONE DEACETYLASE6 Controls Gene Expression Patterning and DNA Methylation-Independent Euchromatic Silencing. *Plant Physiol* **168**, 1298-308.
Hsieh TF, Ibarra CA, Silva P*, et al.*, 2009. Genome-wide demethylation of *Arabidopsis* endosperm. *Science* **324**, 1451-4.
Hsu YH, Chen W, Owens RA, 1995. Nucleotide sequence of a hop stunt viroid variant isolated from citrus growing in Taiwan. *Virus Genes* **9**, 193-5.
Huh WK, Song YB, Lee YS, Ha CW, Kim ST, Kang SO, 2008. D-Erythroascorbic acid activates cyanide-resistant respiration in Candida albicans. *Biochem Biophys Res Commun* **369**, 401-6.
Hwang JJ, Kim YS, Kim MJ*, et al.*, 2009. A novel histone deacetylase inhibitor, CG0006, induces cell death through both extrinsic and intrinsic apoptotic pathways. *Anticancer Drugs* **20**, 815-21.
Itaya A, Folimonov A, Matsuda Y, Nelson RS, Ding B, 2001. Potato spindle tuber viroid as inducer of RNA silencing in infected tomato. *Mol Plant Microbe Interact* **14**, 1332-4.
Itaya A, Matsuda Y, Gonzales RA, Nelson RS, Ding B, 2002. Potato spindle tuber viroid strains of different pathogenicity induces and suppresses expression of common and unique genes in infected tomato. *Mol Plant Microbe Interact* **15**, 990-9.
Itaya A, Zhong X, Bundschuh R*, et al.*, 2007. A structured viroid RNA serves as a substrate for dicer-like cleavage to produce biologically active small RNAs but is resistant to RNA-induced silencing complex-mediated degradation. *J Virol* **81**, 2980-94.
Ito H, Gaubert H, Bucher E, Mirouze M, Vaillant I, Paszkowski J, 2011. An siRNA pathway prevents transgenerational retrotransposition in plants subjected to stress. *Nature* **472**, 115-9.
Jackson JP, Lindroth AM, Cao X, Jacobsen SE, 2002. Control of CpNpG DNA methylation by the KRYPTONITE histone H3 methyltransferase. *Nature* **416**, 556-60.
Jamalkandi SA, Masoudi-Nejad A, 2009. Reconstruction of *Arabidopsis* thaliana fully integrated small RNA pathway. *Funct Integr Genomics* **9**, 419-32.
Ji L, Chen X, 2012. Regulation of small RNA stability: methylation and beyond. *Cell Res* **22**, 624-36.
Jin H, Vacic V, Girke T, Lonardi S, Zhu JK, 2008. Small RNAs and the regulation of cis-natural antisense transcripts in *Arabidopsis*. *BMC Mol Biol* **9**, 6.
Jirtle RL, Skinner MK, 2007. Environmental epigenomics and disease susceptibility. *Nat Rev Genet* **8**, 253-62.

Johnson LM, Bostick M, Zhang X*, et al.*, 2007. The SRA methyl-cytosine-binding domain links DNA and histone methylation. *Curr Biol* **17**, 379-84.
Johnson MD, Mueller M, Game L, Aitman TJ, 2012. Single nucleotide analysis of cytosine methylation by whole-genome shotgun bisulfite sequencing. *Curr Protoc Mol Biol* **Chapter 21**, Unit21 3.
Jones-Rhoades MW, Bartel DP, Bartel B, 2006. MicroRNAS and their regulatory roles in plants. *Annu Rev Plant Biol* **57**, 19-53.
Juarez MT, Kui JS, Thomas J, Heller BA, Timmermans MC, 2004a. microRNA-mediated repression of rolled leaf1 specifies maize leaf polarity. *Nature* **428**, 84-8.
Juarez MT, Twigg RW, Timmermans MC, 2004b. Specification of adaxial cell fate during maize leaf development. *Development* **131**, 4533-44.
Kanno T, Bucher E, Daxinger L*, et al.*, 2010. RNA-directed DNA methylation and plant development require an IWR1-type transcription factor. *EMBO Rep* **11**, 65-71.
Kanno T, Habu Y, 2011. siRNA-mediated chromatin maintenance and its function in *Arabidopsis* thaliana. *Biochim Biophys Acta* **1809**, 444-51.
Kanno T, Huettel B, Mette MF*, et al.*, 2005. Atypical RNA polymerase subunits required for RNA-directed DNA methylation. *Nat Genet* **37**, 761-5.
Kasschau KD, Fahlgren N, Chapman EJ*, et al.*, 2007. Genome-wide profiling and analysis of *Arabidopsis* siRNAs. *PLoS Biol* **5**, e57.
Katsarou K, Rao AL, Tsagris M, Kalantidis K, 2015. Infectious long non-coding RNAs. *Biochimie* **117**, 37-47.
Keese P, Symons RH, 1985. Domains in viroids: evidence of intermolecular RNA rearrangements and their contribution to viroid evolution. *Proc Natl Acad Sci U S A* **82**, 4582-6.
Kidner CA, Martienssen RA, 2003. Macro effects of microRNAs in plants. *Trends Genet* **19**, 13-6.
Kim JM, To TK, Seki M, 2012. An epigenetic integrator: new insights into genome regulation, environmental stress responses and developmental controls by histone deacetylase 6. *Plant Cell Physiol* **53**, 794-800.
Kofalvi SA, Marcos JF, Canizares MC, Pallas V, Candresse T, 1997. Hop stunt viroid (HSVd) sequence variants from Prunus species: evidence for recombination between HSVd isolates. *J Gen Virol* **78**, 3177-86.
Kovalskaya N, Hammond RW, 2014. Molecular biology of viroid-host interactions and disease control strategies. *Plant Sci* **228**, 48-60.
Kurihara Y, Takashi Y, Watanabe Y, 2006. The interaction between DCL1 and HYL1 is important for efficient and precise processing of pri-miRNA in plant microRNA biogenesis. *RNA* **12**, 206-12.
Kurihara Y, Watanabe Y, 2004. *Arabidopsis* micro-RNA biogenesis through Dicer-like 1 protein functions. *Proc Natl Acad Sci U S A* **101**, 12753-8.
Law JA, Ausin I, Johnson LM*, et al.*, 2010. A protein complex required for polymerase V transcripts and RNA- directed DNA methylation in *Arabidopsis*. *Curr Biol* **20**, 951-6.
Law JA, Jacobsen SE, 2010. Establishing, maintaining and modifying DNA methylation patterns in plants and animals. *Nat Rev Genet* **11**, 204-20.
Law JA, Vashisht AA, Wohlschlegel JA, Jacobsen SE, 2011. SHH1, a homeodomain protein required for DNA methylation, as well as RDR2, RDM4, and chromatin remodeling factors, associate with RNA polymerase IV. *PLoS Genet* **7**, e1002195.
Lee TF, Gurazada SG, Zhai J*, et al.*, 2012. RNA polymerase V-dependent small RNAs in *Arabidopsis* originate from small, intergenic loci including most SINE repeats. *Epigenetics* **7**, 781-95.
Lee Y, Kim M, Han J*, et al.*, 2004. MicroRNA genes are transcribed by RNA polymerase II. *EMBO J* **23**, 4051-60.
Lelandais-Briere C, Naya L, Sallet E*, et al.*, 2009. Genome-wide Medicago truncatula small RNA analysis revealed novel microRNAs and isoforms differentially regulated in roots and nodules. *Plant Cell* **21**, 2780-96.

Li C, Xu J, Li J, Li Q, Yang H, 2014. Involvement of *Arabidopsis* histone acetyltransferase HAC family genes in the ethylene signaling pathway. *Plant Cell Physiol* **55**, 426-35.
Li L, Liu Y, 2011. Diverse small non-coding RNAs in RNA interference pathways. *Methods Mol Biol* **764**, 169-82.
Li YF, Zheng Y, Jagadeeswaran G, Sunkar R, 2013. Characterization of small RNAs and their target genes in wheat seedlings using sequencing-based approaches. *Plant Sci* **203-204**, 17-24.
Lima MI, Fonseca ME, Flores R, Kitajima EW, 1994. Detection of avocado sunblotch viroid in chloroplasts of avocado leaves by in situ hybridization. *Arch Virol* **138**, 385-90.
Lindroth AM, Cao X, Jackson JP*, et al.*, 2001. Requirement of CHROMOMETHYLASE3 for maintenance of CpXpG methylation. *Science* **292**, 2077-80.
Lindroth AM, Shultis D, Jasencakova Z*, et al.*, 2004. Dual histone H3 methylation marks at lysines 9 and 27 required for interaction with CHROMOMETHYLASE3. *EMBO J* **23**, 4286-96.
Lippman Z, Gendrel AV, Black M*, et al.*, 2004. Role of transposable elements in heterochromatin and epigenetic control. *Nature* **430**, 471-6.
Lippman Z, Martienssen R, 2004. The role of RNA interference in heterochromatic silencing. *Nature* **431**, 364-70.
Lisch D, 2009. Epigenetic regulation of transposable elements in plants. *Annu Rev Plant Biol* **60**, 43-66.
Lison P, Tarraga S, Lopez-Gresa P*, et al.*, 2013. A noncoding plant pathogen provokes both transcriptional and posttranscriptional alterations in tomato. *Proteomics* **13**, 833-44.
Lister R, O'malley RC, Tonti-Filippini J*, et al.*, 2008. Highly integrated single-base resolution maps of the epigenome in *Arabidopsis*. *Cell* **133**, 523-36.
Liu B, Tabler M, Tsagris M, 2000. Episomal expression of a hammerhead ribozyme directed against plum pox virus. *Virus Res* **68**, 15-23.
Liu C, Lu F, Cui X, Cao X, 2010. Histone methylation in higher plants. *Annu Rev Plant Biol* **61**, 395-420.
Liu S, Yeh CT, Ji T*, et al.*, 2009. Mu transposon insertion sites and meiotic recombination events co-localize with epigenetic marks for open chromatin across the maize genome. *PLoS Genet* **5**, e1000733.
Liu X, Hao L, Li D, Zhu L, Hu S, 2015. Long non-coding RNAs and their biological roles in plants. *Genomics Proteomics Bioinformatics* **13**, 137-47.
Liu X, Luo M, Wu K, 2012a. Epigenetic interplay of histone modifications and DNA methylation mediated by HDA6. *Plant Signal Behav* **7**, 633-5.
Liu X, Yu CW, Duan J*, et al.*, 2012b. HDA6 directly interacts with DNA methyltransferase MET1 and maintains transposable element silencing in *Arabidopsis*. *Plant Physiol* **158**, 119-29.
Liu YX, Wang M, Wang XJ, 2014a. Endogenous small RNA clusters in plants. *Genomics Proteomics Bioinformatics* **12**, 64-71.
Liu ZW, Shao CR, Zhang CJ*, et al.*, 2014b. The SET domain proteins SUVH2 and SUVH9 are required for Pol V occupancy at RNA-directed DNA methylation loci. *PLoS Genet* **10**, e1003948.
Lobbes D, Rallapalli G, Schmidt DD, Martin C, Clarke J, 2006. SERRATE: a new player on the plant microRNA scene. *EMBO Rep* **7**, 1052-8.
Long JA, Ohno C, Smith ZR, Meyerowitz EM, 2006. TOPLESS regulates apical embryonic fate in *Arabidopsis*. *Science* **312**, 1520-3.
Lopez A, Ramirez V, Garcia-Andrade J, Flors V, Vera P, 2011. The RNA silencing enzyme RNA polymerase v is required for plant immunity. *PLoS Genet* **7**, e1002434.
Lu C, Tej SS, Luo S, Haudenschild CD, Meyers BC, Green PJ, 2005. Elucidation of the small RNA component of the transcriptome. *Science* **309**, 1567-9.
Luna E, Ton J, 2012. The epigenetic machinery controlling transgenerational systemic acquired resistance. *Plant Signal Behav* **7**, 615-8.
Luo M, Liu X, Singh P, Cui Y, Zimmerli L, Wu K, 2012. Chromatin modifications and remodeling in plant abiotic stress responses. *Biochim Biophys Acta* **1819**, 129-36.

Llave C, 2010. Virus-derived small interfering RNAs at the core of plant-virus interactions. *Trends Plant Sci* **15**, 701-7.

Machida S, Yamahata N, Watanuki H, Owens RA, Sano T, 2007. Successive accumulation of two size classes of viroid-specific small RNA in potato spindle tuber viroid-infected tomato plants. *J Gen Virol* **88**, 3452-7.

Malagnac F, Bartee L, Bender J, 2002. An *Arabidopsis* SET domain protein required for maintenance but not establishment of DNA methylation. *EMBO J* **21**, 6842-52.

Markarian N, Li HW, Ding SW, Semancik JS, 2004. RNA silencing as related to viroid induced symptom expression. *Arch Virol* **149**, 397-406.

Martin R, Arenas C, Daros JA, Covarrubias A, Reyes JL, Chua NH, 2007. Characterization of small RNAs derived from Citrus exocortis viroid (CEVd) in infected tomato plants. *Virology* **367**, 135-46.

Martinez De Alba AE, Flores R, Hernandez C, 2002. Two chloroplastic viroids induce the accumulation of small RNAs associated with posttranscriptional gene silencing. *J Virol* **76**, 13094-6.

Martínez de Alba AE, Sägesser R, Tabler M, Tsagris M, 2003. A bromodomain-containing protein from tomato specifically binds potato spindle tuber viroid RNA in vitro and in vivo. *J. Virol* **77**, 9685–9694**.**

Martinez G, Donaire L, Llave C, Pallas V, Gomez G, 2010. High-throughput sequencing of Hop stunt viroid-derived small RNAs from cucumber leaves and phloem. *Mol Plant Pathol* **11**, 347-59.

Marzluff WF, Huang RC,1984. Transcription of RNA in isolated nuclei. *Transcription and translation: A practical approach* (B. D. Hames y S. J. Higgins Eds.) 89-129.

Matzke MA, Birchler JA, 2005. RNAi-mediated pathways in the nucleus. *Nat Rev Genet* **6**, 24-35.

May BP, Lippman ZB, Fang Y, Spector DL, Martienssen RA, 2005. Differential regulation of strand-specific transcripts from *Arabidopsis* centromeric satellite repeats. *PLoS Genet* **1**, e79.

Mc CB, 1950. The origin and behavior of mutable loci in maize. *Proc Natl Acad Sci U S A* **36**, 344-55.

Mccue AD, Nuthikattu S, Reeder SH, Slotkin RK, 2012. Gene expression and stress response mediated by the epigenetic regulation of a transposable element small RNA. *PLoS Genet* **8**, e1002474.

Meyers BC, Axtell MJ, Bartel B*, et al.*, 2008. Criteria for annotation of plant MicroRNAs. *Plant Cell* **20**, 3186-90.

Mlotshwa S, Pruss GJ, Vance V, 2008. Small RNAs in viral infection and host defense. *Trends Plant Sci* **13**, 375-82.

Mohamed N-A., Thomas W, 1980. Viroid-like properties of an RNA species associated with the sunblotch disease of avocado. *J Gen Virol*, **46**,157-67.

Molnar A, Csorba T, Lakatos L, Varallyay E, Lacomme C, Burgyan J, 2005. Plant virus-derived small interfering RNAs originate predominantly from highly structured single-stranded viral RNAs. *J Virol* **79**, 7812-8.

Morgan DK, Whitelaw E, 2008. The case for transgenerational epigenetic inheritance in humans. *Mamm Genome* **19**, 394-7.

Mosher RA, Schwach F, Studholme D, Baulcombe DC, 2008. PolIVb influences RNA-directed DNA methylation independently of its role in siRNA biogenesis. *Proc Natl Acad Sci U S A* **105**, 3145-50.

Muhlbach HP, Sanger HL, 1979. Viroid replication is inhibited by alpha-amanitin. *Nature* **278**, 185-8.

Murcia N, Bernad L, Duran-Vila N, Serra P, 2011. Two nucleotide positions in the Citrus exocortis viroid RNA associated with symptom expression in Etrog citron but not in experimental herbaceous hosts. *Mol Plant Pathol* **12**, 203-8.

Murfett J, Wang XJ, Hagen G, Guilfoyle TJ, 2001. Identification of *Arabidopsis* histone deacetylase HDA6 mutants that affect transgene expression. *Plant Cell* **13**, 1047-61.

Navarro B, Flores R, 1997. Chrysanthemum chlorotic mottle viroid: unusual structural properties of a subgroup of self-cleaving viroids with hammerhead ribozymes. *Proc Natl Acad Sci U S A* **94**, 11262-7.

Navarro B, Gisel A, Rodio ME, Delgado S, Flores R, Di Serio F, 2012. Viroids: how to infect a host and cause disease without encoding proteins. *Biochimie* **94**, 1474-80.

Navarro B, Pantaleo V, Gisel A*, et al.*, 2009. Deep sequencing of viroid-derived small RNAs from grapevine provides new insights on the role of RNA silencing in plant-viroid interaction. *PLoS One* **4**, e7686.
Navarro JA, Daros JA, Flores R, 1999. Complexes containing both polarity strands of avocado sunblotch viroid: identification in chloroplasts and characterization. *Virology* **253**, 77-85.
Navarro JA, Vera A, Flores R, 2000. A chloroplastic RNA polymerase resistant to tagetitoxin is involved in replication of avocado sunblotch viroid. *Virology* **268**, 218-25.
Nguyen HN, Kim JH, Jeong CY, Hong SW, Lee H, 2013. Inhibition of histone deacetylation alters *Arabidopsis* root growth in response to auxin via PIN1 degradation. *Plant Cell Rep* **32**, 1625-36.
Nohales MA, Flores R, Daros JA, 2012a. Viroid RNA redirects host DNA ligase 1 to act as an RNA ligase. *Proc Natl Acad Sci U S A* **109**, 13805-10.
Nohales MA, Molina-Serrano D, Flores R, Daros JA, 2012b. Involvement of the chloroplastic isoform of tRNA ligase in the replication of viroids belonging to the family Avsunviroidae. *J Virol* **86**, 8269-76.
Onodera Y, Haag JR, Ream T, Costa Nunes P, Pontes O, Pikaard CS, 2005. Plant nuclear RNA polymerase IV mediates siRNA and DNA methylation-dependent heterochromatin formation. *Cell* **120**, 613-22.
Owens RA, Hammond RW, 2009. Viroid pathogenicity: one process, many faces. *Viruses* **1**, 298-316.
Owens RA, Tech KB, Shao JY, Sano T, Baker CJ, 2012. Global analysis of tomato gene expression during Potato spindle tuber viroid infection reveals a complex array of changes affecting hormone signaling. *Mol Plant Microbe Interact* **25**, 582-98.
Owens RA, Blackburn M, Ding B, 2001. Possible involvement of a phloem lectin in long distance viroid movement. *Mol. Plant-Microbe Interact* **14**, 905-909.
Palatnik JF, Allen E, Wu X*, et al.*, 2003. Control of leaf morphogenesis by microRNAs. *Nature* **425**, 257-63.
Pallas V, Flores R, 1989. Interactions between citrus exocortis and potato spindle tuber viroids in plants of Gynura aurantiaca and Lycopersicon esculentum. *Intervirology* **30**, 10-17.
Pallas V, Gomez G, Duran-Vila N. 2003. Viroids in Europe. In: Viroids, Hadidi, A., Randles, J., Semancik, J. and Flores, R. (eds.). St Paul, USA. 268-274.
Pallás V, Gómez G, 2013. Phloem RNA-binding proteins as potential components of the long-distance RNA transport system. *Front. Plant Sci* **4**, 130.
Pallas, V. 2013. Una breve historia del fenómeno del silenciamiento del RNA. Contribuciones de la virología a su descubrimiento. Virologia **16** (1), 14-21.
Palukaitis P, 1987. Potato spindle tuber viroid: investigation of the long-distance, intra-plant transport route. *Virology* **158**, 239-241.
Pandey R, Muller A, Napoli CA*, et al.*, 2002. Analysis of histone acetyltransferase and histone deacetylase families of *Arabidopsis* thaliana suggests functional diversification of chromatin modification among multicellular eukaryotes. *Nucleic Acids Res* **30**, 5036-55.
Papaefthimiou I, Hamilton A, Denti M, Baulcombe D, Tsagris M, Tabler M, 2001. Replicating potato spindle tuber viroid RNA is accompanied by short RNA fragments that are characteristic of post-transcriptional gene silencing. *Nucleic Acids Res* **29**, 2395-400.
Parent JS, Martinez De Alba AE, Vaucheret H, 2012. The origin and effect of small RNA signaling in plants. *Front Plant Sci* **3**, 179.
Pecinka A, Dinh HQ, Baubec T, Rosa M, Lettner N, Mittelsten Scheid O, 2010. Epigenetic regulation of repetitive elements is attenuated by prolonged heat stress in *Arabidopsis*. *Plant Cell* **22**, 3118-29.
Pecinka A, Mittelsten Scheid O, 2012. Stress-induced chromatin changes: a critical view on their heritability. *Plant Cell Physiol* **53**, 801-8.
Peragine A, Yoshikawa M, Wu G, Albrecht HL, Poethig RS, 2004. SGS3 and SGS2/SDE1/RDR6 are required for juvenile development and the production of trans-acting siRNAs in *Arabidopsis*. *Genes Dev* **18**, 2368-79.
Pikaard CS, Haag JR, Pontes OM, Blevins T, Cocklin R, 2012. A transcription fork model for Pol IV and Pol V-dependent RNA-directed DNA methylation. *Cold Spring Harb Symp Quant Biol* **77**, 205-12.

Polivka H, Staub U, Gross HJ, 1996. Variation of viroid profiles in individual grapevine plants: novel grapevine yellow speckle viroid 1 mutants show alterations of hairpin I. *J Gen Virol* **77**, 155-61.
Pontes O, Lawrence RJ, Silva M*, et al.*, 2007. Postembryonic establishment of megabase-scale gene silencing in nucleolar dominance. *PLoS One* **2**, e1157.
Pontier D, Yahubyan G, Vega D*, et al.*, 2005. Reinforcement of silencing at transposons and highly repeated sequences requires the concerted action of two distinct RNA polymerases IV in *Arabidopsis*. *Genes Dev* **19**, 2030-40.
Pontvianne F, Blevins T, Chandrasekhara C*, et al.*, 2012. Histone methyltransferases regulating rRNA gene dose and dosage control in *Arabidopsis*. *Genes Dev* **26**, 945-57.
Probst AV, Fagard M, Proux F*, et al.*, 2004. *Arabidopsis* histone deacetylase HDA6 is required for maintenance of transcriptional gene silencing and determines nuclear organization of rDNA repeats. *Plant Cell* **16**, 1021-34.
Rackwitz HR, Rohde W, Sanger HL, 1981. DNA-dependent RNA polymerase II of plant origin transcribes viroid RNA into full-length copies. *Nature* **291**, 297-301.
Raja P, Sanville BC, Buchmann RC, Bisaro DM, 2008. Viral genome methylation as an epigenetic defense against geminiviruses. *J Virol* **82**, 8997-9007.
Rajakumara E, Law JA, Simanshu DK*, et al.*, 2011. A dual flip-out mechanism for 5mC recognition by the *Arabidopsis* SUVH5 SRA domain and its impact on DNA methylation and H3K9 dimethylation in vivo. *Genes Dev* **25**, 137-52.
Reik W, 2007. Stability and flexibility of epigenetic gene regulation in mammalian development. *Nature* **447**, 425-32.
Rhoades MW, Reinhart BJ, Lim LP, Burge CB, Bartel B, Bartel DP, 2002. Prediction of plant microRNA targets. *Cell* **110**, 513-20.
Richards JT, Corey KA, Paul AL, Ferl RJ, Wheeler RM, Schuerger AC, 2006. Exposure of *Arabidopsis* thaliana to hypobaric environments: implications for low-pressure bioregenerative life support systems for human exploration missions and terraforming on Mars. *Astrobiology* **6**, 851-66.
Rivera-Bustamante RF y Femancik JS, 1989. Properties of a viroid-replicating complex solubilized from nuclei. *J. Gen. Virol*. **70**, 2707-2716.
Rodio ME, Delgado S, De Stradis A, Gomez MD, Flores R, Di Serio F, 2007. A viroid RNA with a specific structural motif inhibits chloroplast development. *Plant Cell* **19**, 3610-26.
Rodriguez-Negrete E, Lozano-Duran R, Piedra-Aguilera A, Cruzado L, Bejarano ER, Castillo AG, 2013. Geminivirus Rep protein interferes with the plant DNA methylation machinery and suppresses transcriptional gene silencing. *New Phytol* **199**, 464-75.
Roeder RG, Schwartz LB, Sklar VE, 1976. Function, structure, and regulation of eukaryotic nuclear RNA polymerases. *Symp Soc Dev Biol* **34**, 29-52.
Roudier F, Ahmed I, Berard C*, et al.*, 2011. Integrative epigenomic mapping defines four main chromatin states in *Arabidopsis*. *EMBO J* **30**, 1928-38.
Ruby JG, Jan CH, Bartel DP, 2007. Intronic microRNA precursors that bypass Drosha processing. *Nature* **448**, 83-6.
Ruiz-Ferrer V, Voinnet O, 2009. Roles of plant small RNAs in biotic stress responses. *Annu Rev Plant Biol* **60**, 485-510.
Sano T, Hataya T, Terai Y, Shikata E, 1989. Hop stunt viroid strains from dapple fruit disease of plum and peach in Japan. *J Gen Virol* **70**, 1311-9.
Sasaki T, Saze H, Kakutani T, 2008. [Mechanisms to control DNA methylation in *Arabidopsis* thaliana]. *Tanpakushitsu Kakusan Koso* **53**, 809-14.
Sasaki M y Shikata E, 1977. Some properties of hop stunt disease agent, a viroid. *Proceed Japan Acad Series B-Physic Biol Sci* **53**,109-112.
Saze H, Tsugane K, Kanno T, Nishimura T, 2012. DNA methylation in plants: relationship to small RNAs and histone modifications, and functions in transposon inactivation. *Plant Cell Physiol* **53**, 766-84.

Schindler IM y Mülbach H P, 1992. Involvement of nuclear DNA-dependent RNA polymerases in Potato spindle tuber viroid replication: a reevaluation. *Plant Sci.* **84**, 221-229.
Schmitz RJ, Tamada Y, Doyle MR, Zhang X, Amasino RM, 2009. Histone H2B deubiquitination is required for transcriptional activation of FLOWERING LOCUS C and for proper control of flowering in *Arabidopsis*. *Plant Physiol* **149**, 1196-204.
Schnable PS, Ware D, Fulton RS*, et al.*, 2009. The B73 maize genome: complexity, diversity, and dynamics. *Science* **326**, 1112-5.
Schoft VK, Chumak N, Mosiolek M*, et al.*, 2009. Induction of RNA-directed DNA methylation upon decondensation of constitutive heterochromatin. *EMBO Rep* **10**, 1015-21.
Sekhon RS, Chopra S, 2009. Progressive loss of DNA methylation releases epigenetic gene silencing from a tandemly repeated maize Myb gene. *Genetics* **181**, 81-91.
Semancik JS, Weathers LG, 1972. Exocortis disease: evidence for a new species of "infectious" low molecular weight RNA in plants. *Nat New Biol* **237**, 242-4.
Serra P, Gago S, Duran-Vila N, 2008. A single nucleotide change in Hop stunt viroid modulates citrus cachexia symptoms. *Virus Res* **138**, 130-4.
Sha AH, Lin XH, Huang JB, Zhang DP, 2005. Analysis of DNA methylation related to rice adult plant resistance to bacterial blight based on methylation-sensitive AFLP (MSAP) analysis. *Mol Genet Genomics* **273**, 484-90.
Shikata E, 1990. New viroids from Japan. *Sem Virol* **1,**107-115.
Shyu A.B, Wilkinson M.F, van Hoof A, 2008. Messenger RNA regulation: to translate or to degrade. *EMBO J*. **27**, 471-481.
Slotkin RK, Martienssen R, 2007. Transposable elements and the epigenetic regulation of the genome. *Nat Rev Genet* **8**, 272-85.
Slotkin RK, Vaughn M, Borges F*, et al.*, 2009. Epigenetic reprogramming and small RNA silencing of transposable elements in pollen. *Cell* **136**, 461-72.
Smith LM, Pontes O, Searle I*, et al.*, 2007. An SNF2 protein associated with nuclear RNA silencing and the spread of a silencing signal between cells in *Arabidopsis*. *Plant Cell* **19**, 1507-21.
St-Pierre P, Hassen IF, Thompson D, Perreault JP, 2009. Characterization of the siRNAs associated with peach latent mosaic viroid infection. *Virology* **383**, 178-82.
Stroud H, Do T, Du J*, et al.*, 2014. Non-CG methylation patterns shape the epigenetic landscape in *Arabidopsis*. *Nat Struct Mol Biol* **21**, 64-72.
Suzuki MM, Bird A, 2008. DNA methylation landscapes: provocative insights from epigenomics. *Nat Rev Genet* **9**, 465-76.
Symons RH, 1981. Avocado sunblotch viroid: primary sequence and proposed secondary structure. *Nucleic Acids Res* **9**, 6527-37.
Tabach Y, Billi AC, Hayes GD*, et al.*, 2013. Identification of small RNA pathway genes using patterns of phylogenetic conservation and divergence. *Nature* **493**, 694-8.
Tabara H, Yigit E, Siomi H, Mello CC, 2002. The dsRNA binding protein RDE-4 interacts with RDE-1, DCR-1, and a DExH-box helicase to direct RNAi in C. elegans. *Cell* **109**, 861-71.
Tabler M, Tsagris M, 2004. Viroids: petite RNA pathogens with distinguished talents. *Trends Plant Sci* **9**, 339-48.
Takeda R, Petrov AI, Leontis NB, Ding B, 2011. A three-dimensional RNA motif in potato spindle tuber viroid mediates trafficking from palisade mesophyll to spongy mesophyll in Nicotiana benthamiana. *Plant Cell* **23**, 258-272.
Takeda S, Paszkowski J, 2006. DNA methylation and epigenetic inheritance during plant gametogenesis. *Chromosoma* **115**, 27-35.
Tanaka M, Kikuchi A, Kamada H, 2008. The *Arabidopsis* histone deacetylases HDA6 and HDA19 contribute to the repression of embryonic properties after germination. *Plant Physiol* **146**, 149-61.

Tang B, Zhao R, Sun Y*, et al.*, 2011. Interleukin-6 expression was regulated by epigenetic mechanisms in response to influenza virus infection or dsRNA treatment. *Mol Immunol* **48**, 1001-8.
Terai Y, 1985. Symptoms and graft transmission of plum dapple fruit disease. *Ann Phytopath Soc Japan* **51**, 363
Tessadori F, Van Zanten M, Pavlova P*, et al.*, 2009. Phytochrome B and histone deacetylase 6 control light-induced chromatin compaction in *Arabidopsis* thaliana. *PLoS Genet* **5**, e1000638.
Tessitori M, Maria G, Capasso C*, et al.*, 2007. Differential display analysis of gene expression in Etrog citron leaves infected by Citrus viroid III. *Biochim Biophys Acta* **1769**, 228-35.
To TK, Kim JM, Matsui A*, et al.*, 2011a. *Arabidopsis* HDA6 regulates locus-directed heterochromatin silencing in cooperation with MET1. *PLoS Genet* **7**, e1002055.
To TK, Nakaminami K, Kim JM*, et al.*, 2011b. *Arabidopsis* HDA6 is required for freezing tolerance. *Biochem Biophys Res Commun* **406**, 414-9.
Tsagris EM, Martinez De Alba AE, Gozmanova M, Kalantidis K, 2008. Viroids. *Cell Microbiol* **10**, 2168-79.
Vance V, Vaucheret H, 2001. RNA silencing in plants--defense and counterdefense. *Science* **292**, 2277-80.
Vaucheret H, 2006. Post-transcriptional small RNA pathways in plants: mechanisms and regulations. *Genes Dev* **20**, 759-71.
Vazquez F, 2006. *Arabidopsis* endogenous small RNAs: highways and byways. *Trends Plant Sci* **11**, 460-8.
Vazquez F, Vaucheret H, Rajagopalan R*, et al.*, 2004. Endogenous trans-acting siRNAs regulate the accumulation of *Arabidopsis* mRNAs. *Mol Cell* **16**, 69-79.
Veiseth SV, Rahman MA, Yap KL*, et al.*, 2011. The SUVR4 histone lysine methyltransferase binds ubiquitin and converts H3K9me1 to H3K9me3 on transposon chromatin in *Arabidopsis*. *PLoS Genet* **7**, e1001325.
Vogt U, Pelissier T, Putz A, Razvi F, Fischer R, Wassenegger M, 2004. Viroid-induced RNA silencing of GFP-viroid fusion transgenes does not induce extensive spreading of methylation or transitive silencing. *Plant J* **38**, 107-18.
Voinnet O, 2001. RNA silencing as a plant immune system against viruses. *Trends Genet* **17**, 449-59.
Voinnet O, 2008. Post-transcriptional RNA silencing in plant-microbe interactions: a touch of robustness and versatility. *Curr Opin Plant Biol* **11**, 464-70.
Voinnet O, 2009. Origin, biogenesis, and activity of plant microRNAs. *Cell* **136**, 669-87.
Wada Y, Miyamoto K, Kusano T, Sano H, 2004. Association between up-regulation of stress-responsive genes and hypomethylation of genomic DNA in tobacco plants. *Mol Genet Genomics* **271**, 658-66.
Wang CY, Zhang S, Yu Y*, et al.*, 2014. MiR397b regulates both lignin content and seed number in *Arabidopsis* via modulating a laccase involved in lignin biosynthesis. *Plant Biotechnol J* **12**, 1132-42.
Wang L, He Y, Kang Y*, et al.*, 2013. Virulence determination and molecular features of peach latent mosaic viroid isolates derived from phenotypically different peach leaves: a nucleotide polymorphism in L11 contributes to symptom alteration. *Virus Res* **177**, 171-8.
Wang MB, Bian XY, Wu LM*, et al.*, 2004. On the role of RNA silencing in the pathogenicity and evolution of viroids and viral satellites. *Proc Natl Acad Sci U S A* **101**, 3275-80.
Wang MB, Waterhouse PM, 2002. Application of gene silencing in plants. *Curr Opin Plant Biol* **5**, 146-50.
Wang WB, Fei JM, Wu Y*, et al.*, 2010. A new report of a mosaic dwarf viroid-like disease on mulberry trees in China. *Pol J Microbiol* **59**, 33-6.
Wang X, Zhu WG, 2008. [Advances in histone methyltransferases and histone demethylases]. *Ai Zheng* **27**, 1018-25.
Wang Y, Liang Y, Lu Q, 2008. MicroRNA epigenetic alterations: predicting biomarkers and therapeutic targets in human diseases. *Clin Genet* **74**, 307-15.
Wang Y, Ding B, 2010. Viroids: small probes for exploring the vast universe of RNA trafficking in plants. *Plant Biol*. **52**, 17-27.
Warrilow D, Symons RH, 1999. Citrus exocortis viroid RNA is associated with the largest subunit of RNA polymerase II in tomato in vivo. *Arch Virol* **144**, 2367-75.

Wassenegger M, Heimes S, Riedel L, Sanger HL, 1994. RNA-directed de novo methylation of genomic sequences in plants. *Cell* **76**, 567-76.
Waterhouse PM, Wang MB, Finnegan EJ, 2001. Role of short RNAs in gene silencing. *Trends Plant Sci* **6**, 297-301.
Wierzbicki AT, 2010. Silencing: new faces of Morpheus' molecule. *EMBO J* **29**, 279-80.
Wierzbicki AT, Cocklin R, Mayampurath A*, et al.*, 2012. Spatial and functional relationships among Pol V-associated loci, Pol IV-dependent siRNAs, and cytosine methylation in the *Arabidopsis* epigenome. *Genes Dev* **26**, 1825-36.
Wierzbicki AT, Haag JR, Pikaard CS, 2008. Noncoding transcription by RNA polymerase Pol IVb/Pol V mediates transcriptional silencing of overlapping and adjacent genes. *Cell* **135**, 635-48.
Wierzbicki AT, Ream TS, Haag JR, Pikaard CS, 2009. RNA polymerase V transcription guides ARGONAUTE4 to chromatin. *Nat Genet* **41**, 630-4
Wingard SA, 1928. Hosts and symptoms of ring spot, a virus disease of plants. J. *Agric. Res.* **37**,127–153
Wolff P, Gilz R, Schumacher J, Riesner D, 1985. Complexes of viroids with histones and other proteins. *Nucleic Acids Res* **13**, 355-67.
Woo YM, Itaya A, Owens RA, Tang L, Hammond RW, Chou HC, Lai MMC, Ding B, 1999. Characterization of nuclear import of potato spindle tuber viroid RNA in permeabilized protoplasts. *Plant J* **17**, 627-635.
Wu L, 2013. DICER-LIKE1 processed trans-acting siRNAs mediate DNA methylation: case study of complex small RNA biogenesis and action pathways in plants. *Plant Signal Behav* **8**, e22476.
Xie M, Ren G, Costa-Nunes P, Pontes O, Yu B, 2012. A subgroup of SGS3-like proteins act redundantly in RNA-directed DNA methylation. *Nucleic Acids Res* **40**, 4422-31.
Xie Z, Johansen LK, Gustafson AM*, et al.*, 2004. Genetic and functional diversification of small RNA pathways in plants. *PLoS Biol* **2**, E104.
Xie Z, Qi X, 2008. Diverse small RNA-directed silencing pathways in plants. *Biochim Biophys Acta* **1779**, 720-4.
Yang LP, Fang YY, An CP*, et al.*, 2013. C2-mediated decrease in DNA methylation, accumulation of siRNAs, and increase in expression for genes involved in defense pathways in plants infected with beet severe curly top virus. *Plant J* **73**, 910-7.
Yang XJ, Seto E, 2008. The Rpd3/Hda1 family of lysine deacetylases: from bacteria and yeast to mice and men. *Nat Rev Mol Cell Biol* **9**, 206-18
Yoshikawa N, Takahashi T, 1986. Inhibition of hop stunt viroid replication by α-amanitin. *Pflanzenschutz* **93**, 62–71
Yu A, Lepere G, Jay F*, et al.*, 2013. Dynamics and biological relevance of DNA demethylation in *Arabidopsis* antibacterial defense. *Proc Natl Acad Sci U S A* **110**, 2389-94.
Yu B, Bi L, Zhai J*, et al.*, 2010. siRNAs compete with miRNAs for methylation by HEN1 in *Arabidopsis*. *Nucleic Acids Res* **38**, 5844-50.
Yu B, Bi L, Zheng B*, et al.*, 2008. The FHA domain proteins DAWDLE in *Arabidopsis* and SNIP1 in humans act in small RNA biogenesis. *Proc Natl Acad Sci U S A* **105**, 10073-8.
Zaitlin M, Niblett CL, Dickson E, Goldberg RB, 1980. Tomato DNA contains no detectable regions complementary to potato spindle tuber viroid as assayed by solution and filter hybridization. *Virology* **104**, 1-9.
Zamore PD, Tuschl T, Sharp PA, Bartel DP, 2000. RNAi: double-stranded RNA directs the ATP-dependent cleavage of mRNA at 21 to 23 nucleotide intervals. *Cell* **101**, 25-33.
Zemach A, Kim MY, Hsieh PH*, et al.*, 2013. The *Arabidopsis* nucleosome remodeler DDM1 allows DNA methyltransferases to access H1-containing heterochromatin. *Cell* **153**, 193-205.
Zemach A, Mcdaniel IE, Silva P, Zilberman D, 2010. Genome-wide evolutionary analysis of eukaryotic DNA methylation. *Science* **328**, 916-9.

Zhang B, Pan X, Cobb GP, Anderson TA, 2006. Plant microRNA: a small regulatory molecule with big impact. *Dev Biol* **289**, 3-16.
Zhang CJ, Ning YQ, Zhang SW*, et al.*, 2012. IDN2 and its paralogs form a complex required for RNA-directed DNA methylation. *PLoS Genet* **8**, e1002693.
Zhang X, Henderson IR, Lu C, Green PJ, Jacobsen SE, 2007. Role of RNA polymerase IV in plant small RNA metabolism. *Proc Natl Acad Sci U S A* **104**, 4536-41.
Zheng B, Wang Z, Li S, Yu B, Liu JY, Chen X, 2009. Intergenic transcription by RNA polymerase II coordinates Pol IV and Pol V in siRNA-directed transcriptional gene silencing in *Arabidopsis*. *Genes Dev* **23**, 2850-60.
Zhong X, Hale CJ, Law JA*, et al.*, 2012. DDR complex facilitates global association of RNA polymerase V to promoters and evolutionarily young transposons. *Nat Struct Mol Biol* **19**, 870-5.
Zhou DX, 2009. Regulatory mechanism of histone epigenetic modifications in plants. *Epigenetics* **4**, 15-8.
Zhou J, Wang X, He K, Charron JB, Elling AA, Deng XW, 2010. Genome-wide profiling of histone H3 lysine 9 acetylation and dimethylation in *Arabidopsis* reveals correlation between multiple histone marks and gene expression. *Plant Mol Biol* **72**, 585-95.
Zhu QH, Shan WX, Ayliffe MA, Wang MB, 2016. Epigenetic Mechanisms: An Emerging Player in Plant-Microbe Interactions. *Mol Plant Microbe Interact* **29**, 187-96.
Zhu Y, Rowley MJ, Bohmdorfer G, Wierzbicki AT, 2013. A SWI/SNF chromatin-remodeling complex acts in noncoding RNA-mediated transcriptional silencing. *Mol Cell* **49**, 298-309.
Zhu Z, An F, Feng Y*, et al.*, 2011. Derepression of ethylene-stabilized transcription factors (EIN3/EIL1) mediates jasmonate and ethylene signaling synergy in *Arabidopsis*. *Proc Natl Acad Sci U S A* **108**, 12539-44.
Zilberman D, Gehring M, Tran RK, Ballinger T, Henikoff S, 2007. Genome-wide analysis of *Arabidopsis* thaliana DNA methylation uncovers an interdependence between methylation and transcription. *Nat Genet* **39**, 61-9.